Atmospheric Microplastic Pollution

Steve Allen

Submitted for the degree of Doctor of Philosophy

University of Strathclyde

Centre for Water, Environment, Sustainability and Public Health (WESP)

Department of Civil and Environmental Engineering

July 2020

Supervisors: Prof. Vernon Phoenix, Dr Iain Beverland

Acknowledgements

Chapters 2, 3 and 5 of this thesis have been published with the support of my supervisor, Prof. Vernon Phoenix, sample access field support from GET and EcoLab, and µRaman access support from CMAC.

The review chapter (Chapter 2) has been published in Earth Science Reviews (https://doi.org/10.1016/j.earscirev.2020.103118) with thanks and acknowledgement to Dr Yulan Zhang for the editing of the review submission, publication cost support and comments specific to the Tibetan Plateau microplastic research.

Chapter 3, Atmospheric transport and deposition of microplastics in a remote mountain catchment, has been published in Nature Geoscience (https://doi.org/10.1038/s41561-019-0335-5), with thanks to EcoLab for the support in accessing the Bernadouze field site and sample collection.

Chapter 4, Evidence of long-range transport of free-tropospheric microplastic found at 2877mASL, has been submitted and is under review with Science Advances, with acknowledgement to GET for access to Pic du Midi Bigorre.

Chapter 5, Examination of the ocean as a source for atmospheric microplastics, has been published in PlosOne (https://doi.org:10.1371/journal.pone.0232746) with acknowledgement to GET and EcoLab for access to field sampling equipment and financial support in field accommodation costs.

Table of contents

1 Research Introduction

Abstract

The following research marks the beginning of the new field of research on the atmospheric transport of microplastic and its potential terrestrial and oceanic source. Taking atmospheric deposition samples from the French Pyrenees I was able to illustrate the first atmospheric transport of microplastics of at least 95km using hysplit4 back trajectory modelling. Further to this I used high volume sampling technique to show first evidence of free-tropospheric microplastic at an altitude of 2877masl at the Pic du Midi observatory in France. I also showed the ocean to be a source of atmospheric microplastics by sampling the sea breeze in varying wind events showing first evidence of ocean to atmosphere transfer.

1.1 Introduction to current Microplastic understanding and the research focus

Plastic is one of the most useful anthropogenic materials created. For much of the world's population, plastic has completely changed the way we live. Since the first commercialisation of PVC in the 1930's and Wallace Carothers first gave us Nylon fibres in 1938(*1*) (*2*) plastic has invaded almost every aspect of our lives. The durability of this modern marvel also means that if improperly handled, it can persist for long durations in the environment and cause devastation to wildlife(*3*). One of the first journal papers documenting oceanic plastic pollution was as far back as 1969 which describes 74% of the 100 Laysan Albatross chick carcases examined, contained plastic debris (*4*). Then in the early 70's Stephen Rothstein (1973) examined the stomach contents of seven birds collected in 1962 at Gull Island, Newfoundland and found plastic

debris in one of the stomachs. He then looked at seven birds from a 1964 collection from Kent Island, New Brunswick and found four of the seven contained plastic. Rothstein however felt that oceanic plastic would have almost certainly have been present before 1962 (*5*). Carpenter and Smith found particle counts of 3500 pieces/km2 stretching over 1300km of the Sargasso sea in 1971 which indicates that whilst oceanic litter and its effect has only recently become widely publicised, it has existed for well over 50yrs (*6*).

Today oceanic microplastic (MP) is still being quantified and whilst we know a good deal about it, there is still much to know.

Atmospheric MP however has been almost completely overlooked in scientific research with a few notable exceptions such as Dris et al., who demonstrated fallout of MicroP fibres in Paris (*7*) and Cai et al., fallout study in Dongguan in (*8*). Both these studies were in very large cities with potentially quite distinct urban microclimates. Another city based survey in Tehran (Iran) found substantial amounts of plastic in the dust collected from the streets however the studies lower size limit of 250µ limits comparison with other studies (*9*). In 2016 Zhang et al. found microP in remote lake beaches on the Tibetan plateau (*10*). Their research states the area is rarely visited by humans so could not explain the presence of microP. Their samples showed surface cracking and gouging that they felt was possibly caused by sand particles as the microP moved through the environment by wave action/saltation. The material abraded from the scratches on these <2mm samples could be plastic debris in the nano scale, >1µm. Corcoran et.al. (2009) similarly found what they termed “beach weathering”, surface abrasions and cracking consistent with environmentally induced collision alongside ultra-violet light degradation to be a significant factor in the breakdown of plastics in their study of microP on Hawaiian beaches. Conversely, this thesis precipitation study (*11*) on a remote site in the Pyrenees

mountains shows that airborne MicroP is not restricted to urban micro climates and provided the first evidence of airborne MicroP transport within the Planetary Boundary Layer(PBL).

1.2 Hypotheses' and research objectives

Given the limited understanding of how MP were being transported to places such as the Tibetan plateau, and how they were being found in atmospheric deposition in cities, this research set out to explore the potential of long-range atmospheric transport as an unexplored environmental compartment.

Three hypotheses were posed.

1. Are MP in the atmosphere outside of cities and could it be subject to Aeolian transport?
    1.1. Using deposition samplers in a remote location to show presence and atmospheric transport of MP.
2. If MP are present in the Planetary Boundary Layer (PBL) then could convection and topography allow it to enter the Free Troposphere (FT)?
    2.1. Examine an FT site for MP presence.
3. If MP is present in both the PBL and FT then where is it coming from and given the unexplained loss of plastic litter in the ocean, could the ocean be a source of atmospheric MP?
    3.1. Study sea breeze and mist for MP presence.

1.3 Thesis structure

The research is presented in the following format.

Chapter 1: Research Introduction

Chapter 1 provides a contextual basis for the hypotheses' and an introduction to the research.

Chapter 2: Literature Review

The literature review is centred around giving an understanding of the current MP pollution situation and provide the necessary background information to explain the processes of Aeolian MP entrainment and transport.

Chapter 3: **Atmospheric transport and deposition of microplastics in a remote mountain catchment.**

Here we present the observations of atmospheric microplastic deposition in a remote, pristine mountain catchment (French Pyrenees). We analysed samples, taken over five months, that represent atmospheric wet and dry deposition and identified fibres up to ~750 µm long and fragments ≤300 µm as microplastics. We document relative daily counts of 249 fragments, 73 films and 44 fibres per square metre that deposited on the catchment. An air mass trajectory analysis shows microplastic transport through the atmosphere over a distance of up to 95 km. We suggest that microplastics can reach and affect remote, sparsely inhabited areas through atmospheric transport.

Chapter 4: Evidence of long-range transport of free-tropospheric microplastic found at 2877mASL

This study provides evidence of between 0.2 and 0.69 particles of micro-plastics per cm^3 in PM10 filters (over 4 months) from the Pic Du Midi observatory at 2877m ASL. These results exhibit true free tropospheric and planetary boundary layer presence of particles up to 200µm in diameter and fibres. Analysis of back trajectory modelling shows intercontinental transport of

micro-plastics (MicroP) illustrating the potential for global aerosol microplastic transport.

Chapter 5: The ocean as a source for atmospheric microplastic pollution: an examination of potential mechanisms and evidence of ocean to atmosphere transmission.

Examining the mechanisms of Sea Salt Aerosol (SSA) production from the ocean revealed the potential for MP to follow the same route. Here we show first evidence of MP particles, analysed by µRaman, in marine boundary layer air samples on the French Atlantic coast during both onshore (avg 2.9MP/m^3) and offshore (avg 9.6MP/m^3) winds with a peak of 19.38MP/m^3 during a sea fog event.

Chapter 6: Conclusions and Future research.

In this chapter the key research findings from each of the chapters and research questions are highlighted, alongside the research limitations. Future research opportunities and needs based on the findings in this thesis work are highlighted with acknowledgement of global microplastic research needs and knowledge gaps.

2 Atmospheric microplastics: A review on current status and perspectives

Abstract

Microplastics have recently been detected in the atmosphere in urban, suburban, and even remote areas far away from source regions of microplastics, suggesting the potential for long-distance microplastics atmospheric transport. There are questions regarding the occurrence, fate, transport, and effect of atmospheric microplastics. These questions arise due to limited physical analysis and understanding of atmospheric microplastic pollution in conjunction with a lack of standardized sampling and identification methods. This paper reviews the current state of knowledge of atmospheric microplastics, the methods for sample collection, analysis and detection. We review and compare the methods used in the previous studies and provide recommendations for atmospheric microplastic sampling and detection. Furthermore, we summarize the findings related to atmospheric microplastic characteristics, including abundance, size, shapes, colours, and polymer types. Microplastics are occurring in the atmosphere from urban to remote areas, with an abundance/deposition spanning 1-3 orders of magnitude across different sites. Fibres and fragments are the most frequently reported shapes and the types of plastic generally aligns with world plastic demand. We conclude that atmospheric microplastics require further research and greater understanding; to identify its global distributions and potential exposure to human health through further field sampling and implementation of standardized analytical protocols.

Keywords: microplastics, atmospheric transport, atmospheric pollution, remote area

2.1 Introduction

Microplastics are an emerging concern worldwide (*12–14*). The common definition of microplastics is a plastic particle 5 mm to 100 nm in size (*15–17*). A more recent definition of microplastics follows the logical differentiation along standard international unit nomenclature (SI units) of microplastics = 5 mm-1 µm (*18*). Due to the evolving research on plastic particles, nanoplastics are also of particular concern because it is expected to be as ubiquitous as its bulk counterparts (*18–20*). Nanoplastics is usually categorized in environmental science as plastic particles smaller than 1 µm, which is also an important priority with regard to seafood safety as well as enhancement of contaminant transport in the environment and potential risks to human health (*14*, *18*, *19*, *21*). The true definition of nano material is a material whose size was small enough that it behaves differently to its larger counterparts (*22*, *23*). In engineering and nano science this is deemed to occur below 100nm. Among environmental scientists this limit is contentious, and many would like to see everything 1-999nm labelled as nanoplastic. However, as environmental nanoplastics are yet to be quantified widely, microplastics are the targeted plastic particles to review in this study.

Microplastics can be categorized as primary or secondary plastics. The primary microplastics are intentionally manufactured microplastic particles for particular applications (for example microbeads); secondary microplastics are created by fragmentation and degradation of macroplastics, including fibres from synthetic textiles (*14*, *15*). Such a distinction is of possible importance to the study of atmospheric transport due to the difference in shape that may affect its aerodynamics and therefore atmospheric transport. There is strong evidence that microplastics are entering into the environment at all steps in the life cycle

of a plastic product - from producers to waste management, with the potential for trophic transfer and human health exposure (*15*, *21*).

Microplastics have been found in quite diverse media, from soils to aquatic systems (e.g., oceans, rivers, shorelines, and swamps), and digestive tracts of both vertebrates and invertebrates (*24–28*). The majority of research to date has focused on the marine environment; however, attention is increasingly being paid to other environmental compartments (*21*, *29*). The atmosphere is an important pathway by which many suspended materials are transported regionally or globally (*15*, *30*). Recent studies have illustrated that atmospheric microplastic particles can be transported to ocean surface air and even remote areas (*11*, *31–35*). Atmospheric dynamics including the wind speed, direction, up/down drafts, convection lift and turbulence are considered important vectors in microplastic transport and influence the flux mechanism and source-sink dynamics of plastic pollution in both marine and terrestrial environments (*21*, *34*, *35*). Currently, due to their inhalation and combination with other pollutants (mercury or PAHs), microplastics are thought to be an emergent component of air pollution (*13*, *36–40*).

Compared to the plethora of microplastics studies in marine environment and growing number of studies in terrestrial environments (*24*, *26*, *41*), research on atmospheric microplastics has only recently gained attention. To date, very few studies have been conducted on atmospheric microplastic. The majority of studies so far published focus on atmospheric deposition, a passive collection of deposited material at a selected location. Several studies have been longitudinal (extending over multiple seasons up to 12 months) (*7*, *32*) but extended or long-term monitoring and a global perspective of atmospheric microplastic pollution has yet to been undertaken.

The characteristics, including abundance, size, shapes, and components haven been studied and reported for urban, suburban, and remote areas (*11*, *32*, *42*). Dris et al. (2017) and Liu et al. (2019) investigated fibres in indoor and outdoor air, identifying that indoor dust is a non-negligible source of human exposure to microplastics. To better understand current status of atmospheric microplastics, it is necessary to collate and compare current research findings, to determine the current state of knowledge and to compare atmospheric microplastic characteristics with microplastics from other environments. Furthermore, the potential impact of atmospheric microplastics on transport and deposition to remote areas and humans via food webs is as an emerging global concern. This review presents the state of knowledge in atmospheric microplastic pollution research with a focus on its current progress, knowledge gaps and recommendations to support standardized and comparable future research.

2.2 Microplastic analysis methodology

2.2.1 Sample collection

The majority of the published atmospheric microplastics research published to date has been undertaken using a passive collector (total deposition), described in the methodologies published by Allen et al. (2019), Cai et al. (2017), Dris et al. (2017) and Klein and Fischer (2019). Early studies used non-standardized collection equipment, collecting a range of wet and/or dry deposition for varying periods and precipitation quantities. However, recent advances in passive sampling of atmospheric deposition have resulted in a metallic/glass standardized system designed by NILU (Norwegian Institute for Air Research). This system provides a plastic-free standardized method for passive atmospheric deposition, which is ideal for microplastic research. The benefits of these total or bulk deposition samplers is ease of use, methodology

standardization (as in the case of Allen et al. (2019) who used the early design standard NILU collectors) and no requirement for power to the study site. Implementation of this standardised sampling method allows studies to be performed in remote locations with minimal infrastructure at a very low cost but to a standard protocol for collection. Another reason for using a standardized sampler is that the amount of blowby (wind lifting particles out of the collection funnel before entrapment) is a known amount which allows for comparison to other deposited material in addition to other plastic studies.

Road and indoor dust have been sampled using sweeping, vacuum and active pumped sample methods. This results in data that are difficult to compare. Lui et al. (2019) collected indoor dust deposition using hog bristle brushes which they transferred to sample bags as completely as possible (unknown amount of material retained in the brush). While this method is easily replicable, it is difficult to determine the relative quantity of air sampled or whether the collected microplastics were solely atmospheric deposition. Abbasi et al., (2017) investigated road dust for heavy metals, microplastics and mineralogical characteristics, collecting sampled using a dustpan and brush. Similarly, Dehghani et al. (2017) collected road dust for microplastic analysis using an anti-static wooden brush. This study was careful to note the meteorological conditions prior to and during the sampling, selecting sampling times with specific dry periods preceding the sample time periods to try and provide an indication of the duration of dry deposition. This is useful in further comparative analysis of microplastic deposition (MP/m^2/day) however it is difficult to directly compare these findings to true atmospheric deposition collectors (such as the NILU collector) as the quantity of residual microplastic left on the sample surface is unknown

Active pumped samples, and effective atmospheric microplastic sampling method, are effective in sampling known quantities of air over defined periods at selected locations (*45*). This is a highly effective sample collection method that follows a standard protocol for collection, can be correlated to site specific meteorological conditions and known terrestrial/ocean surface conditions. Active pumped air sampling is an established method of atmospheric pollution monitoring (microplastic and other established atmospheric pollutants), used over the past decade and more to monitor atmospheric chemistry such as mercury, lead, carbon and microbes (*46*). Dris et al. (2017) used active air pumped sampling methodology to enable a known volume of indoor air to be sampled (filtered). This provides an advancement in standardization of sampling protocol and, while being more intensive in sample resources (electricity and equipment requirements) is highly replicable. In conjunction with the Dris et al. (2017) studies use of active air pumped sampling method, K. Liu et al., (2019a) used active samplers placed on rooftops, pumping 100±0.1 L/min, to sample Shanghai city air mass microplastic content and in a further study to sample ocean air microplastic in a marine voyage across the China Sea (Shanghai-Mariana Islands study)(*34*).

Passive atmospheric deposition samplers provide a location and time specific indication of the quantity of microplastic falling on the surface (e.g. urban road surface, rural field or remote mountain top). Active samplers sample pumped air and therefore provide a sample of microplastics in the air mass rather than deposited microplastic pollution. Active pumped air samples provide an indication of the quantity of microplastics in the airmass that may not deposit. As a result, the use of passive samplers to collect atmospheric deposition (wet and/or dry) is recommended in conjunction with active pumped air sampling to gain a full picture of air MP content. To ensure the validity, rigor and future comparative capacity of all microplastic research published, it is vital to clearly

state the following in all field and laboratory studies: the type of equipment used to sample microplastics; the duration and dates of all sampling (representing the time period); the spatial location of the samples (location and elevation). This information, in conjunction with the equipment analytical limitations (e.g. the limitation on particle size, particle type) will ensure the research findings can be compared to other, international, microplastic studies. Furthermore, use of multiple sampling methods at one location (i.e. air pump + dry/wet deposition sampler) will provide microplastic samples representative of both air mass and deposition, and will enable future scavenging (e.g. by rainfall) to be quantified.

2.2.2 Criteria for visual identification of microplastics

A great majority of plastics produced globally are based on non-renewable fossil fuel resources (*15*). In general, plastic particles > 500 µm are visually identified by their shape and colour under a stereomicroscope , with subsequent confirmation using a chemical analytical method (*47*, *48*). The technique used for identification of atmospheric microplastics is not entirely the same due to the weathering and size of the particles. However, during identification of atmospheric microplastics, the following guidelines are usually used:

- Plastics must have no biogenic (cellular or organic) structures (*42*).
- Biofilms and other organic or inorganic adherents have to be removed from the microplastics particles to avoid artefacts that impede clear and accurate identification (*20*).
- Fibres are expected to have a relatively even or consistent thickness along their entire length and illustrate three dimensional bending (*42*).
- Fragments and films are expected to have relatively homogeneous colouring and illustrate a level of transparency or clarity (*20*). However, extremely weathered particles may show strong internal colouring

'spots' with a loss or bleaching of colour at the particle edges and surface.

- Aged plastic, such as expected in environmental samples present embrittled and weathered surfaces, and to have irregular shapes with broken and sharp edges (*47*). Weathered plastics may also show pitting, gouging and scratched/torn surfaces (*49*).
- Colour can be a plastic identifier and ranges from transparent and variations of white to bright orange, blues, greens and purples through to black (*20*, *47*, *48*). Transparent, red and green fibres should be examined with high magnification to confirm their nature (*42*). It is noted that biogenic and plastic material becomes bleached during the sample preparation process (H_2O_2 digestion) that makes coloured plastic particulates less visible and more difficult to differentiate from residual (post digestion) biogenic material (*11*).

2.2.3 Sample preparation

2.2.3.1 Organic matrix removal

There is an ongoing evolution and advancement in sample preparation for microplastic analysis. Early research identified microplastics through visual techniques without sample preparation beyond simple filtration (placing the material onto a filter platform), using color, shape, size and reaction to heat (hot needle test) as methods to indicate plastic composition (*47*, *50*, *51*). As microplastic research has extended beyond simple sample matrices and the analytical methods have advanced to allow smaller particle analysis, it has become necessary to separate small microplastics, <500µm, from the remaining sample material. This is particularly important when samples include significant organic material as the organic matter creates interference in spectrographic analysis; causing increased noise in the spectra, screening and

bio-coating of plastic particles (*20*). Organic removal has been undertaken through a variety of methods, including KOH, NaOH, HNO_3, HCl, H_2O_2, H_2O_2+H_2SO_4, H_2O_2+Fe, and enzymatic methods (*52–54*). Atmospheric deposition studies have used sodium hypochlorite (NaClO) or hydrogen peroxide (H_2O_2) as digestion methods for organic removal to date (*7*, *11*, *32*, *55*). A level of consensus regarding effective methodology is growing in microplastics research in general, using a form of H_2O_2 digestion in controlled temperature environment for a selected period (relative to the quantity of organic material). Recent research has identified Fenton's reagent as an effective advancement in sample preparation methodology (*26*, *56*, *57*).

2.2.3.2 Density separation

The methods of sample preparation are not yet standardized, and a variety of organic removal and density separation methods have been used. Density separation is relatively simple, requiring material to be suspended or settled in liquid of various densities. Density separation has been undertaken using freshwater (1.0 g/ml), sea water (1.03 g/ml), sodium chloride (>1.2 g/ml), calcium chloride (>1.35 g/ml), sodium polytungstate solution (>1.5g/ml), sodium bromide (>1.6 g/ml), zinc bromide(>1.7 g/ml), zinc chloride (>1.7 g/ml) and sodium iodide (>1.8 g/ml) (*25*, *58*). To date, density separation for atmospheric samples has been completed zinc chloride (*11*, *43*). It is noted that when settling fine dust particles in atmospheric deposition (Saharan dust and similar material) it was necessary to lightly agitate the settling tubes (60rpm) to prevent collation of fine dust on/around microplastic particles and subsequent loss of microplastic sample material through deposition.

2.2.4 Analytical measurements

2.2.4.1 Visual methods

Early atmospheric microplastic research involved a simple visual microscopic reporting of plastic presence and quantification (*42*). While effective for large obvious microplastic particles, it can be difficult to accurately determine if particulates are plastics when considering particles <500 µm (*51*, *59*). This severely limits the size fractions which can be examined using only visual reporting, because the abundance of microplastic particles appear to increase almost exponentially with decreasing particle size (*60*). More recent studies have used visual identification coupled with confirmation of plastics presence (as opposed to organic or inorganic material) by various hot-needle techniques (*47*, *50*, *51*, *61*). However, visual identification and sorting of microplastic is strongly affected by human bias, microscopy quality, sample matrix and size limitation due to microscope resolution (*25*, *47*). For particles <500 µm, it is recommended that non-visual, spectroscopy methods be used to determine if particles are plastic (overview of microplastic analysis methods is provided in Table 1).

Table 1: Summary of sampling methods for atmospheric MP

Sampling method	Related equipment	Types	Study area	References
Active sampling				
A pump (Stand-alone sampling pump GH300, Deltanova, France) allowed to sample 8 L/min of indoor air on quartz fiber GF/A Whatman filters (1.6 mm, 47 mm)		Dry deposition	Paris, France	Dris et al., 2018, 2017
Suspended atmospheric microplastics were collected using a KB-120F type intelligent middle flow total suspended particulate sampler (Jinshida, Qingdao) with an intake flow rate of 100 ± 0.1 L/min.		Dry deposition	Shanghai, China & West Pacific Ocean	Liu K et al., 2019a, 2019b
The dust collection system comprised a low-volume sampler unit and a filter changer with an intake tube and sampling head (inlet) to collect PM from air that is drawn through a size-selective inlet and through the filter media.		Air	Asaluyeh County, Iran	Abbasi et al., 2019
Passive sampling				

Sampling method	Related equipment	Types	Study area	References
	Palmex Rain Sampler with a sampling area of 0.014 m2 (diameter of 135 mm) constructed of ultraviolet-resistant polyvinyl chloride (PVC) and stainless steel NILU Particulate Fallout Collector (p.no. 9721) with a sampling area of 0.03 m2 (diameter 200 mm) constructed of high-density PE and stainless steel	Dry and wet atmospheric fallout	the Pyrenees mountains, remote area	Allen et al., 2019
	A sampling device equipped with a glass bottle	Dry and wet deposition	Yantai, China	Zhou et al., 2017
	A sampling device was equipped with a glass bottle (30 cm × Φ15 cm, i.e., opening area is 0.0177 m2, volume is 5.31 L) and a fixed support	Dry and wet deposition	Dongguan, China	Cai et al., 2017
	A funnel in a 20 L glass bottle on the rooftop of Paris-Est Creteil University	Wet and dry deposition	Paris, France	Dris et al., 2015 Dris et al., 2016

Sampling method	Related equipment	Types	Study area	References
				Dris et al., 2017
Total particulate samplers consist of a 150 cm long PVC-pipe, a PE-funnel and a 2 l PE-bottle.		wet and dry deposition	Hamburg, Germany	Klein and Fischer, 2019
1. The indoor dust was collected from 4m^2 of floor in each bedroom and 4m^2 in the living room using hog bristle brushes. 2. The outdoor dust was collected simultaneously from the windowsills and open-air balconies connected to the apartments following the same protocol.		indoor and outdoor dust	39 major cities of China	Liu C et al., 2019

2.2.4.2 Thermochemical methods

Thermal Desorption Proton Transfer Mass Spectrometry is currently the best system for characterisation of sub micron nanoplastics (Materic et al. 2019). It can quantify mass and type down to 1ng/ml of PS and 10 of others(*62*). The use of pyrolysis coupled with mass spectrometry is one of the non-visual methods to determine microplastic in a sample. To date, pyrolysis mass spectrometry (e.g. Py/GC/MS) analysis has not been undertaken on atmospheric samples. Py/GC/MS can identify the type of plastic in a sample (e.g. PET, PVC, PE) and the concentration of this plastic type (ppb) through thermoanalytical methods. It is not possible to define the number of particles or the shapes using this method, and thermoanalytical methods are by nature destructive. The quantity or size of plastic particles necessary within the sample to obtain a clear results has been suggested as 100 µm (*20*, *59*, *63*, *64*). However, there have been significant recent advancements in pyrolysis methods coupled with spectrometry techniques have been used to identify smaller quantities of particles in environmental and laboratory experiment samples (*65–68*). These advancements, including the use of thermal desorption (TDS-GC/MS) coupled with thermogrametric analysis (TGA) and solid phase extraction may provide enhanced analysis.TDS-GC/MS may enable identification of sample composition in environmental samples with very small particles and plastic quantities and are potentially usefully atmospheric microplastic analysis methods in the future (*54*, *69–71*).

2.2.4.3 FTIR spectroscopy

Both FTIR and Raman spectroscopy measure the reaction of the various chemical bonds in materials to an energy (light) source (*72*). The use of vibrational spectroscopy for atmospheric microplastic started with Dris et al. (2016) where Attenuated Total Reflectance Fourier Transform Infra Red (ATR-

FTIR) and Focal Plane Array (FPA-FTIR)spectroscopy was used to study fibres (with a minimum size limit of 50µm). FTIR has been used extensively as a tool for characterization and more recently mapping for particle counting and size distribution (*73*, *74*). FTIR determines a particles composition (it's molecular structure) through examination of the sample using an IR wavelength range of 400-4000cm^{-1}. A proportion of the wavelengths are absorbed by the particle being analysed. By determining which wavelengths were absorbed and transforming the absorption using the Fourier Transform function a spectrum describing the particles composition is created. This spectrum is cross referenced against reference libraries and/or analysed for its individual chemical structure to define the particle composition (*27*, *75*).

The early popularity of FTIR for all microplastics research potentially stemmed from the easy to use libraries and ease of analytical and equipment operation. The advantage of FTIR is a higher throughput (compared to hot-needle and visual analysis), the ability to analyse a smaller particle size (below 500µm), characterize it and automation of particle spectral analysis through polymer spectral libraries. FTIR's long history of use for polymer industry quality control offers substantial library spectra of virgin polymer types though environmentally aged plastics spectra are often not as clear. Some early studies used Attenuated Total Reflectance (ATR) to gain spectra from a particle. This system requires placing the individual particles (particles large enough to be manipulated using tweezers) between two points before running the analysis. The minimum size that can be physically manipulated for ATR limits its practical use for atmospheric microplastics (Dris, 2016, 50µm).

FTIR equipped to include a confocal microscope (known as µFTIR) and focal Plane Array (FPA) with Mercury Cadmium Telluride (MCT) liquid nitrogen cooled detectors has reduced the practical particle size down toward the

diffraction limit. For infrared (IR) this limit is theoretically 10µm (particle diameter) as the whole wavelength must pass through the material, however given the normally weathered surface of environmental microplastic samples it is difficult to get reliable signals below ~20µm, especially when automated (*63*). The application of FPA µFTIR for atmospheric microplastic is limited by this diffraction limit and has been shown to illicit 35 % underestimation of particles below 20 µm (*59*). MCT detectors must be cooled using liquid nitrogen to minimize the noise created by dark energy passing through the detector. This means the liquid nitrogen dewer must be maintained at least every 8 hours for most machines.

2.2.4.4 Raman spectroscopy

Though both Raman and FTIR are both considered vibrational spectroscopy, Raman is different to FTIR in that it uses a higher frequency (normally 532nm) laser to excite the surface of a material until it emits photons. The photons are normally emitted in line with the laser (Rayleigh scatter) but 1 in 10-7 photons are emitted at right angles and are known as Raman scattering. Raman is relatively new to microplastics research and does not have the history in industrial polymer research, as such the libraries are not yet well developed. The theoretical limitations of Raman are sub-micron however 2.5µm is the current smallest published due to surface weathering and the energy imparted to the particle can be destructive however it is expected to reduce to 2 µm with improved techniques (*11*, *60*). The smallest atmospheric plastic particle using µFTIR is 11 µm (*76*).

The main issue with short wavelength Raman lasers is fluorescence. The wavelengths traditionally used for Raman are very close to many maximum excitation wavelengths for polymers which causes the particle to fluoresce. This fluorescence obfuscates the signal denying analysis of the chemical bonds. To

get past this, studies are now using a near IR laser of 785nm (*11*). This has an impact on particle sizes and more power is needed to elicit the same Raman response which may increase the possibility of particle destruction. Though initial purchase costs of µRaman is higher than the equivalent µFTIR, the Raman generally uses Thermo Electrically Cooled (TEC) detectors which obviates the necessity for liquid nitrogen cooling. This simplifies operation, reduces costs and makes it possible to operate overnight without supervision increasing runtime per day. It is thought that with further library and technique development that µRaman will be the preferred tool for atmospheric microplastics due to the smaller particle size in this emerging field. Recent advances in nano-FTIR, Raman Enhanced Atomic Force Microscopy (RE-AFM), and Raman tweezers (RT) may change this with particle characterization as small as 20nm (*63*, *77*, *78*). Raman tweezers use the same principle as optical tweezers (OT) which traps particles in liquid with the force of interactions with light between the tips and particle. RT adds the ability to gain a spectra from the particles as well as size and shape making it a promising technique. It is noted that the material must be suspended in liquid which may make it unsuitable for all atmospheric samples types as suspension in an added liquid may contaminate. It is noted by Meyns et al. (2019) that Nano-FTIR has trouble identifying polystyrene which will limit the applicability for environmental samples. Though it may be possible to characterize nanoplastic on these machines, current technology means a very slow throughput and significantly higher costs.

µFTIR and µRaman spectroscopy (FTIR and Raman advanced to allow microparticle analysis rather than meso or macro particle analysis) enables the analysis of small microplastics directly on filters without any visual pre-sorting and open the possibility for automatization. The current preferred filter for both is .2 µm Anodisc (aluminium oxide) (*73*)(*11*) however it is noted that Anodisc is

active in the near IR wavelength (785nm) making sub 10 micron analysis difficult. The use of plastic filter types (such as polycarbonate, PTFE, etc) are discouraged for FTIR as in transmittance the light must pass through the filter. Similarly, when approaching the detection limits stray light from the Raman laser may gain signal from the filter and obscure the signal from the target particle. Cellulosic type filters tend to warp when drying which makes automation of focus difficult, so they are not recommended for either technique. Both µFTIR and µRaman are effective in identifying >20µm microplastic particles, with advances enabling particle mapping and automated counts. Compared with µFTIR spectroscopy, µRaman techniques can theoretically analyse particles down to sub-µm (diffraction limit of 785nm compared to µFTIR ~ 10µm), providing a higher resolution analysis for these increasingly important small microplastic particles (*54*, *60*). The practical limit of µFTIR on aged microplastics appears to be around 20µm without substantial extra effort and expertise provided by the analyst. Käppler et al. (2016) reports that a significant amount (35%) of small microplastics (<20 µm) are lost (underestimation of MP) during µFTIR analysis compared to µRaman imaging. µFTIR analysis has the benefit of extensive polymer library resources for identification and comparative analysis However, as µRaman use increases it is expected a similar library resource will evolve, providing an identification and comparison functionality equivalent to the current µFTIR detail and availability. As a result, µRaman provides a slight advantage at present with regards to the lower limitation of particle size analysed and in the cost to perform the analysis.

It is recommended that atmospheric microplastic analysis be undertaken using a spectroscopic analysis methodology due to visual methods being ineffective for small particle sizes such as those found in atmospheric deposition samples. It is recommended that spectroscopy, µRaman or µFTIR, be used to characterize and quantify atmospheric microplastics to aid in understanding

sources and fates of this material. Analysis of microplastic <1µm in environmental samples is still in the early stages of technological advancement. Further research to support sub-micron microplastic analysis techniques is essential. Development of thermochemical (Py-GCMS, TD) analysis methods may provide an avenue to identifying concentration and plastic type in samples containing microplastics <1µm, acknowledging information on particle counts and shapes are not possible following these destructive methodologie however Brownian motion Dynamic light scattering is an interesting direction.

2.3 Current knowledge of atmospheric microplastics

2.3.1 Occurrence and Abundance

The spatial distribution of atmospheric microplastic studies, presented in Figure 1, illustrates the new and developing nature of this research focus. Using a number of the different sampling and analytical methods discussed, the published atmospheric MP studied (Figure 1) have identified, quantified and characterized atmospheric microplastics at these remote to urban or industrial locations.

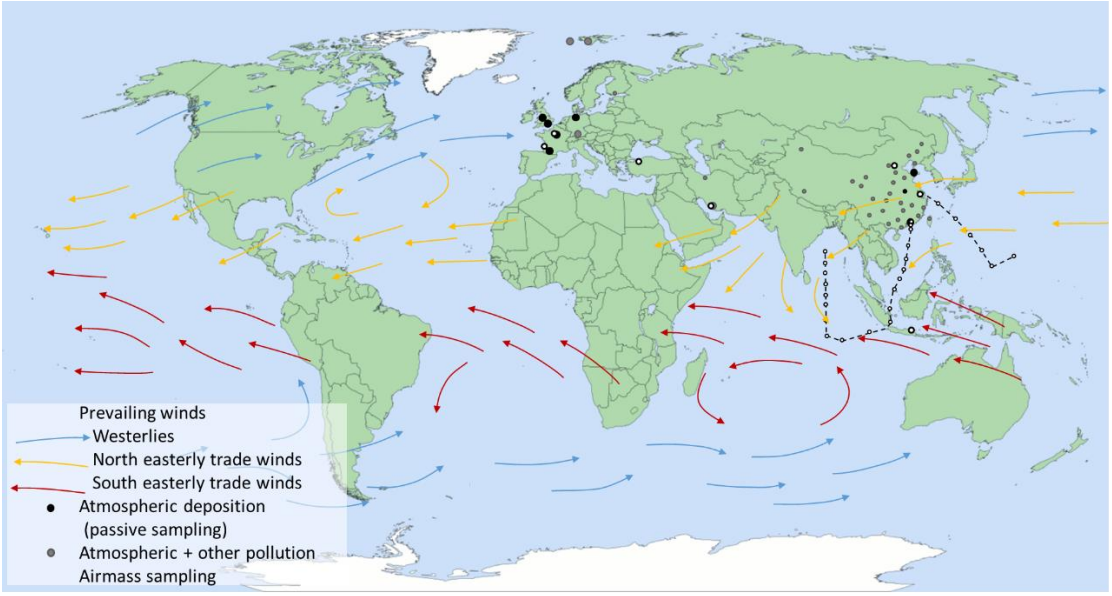

Figure 1. A mapped representation of the atmospheric microplastic studies published to date. For further details on plastic quantities and characterization in these studies, refer toTable 2.

The overall abundance for atmospheric microplastics are presented in Table 2. The average abundance of atmospheric microplastics varied greatly among different studied areas. In the European cities, the mean microplastic abundance from dry and wet deposition has been found between 118 (Paris) and 275 (Hamburg) particles m^{-2} d^{-1} (*32*, *42*, *79*). While in Dongguan city of China, the abundance of non-fibrous microplastics and fibres ranged from 175 to 313 particles m^{-2} d^{-1} in the atmospheric deposition (*8*). Deposition flux of atmospheric microplastics in Yantai (a coastal city) of China attained a maximum of 602 particles m^{-2} d^{-1} (*49*). In the remote area of the Pyrenees Mountains, the result illustrates an average microplastic particles deposition of 365 particles m^{-2} d^{-1} (*11*). Atmospheric microplastics observed from urban cities to remote pristine areas further indicates that microplastic pollution has become a global issue (*21*).

The deposition rate of fibres in indoor environments of Paris is between 1,586 and 11,130 fibres m^{-2} d^{-1} with an abundance of fibres between 0.3-1.5 particle m^{-3} (*43*). Abundance of suspended atmospheric microplastics in Shanghai from filtered air ranges from 0 to 4.18 particles m^{-3}, with an average level of 1.42±1.42 particles m^{-3} (*33*). Higher abundance was observed in Shanghai compared to Paris, possibly due to more anthropogenic activities, population densities, and industrialization levels.

Precipitation (wet deposition, including rainfall and snowfall) events may be a positive drivers in atmospheric microplastics deposition (*11*, *79*). Micro/nano plastic was recently shown by Ganguly and Ariya (2019) (laboratory study) to be an efficient cloud ice nuclei which may explain the slight correlations with

MP counts to snow events from Allen et al. (2019). Snow is considered as a positive method of microplastic deposition (atmospheric particle scrounging) depositing atmospheric particulates in urban areas and on the sea or Arctic regions. The recent study by Bergmann et al. (2019) indicates that deposition of microplastics ranged from 190-154×10^3 particles L^{-1} and 0-14.4×10^3 particles L^{-1} in melted snow sampled from Europe and the Arctic respectively. This abundance was suggested by the authors (*73*) to be 4-7 orders of magnitude higher than concentrations previous reports from Dongguan and Paris (*8*, *43*). A large proportion of this discrepancy is expected to result from significant differences in methodology, most specifically the limit of particle size analysed (11µm in the Arctic study, ~50µm in Paris and ~200µm in Dongguan). Rain and snow are thought to be effective scavenging mechanisms for aerosol particles and the findings in these studies emphasize the need for event specific sampling enabling individual rain/snowfall event atmospheric deposition to be determined, and for short time period dry deposition sampling to occur to support meteorological correlation to atmospheric deposition. Spatially, the Artic and Pyrenees studies illustrate the encroachment of atmospheric microplastic pollution in remote areas These studies provide a new perspective on transport of atmospheric microplastics.

Outdoor abundance of microplastics is significantly lower than that of indoor environments. Dris et al. (2017) found indoor concentrations ranged between 1.0 and 60.0 fibres m^{-3}, while outdoor concentrations ranged between 0.3-1.5 fibres m^{-3}. In China, outdoor atmospheric microplastic abundance has been reported as up to 4.18 particles m^{-3} (Shanghai) and in Surabaya, Indonesia, up to 174 particles m^{-3}. In the indoor dust samples from 39 major cities of China, microplastics (detected PET) abundance ranges from 1550 to 120000 mg kg^{-1} with a median abundance of 26800 mg kg^{-1} (*38*). These findings show that

indoor microplastics may be an important source of atmospheric microplastics and contribute to atmospheric deposition (*43*).

At present, one of the major limitations of current perspectives on microplastic pollution research is the lack of harmonization or standardisation of data and methodologies that are widely used within the research community. However, this is improving as scientists have now developed formal definitions to ensure transferability and reproducibility of research results and greater clarity in the reporting structure (detailing sampling and analytical methods and their limitations) (*18*). Correlation to meteorological conditions and sample period representation are further important study data that need to be considered in the design and provided in the reporting of future atmospheric microplastic research.

2.3.2 Physical characterization: shapes, size, and colours

2.3.2.1 Shapes

Microplastics in environment appear in a wide diversity of shapes and size (*81*). Frequent description of microplastic shapes includes spheres, beads, pellets, foam, fibres, fragments, films, and flake (*47*). These shapes depend on the original form of primary microplastics, the degradation and erosion processes of plastic particle surface, and residence time at the environment. It has been suggested that degraded microplastics with sharp edges illustrate a recent introduction into the environment while smooth edges are associated with a large residence time (*47*, *81*). Diverse shapes including fibre, foam, fragment, and film have been detected in the atmospheric microplastics proved by previous studies. In Dongguan, Shanghai, Yantai, and Paris (urban centres), fibres were the dominant shape (>60%) for the atmospheric microplastics (Table 2). However, in Hamburg, the dominant shape of atmospheric

microplastics detected were fragments, contributing to 95% of the total particle numbers and only 5% comprised fibres (*82*). Atmospheric deposition studies in remote areas also suggested dominant fragment shape (*11*, *73*). In Iran, fibrous (33.5%) and granule (65.9%) microplastics were the most abundant shapes in street dust (*9*, *83*).

The shape of microplastics has been often used to infer their origin and pathway because certain shapes may be more prolifically shed from particular products (*13*, *84*). Fibres, for example, are the dominant shape found in the urban atmospheric deposition of Shanghai, are likely closely connected to the increasing production of synthetic fibre (clothing, upholstery, or carpet); while fragmented microplastics could possibly result from the exposure of larger plastic items to strain, fatigue, or UV light (*33*). Surface texture (e.g., adhering particles, grooves pits, fractures and flakes) of fibres indicate that mechanical abrasion and chemical weathering might play a key role on the degradation of microplastics in the atmospheric environment (*8*, *49*). Microplastic fibres can range in thickness and/or width from 1 to ~500 µm (*85–87*). It is noted that for small microplastics it can be difficult to identify if the particle is a fibre due to the mechanical and/or chemical degradation of the material resulting in reduction of the fibre length such that the width and length of the fibre are similar. The differentiation between fibre and fragment for smaller microplastics may therefore be ineffective.

The different shapes of microplastics may affect the transport of this pollutant through the environment. For instance, films can be very thin and flat, and therefore provide a greater surface area for atmospheric conveyance relative to fragments of the same mass (*11*). The influence of shape on atmospheric transport is currently unknown and required further research. Specific shapes or sizes of microplastics may have greater potential to cause physical harm to

organisms, with smaller angular particles passing membrane barriers more easily than particles presenting regular surfaces or longer edges (*13*, *47*).

2.3.2.2 Size

Plastic particle size is a major factor determining the item's interaction with biota and its environment fate (*88*, *89*). Generally, microplastic size limits are operationally defined by the sampling and analysis method (*18*). Microplastics encompass a broad range of sizes, which are typically considered to be 1μm to 5mm in length (*15*, *18*). Compared to microplastics from aquatic and sediment environments (*24*, *26*, *53*), the predominant size of atmospheric microplastics is much smaller (Table 2). For example, in the Pyrenees Mountains, the predominant length of plastic fibres was less than 300 μm (~50%) with a greater proportion of fragments (fragment sizes <50 μm, 70% of microplastic particles) within the samples (*11*). In a European urban city of Hamburg, the majority of fragments were <63 μm (~60%), followed by 63-300 μm (~30%); while fibres were predominantly between 300-5000 μm in length (*32*). Dris et al. (2016) primarily found fibres of 200-600 μm (~40%), whereas Cai et al. (2017) report predominant fibre lengths of 200-700 μm (~30%). In Yantai and Shanghai, the predominant particle size is <500 μm (~50%) (*33*). Among the previous studies, the longest atmospheric microfibre identified is ~5000 μm (*8*, *79*). Film and foam size have not been specifically evaluated in the majority of previous atmospheric microplastic research. Only the study in Pyrenees Mountains shows the predominant film diameter is 50–200 μm, larger than the predominant fragment size (*11*). For snow in European and Arctic regions, 80% of the detected microplastics were ≤25 μm, and 98% of all particles were < 100 μm (*73*). Such results indicates that particle number increases as particles get smaller(*73*, *90*) and that particle size is a highly important aspect of atmospheric microplastic analysis and research.

2.3.2.3 Colour

Microplastics have been reported in a range colours, including red, orange, yellow, brown, tan, off white, white, grey, blue, green, and so on (*13*, *73*). The most commonly reported are blue and red fibres (*47*). Dark, white, transparent, or translucent particles may be underrepresented during visual inspection (*18*). Colour is useful to identify potential sources of plastic debris as well as potential contaminations during sample preparation (*18*, *81*). Clear and transparent items have been ascribed to polypropylene, white to polyethylene and opaque colours to LDPE (*81*). However, the colour of a plastic particle cannot easily be used to deduce the type or origin. Importantly, colour information can be biased as brighter colours are spotted more easily during visual inspection (*13*).

In the study of Paris atmospheric microplastics, Dris et al. (2015) pointed out that there is a tendency to overestimate brightly coloured fibres (blue, red) in comparison with other particles because they are more easily recognized. In Shanghai city, atmospheric microplastics were variously coloured including black, blue, red, transparent, brown, green, yellow, and grey particles (*33*) (Appendix 1). Among them, blue and black microfibres comprised the majority of the atmospheric microplastics, accounting for 25% and 28% of the total microplastics, respectively. For microplastic from supraglacial debris, both fragment and fibres were of diverse colours, with black and blue dominating (31% and 22%, respectively) (*31*). Optical microscope images of selected polymers from Dongguan city showed atmospheric microplastics have colour of blue, red, grey, and transparent (*8*). Discoloration of microplastics can take place during weathering as well as sample preparation (particularly with oxidative digestion such as H_2O_2), which should be considered in data reporting and interpretation (*11*, *13*). It is considered that colour can be helpful in the initial visual assessment of microplastics in atmospheric samples, but due to

the predominantly small particle size and often significant weathering of these particles colour analysis is less important than spectral or chemical identification of these microplastics.

Table 2. Summary of characteristics of microplastics in possible atmospheric depositions presented in published studies. Studies which are a mix of atmospheric and other sources of MP (e.g. road dust + atmospheric deposition) are indicated with an *.

Study area	Sample types	MP abundance	MP size	Shapes	Colours	Composition	Method	References
Paris, France	Total atmospheric fallout (dry&wet deposition)	29–280 particles m^{-2} d^{-1} Ave: 118 particles m^{-2} d^{-1} (110 in urban, 53 in suburban)	100-500 µm 500-1000 µm 1-5 mm (50% fibres > 1000 µm)	>90% fibres ~10% fragments	Blue Red	N/A	Stereomicroscope µFT-IR	Dris et al., 2015
Paris, France	Atmospheric fallout	2.1-355.4 fibers m^{-2} d^{-1}	50-200 µm:3% 200-600 µm: 42% 600-1400µm: ~40% (50-4850 µm)	Fibers	N/A	29% synthetic	Stereomicroscope µFT-IR	Dris et al., 2016

Study area	Sample types	MP abundance	MP size	Shapes	Colours	Composition	Method	References
Paris, France	Indoor and outdoor air	Outdoor: 0.3-1.5 fibers m^{-3} (1586-11130 fiber m^{-2} d^{-1}) Indoor: 1-60 fibers m^{-3}	50-450 µm: >80%	Fibers	N/A	PP	Stereomicroscope µFT-IR	Dris et al., 2017
Hamburg, Germany	Atmospheric deposition	275 particles m^{-2} day^{-1} (Range: 136-512)	Fragment: <63 µm: ~60% 63-300 µm:~30% >300µm: ~20% Fibers: 300-5000µm: 68% 63-300µm: 25% <63µm: 7%	Fragment: >90% Fibers: <10%	N/A	PE: 48.8% EVAC: 22% PTFE PAV	µ-Raman	Klein and Fischer, 2019

Study area	Sample types	MP abundance	MP size	Shapes	Colours	Composition	Method	References
* Tehran metropolis, Iran	Urban dust	88-605 items per 30g dry dust	Predominant: 250-500 µm (100-1000µm)	Granule dominant:60% Fibers:35% Sphere:5%	Black, grey, orange, yellow, white, transparent, green, blue, red, pink	N/A	Fluorescence microscopy SEM/EDS	Dehghani et al., 2017
* Asaluyeh County, Iran	Suspended dust, urban dust	0.3-1.1 item m^{-3}	100 -1000 µm:	Fibres Granules	White-transparent: >70% blue-green: Yellow-orange Black	N/A	Fluorescence microscopy SEM/EDS	Abbasi et al., 2019
Dongguan , China	Atmospheric fallout (dry&wet deposition)	175-313 particles m^{-2} d^{-1} (natural fibers 73%; PP 9%, PE 14%)	majority of fibers to be 200–700 µm in length (200-4200 µm)	Fibers (80%) foams Fragments Films	Blue Red Transparent Grey	PE, PP, PS	Stereomicroscope µ-FTIR	Cai et al., 2017

Study area	Sample types	MP abundance	MP size	Shapes	Colours	Composition	Method	References
Shanghai, China	Suspended atmospheric microplastics	1.42 ± 1.42 items m^{-3} (maximum 4.18 items m^{-3})	23-500μm: >50% (23-5000 μm)	Fibers: 67% Fragment: 30% Granules: 3%	black, blue, red, transparent, brown, green, yellow, and grey	PET, PE, PES, PAN, PAA, and Rayon	Stereomicroscope μ-FT-IR analysis	Liu K et al., 2019a
Yantai, China	Atmospheric deposition	Fibers: 115-602 items m^{-2} d^{-1} Others: 40 items m^{-2} d^{-1}	<500 μm: 50% (100-300 μm dominant) followed by 0.5-1 mm	Fibers:95% Fragment Film Foam	N/A	N/A	Stereomicroscope μ-FT-IR analysis	Zhou et al., 2017
* 39 major cities in China	Indoor and outdoor dust	PET: 1550-120000 mg/kg (indoor) 212-9020 mg/kg (outdoor) PC:	N/A	Fibers dominant: 75% outdoor 85% indoor Granule	N/A	PET: >60% PC, Nylon, PE, PP, PMMA, PU, PEI, Alkyd	μ-FT-IR	Liu C et al., 2019

Study area	Sample types	MP abundance	MP size	Shapes	Colours	Composition	Method	References
		4.6 mg/kg (indoor) 2.0 mg/kg (outdoor)		Cellulose and Rayon: natural sources				
Pyrenees mountains, Europe	Atmospheric dry & wet deposition	249 fragments, 73 films and 44 fibres m^{-2} d^{-1}	predominant fiber lengths of 100–200 μm and 200–300 μm （10-5000 μm）	Fragments; 68% fibers films	N/A	PS, PE, PP, PVC, PET	Stereomicroscope μ-Raman	Allen et al., 2019
* Europe and Arctic	European snow Arctic snow (wet deposition)	190-154×10^3 items L^{-1} European snow 0-14.4 × 10^3 items L^{-1} Arctic snow	11-150 μm 11-250 μm more than 80% ≤ 25 μm (11-475 μm)	Fibers	N/A	Varnish Nitrile rubber PE Polyamide rubber	μ-Raman FTIR imaging	Bergmann et al., 2019

Study area	Sample types	MP abundance	MP size	Shapes	Colours	Composition	Method	References
* Helsinki, Finland	Urban snow (wet deposition)	700 items m^{-2} of melted snow (market place) 1400 (road side) 16600 (residential area)	0.3-4 mm	N/A	N/A	PE, PP	FTIR	Pikkarainen et al., 2019
* Italian Alps	Supraglacial debris	74.4 items kg^{-1} of sediments (dry weight)	N/A	N/A	Black 31% Blue 22% Red 17% Transparent 17% Light blue 9% Violet 4%	Polyester 39% PA 9% PE 9% PP 4% Unknown 39%	µ-FTIR	Ambrosini et al., 2019
Surabaya, Indonesia	Suspended atmospheric microplastics	132.75-174.97 items m^{-3}	<500 µm: 5% 500-1000 µm: ~13%	Fibers dominant,	NA	PE, PET, cellophane	FTIR	Asrin and Dipareza, 2019

Study area	Sample types	MP abundance	MP size	Shapes	Colours	Composition	Method	References
			1000-1500 µm: ~30% 1500-2000 µm: ~14% 2000-2500 µm: ~20% 2500-3000 µm: ~7% 3000-3500µm: ~2% 3500-4000µm: ~2% 4000-4500µm: ~3% 4500-5000 µm: ~4%	fragments, films, pellets				
* Nottingham, UK	Atmospheric wet and dry	0-31 fibres m^{-2} d^{-1}	38µm-5mm	fibres	NA	Acrylic, polyamide,	FTIR	Stantin et al. 2019

Study area	Sample types	MP abundance	MP size	Shapes	Colours	Composition	Method	References
	deposition, urban dust					polyester, polupropolene		
West Pacific Ocean (Open Ocean)	Suspended atmospheric microplastics	0-1.37 items m^{-3} Ave.: 0.06 items m^{-3}	More than 50% <500 µm (20 µm - 2 mm)	Fibers: 60% Fragment: 31% Granule: 8% Microbead	Black, blue, brown, green, grey, orange, pink, purple, red, transparent, white, yellow	PET 57% PE: 10% PE-PP: 6% PES, ALK, EP, PA, PAN, Phe, PMA, PP, PS, PVA, PVC	Stereomicroscope µ-FTIR	Liu K et al., 2019b
London UK	Atmospheric wet and dry deposition	12-925 items/ m^2/day Ave: 771 items/m^2/day	Fibres: 20-25µm dia., 400-500µm length Fragments: 25-350µm dia., ave. 164µm	Fibers: 92% Fragments: 8%	NA	Fibres: PAN 67%, PET 19%, PA 9% Fragments: PS, PP, PE, PET, PUR, PVC	FTIR	Wright et al. 2019

2.3.3 Components

The chemical composition is the most fundamental criterion for defining plastic pollution (*18*). Microplastics are also composed of a diverse suite of polymer types (*13*). A variety of polymers are synthesized and used for domestic and industrial purposes. The structure (backbone) of plastic polymers can define a plastic's physical and chemical properties (categorized to be thermoplastics and thermosets) (*12*). The greatest plastic demand and most highly produced polymer types are polypropylene (PP, 19.3%), low-density polyethylene (LDPE 17.5%), high-density polyethylene (HDPE, 12.3%), polyvinyl chloride (PVC, 10.2%), polyurethane (PUR,7.7%), polyethylene terephthalate (PET; also known as polyester, 7.4%), and polystyrene (PS, 6.6%) (*12*). Polymer composition in seawater reported from published literature indicates that PE is the dominant polymer, followed by PP and PS; while PE, PP, PS, and PES are major polymer types on beaches and subtidal sediments (*14*).

For the atmospheric microplastics, chemical composition varies over different regions (Figure 2). The main polymers in the coastal city of Yantai were PET in the case of most of the fibres, PVC in the case of some fibres and films, PE for the fragments, and PS for the foams (*49*). In Shanghai, synthetic compounds comprised 54% of the observed particles, of which PET, PE, PES, PAN, PAA, and rayon comprised 91% of the microplastics (*33*). In Dongguan city, microplastics of three different polymers (e.g., PE, PP, PS) were identified (*8*). Microplastics in dust deposition from Chinese major cities were mainly determined as PET and PC (*38*). In the Hamburg city of Germany, PE and ethylvinyl acetate (EVA) copolymers dominated in the atmospheric microplastics samples (48.8% and 22.0%, respectively) (Klein and Fischer, 2019). The predominant plastic found in the samples from remote area of Mountains is PS (as fragments), closely followed by PE (*11*). For the snow fallen out in Arctic, polymer types were found to vary extensively; varnish (acrylates), plasticized rubber and polyamides were among the most high identified microplastics. In contrast, in the European snow microplastics composition was primarily (67%) by polyimide, varnish, rubber, EVA, and PE (*73*). In the supraglacial debris of an Alpine glacier, most microplastic items were made of polyesters, followed by PA, PE, and PP (*31*). To date there is no clear correlation or explanation for the

variability or composition of polymer types in atmospheric samples. Further research is needed to establish if there is a predominant group of polymers occurring in atmospheric microplastic pollution and whether this polymer composition changes due to sample location and particle distance travelled.

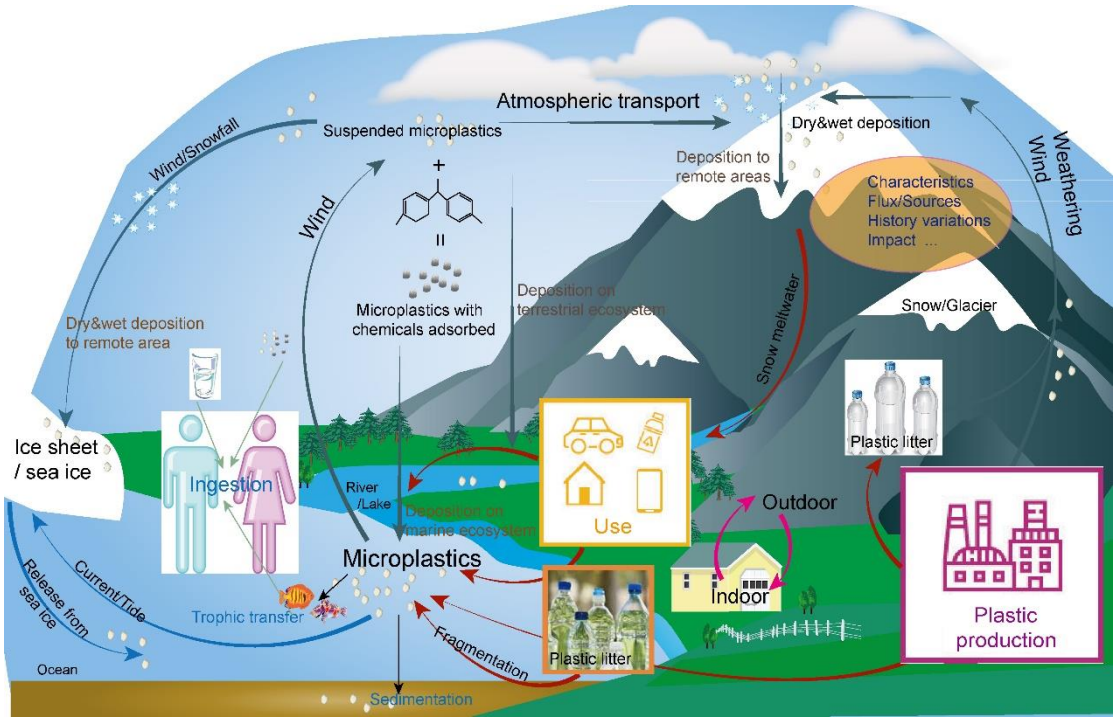

Figure 2. Conceptual model of atmospheric microplastics in the environment.

2.3.4 Comparison with microplastics from marine and terrestrial environments

From the above sections, we notice the characteristics of atmospheric microplastics vary widely among studies from the dry and/or wet depositions and sampling of airmasses. This is also true for microplastics in marine environment with a range from undetected to more than 100 000 items m^{-3} (*14*). Microplastic abundance tends to increase significantly with decreasing size (*90*). Meanwhile, the mean microplastic size reported in individual studies depends on the size range of the microplastic sampled and analysed. For example, in aquatic environments, mean size of microplastics ranges from one to a few millimetre for samples collected using nets with mesh size of 200-1000 μm; however, mean size of microplastics collected by using smaller net mesh size (50-63 μm) have shown a mean size of <700 μm (*14*, *90*). For atmospheric microplastics, particle

size tends to be much smaller. Fibres observed in indoor and outdoor air are mainly in the lower size range (50-80% between 100 and 500 µm) and to with only a small proportion being larger than 500µm (10-30% between 500 and 1000 µm or between 1 000 and 5 000 µm) (*43*). Fragments observed in the atmospheric deposition concentrated on the range of <100 µm (*11*, *32*)

Previous studies indicate that fibres and fragment are dominant shapes of microplastics in seawater, beach sediments, and freshwater (*14*, *90*, *91*). Such findings imply that secondary microplastics contribute to microplastic abundance more than primary plastics in the marine and freshwater environment. In the atmosphere, fibres and fragment are also the dominant shapes (Appendix 1). Fibres originate from fabric, for example, clothes and textiles (*8*, *11*, *92*). Fragments are thought to originate from disposable plastics via fragmentation (*11*, *14*). Textile fibres are an important source of indoor dust (*38*, *43*). PET is commonly used to produce polyester fibre, fabric, and cording for textiles (*93*), and this widespread use can help explain the high levels of PET MPs in indoor dust. As shown in Table 2 (and Appendix 1), the higher concentration of fibres in indoor air compared to those measured outdoors suggest that a large fraction of the fibres may be transferred to outdoors through the air exchange. This could contribute to atmospheric fallout and indoor atmospheric fibres and particles could also enter the aquatic systems through runoff.

Different polymer have different densities (*47*), which can affect the pathway of microplastics into the atmosphere. Less dense polymers, such as PE, PP, and expanded PS, are widespread in the water and atmospheric fallout. The variety of polymer types found in atmospheric samples published to date does not indicate a clear or obvious delineation between less and more dense polymer types. Conversely, other polymers with heavier densities (e.g. PS, PVC, PES) have also been observed in atmospheric deposition/air mass sampling. PS and PE are used in many single-use plastic items and in packaging material as indicated by a European Strategy for Plastic in a Circular Economy (*11*). The link or correlation between marine, terrestrial and atmospheric microplastic composition has not yet been considered in detail, and there is not yet sufficient terrestrial, freshwater or atmospheric microplastic research to provide indications on these interlinkages and source-pathways. While some studies appear to have

similar atmospheric microplastic deposition composition to previously published aquatic studies (e.g. Dongguan (*8*)) other studies show significantly different and variable composition (*11*, *32*, *73*).

Shapes and polymers of microplastics show different sorption of hydrophobic contaminants and can facilitate the transport of contaminants (*19*, *39*). In the aquatic or sediment environment, microplastics are always found as part of a mixture or diverse suite of chemicals (*13*).This indicates that microplastics can adsorb organic chemical and trace metals from the surrounding environment (*28*, *94*). Overall, hydrophobic compounds are attracted to the neutral areas on the microplastic surface, while hydrophilic or charged compounds are attracted to the negative areas on the microplastic surface with electrostatic interactions and media characteristics being most important (*39*). In European seabass, microplastics were found to influence the bioaccumulation of mercury (*36*). Currently, studies on aggregation, toxicity, sorption of contaminants for microplastics in the atmosphere are sparse. Substantial further research is needed to understand the scope of this issue.

2.4 Perspectives

2.4.1 Atmospheric transport of microplastics

Microplastic pollution appears ubiquitous in marine, freshwater, terrestrial and now atmospheric environmental compartments (*11*, *29*, *73*). These environments are interlinked, with a diverse network of source-pathway-sink connections which can influence the flux and retention of microplastics among such environmental matrices. In recent years, atmospheric transport of microplastics has been considered an important vector and that could lead to deposition of microplastics to land or aquatic environments (*11*, *35*, *73*). Such transportation strongly impacts the source-sink dynamics of plastic pollution in different ecosystems including transfer between terrestrial and marine environment (*21*, *95*). In Shanghai city and the west Pacific Ocean, a study based on characteristics of atmospheric microplastics suggests that marine microplastics may ultimately derive from terrestrial environments (*33*). Suspended atmospheric microplastics may be an importance source of microplastics pollution in the ocean, including the pollution caused by textile microfibres (*34*). Atmospheric transport plays a significant role

on the transport and potential environmental sinks for microplastics. The density and shape of microplastic particles will have important effects on their transport (*29*). However, little is known about the processes governing transport of microplastics within air (*11*, *43*). Specifically, it is not known to what extent atmospheric fallout contributes to aquatic and terrestrial contamination. There is a need to significantly more research is needed in this area, spatially, with regards to source-pathway-sink processes, transport parameters and relative to meteorological conditions.

Latest research show that atmospheric transport of microplastics can reach remote areas without any local source of plastics (*11*). Evidence of microplastics on an Alps and Tibetan glaciers has been observed (*31*, *35*). Microplastics transported by wind to high latitudes may be the cause of microplastics deposition on glaciers (Figure 2, Table 2). Microplastics in snowfall (and rainfall) may be another important way for microplastics occurrence in surface ocean and Arctic environments (*73*).

Measurement of atmospheric microplastic flux could help quantify the contributions of atmospheric microplastics to the marine or terrestrial ecosystems. However, microplastics flux from atmospheric deposition has not been widely studied at present. Glaciers in the cryosphere regions are ideal environments to accumulate pollutants from the atmosphere through dry deposition or snowfall. Due to its low temperature and remoteness from human activities, pollutant records in snow have been effectively used to calculate the flux from atmospheric deposition. Similar processes may also be effective in analysis of microplastics, one of the most ubiquitous pollutants released by anthropogenic activities. More importantly, accumulation of microplastic particles in ice cores will provide temporal variations, in a similar way to lacustrine archive microplastics (lake sediments) (*96*).

To date, only two atmospheric microplastic studies have attempted to examine the transport pathway or trajectory of these particles. The first attempt at analysing atmospheric microplastic transport was presented in Allen et al. (2019) where the particle transport was evidenced to be greater than 95km. This study used simplistic meteorological and particle settling velocity calculation and well-

known atmospheric Hybrid Single Particle Lagrangian Integrated Trajectory Model (HYSPLIT) to examine dynamic atmospheric transport. A further study by K. Liu et al., (2019b) has used HYSPLIT to consider the possible sources of atmospheric microplastic (airmass sampling) creating back trajectories relative to the sample period. Lagrangian atmospheric models such as HYSPLIT, LAGRANTO and FLEXPART are useful tools to consider where atmospheric particles and pollutants may have travelled from(*97*). They can be used to identify the potential source of an atmospheric pollutant and the atmospheric trajectory along which it may have travelled (distance, elevation, atmospheric mixing etc.). These models are well established and used of atmospheric modelling of pollutants, particles and gasses such as mercury, caesium and dust and have great potential for more in depth and detailed analysis of atmospheric microplastic transport. However, at present the parameters necessary to adequately describe and characterize atmospheric microplastics are unknown. The density, shape and size of atmospheric particles can be attained from field samples, but global, regional or land use specific generalizations are difficult. The entrainment potential, deposition and detention processes and potentials, atmospheric settling velocities with/without collation or cohesion of homo/heterogeneous atmospheric particles are all unknown. The efficiency of precipitation scavenging, influence of atmospheric microplastics in atmospheric ice nucleation and electrical charge of the particles on atmospheric transport is unknown and so un-parameterized (*80*, *97*, *98*). Atmospheric particle transport modelling is an important future focus of atmospheric microplastic transport research, with significant further research needs and challenges in definition and description of atmospheric microplastic transport dynamics.

It is widely considered that the oceans represent a sink for a large proportion of microplastics, with terrestrial and freshwater environments acting as important sources and pathways for microplastics to the sea (*99*). Atmospheric microplastics link the processes influencing flux and retention of microplastics in environment (*29*, *34*). The atmospheric transport for microplastics to remote areas and its potential global impact on contributions to microplastics in marine and terrestrial ecosystems is a challenge facing the development of the plastic source-pathway-sink model (*21*).

2.4.2 Risk estimation for human exposure

Microplastics present in the environment can be ingested by different types of organisms, including species widely used in the human diet (*25*, *100*, *101*). The recent findings of atmospheric microplastics highlight the broad spatiotemporal scales of the processes that influence the sources, fate, transport and effects of microplastics on the environment and its inhabitants, including humans (*21*). Epidemiologic studies indicated ambient atmospheric particles air pollution is linked to adverse respiratory and cardiovascular effects (*102*). Although the visually observed microplastic fibres are supposedly too large to be inhaled; there is an exposure may occur through dust ingestion, particularly for young children (*40*, *43*). Previous studies identified cellulosic and plastic fibres in human lungs (excised lung cancers and lung biopsies) (*40*, *103*) and for workers in plastic processing factories to demonstrate breathing and health problems (coughing, dyspnea, wheezing, occupational asthma (*104*). Microplastic particles (>100µm) have also been demonstrated as biopersistent and to pass the gastrointestinal tract epithelium (*40*). Human exposure of microplastics especially via dust ingestion can potentially be estimated based on the atmospheric microplastic concentration.

Simplistic modelling has estimated that approximately 7665 particles of microplastics are inhaled annually by people in Shanghai (East China) from outdoor environments (*33*). Meanwhile, indoor dust is a non-negligible source of human exposure to MPs, accounting for a geomean daily intake of 17 300 ng/kg-bw (average body weight) of PET microplastics in children of Chinese major cities (*38*). In Iran, it is estimated that a mean of 3223 and 1063 microplastic particles per year is ingested by children and adults, respectively (*9*). For context, the flocking area of a polyester microfibre plant may have airborne particles of 7mg/m^3, up 1,000,000 fibres/m^3 (*40*). Most of the inhaled microplastic fibres are potentially subjected to mucociliary clearance; however, some may persist in the lung causing localized biological responses, including inflammation, especially in individuals with compromised clearance mechanisms (*37*, *40*).

Microplastic is also a pollutant transport medium for other toxic elements such as DDT and hexachlorobenzene (*105*). The sorption of chemicals (e.g., PAHs,

mercury) to microplastics may become a threat to biota, when ingestion occurs or through leaching and/or desorption of adsorbed and plastic composite chemicals. Associated contaminants such as PAHs desorb and lead to genotoxicity while the plastic itself and its additives (dyes, plasticizers, PFAs, phthalates) lead to health effects including reproductive toxicity, carcinogenicity and mutagenicity (*37*, *40*, *106*, *107*). Microplastic bioaccumulation in the environment is in the early stages of research, with very little known in the marine, freshwater or terrestrial environments and no examination with relation to the atmospheric environment yet (*108*). It is known that phthalates and other plastic components can cause detrimental impacts on human health, as illustrated by past BPA studies (endocrine disruption) and DEHP research (modified gene expression, shortened gestation periods, lower birth weights)(*106*, *109–111*). There is also evidence of phthalates such as BPA in the atmosphere as aerosols in notable quantities (up to 17,4000pg m^{-3})(*112*). The effect of atmospheric microplastics, their chemical components and their adsorbed pollutants on human and ecosystem health is unknown, but the potential of micro and nano plastic to influence this is of concern (*40*, *113*). However, the interactions between microplastics with other organic pollutants and metals in the atmosphere, their impact on and interaction with the environment, humans and ecosystem health are virtually unstudied and need to be better understood.

2.5 Conclusions

Microplastics are now acknowledged as atmospheric pollutants and particulates. Recent studies have demonstrated the existence of microplastic in the atmosphere in urban, rural and remote atmosphere and as atmospheric deposition. As an atmospheric pollutant, there is significant potential for long-range transport and therefore influence on locations far from microplastic pollution sources.

Among the published studies, relative abundance of atmospheric microplastics reflects a wide range of characteristics and quantities across different regions. Fibres and fragments are the most frequently identified microplastic shapes in atmosphere. Conclusion on size distribution in these studies are difficult to draw due to the differences in targeted particle size. Because of its light-weight,

durability, and other intrinsic features, atmospheric microplastics can be transported to remote areas and deposited through dry or wet deposition. Wind, snowfall, and weathering play an important role on atmospheric microplastics from sources to ocean or land surfaces.

Current atmospheric microplastic research is in the early stages, and therefore suffers from insufficient comparable data on abundance and characterization. This is especially the case in remote areas and concerning microplastic composition due to the non-standardized operation protocols for microplastic sampling and detection used to date. Standardized methods for sampling and measurement of atmospheric microplastics will allow reproducibility and comparability of results and will lead to the quality data to necessary conduct risk assessments. Worldwide research on spatial and temporal variations of atmospheric microplastics depositions needs to be further enhanced. Studies are also needed to better understand the interaction between atmospheric microplastics and other chemicals, ecosystems and human exposure.

3 Atmospheric transport and deposition of microplastics in a remote mountain catchment

Abstract

Plastic litter is an ever-increasing global issue and one of this generation's key environmental challenges. Microplastics have reached oceans via river transport on a global scale, but outside two mega-cities, Paris (France) and Dongguan (China), there is a lack of information on atmospheric microplastic deposition or transport. Here we present the observations of atmospheric microplastic deposition in a remote, pristine, mountain catchment (French Pyrenees). We analyse five months of samples representing atmospheric wet and dry deposition and identify fibres up to ~750 µm long and fragments ≤300µm as microplastics. We document relative daily counts of 249 fragments, 73 films and 44 fibres per square metre depositing on the catchment. Air mass trajectory analysis shows microplastic transport through the atmosphere over a distance of at least 95km. We suggest that microplastics can reach and affect remote, sparsely inhabited areas through atmospheric transport.

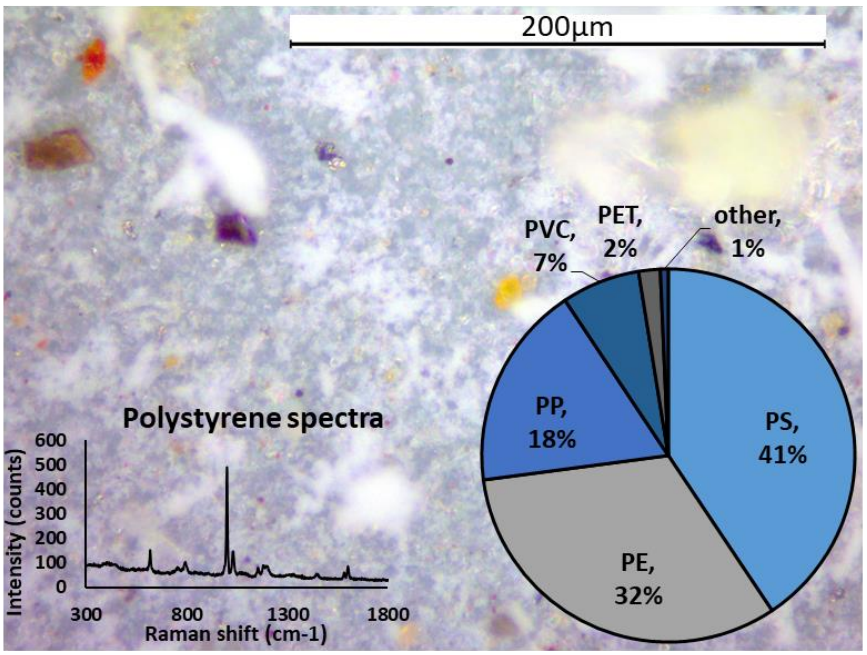

3.1 Introduction

Plastic industry experts estimate global manufacture of 335 million tonnes (Mt) of plastic in 2016(*114*). Of the 335Mt worldwide, 60Mt was produced in Europe, of which ~40% is packaging (short-term or single use). However, in 2016 27.1Mt was recovered as waste for recycling, energy recovery (burning) or placed in landfill(*115*, *116*). Some plastics remain in service for up to 50 years, which helps explain some of the 32.9Mt discrepancy in the plastics mass balance. While plastic is recognised to biodegrade very slowly, degradation to micro (5mm-1µm) and nanoplastics (<1µm) does occur(*117*, *118*). Thus, plastic waste can start as macroplastic pieces (bottles, packaging etc.) and over time degrades to microplastic (MP) particles or smaller. Mattson et al.(*119*) estimate 10% of created plastics enter the ocean annually, accounting for a portion of the 32.9Mt plastics waste. However, this highlights questions on the fate of the remaining plastic. Large amounts of macroplastic waste would be noticed in the terrestrial environment, but if this waste was degraded to micro-sized particles it could evade easy detection. Recent studies have identified MP on alpine river floodplains(*120*) and lake sediment(*121*) illustrating terrestrial MP occurrence, and in mega-cites as aerosol pollution(*8*, *37*, *43*, *79*). The recent research on atmospheric fallout in Paris (France) (*37*, *43*, *79*) and Dongguan (China)(*8*) suggests atmospheric MP conveyance and corresponding deposition. Soil/sediment/lake samples provide an informative terrain-based analysis of plastic(*10*, *120*, *122–124*) occurrence however determination of atmospheric MP beyond intra-city deposition requires source specific and remote atmospheric sampling.

This research provides unequivocal evidence of direct atmospheric fallout of MP in a remote area of the Pyrenees Mountains. The Pyrenees mountainous regions are anecdotally considered pristine wilderness due to limited development, difficulty of human access and distance from major populations or industrial centres. The study site is located at the Bernadouze meteorological station(*125*), 42°48'14.6"N 1°25'06.8"E and 1425m a.s.l., within the Vicdessos catchment and Mid-Pyrenees mountains in south-west of France (Appendix 2 - Detailed site description). The local vicinity is sparsely populated, without industrial, commercial or large agricultural activities and is primarily used for recreational

activities (hiking, skiing, environmental education and scientific research). The closest local residential area is a village ~6km to the south-east (Vicdessos village, population ~540 (*126*)) with a moderately sized town located ~25km to the north-east (Foix, population ~9,720 (*126*)).

The presented research considers five months of atmospheric deposition collected from the field site. Five samples of total atmospheric deposition (wet and dry), from two separate monitoring devices, were analysed to identify if MPs are present in the remote mountain catchment. Regular (monthly) sampling campaigns were proposed, however weather conditions restricted site access resulting in irregular monitoring intervals (Methodology, Appendix 3). The objective in observing the case study atmospheric deposition was to identify (1) if MPs are present in atmospheric fallout in this remote mountainous location and (2) if MP are present, in what quantity, size, shape and plastic type do they occur? The purpose of this study was to take steps towards discovering the extent of MP atmospheric deposition in remote terrestrial locations.

3.2 Methods

3.2.1 Field sampling and data collation

The field meteorology and sample station was visited five times over the five month monitoring period to acquire samples from the atmospheric fallout collectors. The sampling period extended from November 2017 to March 2018. Ideally, samples would be collected every four weeks, but because climatic conditions restricted access, the sample periods were inconsistent (sample durations of 12, 19, 34, 41 and 34 days, respectively, for samples from November to March). Field blanks were also collected. During this period two independent atmospheric deposition collectors were active at the site. The first collector was a Palmex Rain Sampler with a sampling area of 0.014 m^2 (diameter of 135 mm) (constructed of ultraviolet-resistant polyvinyl chloride (PVC) and stainless steel). The second collector installed and sampled from was a NILU Particulate Fallout Collector (p.no. 9721) with a sampling area of 0.03 m^2 (diameter 200 mm) (constructed of high-density PE and stainless steel). Both collectors were open to the atmosphere for the total period of sampling and therefore all the samples are a combination of dry and wet atmospheric fallout. The samples collected from

each atmospheric fallout collector were kept separate (both during the field sampling and the laboratory sample preparation) and thus provide a duplicate sample data set for each monitoring period.

During the collection of the sample material (and at all times when near the sampler), all the personnel were careful to remain downwind of the sampler, samples exposure time was kept to a minimum and, whenever possible, cotton clothing was worn to minimize contamination. The total sample volume was collected (without subsampling). Samples from the Palmex collector were decanted into clean glass 2 litre bottles in the field, capped and transported back to the laboratory. The field sample container from the NILU collector was capped and transported back to the laboratory where samples were decanted into clean glass 2 litre bottles in the laboratory 'clean room'. All the decanted samples were stored in a dark walk-in refrigerator (at 4 °C) until filtration and sample processing commenced.

In conjunction with physical atmospheric samples, wind, humidity, temperature, rainfall and snowfall data were recorded at the monitoring site by the CESBIO (Centre d'Etudes Spatiales de la Biosphere) meteorological gauging station (*125*). This data set provided local microclimate information at a 30 minute timestep.

3.2.2 Sample processing preparation for MP analysis

All samples (2 × 5 field samples) contained varying amounts of organic and inorganic matter, which include biofilm and dust. To aid the analysis, it is necessary to remove as much of the biogenic and non-plastic inorganic material as possible without damaging or losing potential plastic particles. It is also necessary to remove biofilm from the plastic prior to micro-Raman spectroscopy to ensure an effective analysis (spectra clarity). To this end, protocols were selected with the minimum physical manipulation, least number of steps and the least-aggressive digestion chemicals and temperatures possible to achieve the desired results. Sample material was filtered through a 0.45 µm polytetrafluoroethylene 47 mm diameter membrane (Whatman) using borosilicate laboratory glass filtration equipment and then vacuum dried with ethanol (96 vol%). Filters were examined and photographed under a stereomicroscope

Olympus SZX10 with an Olympus SC30 camera attachment (and visually checked using an Axiostar Plus (×50) microscope) to record as much detail of the potential plastic particles as possible prior to digestion. The filter was then rinsed into borosilicate glass test tubes with 10 ml of hydrogen peroxide (H_2O_2) solution 30%, capped with glass stoppers and placed in a static heat block (Thermomix) at 55 °C for 7 d (no agitation). On day 8 a further 5 ml of H_2O_2 solution 30% w/w was added to each sample and the sample was left for a further 7 d. H_2O_2 was chosen as the digestion medium because it was used in previous studies (*120*, *127–129*), but given the low usage temperature of some plastics (PS = 70 °C and PVC = 60 °C) (*130*) and the risk of glassing or melting at elevated temperatures, the temperature was purposefully maintained below 60 °C to ensure the methodology did not affect the characterization or result in the loss of material.

On day 14 the sample was filtered onto a 0.45 µm polytetrafluoroethylene 47 mm diameter filter membrane, rinsed with 250 ml MilliQ (18 MΩ cm) water and dried with ethanol (96 vol%). The filtered material was then rinsed into density separation glassware with zinc chloride (Technipur $ZnCl_2$) at a 1.6 g ml^{-1} density. This was gently agitated (60 revolutions per minute) for 7 d at room temperature (Edmund Buhler KS-15 shaker). the settled material was drained away with the sediment removal valve and the remaining sample filtered onto 0.2 µm, 25 mm diameter aluminium oxide filters (Anodisc 25). Glassware was triple rinsed onto the filter with a pH 4 buffer. The filter was then rinsed with 250 ml MilliQ water and vacuum dried with ethanol. The resulting filter was then examined and photographed again to look for changes in either the number of particles or particle character. Although it is difficult to quantify particles pre-digestion (due to excessive organic/inorganic material) many of the particles photographed previously were identifiable and any visible change in the material was noted, and thus we are confident that the protocols were sufficiently gentle to ensure minimal losses of material.

3.2.3 Blank test

Two sets of laboratory blanks were created in support of this sample preparation process. Two MilliQ samples of 1 litre, instead of field sample material, were put through the full digestion and zinc chloride separation process, which resulted in

two full-process blanks (following in detail the process outlined for the sample preparation).

A further two laboratory blanks (MilliQ water samples) underwent the digestion process, but were filtered onto the Anodisc 25 filters without zinc chloride separation. The purpose of these blanks was to help quantify the possible MP contamination caused by the sampling and sample preparation process.

Field blanks were also collected from each collector. Sample collection containers (glass) were taken out on site, connected to and opened at the sample location and then returned to the laboratory. These 'empty' glass containers were then thoroughly rinsed with MilliQ water and the resulting water processed without the zinc chloride separation, following the preparation described above.

The blank test resulted in a total of six blank samples, two from the complete preparation and $ZnCl_2$ process and four without $ZnCl_2$ separation. The blank filters identified, on average, 3 ± 1 fibres, 1 ± 1 film and 8 ± 1 fragments per filter.

3.2.4 Visual and ImageJ/Fiji particle inspection and count

All filters were visually inspected under a stereo microscope for MP particles using the identification criteria published by Hidalgo-Ruz et al.(*47*), Löder and Gerdts (*131*), and Norén (*132*). Noted that to use visual identification alone is not recommended for MP <500 µm, and so a second technique (Fourier transform infrared and Raman spectroscopy) is recommended to confirm small particles (*47*, *131–133*). Plastic particulates are visually identified by their shape and colour. Plastics must have no biogenic (cellular) structure; fibres are expected to have a relatively even or consistent thickness along the fibre length and illustrate three dimensional bending; fragments and films are expected to have relatively homogeneous colouring and illustrate a level of transparency or clarity (*131*, *132*). Aged plastic, such as expected in environmental samples, is described by Hidalgo-Ruz et al.(*47*) to present embrittled and weathered surfaces, and to have irregular shapes with broken and sharp edges. Weathered plastics may also show pitting. Colour is also a plastic identifier (*47*, *131*) and ranges from transparent and variations of white to bright orange, blues, greens and purples through to black. It is noted that biogenic material becomes bleached during the

sample preparation process (H_2O_2 digestion) that makes plastic particulates with colour highly visible and differentiated from residual (postdigestion) biogenic material.

An initial, indicative fragment, fibre and film count was visually undertaken for each sample using an Olympus SZX10 stereomicroscope. Three locations of 13 mm^2 were randomly selected and investigated on each filter (two filters per sample, with random selection to minimize bias) (*134*). After the visual identification methodology, a count of plastic fragments, fibres and films was undertaken (n = 6 inspected areas for each sample, with a total of 254 MPs identified). The identification was conservative with a focus on obvious coloured particulates, which resulted in a possible overall under-estimation due to the limited count or testing of white and non-transparent materials.

All the filters were then photographed using a Leica DM6000M confocal microscope with a Marzhauser Scan 130 × 85 4 mm *X*–*Y* motorized stage. Photographs were manually focused for each frame using a ×10 lens. Filters were photographed using the automated mosaic software (Leica proprietary software) and automatically stitched to provide a multistep mosaic image for each filter. The visual count was repeated on the photographs and completed using the software ImageJ. Three 13 mm^2 photographed areas of each filter were imported into ImageJ. Particle counts were undertaken using the protocol defined and used by Erni-Cassola et al.(*127*) (ImageJ code provided in the supplementary material of Erni-Cassola et al.(*127*)). A second count was undertaken following the same method using a larger area (6 × 58 mm^2) to provide a visual/ImageJ MP count for 50% of the Anodisc 25 filter surface. All the identified particles (n = 1,147) were sized using ImageJ (as completed in Isobe et al.(*90*) and Imhof et al.(*135*)) to provide a length, width and area appropriate for PSD analysis.

3.2.5 Raman set-up and analysis

Confirmation of the presence and type of plastic was achieved by a micro-Raman (Horiba Scientific Xplora Plus, 50–3,200 cm^{-1} with a 1.5 cm^{-1} resolution and confocal imaging accuracy of 0.5 µm) confocal microscope with a motorized *X*–*Y* stage. Micro-Raman spectroscopy was used in previous studies to confirm visual and Nile Red fluorescence-assisted MP quantification in environmental

samples (*59*, *127*, *136–138*) and has been shown to be effective in MP characterization down to 1 µm (*60*). Three areas of each filter (6 × 13 mm^2) were randomly selected and analysed for the total plastic presence using the 785 nm laser (spatial resolution of 1 µm) and 200–2,000 cm^{-1} Raman shift range. Spectra were collected using an acquisition time of 15 s and ten accumulations at a maximum of 25% power (filter) (general settings: 1,200 gratings mm^{-1} with a 50 µm slit, modified to achieve effective spectra results as necessary during the analysis). Laser power settings were tested on plastic particles to establish the strength necessary for effective spectra imaging with the minimal particulate damage. A laser power of 25% resulted in no visible damage to the plastics and an acceptable spectra delineation. Laser powers of 50% and 100% resulted in damage (burning or melting) of the plastic, as shown in Appendix 4.

Each suspected plastic particle was analysed individually, which resulted in a data set of Raman shift spectra (n = 245 particulates). Each potential identified MP was analysed twice (at two unique locations on the particle) to confirm the Raman spectra. Where the spectra were unclear or not definitive, a third analysis was undertaken. Samples that illustrated three unclear spectra were defined as ‘not plastic’. The blank filters were tested to quantify the level of contamination (through sample processing and analysis). A new Anodisc 25 filter was also analysed to confirm the background filter spectra. The micro-Raman spectral analysis provided confirmation of the visual identification, which supports the extrapolation of visual counts to consider spatial and temporal trends.

3.2.6 Raman spectra analysis

Open source Spectragryph software and databases (*139*) were used to analyse the micro-Raman spectral results. An individual evaluation of each spectrum was completed, similar to methods of spectral analysis followed in Lenz et al. (*136*), Khashaba et al. (*140*) and Ševčík and Mácová (*141*) in conjunction with Lagaron et al. (*142*), to provide a clear definition of the chemical and bond spectra peaks.

3.2.7 Statistical analysis

Visual and ImageJ MP counts of all the filters were confirmed using micro-Raman spectrometry (11% of the filters were analysed using micro-Raman and 50% of the filters were inspected visually and with ImageJ). The micro-Raman confirmed count of MP mm^{-2} was extrapolated to provide an indication of the quantity of MPs per filter and therefore per sample. It is acknowledged that extrapolation from subsampled filters does not provide a definitive MP count and ideally all MP particulates would be counted and confirmed with micro-Raman analysis. Due to analysis constraints, a complete filter analysis was not possible.

The calculation of MP m^{-2} d^{-1} was calculated through a simple sum of sample area MP counts, scaling using known filter and collector areas and known monitoring period durations. The calculations used the following simple

$$\bar{X} = \frac{(\sum X_{1-n})}{n}$$

$\bar{X}$ = the average MP count for a sample area (13mm^2) Eqn. 1

$X_{1, 2, 3}$ = the MP count for a sample area 1, 2, 3 etc. (sample area = 13mm^2)

n = sample area number (6 sample areas were investigated for each sample period)

$$\mu P = \left(\bar{X} \times \frac{Y}{y}\right) - \varepsilon$$

μP = total MP count per filter Eqn. 2

y = sample area (13mm^2 or 0.000013m^2)

Y = total filter area (346 mm^2 or 0.0003m^2)

ε = sampling error, the number of MP particulates found on the blank samples

$$MP = \left(\mu P \times \frac{1}{a}\right) / d$$

MP = MP count per m^2 / day Eqn. 3

a = sample area of the atmospheric collector (m^2)

d = duration of the sampling period (days)

The quantity of MPs per filter is accepted to be representative of the atmospheric deposition for the monitoring period relative to the collection area (Palmex collector = 0.014 m^2, NILU collector = 0.03 m^2). The provision of MP quantity per square metre has been previously published and accepted as a method that supports the comparison of the results of multiple studies (*121*). Therefore, the results per monitoring period were normalized for time period of 1 d (for comparison with Dris et al. (*79*) and Cai et al. (*8*)) and a 1 m^2 area using the known collector surface areas. The two collectors provide replicate samples for each sample period and therefore were treated as such. Thus, two independent samples were collected for each sample period, which provided two Anodisc 25 filters, with a total of six randomly selected areas analysed for MPs and resulted in n = 6 per monitoring period.

Statistical analysis of the MP counts and characteristics were purposefully kept to a minimum due to the data set duration (five monitoring periods) and the constraints of a single site case study (it is not considered appropriate to generalize from a single case study, so the study is presented as a first indication and presentation of remote MP presence only). Simple correlation analysis between the particle counts and meteorological data was completed using R Studio (R version 3.4.1) software and standard significance (P value), and Pearson and Spearman correlation tests appropriate to the data (CRAN packages hydroGOF, Hmisc, Performance Analytics and subsidiaries) were used.

3.2.8 Bias

Use of a non-automated system in particle counting and analysis induces a level of human bias in the results. To reduce the potential human bias in the results due to the lack of automation, random sampling was employed for all filter counting and micro-Raman analysis site selection. MP visual, ImageJ and micro-Raman analysis was undertaken in triplicate on all filters to further limit bias and uncertainty in the results. MP identification was completed following an identification protocol that was consistently employed on all the areas analysed. The identification protocol was conservative; any particles that did not meet the visual identification protocol as described by Hidalgo-Ruz et al.(*47*)

and Norén (*132*) and/or did not provide a clear Raman plastic signature were discounted from the analysis to limit misidentification and bias.

3.2.9 Local transport trajectory and source area assessment

The recorded wind, rain and snow meteorological data were used to support a local MP transport assessment and to help consider potential source and trajectories of MP particles relative to the field site. The simple numerical assessment of distance and transport duration of MP particles relative to rainfall events, snowfall events and wind occurrences (events) were calculated using the known field site elevation, upper elevation of MP entrainment (*143*), wind speed and assumed settling velocity (*144*) (based on a 25 µm dust particle). Once elevated, it was assumed that no further meteorological updraft or conveyance assistance (other than the recorded horizontal wind speed and direction) influenced the MP (to provide a simplified assessment of possible MP transport):

$$distance = back - trajectory\ duration\ x\ wind\ direction$$

distance = potential horizontal trajectory of MP (m) Eqn. 4

back-trajectory duration = the duration MP is airborne (sec); calculated as maximum elevation (600m a.g.l)(*143*)/ settling velocity (0.1 m/s)(*144*)

wind speed = maximum recorded wind speed (at the meteorological station) during each rain, snow or wind event (m/s)

The wind directions recorded for the rain, snow and wind events were used in conjunction with the calculated horizontal transport distances to create event specific wind rose maps to spatially illustrate the local MP trajectories. It is acknowledged that this is a highly simplified assessment of the potential horizontal transport trajectories and does not take into account the complex atmospheric dynamics of mountain terrain or atmospheric mixing. However, it does provide a first simplified assessment of local MP transport.

3.2.10 HYSPLIT4 analysis

The open source modelling software HYSPLIT4(*145*, *146*) was used to model the back trajectory of air parcel movement from the field site during the five

monitoring periods. HYSPLIT4 was used to download and model global wind and/atmospheric meteorology data provided by the National Oceanic and Atmospheric Administration (Global Data Assimilation System data) (similarly used in Su et al.(*147*), Ashrafi et al.(*148*) and Reche et al.(*149*)). Each rainfall (n = 165), snowfall (n = 186) and wind event >2 m s^{-1} (n = 197) was individually modelled with the back-trajectory duration defined as in equation (4). The multiple individual trajectories were then collated to create a frequency chart of trajectory potentials across the local area. The source point (deposition location in a back trajectory model) was set to 43° N 1° E and 100 m a.g.l.

3.3 MP particles in the remote mountain catchment

MP fragments, fibres and films were found, and confirmed (through visual microscopy inspection and µRaman analysis (*60*)) in all atmospheric deposition samples collected from the field site. This illustrates that for this location there is an atmospheric MP presence. The atmospheric MP deposition captured in the collectors are presented in Figure 3.

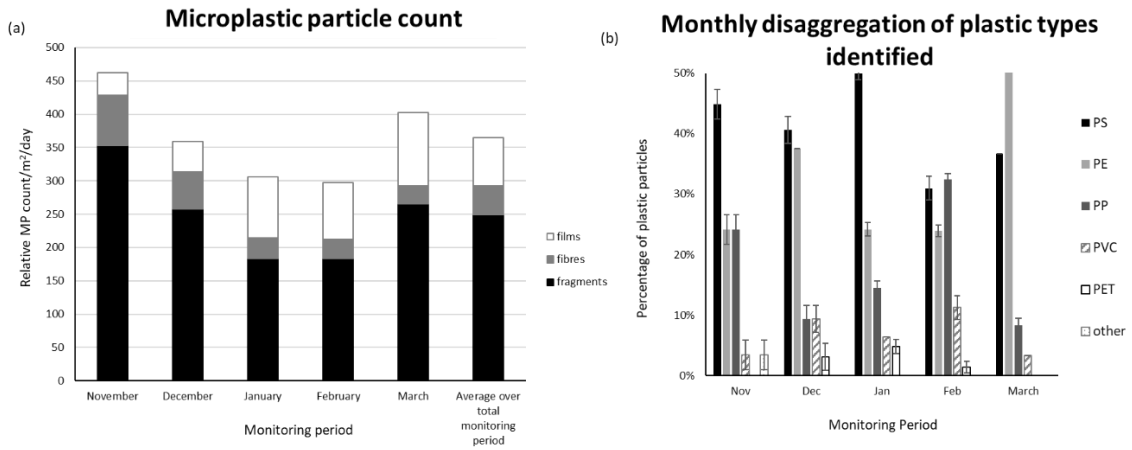

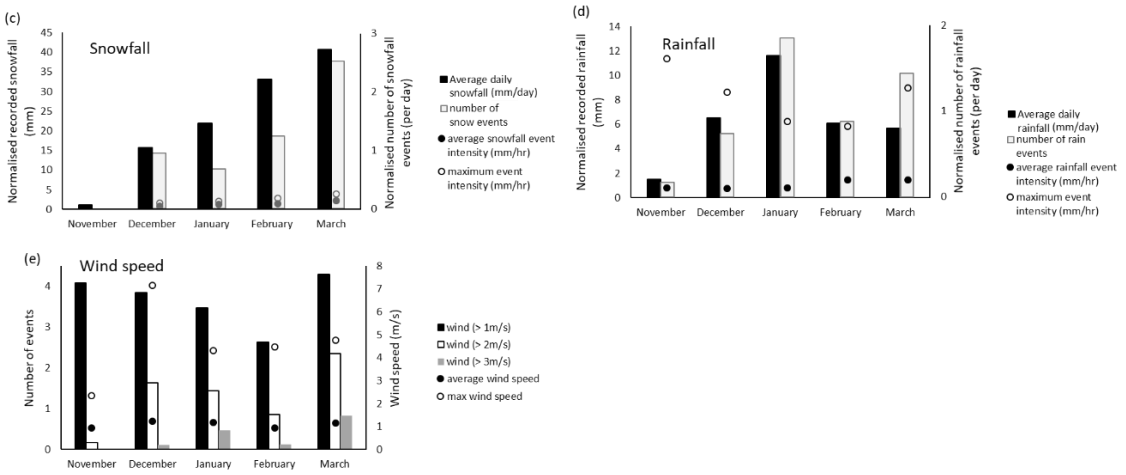

Figure 3. MP occurrence, MP type, recorded local rain and snow fall for the monitored period, wind speed and wind events. See Appendix 5 for comment on the fragment, fibre and film ratio. The types of plastics found in the atmospheric fallout derived from Raman spectroscopy analysis, SpectraGryph© spectral analysis software and libraries(*59*, *135–138*). The plastic types are presented as abbreviations: PS (polystyrene); PE (polyethylene); PP (polypropylene); PVC (polyvinyl chloride); PET (polyethylene terephthalate); other (uncharacterised).

Details of local meteorological conditions recorded at the sampling site are provided in Appendix 3 in conjunction with normalised MP counts (MP/m^2/day) per day. The meteorological record illustrates lower relative precipitation and fewer storms (rain or snow) in November compared to the following months. The relative snowfall increased over the monitoring period while rainfall was greatest in the January. Monthly average wind speed fluctuated around 1.1(±0.6) m/s with a maximum recorded wind speed of 7.1m/s in December. December-March illustrate wind speeds >4m/s and the greatest relative number of wind events (>2m/s and >3m/s) occurred in March. The number of >1m/s events were greatest in November and March, declining to the lowest frequency in February.

Field sample MP counts illustrate an average daily particle deposition of 365/m^2/day (±69, standard deviation). Sample MP counts were normalised to represent daily atmospheric deposition (MP/m^2/day) as site access limitations resulted in inconsistent monitoring durations (November extended 12 days, December 19 days, January and March 34 days, February 41 days).

Both rainfall and snowfall show moderate to strong significant correlations with MP count in the original dataset ($r \geq 0.8$, $p < 0.05$) and to the monitoring duration (days) (Supplementary Note 2). The normalised dataset presents a positive correlation to the frequency of wind speeds >1m/s (light air-strong wind movement) ($r>0.8$, $p<0.05$) suggesting MP transport and deposition may be influenced by wind movement. The maximum rainfall intensity also presents a strong positive correlation ($r>0.9$, $p <0.05$) suggesting that individual events and the intensity of events may influence atmospheric MP deposition (scavenging)(*150*). While it is acknowledged that the dataset is limited, the number of snowfall events also shows a positive correlation with normalised MP deposition ($r\geq0.6$, $p<0.05$). The duration (average and maximum) of both rainfall and snowfall events illustrate negative correlations with MP deposition ($r\leq-0.6$) suggesting event occurrence and intensity rather than duration may positively influence MP deposition(*30*, *151*). Despite long durations (≤41 days) represented by the samples, this preliminary dataset suggests that rain, snow and wind events may be drivers in MP deposition at this site. This supports the suggestion by Dris et al.(*43*) that precipitation events may be a positive driver in atmospheric MP fallout.

The samples collected for the January – March monitoring period contained a visible quantity of orange quartz-like fine dust. This dust presented size (d50 ~8µm), colour and indicative chemical signature descriptive of Saharan dust (*152*, *153*) (further details in Appendix 6). The fine dust, and other particulate matter potentially including some MP particles, are possibly Saharan, North Africa or Iberic sourced material (or potentially sourced along this trajectory)(*154*). For example, long-range transport of dust has been shown by van der Does et al.(*98*) findings of ultra-giant particles (<400µm) traveling trans-oceanic up to 3,500km. The distance MP can travel is currently unknown and further event–based research is needed to identify source and transport vectors of atmospheric MP particles.

3.4 Characteristics of MP particles

Characterisation was completed following the identification guide presented by Hidalgo-Ruz et al. and Noren et al.(*47*, *132*) in conjunction with µRaman analysis.

MP particle size or length was defined using the particle characterisation and count functions in ImageJ/FIJI (*155*), following the method presented by Erni-Cassola et al.(*127*). The overall particle size for MP particles are presented in Figure 4, with individual monitoring period sample fragment sizes illustrated in Figure 4b.

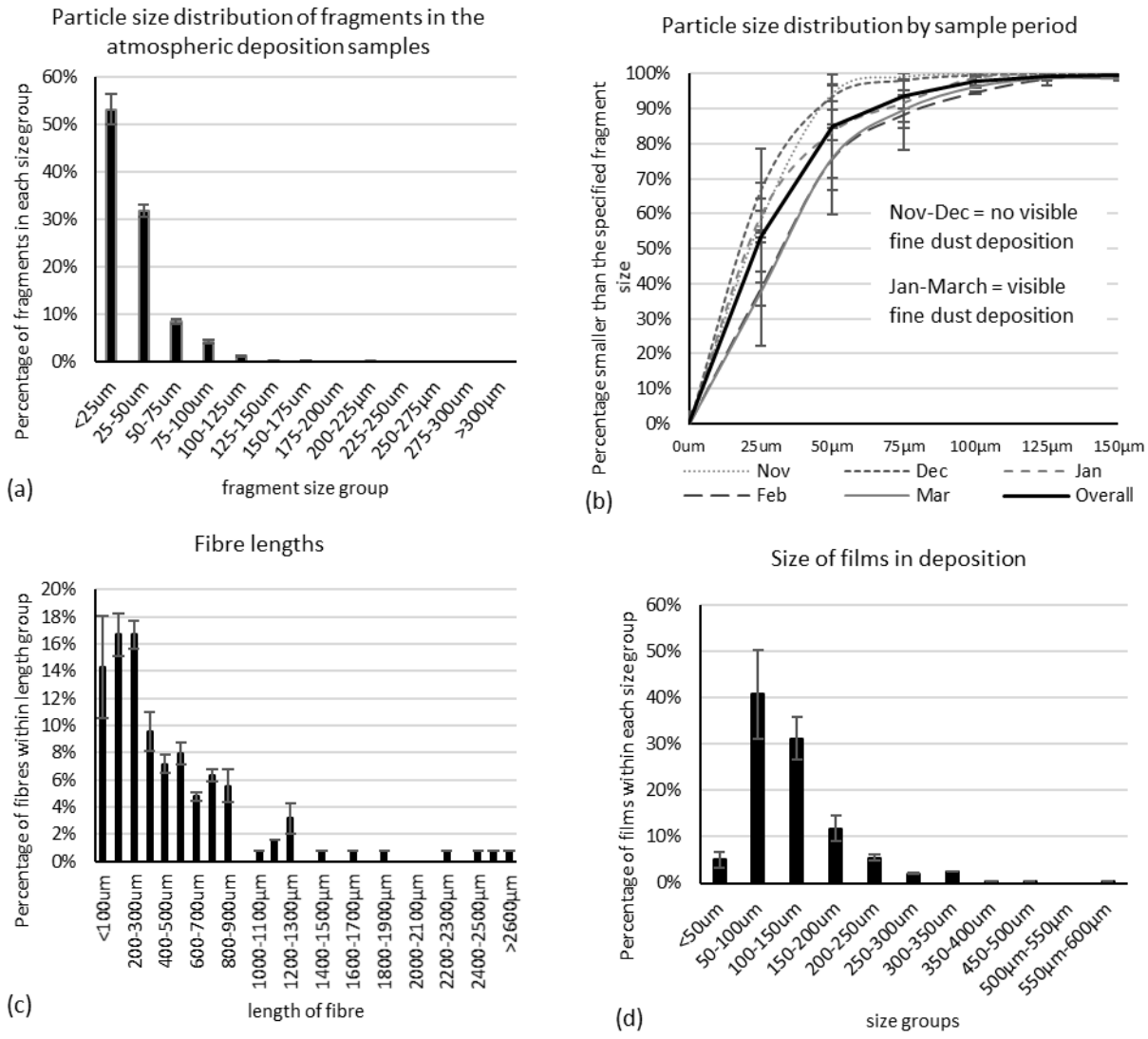

Figure 4. Deposited MP characterisation. (a) and (b) illustrate the particle size distribution for the MP particles identified in the monitoring period. (c) illustrates the range and predominant fibre lengths. (d) illustrates the average diameter of films collect.

The majority of environmental MP studies that have considered particle size distribution (PSD) illustrate an increasing trend in the number of finer fragments (significantly greater number of MP fragments with smaller particle size)(*8*, *37*,

156). The remote atmospheric deposition samples illustrate the majority of identified MP fragments to fall ≤50µm and the overall fragment size trend to follow previous MP particle size trends. When considered relative to the monitoring period (Figure 4b) there is a slight shift in PSD curve that appears to correspond to the fine dust deposition. Samples with no visible quantity of fine dust (November, December) show a greater quantity of smaller fragments. The fine dust laden samples show a small increase in primary fragment size (February-March). It is noted that for the fine dust sample periods there are a greater number of elevated wind periods (wind events >2m/s and greater), higher maximum recorded wind speeds and interspersed periods of calm (wind speed <0.5m/s) that may assist in the conveyance and deposition of the MP fragments.

The length of plastic fibres found in the atmospheric fallout samples (Figure 4c) suggests the predominant fibre lengths to be 100-200µm and 200-300µm. Cai et al.(*8*) found the majority of fibres in Dongguan to be 200-700µm in length with fibres of ≥4200µm (longest fibre), while Dris et al.(*43*, *79*) primarily found fibres of 200-600µm, with the longest recorded fibre ~5000µm. When the scale for fibre length analysis is modified to fit previous studies, the Pyrenees site fibre lengths fall predominantly between 200-700µm (47%) (Cai et al.(*8*) present ~30% in this predominant category) and 50-200µm (30%) (Dris et al.(*43*, *79*) illustrate a higher predominant fibre length of 400-600µm, ~23%). The longest fibre identified as a plastic fibre in this mountain field study was 3000µm. Film size has not specifically been evaluated in previous atmospheric MP analysis so limited comparative information is currently available. Films can be very thin, flat and therefore provide a greater surface area for atmospheric conveyance relative to a fragment of the same mass (Figure 4a and 2d). Within this mountain field study, the predominant film diameter was 50-200µm, larger than the predominant fragment size.

Raman spectroscopic analysis provides a verification of fragments, fibres and films as plastic(*156*) and characterisation of plastic type (Figure 3). The predominant plastic found in the samples is polystyrene (PS) (as fragments), closely followed by polyethylene (PE). PS and PE are used in many single use plastic items and in packaging material. Approximately 40% of plastic demand is for plastic packaging and PS or PE products(*157*). PS and PE are recyclable products, however the European recycling rate is currently ~31% overall (all

plastics) and ~41% for plastic packaging (2016(*157*)) with 3.4Mt of plastic packaging disposed in EU landfill. PE has a low density compared to other plastics, 0.92-0.97g/cm(*47*) and is a common film plastic (including plastic bags)(*158*). PS is a common packaging material having thermal insulating features and the ability to provide both strong and light weight plastic products. PS has a higher density than PE, 0.96-1.1g/cm^{3,}(*47*) however it is often used in a foam form for packaging, insulation and protection, resulting is a significantly lowered density. Polypropylene (PP) comprises 18% of the identified plastic particles (fibres primarily PP and PET). PP is used in packaging, textiles and re-usable products. It is the least dense of all plastics (0.9-0.91g/cm^3)(*47*) and due to its use in textile industry is constructed as fibres as well as objects or films.

The composition of plastic fallout varies over the monitoring period. Initial correlation analysis does not indicate any strong, significant correlations between plastic type and recorded meteorology (rainfall, snowfall, wind speed or events). The complexity of the plastic composition may be due to the source of plastic particles (and therefore wind direction, wind strength), the occurrence of storm events and the duration of calm days relative to event occurrence. The initial consideration of atmospheric MP fallout to meteorological conditions does not suggest a simple meteorological mechanism driving specific or preferential plastic deposition at this field site but does illustrate PS, PE and PP to be the three greatest contributors to the atmospheric fallout at this location.

3.5 Remote MP deposition compared to mega-city MP

The MP deposition recorded at this field site equates to an average daily MP deposition of 365/m^2/day (±69, particles ≥ 5µm). Previous atmospheric fallout monitoring(*8*, *79*) undertaken in high density urban areas identified daily fallout of 110(±96) and 53(±38) particles/m^2/day (Paris)(*43*, *159*) and 228(±43) particles/m^2/day (36 MP particles/m^2/day confirmed) (Dongguan)(*8*). Both the Paris and Dongguan studies counted and analysed particles ≥100µm, ≥50 µm and ≥200µm respectively. If only ≥200µm particles are counted in the remote mountain field samples, this equates to 40(±20) particles/m^2/day, 70% as fibres. The Pyrenees field site MP deposition is comparable to the reported mega-city

and suburban atmospheric MP deposition despite the remote and mountainous location of notable distance from urban city development or infrastructure.

Both the Paris and Dongguan studies primarily focused on MP fibres. If only fibres are considered, the relative daily MP fibre deposition is 36(±18) fibres/m^2/day ≥100µm, or 28(±13) fibres/m^2/day ≥200µm. This is lower but comparable to mega-city average MP counts. The fibre count for the Pyrenean site for MP fibres ≥100µm ranges from 22-62 fibres/m^2/day. The Paris mega-city study includes periods of lower MP deposition than seen in this field study (Paris MP deposition range 2-355 MP/m^2/day) potentially due to the greater precipitation quantity and frequency at the Pyrenees field site compared to the Paris study period. It is noted that, in concurrence with the Paris and Dongguan findings, there appears to be no direct correlation between MP deposition and average daily rainfall but that the occurrence of precipitation events (rain or snow) and their specific characteristics, intensity and frequency, may be drivers in atmospheric fallout.

The Paris and Dongguan studies MP sample composition differs in plastic type as well as shape to this study's findings. PS and PE form a large portion of the plastic type found in the Pyrenees field site. The majority of PS particles were fragments while most fibres were PET or PP. The Pyrenees field study, similarly to the Swiss floodplain findings(*120*) found MP composition to differ from the city atmospheric findings(*8*, *79*). While acknowledging the different environmental compartment, there have also been several oceanic focused studies that identified high counts of PS alongside PE and PP(*160*). Emerging research on the degradation rate of plastics by type suggest that PS, especially EPS, is highly sensitive to mechanical and UV degradation (when compared to PP and PE)(*117*). Expanded PS microplastics may be less dense and more easily entrained (therefore transported), and this may help explain the findings at this field site. The composition of plastic waste lost to the environment (not recycled or recovered) is not well documented and this, combined with limited knowledge on degradation rates makes establishing the plastic waste type, shape and size 'escaping' to the environment difficult to quantify or characterize.

3.6 Remote atmospheric MP source and transport analysis

Atmospheric MP source and transport analyses are new to MP research. Local to regional transport has been considered for this field site using two methods, a simple MP settling calculation and short-duration Hysplit4 back-trajectory modelling (see Methodology). Back-trajectory duration is defined as ~2hrs (0.1m/s settling velocity(*144*) for 600m a.g.l. Pyrenean planetary boundary layer depth(PBL)(*143*)) and each individual wind (>2m/s), rain and snow event has been analysed to provide a spatial context for local MP transport. The simple MP settling calculations, using MP settling velocity, event wind speed and direction and PBL depth(*143*), provide basic, linear back-trajectories for MP deposited at the field site due to initial entrainment or uplift and horizontal (wind) conveyance (without further mechanical or convective lift). The MP source area or zone of influence defined by this method extends 28km north-west to south-west, along the sparsely populated Aulus-les-Bains, Ercé and Massat valleys, over the Guzet-Neige ski fields and south-east along the Vicdessos valley (Figure 5 a-b). Wind events >2m/s illustrate a local MP source area across Aulus-les-Bains and the Saint-Girons valleys (42km to the north-west) and 20km to the north-east over Tarascon-sur-Ariège (village populations <6000).

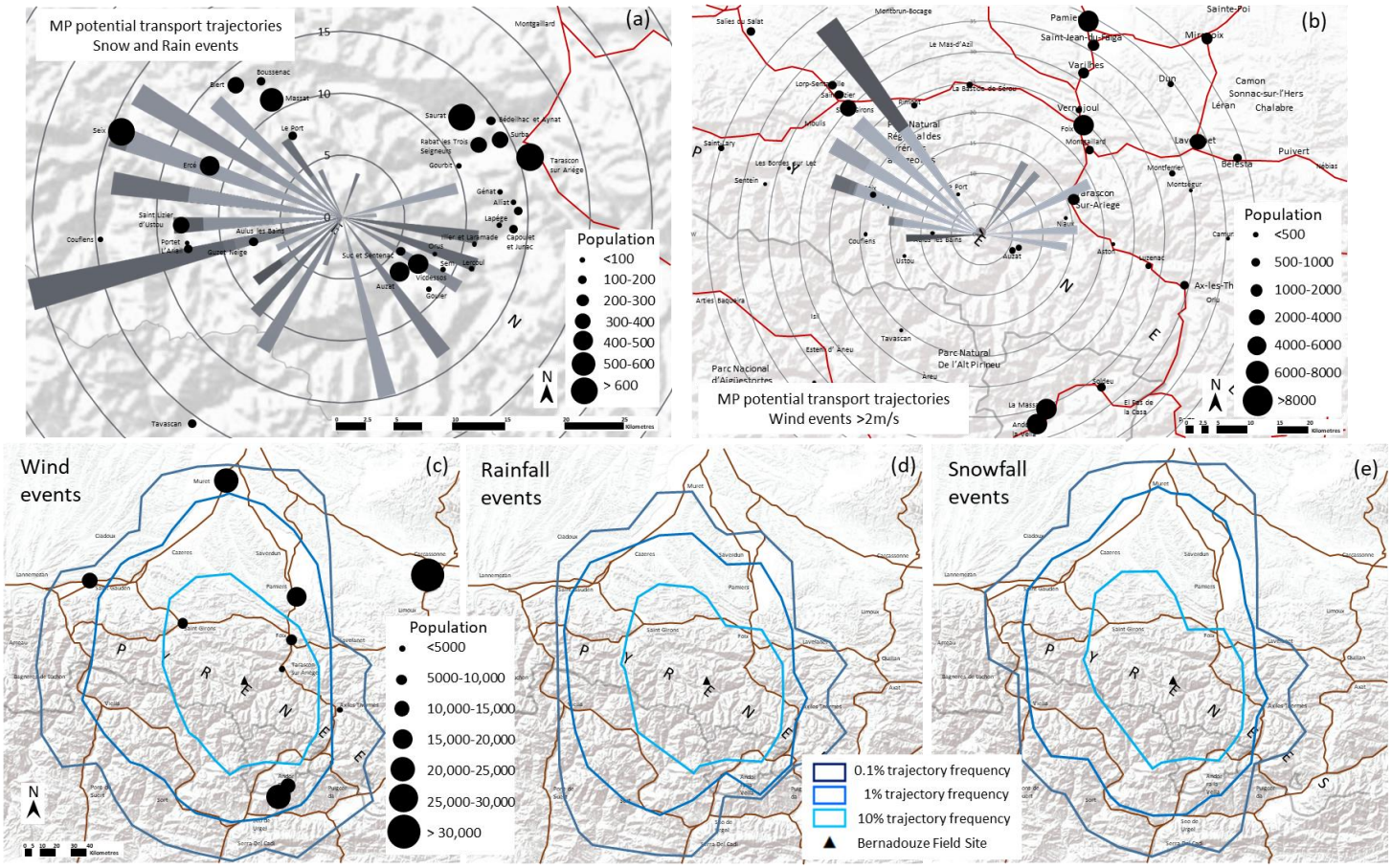

Figure 5. MP transport trajectories relative to recorded meteorology (simplistic MP settling velocity trajectory calculation, Methodology Eqn.4) and Hysplit4 back-trajectory modelling. Figure 5a illustrates the rain (n=165) and snow (n=186) event trajectories calculated from the maximum recorded wind speed and wind direction of each storm. Figure 5b illustrates the trajectories of wind events >2m/s (n=197). Figure 5c-e present the Hysplit4 back-trajectory model results for each individual rain, snow or wind event >2m/s. The results have been collated and are presented as trajectory frequency graphs. The wind direction data is presented in reference to local populated areas to provide spatial reference.

Hysplit4 back-trajectory modelling allows individual event air parcels to be back-traced illustrating the air parcel trajectory. Using the calculated back-trajectory duration (see Methodology), models for individual rain, snow and wind events were created and collated to provide event-based back-trajectory frequency maps (Figure 5 c-e). These short duration back-trajectories include localised updraft, convective mixing and advection, thus extending the MP transport trajectories and the source area 60km to the east, 75km to the west and south and 95km to the north of the site. Hysplit4 MP source areas extend into western Andorra (Andorra le Vella, population ~22,250), the Spanish Pyrenees, the Saint Gaudens valley, across Foix to Muret (population ~24,975). However, like the MP settling calculations, they still fall short of the more densely populated and industrialised areas likely to be significant MP emission sources (Toulouse (population ~466,000), Barcelona (population 1.6million), Zaragoza (population ~661,000). This dataset does not support long-range transport analysis due to the sampling time-step, however MP emissions are unlikely to be limited to local sources (<100km) due to low local population density.

3.7 Evidencing remote atmospheric deposition and transport

This study reports atmospheric deposition of MP in a remote Pyrenean mountain location. The research shows the monitored site received large numbers of MP particles (365 MP particles/m^2/day) in atmospheric deposition collectors over the winter period of 2017-2018. The presented research illustrates the presence of MP in non-urban atmospheric fallout. Analysis for this single site suggests a tentative but possibly important link between precipitation (rain and/or snow), wind speed and direction to MP deposition. Initial local MP trajectory assessment indicates an MP source area extending to 95km from the site, reaching several towns (populations <25,000) but not the city MP emission sources such as Toulouse or Zaragoza. The data cannot prove long-range transport, however air mass trajectory, MP transport and settling considerations suggest MP emission sources to at least be regional (>100km) given the population density within this local area. Longer-distance transport modelling may be possible but requires event specific sampling and back-trajectory analysis to identify the extent of this transport. It is highly recommended that further monitoring and analysis be undertaken using separate dry and wet deposition sampling equipment. This would advance the understanding of precipitation influence on atmospheric MP

deposition and wind trajectory impact on quantity and composition of atmospheric MP fallout.

4 Evidence of long-range transport of free-tropospheric microplastic found at 2877mASL

Abstract

The emerging threat of atmospheric micro-plastic pollution has prompted researchers to seek areas previously considered beyond the reach of plastic. Investigating the extent of microplastic transport and the vectors that may facilitate its transport is key to understanding the global extent of this problem. While atmospheric microplastics have been discovered in the planetary boundary layer, their occurrence in the free troposphere has yet to be examined. Answering this is important because their presence in the free troposphere would facilitate transport over greater distances and thus the potential to reach more distal and remote parts of the planet. This study provides evidence of 0.09-0.66 particles of microplastics per m^3 in PM10 filters (over 4 months) from the free tropospheric Pic du Midi Bigorre observatory at 2877m a.s.l. These results exhibit true free tropospheric presence of microplastic particles and fibers up to 160µm in size. Analysis of back trajectory modelling shows intercontinental and trans-oceanic transport of microplastics illustrating the potential for global aerosol microplastic transport.

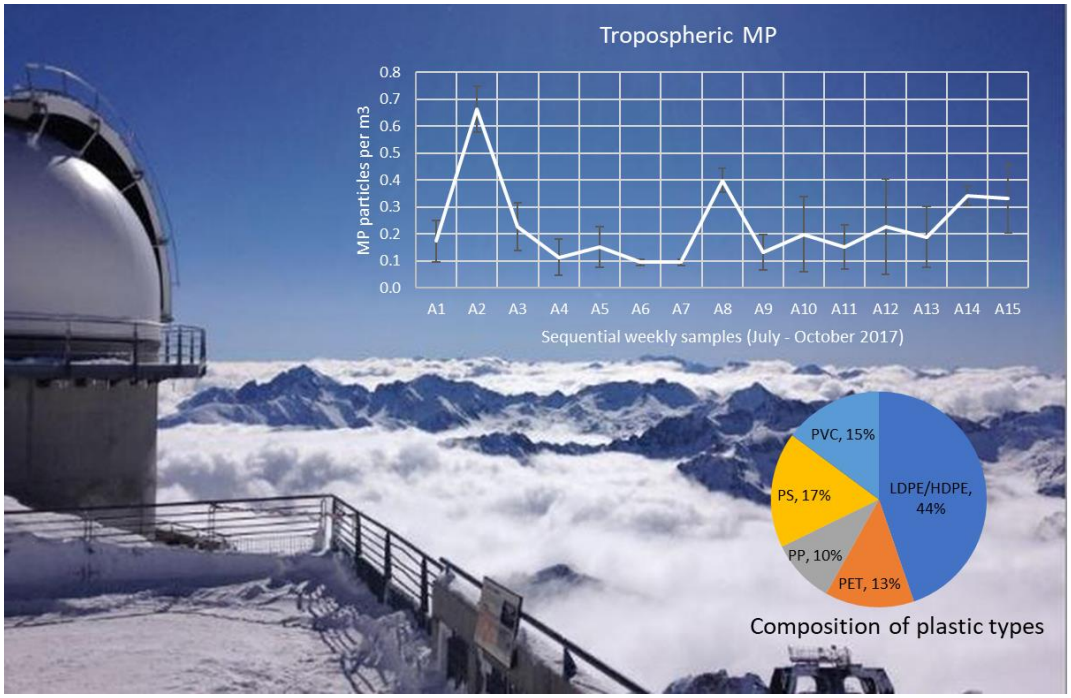

4.1 Introduction

Much has been written on oceanic plastic debris since Carpenter & Smith first published the results of their neuston net tows in the Sargasso sea in 1972 (*6*). Conversely, airborne microplastic (MP) has only recently been considered. Of the limited studies considering atmospheric microplastics, the majority focus on quantifying deposition. The three megacity studies in Paris (*161*), London (*162*) and Dongguan (China) (*8*) found fallout of microplastics the order of 175-1008 MP particles/m^2/day, prompting more cities to begin monitoring their air for microplastic. Monitoring completed in urban and rural Hamburg illustrated similar atmospheric deposition quantities, ~215MP/m^2/day and ~396MP/m^2/day respectively (*32*). Very few studies have attempted to analyses microplastic atmospheric transport. The recent findings of microplastics in the French Pyrenees Mountains identified daily MP deposition of ~365 MP/m^2/day at an altitude of 1425m a.s.l. with atmospheric transport of over 100km (*11*). Analysis of London city atmospheric MP illustrated 12-60km local MP transport (particles and fibres) with a long-range transport area of influence of up to 8700km^2(*162*). Complementary to this, marine studies collecting samples from Shanghai to the Mariana Island (ocean voyage) and the Pearl River to the Indian Ocean identified notable MP (up to 1.37 MP/m^3) in particulate pumped marine aerosol samples up to ~300 nautical miles offshore (*34*, *163*). HYSPLIT back-trajectory modelling, similar to that used in the Pyrenees study, illustrated marine aerosol MP particles to potentially have come from Japan, mainland China and Korea (*34*) and the Philippines (*163*). Furthermore, the recent study by Bergmann et al. (2019) (*164*) showed large amounts of MP in snow collected from various sites from the French Alps to Greenland icebergs. The Bergmann et al. study suggests MP was possibly transported by wind on the same air currents that carry mercury to the Arctic (*165*, *166*). The evidence is clear that MP is present in the planetary boundary layer (PBL), at least at the sites tested, but how far these particles can travel is at least partially dependent on the altitude they can reach within the atmospheric environment. With is in mind the next logical question to ask is how ubiquitous is MP pollution in our atmosphere and has it reached the free troposphere?

Wind within the free tropospheric (FT) is a global transport vector for many anthropogenic pollutants including mercury, lead and carbon particulates. The

lack of friction from surface topography results in elevated wind speeds and a greater potential for long-distance transport of particle matter. Dust that enters the FT has been recorded to circuit the globe, illustrating the extensive transport distances of particulate matter entrained into the FT(*167*). This study presents samples collected at the free troposphere terrestrial observatory, Pic du Midi Bigorre in the French Pyrenees, to determine if MP is within and transported through the FT. The Pic du Midi Bigorre research station (PdM) is an established FT long-term monitoring location at 2877m a.s.l, 42°56′11″N 0°08′34″E. This station provides extensive FT aerosol datasets for humidity and chemical compounds including ozone, particulate and elemental mercury, carbon monoxide, methane and carbon dioxide (*168*, *169*). PdM is defined as a 'clean station' due to its limited influence by local climatic conditions or environment (*170*). The PdM only has occasional planetary boundary level (PBL) influence from upslope winds (*169*), making it an ideal site for free troposphere monitoring and analysis. As a result, it is an established and extensively used site for sampling the free troposphere (cite several papers which have done this as examples). This study investigates the occurrence, quantity and characteristics of MP in the FT airmass and its transport pathways. Knowledge of PBL MP pollution illustrates regional atmospheric transport (from key MP sources such as cities, agriculture activities, industry, landfills to remote areas) but illustration of MP in the FT identifies a greater, trans-continental and trans-oceanic MP transport. The discovery of MP in the FT illustrates that atmospheric MP pollution has the potential to influence the most remote and isolated areas of the globe through FT transport, and that local atmospheric MP pollution may influence a spatial area far beyond the regional source location if the MP are entrained into the FT. With the knowledge of FT MP pollution and FT atmospheric MP transport the presence of MP in the Arctic, Antarctic and remote mountain regions can be explained, and back trajectory and dispersion modelling of FT MP particles identifies the possible remote area MP pollution sources.

4.2 Materials and Methods

4.2.1 Study Site and Sampling Method

The field study site is the free tropospheric long-term monitoring platform located on Pic du Midi Bigorre in the French Pyrenees Mountains. The sampling location latitude and longitude is 42°56'11" N, 0°08'34" E at an altitude of 2877m a.s.l.

The atmospheric monitoring platform forms part of the long-term monitoring ongoing at this station, as described in (*46*, *169*, *171*). The site is defined as a free tropospheric monitoring platform and as remote due to elevation and location. Access to the site is primarily by cable car, with the closest public road ~2.5km to the south and 1700m a.s.l.

Aerosol sampling was completed using a TISCH high volume PM10 sampler with a 49833mm^2 letterbox format quartz fibre filter membrane over four months of summer/autumn of 2017 (23/06/2017-23/10/2017). Samples were collected over an average of 8.2 days (standard deviation ±1.2 days), with an average pumped air mass sample volume of 7880 m^3 per sample (standard deviation ±1206 m^3) (full details provided in the supplementary dataset). Sampling was continuous from 23:00 to 16:00, with a shut-down period between 16:00-23:00 every day due to telescope and electrical interference requirements at the PdM platform. A total of 15 samples were collected and analysed for MP content and FT transport plus two field and two laboratory blanks.

All samples were collected on Whatman quartz microfibre (8 x 10 inch) filters with a pore size of 2.2µm, and all filters were sanitized in an autoclave at 300°C prior to use to ensure filters were clean of contaminants. Filters were then placed in the TISCH high volume sampler and the air suction pump activated of the monitoring period, with automatic shut down each day between 16:00 – 23:00. At the end of each sampling period samples were collected and placed in oven baked 450c/3hrs aluminium foil envelopes and stored in the dark under refrigeration conditions. Cotton laboratory coats and nitrile gloves were worn at all times when manipulating sample filters and equipment. Material collected on the quartz filters was analysed for MP, PM10 and black carbon content.

Alongside air mass filter samples (for PM10 and MP quantification) ozone, carbon monoxide, relative humidity, wind speed and direction, air temperature, global radiation, red, green and blue light diffraction were measures (as part of the ongoing long term PdM monitoring activities. This monitoring is undertaken by Laboratoire d'Aérologie and the Observatoire Midi-Pyrénées and is provided online via http://paes.aero.obs-mip.fr/ (last accessed 20.03.2020, hourly data accessed for all long-term atmospheric monitoring parameters).

4.2.2 Analytical procedure for the detection of MP particles

Three 30mm diameter circular area or the quartz filter was analysed for MP. There is a necessary assumption that the TISCH high volume sampler collects MP evenly across the filter in a similar manner to PM10 particulates. The three 30mm diameter sub-samples were removed from the quartz filter sheet using an autoclave sterilized stainless steel circular stamp in a positively pressurized room and under a fume hood in an ISO 1000 rated clean room. The sub-samples, for MP samples and field blanks, were then placed in autoclave sterilised aluminium envelopes and stored in a glass container in dark, refrigerated conditions.

MP samples (and field blanks) quartz filters were flushed with 250ml MilliQ (18 MΩ.cm) ultrapure water into sterilised borosilicate glass test tubes. Due to the low organic particulate content, no organic removal digestion was included in the protocol. Samples (material + MilliQ) were then filtered onto aluminium oxide filters (Whatman Anodisc 0.2µm pore, 25mm diameter) using borosilicate glass vacuum filtration. The filters were vacuum air dried (sterilised aluminium and glass test tube caps to minimise air MP contamination) and placed in borosilicate glass capped dishes prior to µRaman analysis.

µRaman analysis was completed for each sample using a Horiba XploraPlus (50-3200cm^{-1} with a 1.5cm^{-1} resolution, confocal imaging accuracy 0.5 µm with motorised X-Y stage). Three areas of each filter (6 x 13mm^2) were randomly selected and analysed for total plastic presence using the 785nm laser (spatial resolution of 1 µm) and 200-2000cm^{-1} Raman shift range. Spectra were collected using an acquisition time of 15 seconds and 10 accumulations, maximum of 25% power (filter) (general settings: grating of 1200gr_mm and 50µm split, modified to achieve effective spectra results as necessary during analysis) (*11*). µRaman analysis, particle count and shape identification strictly followed the methodology detailed in the Allen et al. 2019 methods (*11*).

The use of µRaman on a subsection of the filters enabled potential MPs to be positively identified as plastic particles. Using the visual characteristics of these confirmed MPs enabled MP size and count to be completed on the full extent of the 25mm aluminium oxide filters using confocal microscopy; the MPs identified and counted using ImageJ software and Nile Red staining (FIJI) (*172*) (Allen et al., 2019). Raman and visual counts are shown in supplemental information.

4.2.3 Contamination and procedural blanks

All MP samples collected at the PdM monitoring station were collected in a manner to minimise contamination. Cotton clothing and laboratory coats were worn at all times when manipulating samples, with all sample filtration material, storage envelopes (aluminium) and manipulation equipment (stainless steel tweezers, spatulas etc) sterilised through autoclave heating (300°C) to minimise contamination. A field blanks was created during this sampling campaign, on the 28/08/2017 and 23/10/2017, following the same protocol for preparation, installation and storage for the MP sample filters. Field blanks (2) were created and analysed following the same protocol as the MP samples and laboratory samples, with values reported in the supplementary dataset. Laboratory blanks (2) were created during the sample preparation period, following the full protocol for MP sample preparation and analysis. In line with all previously published MP analysis to date, the MP counts found on the atmospheric samples was reduced by the MP found on the field and procedural blanks, providing the resultant sample counts (as described in (*11*) methodology.

4.2.4 Back trajectory and dispersion modelling

Hybrid Single-Particle Lagrangian Integrated Trajectory (HYSPLIT) modelling (*173*) undertaken using HYSPLIT version 4 (April 2018). Initial analysis to examine trajectory spatial extents and air mass trajectory elevation were undertaken using archived Reanalysis datasets from the Global NOAA-NCEP/NCAR pressure level archive data using a 2.5° grid (initially) followed by a more detailed analysis undertaken using archived GDAS 0.5° datasets and presented in Fig. 3. HYSPLIT was run in backwards mode, models were run for 168 hours from the PdM sampling platform location, 100m above ground level (~3000m above sea level). A new back trajectory model was run for each hour within the sampling period, resulting in 2175 modelled trajectories. Trajectory pathways, elevation and mixing depth information were extracted. The hourly back trajectory models for each sample period were frequency analysed to create a spatial frequency maps.

4.2.5 Data analysis

Statistical analysis of µRaman spectroscopy to estimate the MP count per analysed filter and total TISCH high volume filter relative to the air mass pumped

through the filter was undertaken through simple extrapolation. MP identified in the µRaman sampled areas (3 x 13mm^2 for each filter) were used to confirm the visual and ImageJ MP counts for the 30mm diameter sub-samples (3 sub-samples per sample period, analysed as replicates to create a representative MP count). The representative airmass passing through each 30mm diameter sub-sample was calculated from the recorded total TISCH high volume airmass sampled per sample period (6624-11799m^3, detailed in the supplementary dataset) (total filter area 0.0516m^2). MP counts were reported relative to 1m^3 of airmass sampled for each sample period (A1-A15).

Atmospheric parameters continuously monitored at the PdM long-term monitoring station (O3, CO, temperature, relative humidity, atmospheric pressure, global radiation) were downloaded from the PAES database in hourly format. The sample MP counts, polymer sample compositions and fibre:fragment content of each sample were analysed relative to the mean, mode, maximum, minimum and variance of each sample period (ensuring shutdown periods were not included). Independence and correlation for parametric and non-parametric datasets were considered (as appropriate to the individual dataset) to identify any statistically significant trends (Pearson, Spearmen and Mann Whitney U tests).

HYSPLIT back trajectory elevations were extracted from individual HYSPLIT model runs and analysed to define the 25th, 50th, 75th, maximum and minimum elevations. Extracted HYSPLIT 3D datasets were converted to ArcGIS (ESRI) shape files and used to calculate trajectory distances from PdM relative to elevation and trajectory duration.

4.3 Results

MP fragments or fibres were found in all samples analysed during the summer-autumn monitoring period. Active aerosol sampling resulted in MP counts of 0.09-0.66 MP/m^3 at the PdM FT sampling platform, with an average of 0.23 MP/m^3 (St.Dev. ±0.15) (Figure 6). 13 of the 15 samples presented MP counts >0.1MP/m^3, with 4 samples presenting >0.3 MP/m^3. Due to their small size (primarily 5µm to 20µm) particles were primarily identified as fragments or fibres (58%, 42% respectively), with fibres defined as presenting a 3:1 length to width ratio (*87*, *174*). MP particles were comprised of (LD/HD)PE, PS, PVC, PET, and PP (in order of abundance 44:18:15:14:10 by percentage). MPs occurred as fragments ranging up to 36µm in diameter and fibres extending up to 163µm in

length. The majority of MP fragments were 5µm – 15µm in diameter (78% of fragments, 46% of MP particles) and predominant fibres lengths were 10-20µm, 25-35µm and 40-45µm (61% of fibres, 26% of MP particles).

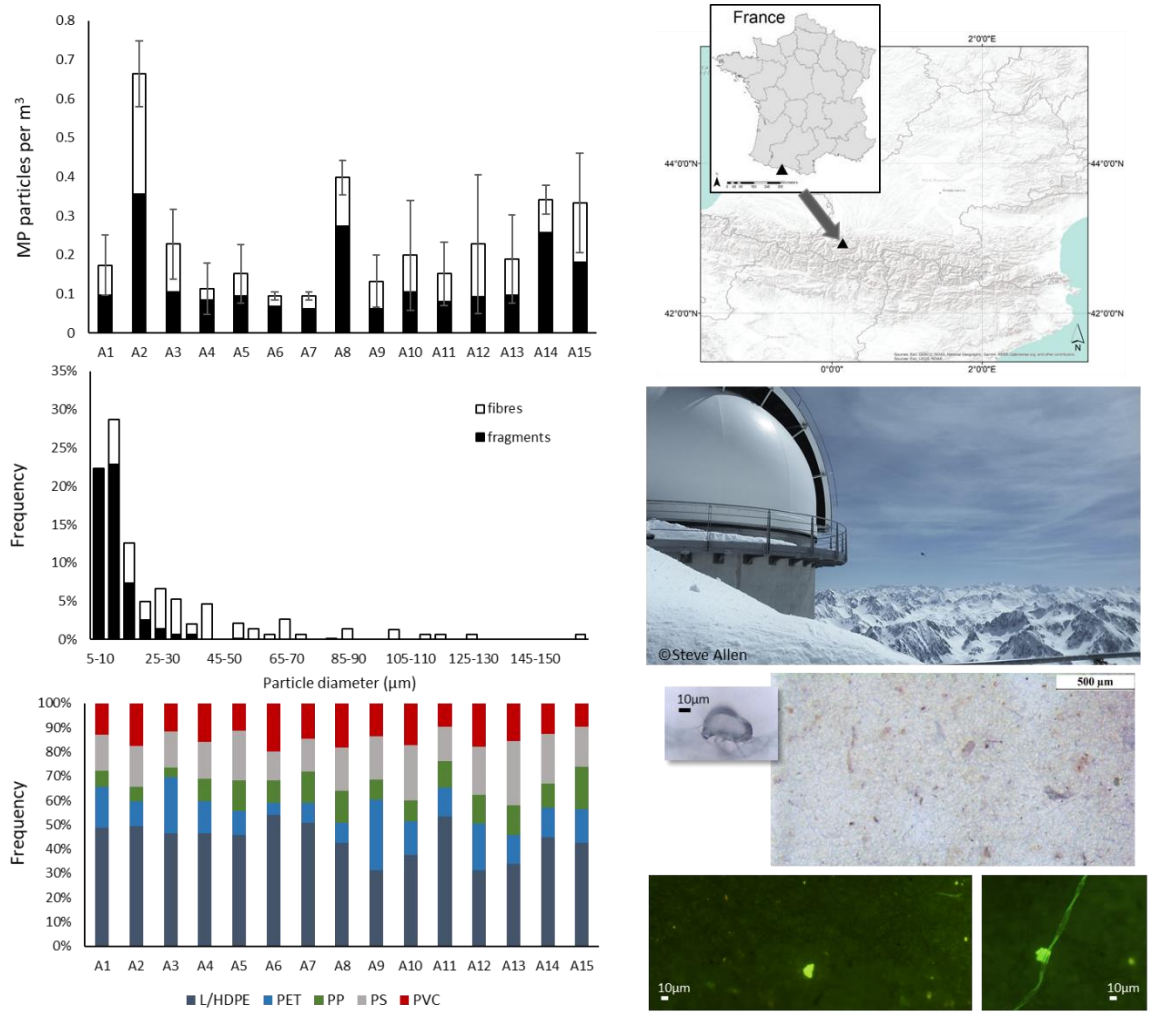

Figure 6. MP quantities (MP/m^3) for the 15 sampling periods (a), size distribution (from all sampling periods combined)(b) and polymer types (c) for the 15 samples collect between 23/06/2017 and 23/10/2017 (f) at Pic du Midi Biggore long term monitoring station (location (d and e)). Underlying data set of MP counts is provided in Appendix 8.

4.3.1 MP quantities relative to FT characteristics, meteorological conditions and PM10

Several meteorological parameters are monitored at the PdM field site, including wind direction, wind velocity, air temperature and relative humidity. Total particulate matter ≤10µm (PM10) is also monitored, however the full sequential dataset was not available for the entire period of MP sampling due to equipment

faults. As a result, 5 of the 15 sampling periods have no comparative PM10 data records. The MP results were analysed alongside these PdM atmospheric parameters to identify any correlating local environmental conditions (Figure 7).

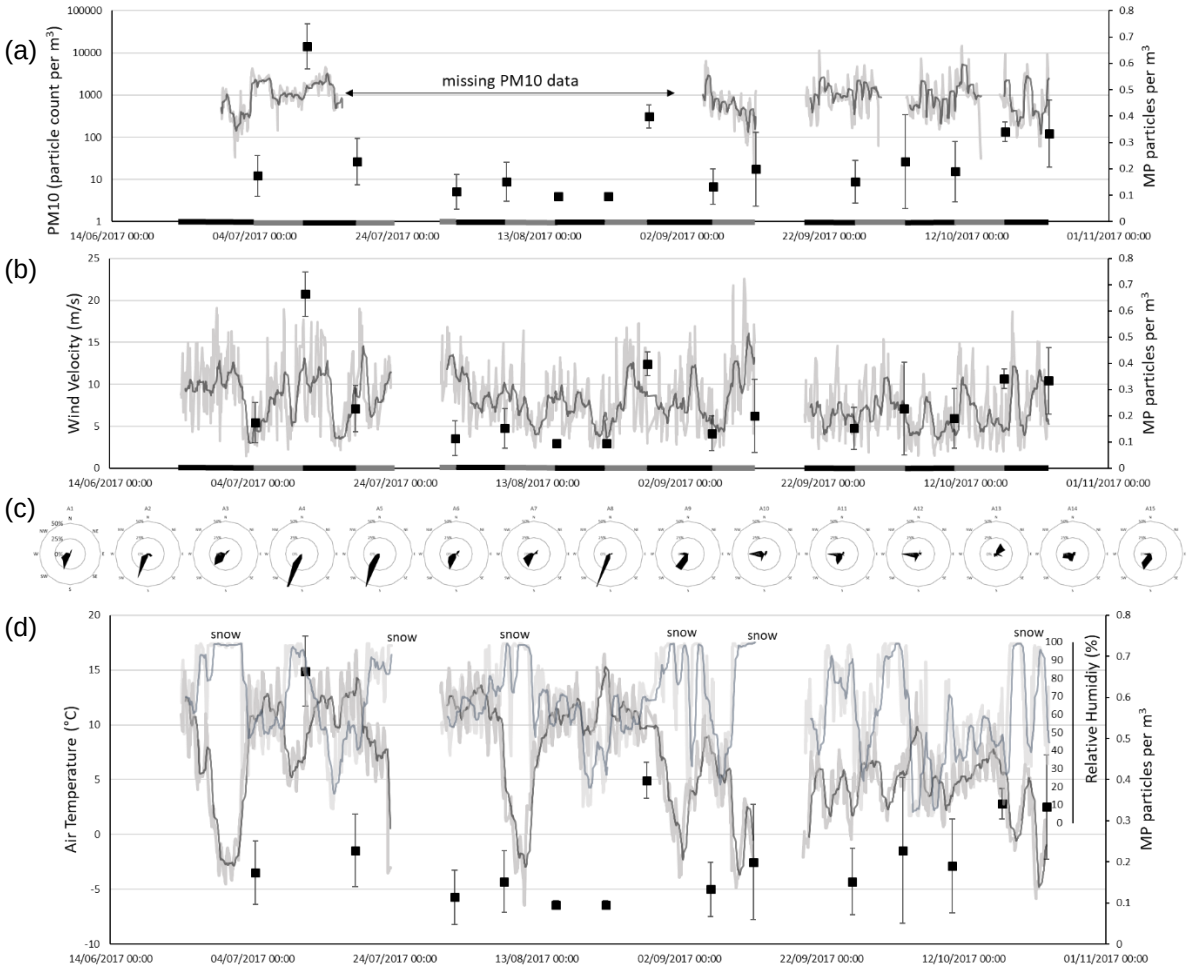

Figure 7. MP quantities plotted relative to the PM10 monitored in conjunction with MP (a), wind velocity (b), wind direction (c) and air temperature (d). PdM local meteorology datasets are provide in Appendix 9.

There appears to be limited correlation or comparable trend between the local meteorological atmospheric conditions monitored (air temperature, relative humidity or local rainfall) and the MP particle counts found for the corresponding monitoring periods ($p>0.05$ for all datasets). The recorded wind direction is predominantly south to south-west with only sample period A13 presenting significant easterly wind influence (NNE-ESE 62% of this monitoring period, less than 25% for all other sample periods). There is limited variation in wind direction over the monitoring period resulting in limited identifiable local wind directional

trends relative to MP. Stronger wind velocities from easterly winds tentatively correlated with elevated MP counts ($p=0.04$), as did stronger (maximum) wind gusts from the north ($p<0.05$). The wind velocity ranged 1.4-22.6 m/s (mean 7.9 m/s ±3.6 m/s), with the stronger winds (≥10m/s) occurring predominantly from the W to SW (71% of the monitoring period). There is notable intra-sample variation in wind speed resulting in no clear local wind velocity trend relative to MP counts. All sample periods present both peak wind velocities for short periods above 10m/s and calmer wind periods (<5 m/s).

PM10 particle sampling has been completed alongside MP analysis at the PdM monitoring platform (Figure 7a). PM10 at PdM has been previously reported to range between 870-2330 particles per m^3 (*175*). PM10 monitoring for the MP sampling period ranged between 21-14623 particles per m^3, with an average PM10 count of 1057 particles per m^3 (StDev. ±1261 particles per m^3). MP results illustrate a positive relative correlation to PM10 results, with MP counts following a similar trend to the total PM10 cumulative values ($r=0.65$, $p=0.04$) and a non-significant positive correlation with average PM10 values ($r=0.30$, $p>0.05$). MP fragments correlate more strongly with PM10 values than fibres (fragments $r=0.7$, $p<0.05$; fibres $r=0.5$, $p>0.05$). When comparing samples with elevated MP results (>0.3 MP/m^3) to samples with lower MP results (<0.3 MP/m^3), a higher PM10 mean, maximum and lower minimum are noted (for >0.3 MP/m^3 PM10 results presented a relative increase/decrease of mean= +267, max=+3855, min=-117 comparatively). This suggests a trend of greater PM10 for periods with elevated MP alongside greater variance during these elevated MP sampling periods (supplementary dataset) despite the limited dataset (n= 10, no comparative data for sample period A4-A8).

PM10 values show correlations with ozone (n=10, r0.6, $p<0.05$), carbon monoxide (n=5, r=-8, $p<0.05$), black carbon (n=3,r>0.5, $p<0.05$), average wind speed in the east and north projection (n=10, r=-0.6, $p<0.05$; n=10, r=0.5, $p<0.05$). MP results show similar trends to carbon monoxide, although not as strong or significant as PM10 to carbon monoxide (n=10 r=-0.5, $p>0.05$), but a negative trend to cumulative ozone values (n=15 r=-0.7, $p<0.05$). This suggests there may be similar transport mechanisms and dynamics for these two particle types or that the MP characteristics can be seen within the PM10 trends (acknowledging that a proportion of the PM10 count will be MP particles), but that

these transport mechanisms are not identical and MP appears to have a more complex transport pathway.

MP found in the PdM samples, collected at high altitude, cannot easily be attributed to any clear or specific local influence. While MP counts appear to follow a similar trend to PM10 counts, these particles may be a result of long-distance atmospheric transport and complex atmospheric mixing away from PdM itself. This is supported by the lack of strong statistical correlation between the MP counts and local wind direction and velocity meteorological conditions (including temperature and relative humidity) for the PdM location during the monitoring period. The occurrence of MP at PdM is therefore considered to be a result of more complex atmospheric transport, mixing and distal source influence.

4.3.2 Long-distance transport and the influence of possible distal MP sources on PdM

Atmospheric transport models can be used to consider the possible trajectory and dispersion pathways of atmospheric air masses and particulates. The MP found in the FT environment of PdM appears to have limited local atmospheric influence (no local atmospheric parameter trends), suggesting long-distance transport. Through back trajectory modelling, the elevation, distance and potential entrainment locations resulting from long-distance atmospheric transport can be visualized using recorded meteorological data.

Analysis of the back-trajectory transport was completed using HYSPLIT. HYSPLIT analysis was undertaken to consider the back trajectory of atmospheric air masses potentially carrying particulate material to establish the probable direction of MP transport to PdM, the associated trajectory and therefore possible source areas (*176*). HYSPLIT back trajectory elevations were also considered to identify the elevation of these air parcels and the duration of flight prior to arrival at PdM.

4.3.3 Back-trajectory analysis of air parcels conveying MP particles

HYSPLIT back-trajectory analysis was run for a 7day (168hrs) backwards period for each trajectory analysis, a duration long enough to establish potential distal sources and trajectory elevation decline (also a standard adopted atmospheric backward modelling period for long distance analysis (*169*, *173*, *177*)) . Back-trajectories were created for each hour during the monitoring periods, resulting in

2175 back-trajectories. Individual back trajectory analysis was run for each hour to ensure that diurnal influences were included in the trajectory spatial and elevation analysis. Alongside spatial location and elevation, the PBL (mixing height), pressure and rainfall were identified along each trajectory.

The back-trajectory air mass modelling for each sample period (A1-A15) was completed, and the trajectory's elevation above mean sea level and above the HYSPLIT modelled ground level (represented through atmospheric pressure maps in hPa) were created (Figure 8, see Appendix 10 - 12). Seven of the field samples (A3 - A7, A11, A13 and A14 illustrated backward trajectory model results that showed negligible decent to mean sea level height or ground surface level. Samples A2 presented the shortest time of flight between <50m above sea level and PdM (113hrs) followed by sample A8 (135hrs). It is noted that samples A2 and A8 are elevated MP sample periods (0.66 ± 0.07 and 0.40 ± 0.04 MP/m^3 respectively). There is a negative correlation between the duration (and therefore distance) of air mass transport and the MP quantities in the PdM samples. MP count/m^3 correlates significantly and inversely to the time taken to move between the trajectory elevation <50m above sea level and the PdM sample location (Log10(MP count r= -0.7, p=0.004, MP count rho = -0.6, p = 0.03). There is also a non-significant but negative correlation between the minimum and average back trajectory elevation and MP count for each sample period (r= -0.4 and r = -0.3, p>0.05). This suggests that high MP counts appear to occur when air mass passes close to the ground nearer to PdM (e.g. 74hr previously rather than 113 hrs previously). It also suggests that great MP counts occur during periods of lower overall trajectory elevation. Higher MP results may contain MP that was entrained closer to PdM while samples with lower MP may contain MP particles that have travelled for longer and potentially further.

The HYSPLIT back trajectory analysis results were divided to illustrate atmospheric transport for MP in the upper 5th percentile of the sample range (MP ≥0.33MP/m^3) and all other MP sample periods (MP<0.33MP/m^3). This was done to try and identify any drivers or correlations between the air mass trajectories and the MP counts within the samples.

Back trajectories presented as elevation above mean sea level (m)

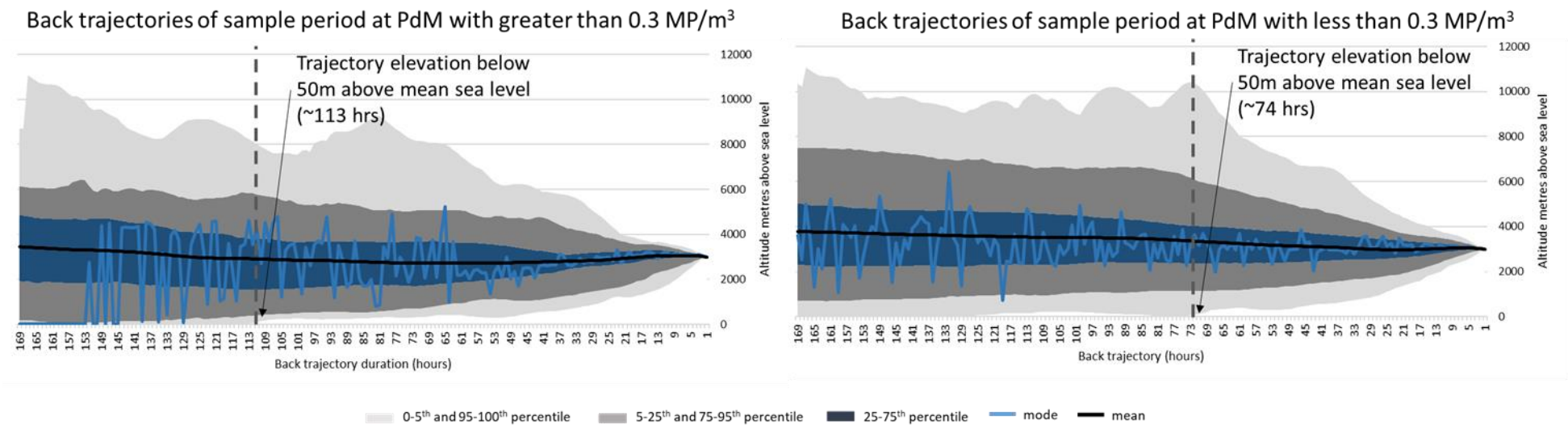

Back trajectories presented as elevation modelled ground level (m)

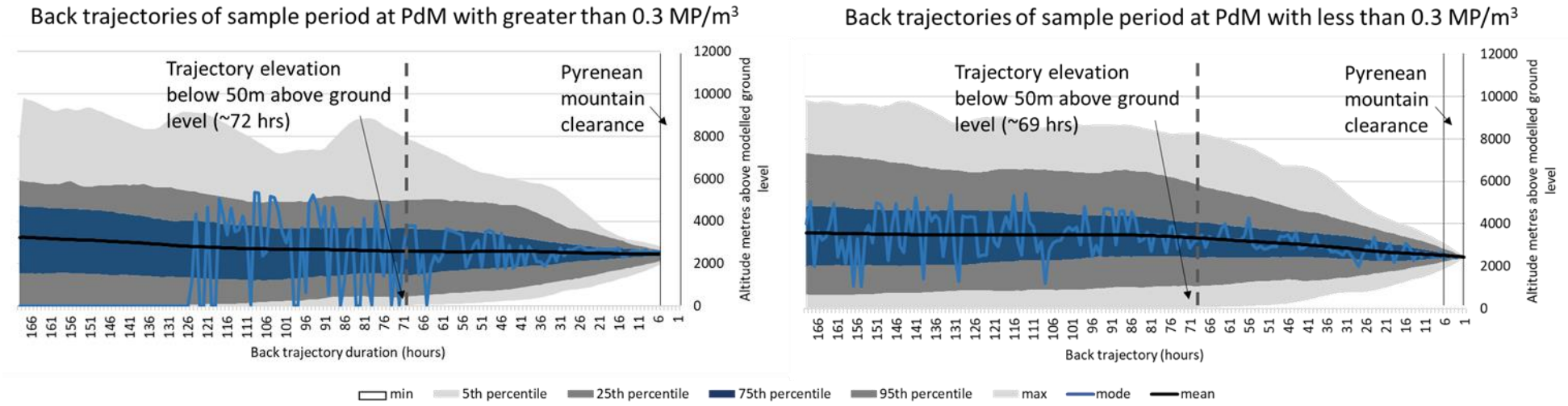

Figure 8. HYSPLIT back trajectory models of air mass movement from PdM sample period. The data is separated to illustrate the higher quantity MP sampling period (MP>0.33MP/m^3, Fig. 8a) and trajectories relating to the lower MP sampling results (Fig. 8b). The graphs beneath the back trajectory spatial illustrations show the 5^{th}, 25^{th}, 75^{th} and 95^{th} percentile, maximum and minimum elevations of the modelled back trajectories respectively (Fig. 8c and d). The mean elevation is indicated as a black line, and the mode (most frequently occurring elevation relative to the back-trajectory analysis time step) is indicated as a blue line. The dotted lines in illustrate the earliest potential entrainment point in the back-trajectory modelling, the shortest duration and distance of air mass movement from surface or sea level elevation to PdM relative to the monitoring period.

The back trajectories relative to the higher MP results (Figure 8 a,c) illustrate high flight paths, with a mean trajectory elevation of >2715m above mean sea level, a mode of greater than 1000 m a.s.l. for at least the first 63 hrs prior to sampling and all trajectories remaining above 50m above sea level for at least 113 hours (dotted line in Fig 3a). The back trajectories relative to samples presenting <0.33 MP/m^3 (Figure 8 b,d) illustrate airmass flight paths similar elevation compared to samples with >0.33mp/m^3. The mean trajectory elevation for these lower MP samples is >2961m above mean sea level, a mode of greater than 1000 m a.s.l. for at least the first 118 hrs prior to sampling and all trajectories remaining above 50m above sea level for at least 74 hours (dotted line in Figure 8 d).

The minimum flight path drops close to ground level after 69-72hrs (light grey shading in Figure 8 c, d), as does the modal trajectory elevation (dark blue line) for general back trajectories for sample periods with >0.33MP/m^3. This suggests that there may be mixing and entrainment of MP and particulate material into the PBL/FT at this time step.

While it is acknowledged that particles will be scavenged by rainfall and dry deposition will be assisted by dynamic air mass movement (e.g. down drafts), due to the limited transport parameterisation and evidence based atmospheric transport characteristics, air mass movement has been used as a simplistic indication of potential particle transport. Therefore, simplistic correlation between the number of airmass trajectories indicating close to surface profiles during the 168h backward trajectory modelling period and MP sample findings have been

considered. The number of air mass back trajectories falling close to ground or sea level (<50m above ground level or 50m above mean sea level) appears to correlate with the MP findings (LOG10(MP) $r=0.72$, $p<0.01$), and the duration of travel from these low altitude points to the PdM sampling site are inversely (but not significantly) correlated (LOG10(MP) $r=-0.50$, $p=0.06$). Sample period A2 and A8 present the greatest number close to ground level back trajectories (n=21, n=11 respectively). This tentatively suggests that samples with higher MP counts occur during periods when a greater quantity of airmass movement has passed close to surface of sea level, during the past 168hrs, prior to arriving at the PdM sampling site and that a longer duration of travel may correlate to lower MP sample counts due to potential deposition or loss during transport.

The HYSPLIT air mass back trajectory modelling illustrates an average air mass movement of 4522km from PdM over the 168hr modelled period (2119-6569km average trajectory distances for samples A1-A15). The shortest distance travelled (in a straight line from PdM) is 272km (A1, average trajectory elevation 1935m above ground level) while the longest distance is 10,248km (A13). The projection of these back trajectories is generally westerly or southerly, across the Atlantic Ocean towards north America or across the Mediterranean Sea towards northern Africa (Figure 9 a, b). Individual sample trajectory projections are provided in Appendix 11. It is noted that all projections from PdM suggest long-distance transport (>100km, (*11*)).

HYSPLIT provides airmass back trajectories as a representation above mean sea level and as an elevation above ground level. Sample periods A1-2, A4, A8-10, A12 and A15 present airmass back trajectories that come close to ground level prior to arriving at PdM ($n \leq 21$). The distances travelled (calculated as a direct line to PdM) from close to ground level to PdM range from 470-6792km. This suggests that, if only air mass transport is considered (not considering wet and dry deposition), the MP could potentially be entrained from ≥ 470km away from PdM.

Back trajectories for samples with MP<0.33MP/m^3

(a)

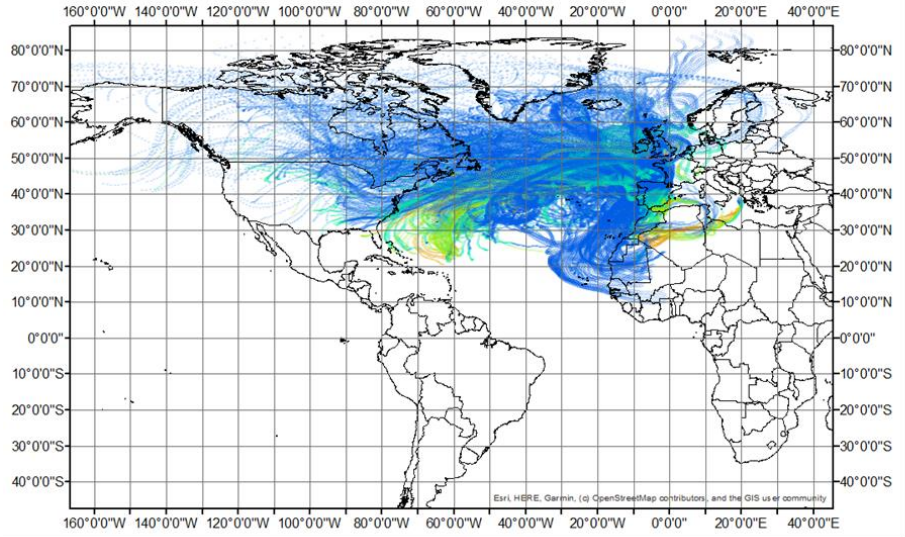

Back trajectories for samples with MP>0.33MP/m^3

(b)

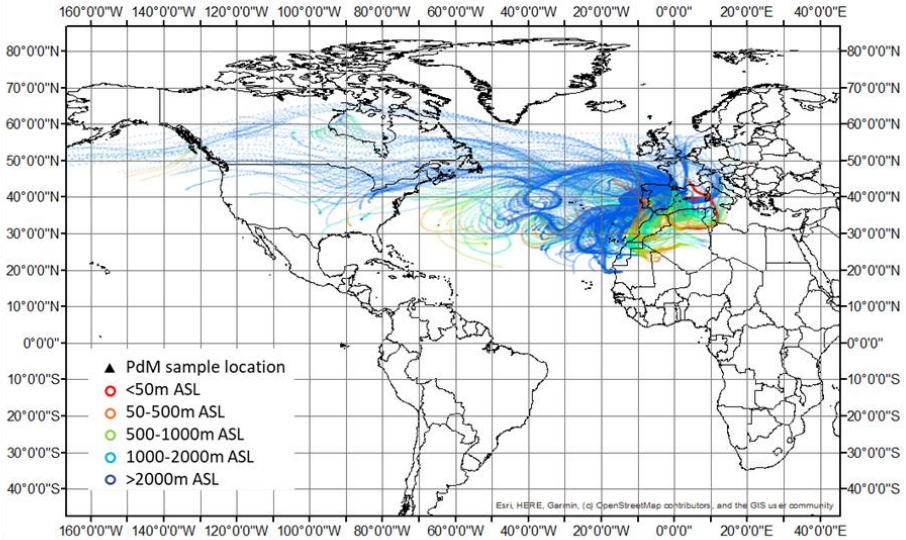

(c)

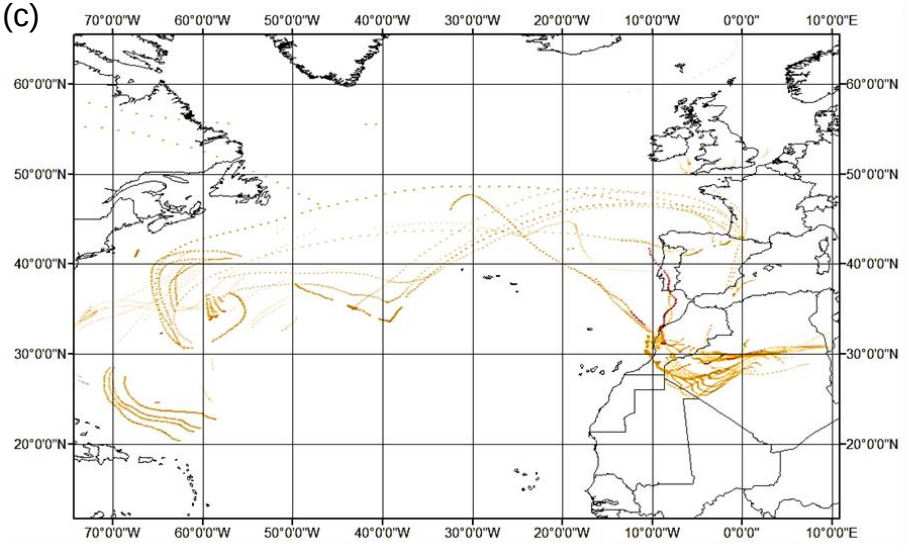

(d)

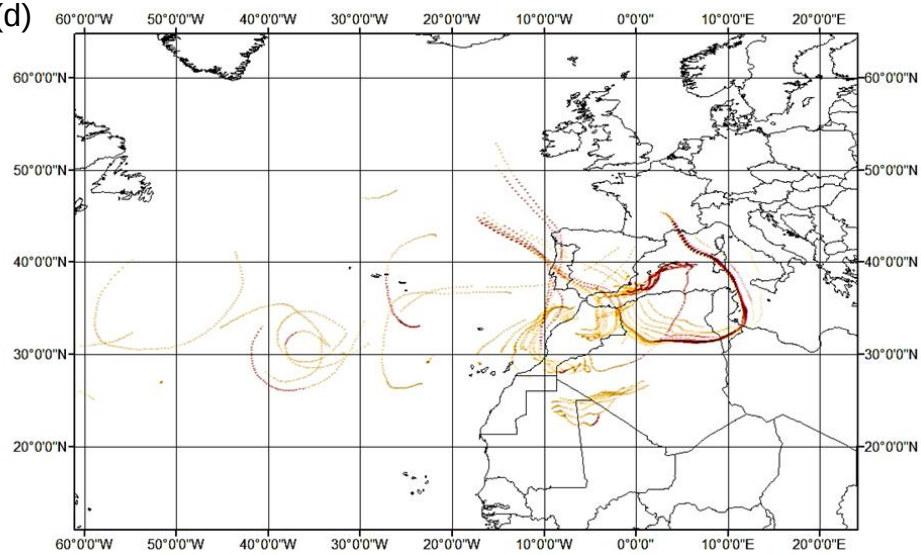

Figure 9. HYSPLIT modelled trajectories for 168 hours in backwards mode for higher MP sample periods (MP>0.33MP/m^3; A2, A8, A14 and A15) (Figure 9a) and the lower MP sample periods (Figure 9b). Figures 9 c and d present the location of airmass backward trajectory points below 50m and 500m above ground level.

All sample periods illustrate an Atlantic Ocean (westerly) trajectory influence. Sample A8 is the only sampling period that does not show airmass trajectories extending across the Atlantic Ocean into/over north America. Samples A1-A3, A5-A6, A9-A11 and A13-A15 illustrate trajectories that pass over the UK and Ireland. Sample periods A1-6, A8-9, A12 and A14-15 show trajectories extending over northern Africa, and there is a positive correlation between MP findings (MP/m^3) and the number of northern African trajectories in each sample period (LOG(10)MP r=0.5, p=0.04). The north African continental influence may therefore be a potential MP source for this monitoring period at PdM. Figures 4c and d illustrate the trajectory points that are close to ground level (<50m above ground level) as modelled by HYSPLIT backward air mass trajectory analysis. While there are some low elevation trajectory points close to north America, the majority occur over France, Spain, Portugal, north Africa and the Mediterranean (with several low trajectories over the Atlantic Ocean). This mapping suggests that that northern Africa and the Mediterranean may be a source or area of potential MP entrainment for the airmass relative to the monitored period at PdM.

4.4 Discussion

Direct comparison of PdM findings to other studies is limited due to the differences in the minimum size of the particles analysed. Only Li et al. (2020) considered MP particles down to >5µm particles in Beijing (*178*) and Allen et al. (2020) identified and quantified MP particles down to >2.5µm on the French Atlantic (*179*) coast. It can be seen in Table 3 that the Beijing study found particles several orders of magnitude (5600-5700 MP/m^3) greater than this study (0.09-0.66 MP/m^3). The French coastal air findings were higher than this study's findings but more relative than those from the mega-city of Beijing, presenting results two orders of magnitude greater than found at PdM (1.47-19 MP/m^3). This is understandable given the inner-city sampling location in Beijing compared to oceanic winds and the relative anthropogenic isolation of PdM.

Table 3. Summary of published air mass microplastic findings

Location	Microplastic count	MP size range	Reference
Shanghai, China	0-4.18 MP/m^3	23µm-5mm	(Liu K et al., 2019a)(*33*)
Paris (indoor)	1.0-60.0 MP/m^3	50µm-5mm	(Dris et al., 2017)(*43*)
Paris (outdoor)	0.3-1.5 MP/m^3	50µm-5mm	(Dris et al., 2017)(*43*)
Sakarya Province, turkey	116-3424 MP/m^3	50µm-5mm	(Yurtsever et al. 2018)(*180*)
Western Pacific Ocean (Shanghai - Mariana Islands)	0-1.37 MP/m^3	20µm-2mm	(Liu K et al., 2019b)(*34*)
Surabaya, Indonesia	131-174 MP/m^3	~500µm-5mm	(Asrin and Dipareza, 2019)(*181*)
Asaluyeh County, Iran	0-1 MP/m^3	100µm-1mm	(Abbasi et al., 2019)(*44*)
Beijing, China	5600-5700 MP/m^3	5µm – 2mm	(Li et al. 2020)(*178*)
Atlantic coast, France	1.47-19 MP/m^3	2.5-300µm	(Allen et al. 2020 *in press*)
Pearl River Estuary, South China Sea, Indian Ocean	0-0.077 MP/m^3	58-2252µm	(Wang et al., 2019)(*33*)
Pic du Midi Bigorre, France	**0.09-0.66 MP/m^3**	**5-163µm**	**This Study**

MP are clearly present in FT atmospheric samples from the monitoring station at PdM and potential long-range MP transport has been illustrated through airmass backward mode trajectory modelling. Potential source areas identified include locations across North Africa, Spain, Portugal, France, UK/Ireland and as far as USA/Canada. Higher MP sample periods appear to be tentatively influenced by northern African airmass trajectories, with lower MP sample periods showing less northern African influence.

MP numbers showed little comparable trend and no statistically significant correlation with local meteorological conditions suggesting long-distance atmospheric transport and distal MP source(s). The variance in particle numbers with similar modelled pathways also suggests events further out than the 168hr study period both spatially and temporally, may be responsible for entrainment. These entrainment mechanisms are an area that requires a substantial further research to fully understand the processes at work.

The mechanics and dynamics of MP atmospheric transport are relatively unknown and unevidenced. The in-cloud and below-cloud scavenging coefficients have tentatively been considered for tyre and brake wear in a recent study (using statistical assumptions due to lack of physical parameterisation (*182*)), MP particles that are notably more dense than those found in the PdM

atmospheric study. The wet and dry deposition rate, triboelectric effect, chemical and physical particle interaction in the atmosphere, influence of humidity, temperature, acidity, precipitation and surface vegetation are all currently unquantified or characterised. The tentative but non-significant correlation between PM10 and MP results in the PdM samples suggest some similar atmospheric transport characteristics but the lack of correlation with local and modelled meteorological conditions suggests MP atmospheric transport to be more complex than dust or black carbon particle movement. Future research is needed to characterise and parameterise MP atmospheric transport dynamics and to identify the key drivers for entrainment, wet and dry deposition and long-distance atmospheric transport. This future parameterisation and transport characterisation will enable more detailed modelling, including particle dispersion analysis, that may provide more detailed insight into atmospheric MP transport.

It should be noted that this study extends over only a short period of the year and seasonal variations are possible and likely. The one-week sample time step could be shortened to improve model reliability however current plastic pollution levels suggest that long sample times are required to obtain a statistically relevant number of particles. With increasing production and mismanagement of waste it may be possible to shorten the sampling times in future research. The Tisch high Volume PM10 sampling system relies on the particle density of dust being 2.65g/cm^3 whereas the plastic materials studied are on average around half this density (~1 g/cm^3). The system does not use a pre filter to exclude larger material but instead redirects incoming air to reverse its direction (~180° turn) and uses the material density and kinetic energy to limit the >10µm particles reaching the sample filter. Heavier material carries too much kinetic energy to make the turn and collides with a silicone grease pad to which it adheres. Particles found in this study were often greater than the PM10 system normally captures and it is possible that this is because the light plastic material can make the turn, avoiding being captured by the grease. It is possible that the types of plastic recorded and/or numbers may be influenced by the PM10 sampling system and we recommend a total particulate system for future studies.

The HYSPLIT models suggest that trans-ocean and trans-continental MP transport may occur. While significant further field and laboratory research is replicate and validate these findings, the indicative airmass modelling suggests

atmospheric MP to travel extended distances and to occur in the FT. These findings have implications for the planet's wild places, transporting this now contaminant (and potential pollutant) far beyond its source location. It also indicates a potential risk to environment and human health due to the possibility of adsorbed chemicals and bacteria/virus being transported and deposited to 'pristine' locations and areas vulnerable to 'exotic' chemicals and bacteria/virus.

5 Examination of the ocean as a source for atmospheric microplastics

Abstract

Global plastic litter pollution has been increasing alongside demand since plastic products gained commercial popularity in the 1930's. Current plastic pollutant research has generally assumed that once plastics enter the ocean they are there to stay, retained permanently within the ocean currents, biota or sediment until eventual deposition on the sea floor or become washed up onto the beach. In contrast to this, we suggest it appears that some plastic particles could be leaving the sea and entering the atmosphere along with sea salt, bacteria, virus' and algae. This occurs via the process of bubble burst ejection and wave action, for example from strong wind or sea state turbulence. In this manuscript we review evidence from the existing literature which is relevant to this theory and follow this with a pilot study which analyses microplastics (MP) in sea spray. Here we show first evidence of MP particles, analysed by µRaman, in marine boundary layer air samples on the French Atlantic coast during both onshore (average of 2.9MP/m^3) and offshore (average of 9.6MP/m^3) winds. Notably, during sampling, the convergence of sea breeze meant our samples were dominated by sea spray, increasing our capacity to sample MPs if they were released from the sea. Our results indicate a potential for MPs to be released from the marine environment into the atmosphere by sea-spray giving a globally extrapolated figure of 136000 ton/yr blowing on shore.

5.1 Missing plastic in the marine microplastic models

Since the first evidence of anthropogenic plastic litter affecting sea birds in the 1960's (*4*, *183*) there has been a steadily growing awareness that plastics are becoming a major pollutant. According to the plastic industries figures, around 359 million tons of plastic was manufactured globally in 2018 (up from 334 million tons in 2016) (*184*), of which 60 million tons were produced in Europe. Mattsson et al. (2015) estimate that around 10% of all plastic produced is lost to the sea each year (*119*). A 2010 estimation suggests between 4.8-12.7 million tons of plastic entered the oceans from coastal and terrestrial areas, with up to 92% of this being <4.75mm in size (*185*).

That this figure is now 10 years old and as around half of all plastics produced has been in the last 15 years, it is likely that figure would significantly underestimate current levels (*186*, *187*). A 2015 estimate by van Sebille et al. suggests 93000-236 000 tons of plastic floating in the world's surface oceans (*188*). Koelmans et al. (2017) (*189*) simulations suggest 99.8% of oceanic plastic has sunk below the ocean surface layer (OSL), however this figure is primarily based on the plastic not being visible or identifiable in surface samples. Various oceanic plastic transport models created, such as Maximenko et al.(2012) (*190*), van Sebille et al. (2015) (*188*), Jambeck et al. (2015) (*99*) and Wichmann et al. (2018) (*191*), make mention of "leaky basins" to explain areas that do not contain the plastic concentrations or quantities the models predict. In spite of the great effort to model oceanic plastic transport and sinks, there does not seem to be a definitive answer for the missing plastics and considering the potential for atmospheric plastic to be depositing in the ocean, the missing plastic quantity could be much greater

The ocean or marine environment is generally been considered a microplastic (MP) sink, with cities, human activities (including waste mismanagement) and industry being primary MP pollution sources. Early transport studies have identified MP moving from cities to rivers, rivers to sea and most recently atmospheric transport of MP across terrestrial environments and out to sea (*11*, *32*, *34*, *163*). With the emergence of atmospheric MP monitoring comes the acknowledgement of local to long-distance atmospheric transport and the potential for MP to reach even remote locations (marine and terrestrial). However, to date there has been no consideration of the oceans as an atmospheric MP source. This research seeks to determine if MP could be leaving the ocean through marine boundary layer interaction with the ocean surface layer. This unexplored secondary source of MP (the sea) and transport pathway (ocean to atmosphere exchange) could help identify at least some of the missing plastic pollution identified in the global marine models. It could also help explain, in part, the occurrence of MP in the air sampled extensive distances offshore (marine air samples (*34*, *163*). While anthropogenic terrestrial atmospheric MP sources are known, and inroads to quantifying their MP emissions are being made, this analysis and pilot study aims to identify if the ocean is a marine MP emission source and take the first steps towards quantifying the influence of this on

terrestrial airmass MP. In addition, we discuss the potential impact of MP emissions.

5.2 Ocean to Atmosphere particle transfer processes

There is evidence that MP is making its way to some of the most remote corners of the globe though limited discussion has been made on how it got there. Given the current state of this knowledge we propose a hypothesis on a previously unexamined potential transport vector to advance the discussion. Most marine particles (non-MP) are sea salt (SS) and organic material. Every year approximately 6700-7400Tg of sea salt aerosols (SSA) and organic matter from a few nanometres up to ~20 µm are produced by wave/wind/interaction which are then transported into the atmosphere through convective updrafts (*192*, *193*). Under normal conditions micro and nano size salt particles are ejected from the sea when breaking waves cause bubbles of trapped air to rise to the surface and burst (*194*) (Fig 1a). The bursting of the unsupported surface of the bubble leaves nano sized particles expelled and suspended in the air available for wind transport (*195*, *196*). With the surface bubble removed the water seeks to fill the void left by the bubble, collision of water from all sides causes the secondary ejection known as a jet to eject the larger micro sized particles (*197*) (Figure 10). This phenomenon also ejects organic matter which is an important element in cloud formation and precipitation rates (particularly in warm air) (*198*, *199*). Bacteria and virus cells have been well documented traveling in wind and as aerosols across continents and oceans (*200*) and these organisms have been reported to exit the sea in a similar fashion to SSA (*201*).

There is a potential for upwelling, through Ekman's transport, Langmuir spirals and surface gravitational waves drawing water from as deep a 200m below the surface (*202*), to act as a form of MP supply to the surface and bubble burst ejection process. Most marine particles (non-MP) are sea salt (SS) and organic material. SS are ejected droplets/aerosols and are infinitely available whereas organics are produced in the OSL and are not directly dependent on upwelling supply. MP in contrast can often be found in greater quantities below the surface (*203*) and the mixing of the surface and deeper marine waters, and associated upwelling processes, may be influential in the availability of MP (*204*).

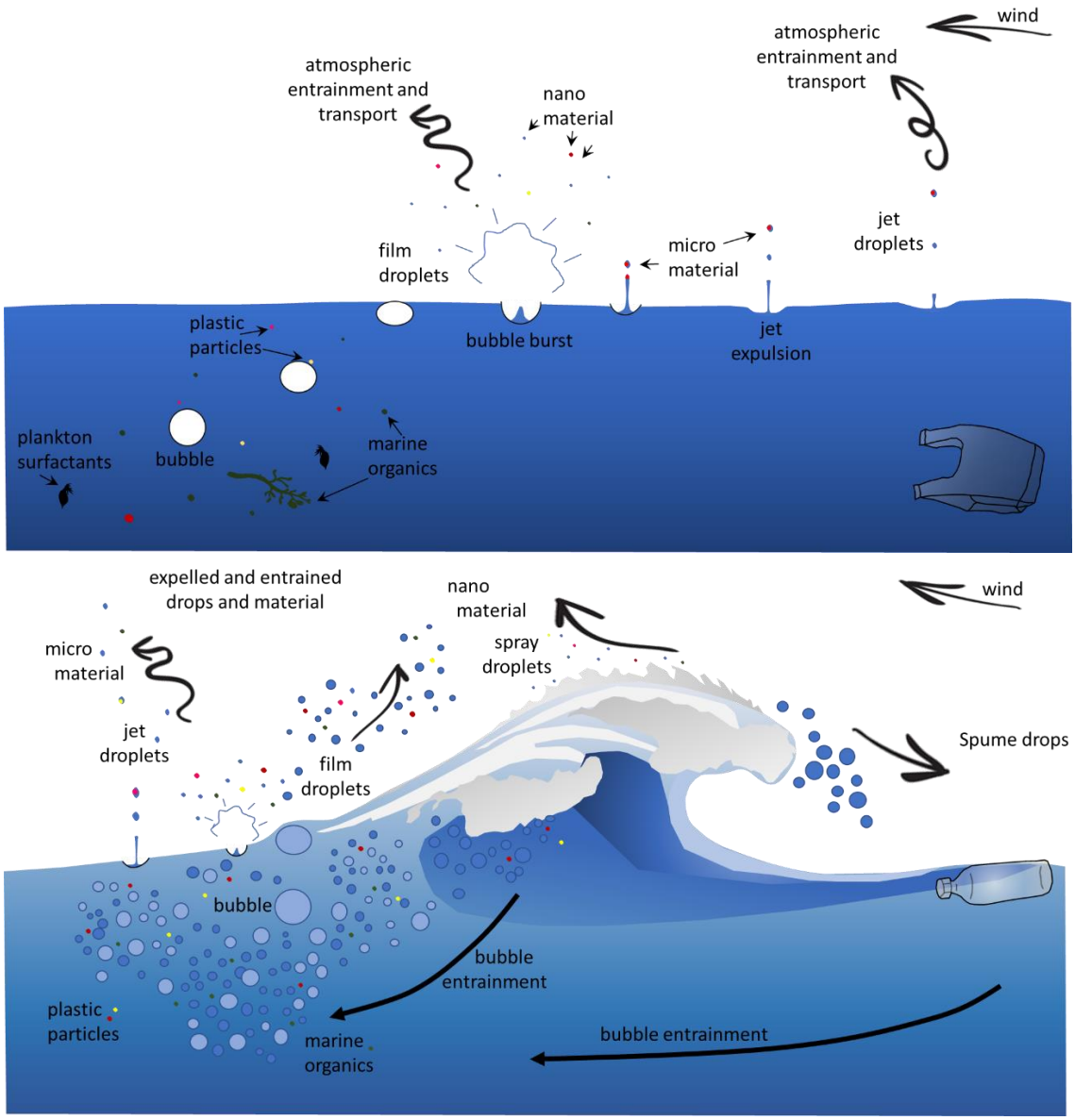

Figure 10. The established SSA and organic matter ocean to atmosphere bubble burst (a) and wave exchange (b), and the potential micro and nano plastic exchange process mimicking these processes.

5.3 Atmospheric microplastic

To date there have been very few atmospheric MP studies. Of the studies undertaken, presented in recently published reviews (*205–207*), it is noted that MP particle of fibre, film, foam and fragment shapes have been found in atmospheric deposition and sampled air masses. MP sizes range down to 10µm (lower limit of detection published to date) and up to 5mm but with a greater proportion of sampled particles <500µm (*205–207*). Atmospheric MP has been sampled by deposition and active air mass (pumped) sampling, presenting up to 1008 MP/m^2/day deposition (*162*) and 60 MP/m^3 in air mass sampling (*43*).

Several studies have considered city MP deposition, identifying types and quantities of atmospheric MP deposition in locations including Paris, Dongguan, Shanghai and Hamburg (*8*, *32*, *43*). Only a few studies have considered remote location MP deposition and a precursor to MP long-distance transport analysis; Tibetan plateau, Arctic snow, Pyrenean Mountains and west Pacific Ocean (*11*, *34*, *73*, *205*). Only the study of Pyrenees Mountain MP deposition considered and attempted to model atmospheric transport (*11*) based on MP deposition findings in the field.

Dris et al. (2016) describe fibres as large as 600µm and smaller than 50 µm collected from atmospheric fallout in the mega-city Paris, France. Their study describes collecting fibres sub 50µm however they did not have the ability to accurately identify the plastics below this level, thus they were excluded from their overall analysis. The source of this fallout was not examined.

The study by Cai et al. (2017) at three locations around Dongguan city in China revealed continuous fallout of MP particles and fibres over the three months of autumn/winter in 2016. The study found 175-313 MP particles m^2/day (~ 100µm or larger) of which the vast majority was fibres (>90%) (*8*). Tentative recognition of weather influence is included but no examination of MP source beyond assumption of urban production.

Klein and Fischer (2019) also studied the deposition of MP in and around Hamburg, Germany (*32*). This passive atmospheric deposition study was the first to compare the influence of urbanisation on atmospheric MP deposition through direct urban/rural sample comparison. The study's findings present surprising data on the topographical effects on deposition numbers; rural (open field and forest, ~396 MP/m^2/day) sites illustrating greater MP deposition counts (MP>50µm) than the urban areas (~215 MP/m^2/day) (*32*).

Research by Bergman et al. (2019) (*73*) on MP content in snow illustrates MP pollution to have reached remote uninhabited locations, specifically the Arctic. Arctic samples, collected from snow deposition on ice platforms within the Fram Strait, were located ≥100km from land (Svalbard, Norway). They state that the snow contamination is atmospheric, propose that MP (>11µm, ~1760 MP/L snow) could be scavenged by snow formation and that MP are potentially arriving in these remote locations via atmospheric transport (*73*).

In 2016 Zhang et al. found MP in remote lake beaches on the Tibetan plateau (*10*). Their research states the area is rarely visited by humans so could not explain the presence of MP. Their samples showed surface cracking and gouging of plastic particles that they felt was possibly caused by sand particles as the MP moved through the environment by wave action/saltation. The material abraded from the scratches on these <2mm MP particles could be plastic debris in the nanometer scale, <1µm (*10*). Corcoran et.al. (2009) similarly found what they termed “beach weathering”, surface abrasions and cracking consistent with environmentally induced collision alongside ultra violet light degradation, to be a significant factor in the breakdown of plastics in their study of MP on Hawaiian beaches (*208*). Lambert and Wagner (2016) demonstrated the breakdown of plastics to the nano scale by simulated sunlight in the laboratory yielded nanoplastic (NP) from polystyrene cup lids in just 56 days (*209*). The breakdown of MP to NP by sunlight is a very real phenomena and coupled with wave action and abrasion to accelerate the process, could mean an increased number of available NP particles in the environment as larger plastic items break up over time (*117*, *210*, *211*). In conjunction with UV, abrasion and temperature MP degradation to NP, emerging research also illustrates aquatic biota’s degradation effect. Plankton such as Antarctic Krill have been shown to cause MP degradation to NP by their digestion processes (*212*), *Zalerion maritimum* (a marine fungus) in laboratory conditions were found to decrease both the mass and size of MP (PE pellets 250-1000µm). There are both mechanical and biological MP to NP degradation pathways within the marine environment that may make these smaller particles available in greater quantities.

Cooper and Corcoran (2010) provide detailed descriptions of weathering effects on plastics on beaches which closely matches those described by both Zhang et al. (2016) and Cai et al. (2017). Cai et al. (2017) acknowledged the Cooper and Corcoran (2010) findings on weathering suggesting that plastics may have been transported to the sea by wind. It is perhaps just as possible that the plastics were transported by wind from a building site in the area and the abrasion is simply caused by the workers activities or vehicle traffic. This is certainly plausible for beaches or sites near population centres similar to Cooper and Corcoran’s (2010) Kauai Hawaii beach study, however less viable when presented by Zhang et al. (2016) findings on a remote Tibetan plateau.

During the period of the Cai et al. (2017) study there were several significant weather events which may have affected the material available for atmospheric fallout; three severe typhoons affected the area in October (*213*), cold fronts and easterly winds through November (*214*) as the North-easterly Monsoon sets up and the two further typhoons in December (*215*). Severe typhoons in the China Sea entrain large amounts of sea salt and organic debris into the atmosphere and produce large wave action on the shoreline. These significant marine weather conditions suggest the need to consider possible MP atmospheric transport and source scenarios beyond microclimate urban MP generation. One possible scenario is that wave action on the shoreline together with strong winds from the typhoons entrained and carried MP particles from the beach to the city sites, ~115km inland. We know from the Allen et al. (2019) (*11*) study that MP particles can be transported over *at least* the medium distance which could link the China Sea atmospheric MP pollutants to the city of Dongguan. Another possibility is that the offshore weather conditions could have atmospherically entrained the plastics alongside the organic matter and SSA (that is normally found in the atmosphere post strong wind events) (*216*, *217*), producing (part of) the fallout found by Cai et.al. (2017) in Dongguan. In either of these latter scenarios it seems there is potential that the degraded particles Cai et al. (2017) found, MP that were similarly degraded to beach plastics, were similar because they may have come from the sea.

Paris is approximately 150km from the sea and in a very different climate to Dongguan. Paris does not experience Typhoons or monsoonal troughs. It does however experience a predominantly onshore wind from the North Sea/Atlantic Ocean, especially strong through winter (*218*). The findings of Dris et al. (2016) showed that the winter months received generally more deposition (with the notable exception of June) (*79*). The ground in winter is damp or snow covered reducing the likelihood of dust or plastic being atmospherically entrained. Potential sources for city fallout are likely to be local or regional land based for the vast majority of this recorded fallout, and the specific urban radiative microclimate hinders comparison at this early stage of investigation.

The marine air sampling campaign published by Liu et al. (2019) (*34*) is an illustration of long range transport and deposition of MP into the sea. Samples, taken along a transect from Shanghai to the Mariana Islands (west Pacific Ocean)

at an elevation of 10m above sea level, showed MP up to 1.37MP/m^3 (>16µm) (*34*). Given the sampling locations (mid-ocean and close proximity to sea surface) there is a high likelihood of SSA and marine organic material that have been released from the sea are on these actively pumped samples. The study found more MP close to the coast, as would be expected, but also found particles at 600 nautical miles from land. It is possible that the particles were blown from land but there is also a potential for (part) of the MP found in the marine air to have come from ocean-to-atmosphere MP exchange in a similar manner to SSA.

The importance of the potential for MP or NP to act in a similar way to SSA is that the potential ocean-atmosphere exchange identifies the earths ocean surface as a possible atmospheric plastic pollution secondary source (a sink that becomes a source through bubble burst ejection and wave action). Once airborne (expelled from the ocean via bubble burst or jet ejection) MP or NP may function in a similar way to dust and salt particles (*98*), acting as cloud condensing nuclei (CCN) for ice or cloud nucleation (*80*, *219*). Once airborne, dust, SSA, bacteria and sand are all known to be rained out (incorporation of particles within cloud droplets) or washed out (collision with precipitation below cloud level) of the atmosphere. If micro or nano plastic particles are similarly atmospheric it is possible they may be similarly affected (at least by the latter process) taking any adsorbed pollutants with it (*144*, *220*). Currently the surface charge and how it could affect dust scavenging by particles is an unknown. It could be possible the triboelectric effect (*98*) of air passing over the plastic will statically charge the particle and make it attract dust. Van der Does et al. (2018) (*221*) suggest this effect could assist particles to remain aloft. The triboelectric effect may also potentially increase plastic particle's potential to be entrained after ocean expulsion (bubble burst/jet expulsion) and transported, similar to ultragiant dust (*98*). This would create larger particles and potentially change the hydrophobic nature of the particle. If MP or NP act as CCN, they may add to the total atmospheric loading of CCN, which could influence albedo and global radiation budgets (*198*, *220*). Cloud coalescing nuclei do not have to be hygroscopic in nature, their presence is often enough to be a factor in the formation of clouds (*220*). As illustrated in recent research by Ganguly and Ariya (2019) MP and NP have a high ice nucleation efficiency and may be important for cloud formation (*80*). While this is theoretical and speculative, the potential for ocean-atmosphere exchange similar to SSA is a first step to the greater questions on the impact of atmospheric MP/NP.

5.4 Laboratory based theory test of MP ejection from water

Testing of the possibility of MP ejection from water was carried out based on similar experiments by Modeni et al. (2010) (*222*) on organic material ejection, however in a much simplified setup. The primary goal was proof of concept, that MP could be ejected from a water body through bubble burst ejection. It should be noted that the experimental design did not aim to quantify MP ejection rates but aimed to evidence the theory and a possibility in nature (field environments).

A water tank, air bubbler and imaging station was created to visually establish if MP could undertake 'ocean' to atmosphere transmission through bubble burst ejection activity (Figure 11). The experimental setup relies on the fluorescence of MP due to their chemical composition by specific light wavelengths. This results in MP particles fluorescing visibly in a darkened environment while other material (water, air, dust, metal, salt) do not fluoresce and therefore remain 'invisible'.

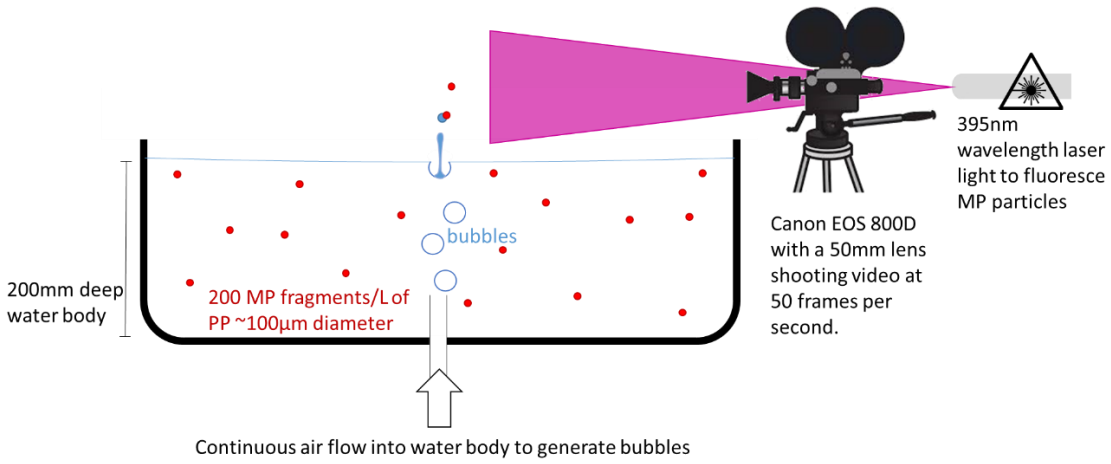

Figure 11. Schematic of bubble burst ejection laboratory theory test (not to scale).

A shallow 200mm high tray was filled with water. The initial test used standard tap (municipal) water to ensure the experimental setup was functional, but for the purposes of ocean to atmosphere theory saline water with the same salinity of seawater was used.

A metal (stainless steel) tray was fitted with an air inlet on the base and placed in a blackout room (no lighting). A 395nm wavelength light was stationed adjacent to one side of the container and focused so that the laser shone along a horizontal path approximately 20mm above the water surface (aiming from one side of the tray to the other). A camera, set to collect 50 frames per second, was stationed alongside the laser and focused to the centre point above the air inlet and laser

path (the centre of the tray, approximately 200mm above the water surface). The laser and camera were set to function continuously.

A saline water mix was created to represent sea water. 3.5L of standard (tap) water was mixed with sodium chloride (salt) to create a saline solution (salinity ~35000ppm, approximately 35g salt (dissolved)/kg water, ~22 ˚C). 100µm polypropylene microplastic particles were manually milled from a virgin macroplastic PP article. PP particles were checked for size using a micrometer grid slide (microscope slide with etched scale) and microscope. 0.27mg of PP particles (~200MP/L at 100µm diameter and 0.86g/cm^3 density) were then added to the saline water mix and mixed thoroughly.

The saline+PP water was then poured into the metal tray in the blackout room. Air was pumped through the air inlet at the base of the tray at a continuous rate of 0.1L/min (as in (*222*)). The laser and camera were activated and all bubble and MP activities recorded over 3 minutes, repeated 8 times to ensure effective capture and replicability of visualised findings.

5.4.1 Early findings from laboratory based bubble burst ejection tests

Images were then viewed in slow motion to identify 1) if PP MP were effectively visible using the 375nm wavelength laser experimental setup; 2) if bubble burst activities occurred; and 3) if MP ejection through bubble burst jet ejection occurred. It was found that PP particles effectively fluoresced (luminous, white particles with a purple ‘jet stream’) under a 375nm wavelength laser, while the metal tray did not and water (when in the direct line of the laser) presented a low level purple shade (Figure 12).

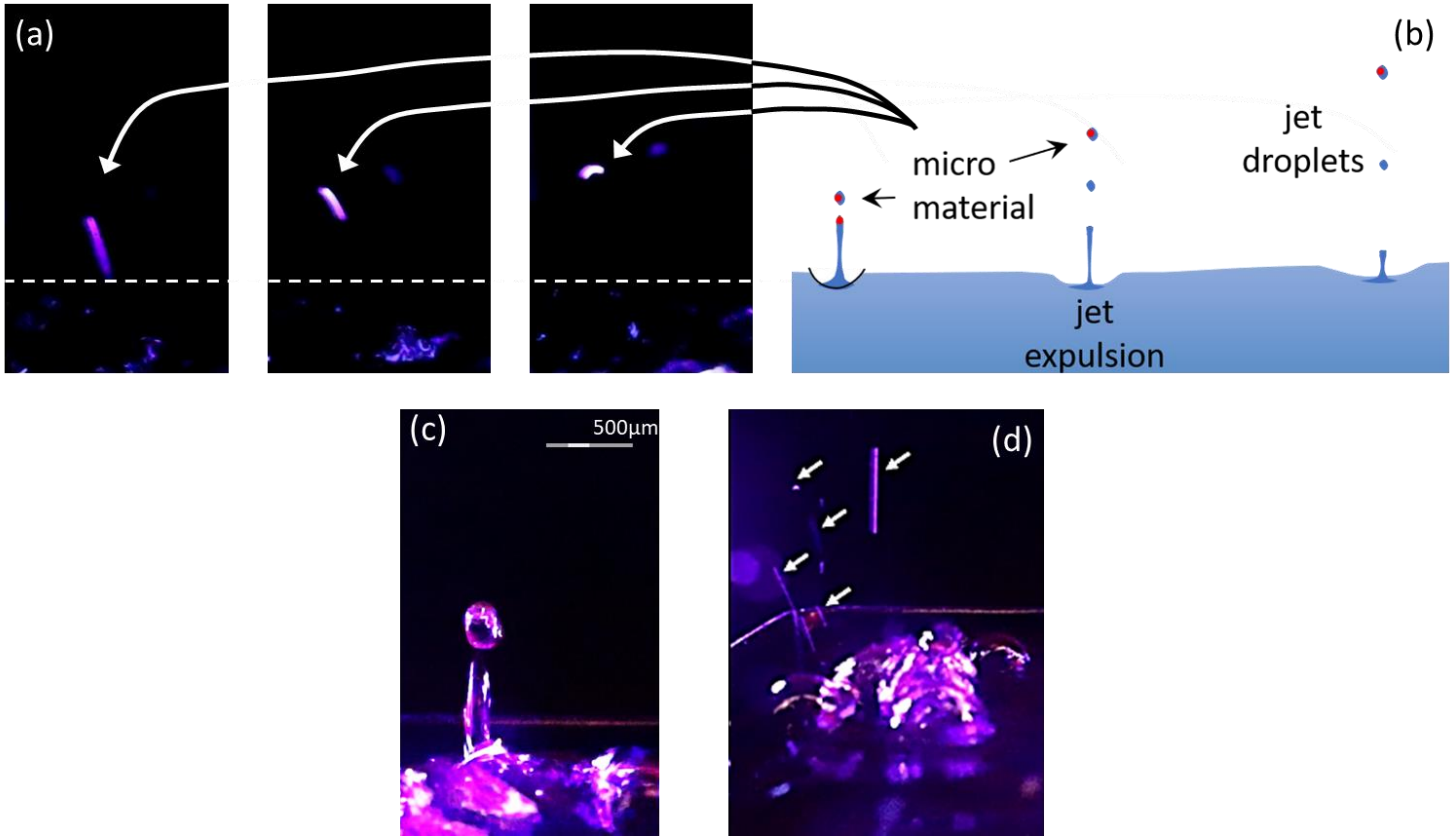

Figure 12. Image of a fluorescent microplastic fragment (PP, ~100µm) being ejected from a water body by jet expulsion. The fragment is illuminated using an ultraviolet light (395nm wavelength) in a darkroom. The water body (standard tap water spiked with 100µm PP fragments at approximately 200 fragments/L) is indicated below the dotted white line. Ejection bubbles were created through manual aeration of the waterbody. Images are still frames captured using a Canon EOS 800D with a 50mm lens shooting video at 50 frames per second.

The microplastic particles used in the laboratory experiment were comparatively large compared to atmospheric microplastic findings of previous research (Chapter 2-4, MP is often 10-20µm in particle size, but ranging up to 300µm). Therefore, the ability of the bubble burst jet propulsion to convey the artificial 100µm MP out of the water in this simple laboratory experiment is erring on the side of conservatism and transfer of smaller MP particles could be more easily achieved.

It is noted in the laboratory study by Fuentes et al. 2010 (*223*) that increased water turbulence and movement can result in a greater number of bubbles created. This work illustrates there also appears to be bubble size distribution, with bubbles occurring in the 30-80µm ranges, and a second preferential larger bubble size created at 200-600µm, but with bubble sizes ranging from <10-1000µm. Bubbles greater than 3mm don't appear to create aerosol or jet ejection effectively (*223*, *224*). These bubbles correspond to film aerosol sizes of <3µm, with jet aerosol sizes of <10-35µm up to ~300µm (ranging from ~400µm down to <5µm) (*223*). Film droplet number (number of droplets generated from bubble surface burst) is directly related to bubble size and inversely related to film thickness (*224*). Published field sea spray data concurs with these laboratory findings, presenting aerosol sizes from bubble burst ejection actions between 300µm down to ~5µm and illustrates a bimodal predominant sizes of ~30µm and ~150µm.

The visual captures, illustrated in Figure 12, show bubble burst and jet ejection of water droplets and particulates (Figure 12c zoomed in image of a jet, Figure 12d over-exposed, low zoom image of multiple jets and ejected particles (indicated by the arrows)). Sizing of the jet ejection bubbles was limited due to the experimental setup and equipment limitations, however visually monitored jet ejection bubbles were estimated to occur between 50-500µm. Visual sizing of the film droplets created in the initial bubble burst was not possible in this experiment.

The experiment illustrates that MP particles are ejected as a result of bubble collapse and jet ejection (white fluorescent points in Figure 12a). A representation of bubble burst activity and MP water-to-atmosphere transmission was found in all repetitions of this experiment, confirming the validity of the theory in controlled conditions. The laboratory test confirmation of MP particles transition from saline water to air enabled the field testing to commence with a level of confidence.

5.5 Field exploration of MP in sea mist – as a possible indicator of ocean MP transfer to atmosphere

A pilot investigation into sea spray and mist was conducted in field environmental conditions. The field test was designed as an indicative early look towards identifying if MP were occurring in expelled sea water droplets and if these were in the onshore blown sea air and mist (Figure 13).

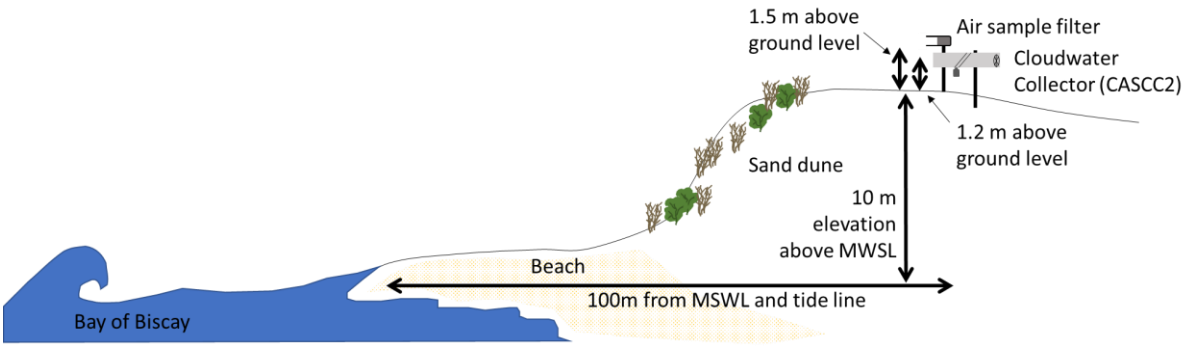

Figure 13. Schematic of field site activities. (Field site location details provided in Appendix 14.)

Sea air was sampled on the French Atlantic coast from a height of 10m above MLWS (mean low water springs) for a period of 8 days. The site was on top of the first dune of Mimizan beach in the Aquitaine region, best known for its surf (44.219N, 1.297W). The site is open to the Bay of Biscay and was ocean facing from north to south via the west, without local island or land mass interference. The study took place at the end of Autumn 2018 at a time when the number of beach goers was minimal, and the meteorology is the most volatile (westerly onshore storms).

Two separate air sampler types were employed in an attempt to find the most effective system to sample sea mist and onshore airmass. Both samplers were located on the top of the dune, with the dune height noted to be 10m above sea level. The first was a standard 50L/min active air pump with a 47mm diameter circular capture area and quartz filter (Millipore QMA) placed 1.5m above ground level (height of stand was 1.5m resulting in a sample elevation of 11.5m above sea level due to the dune elevation (10m) above the sea (high tide)), providing

an average pumped volume of 18m^3/sample. The second was a Caltech Active Strand Cloudwater Collector (CASCC) (*225*) (cloud catcher). The CASCC2 used in this study includes a 220v fan driving air over teflon filaments which trap water droplets and direct them into a glass bottle. It was designed to capture airborne droplets in clouds/fog at 80% efficiency for >10µm droplet size (clouds/fog droplets average 10µm-30µm) (*225*), however it was used in this study as a possible way to capture particles suspended in sea spray fog. The CASCC2 was placed at 1.2m above ground level (height of stand for fixing,), resulting in a sample elevation of 11.2m above sea level. The CASCC2 was run at 5.8m^3/min (an average pumped volume of 6401m^3/sample). Corresponding sea surf water samples were collected during this period in sterilised glass bottles. Both the CASCC and pumped air sampler have been used to collected atmospheric particle samples and have standardised sampling and verified efficiencies. Air particulate monitoring using the quartz filters and active air pump method have been used marine aerosol sampling (*34*, *163*) and the CASCC system has been used to collect cloud water and fog from mountain and valley locations (*226–228*).

Quartz filters were changed daily on the air pump and the litres of air pumped noted from the inline gas volume meter. The cloud catcher receiving bottle was also changed daily at the same time as the quartz filter. Field scientists always wore cotton clothing and stayed down wind of the equipment at all times. Blank filter material was placed in the filter cartridge in the same manner as the samples but without the pump running and removed for later analysis alongside the samples. Cloud catcher receptacle blanks were created using a sterilised glass bottle which was installed then removed without the fan running. Sea water was collected from the surf zone daily using a 2.5Lt sterilised glass bottle plunged into the surf zone at midday. The sea water sample was taken from approximately the same location each day in 0.5m deep water and the bottle was filled to capacity (2.5L). The bottle and cap were rinsed with sea water three times prior to filling to limit contamination.

Wind direction and weather conditions at the monitoring site were noted throughout the sampling periods and compared to the meteorological monitoring station at Mimizan. Mimizan local meteorology was collected from the MeteoFrance data repository (*229*).

All samples collected were processed following published digestions methods (*11*) to remove organic material from the samples. µRaman spectral analysis can be affected by biofilms or other contaminants thus it is important that material undergo a digestion process to remove unwanted organic matter(*230*).

Sea water samples were vacuum filtered onto Whatman 10µm cellulose filters using glass filtration equipment (triple rinsed with milliQ ultrapure water) to collect all MP and other material of 10µm or greater. Liquid collected from the cloud catcher was similarly filtered onto PTFE 0.45µm, 47mm to collect all particulates. All filtered material (from sea water, cloud collector and active air pump filters) underwent organic material removal via digestion. Filtered material was flushed into borosilicate glass vials with approximately 10ml of hydrogen peroxide (H_2O_2 30% by vol). Samples were then capped with foil and heated to 55°c in a heat block for 7 days. Active air pump and cloud catcher samples were then filtered onto aluminium oxide (Anodisc) 0.2µm (25mm) filters for analysis by µRaman spectroscopy. Sea water samples underwent an additional step of density separation before final filtration, to remove all sand and sediment. Sea water samples were density separated using zinc chloride (density 1.6 Kg/L) in density separation tubes, gently agitated at 60rpm on an agitation table for 5 days. Settled material was drained off and the remaining liquid and material filtered onto Whatman 0.45µm cellulose 25mm discs for µRaman analysis (acceptable for sample of MP≥10µm diameter). The CASCC2 and air pumped samples did not present significant visible airborne dust, potentially due to the short (24 hour) sampling period, and therefore the additional density separation step was not used for these samples.

All filters were analysed with an Horiba Xplora-Plus µRaman following protocols and settings used in Allen et al. (2019) (*11*). Full procedure blanks for all sample types were run alongside the samples and their results subtracted from the described MP counts (Appendix 13).

5.6 Early findings of MP in sea mist

5.6.1 Air mass and sea spray aerosol droplet MP counts

The first two days (A1, A2) of sampling had strong onshore winds with heavy rain. The following two days (A3, A4) the wind eased substantially but remained

onshore, the rain ceased however a light sea spray fog was present from the surf zone. Day 5 (A5) commenced with a light onshore sea breeze and accompanying sea mist, but wind swung round to become offshore at midday and throughout the afternoon. Days 6 through to midday day 8 (A5-A8) were influenced by offshore winds. However, late on day 8 a sea breeze convergence set up over the beach allowing for <1 m/s onshore breeze to push sea spray mist from breaking waves onto the beach (A8a). The mist was visible as a local phenomenon; it was possible to see extent of the mist inland (~500m), offshore starting at the first line of breaking waves (glassy sea beyond) and vertically (~20-30m AMLWS). The Mimizan meteorological station recordings are collected several km inland from the site. During the sea spray mist event (A8a) the MeteoFrance station showed ≥4m/s offshore winds, while beach recording indicated westerly (onshore) winds of less than 1m/s. In such a sea breeze convergence the onshore sea breeze cancelled this inland offshore wind movement, resulting in a classic sea breeze convergence occurrence of onshore dense marine air movement (*231*). This microclimate provided an opportunity to sample only sea spray without significant wind influence or inland airmass contribution. The local wind was too light to support plastic entrainment off the beach and therefore suggests a true sea sourced aerosol sample. While the presence of some beach sourced MPs in our samples cannot be ruled out, the results do not illustrate an increase in MP numbers with increasing onshore windspeed, therefore it is unlikely that MPs sourced from the beach are being entrained significantly in our samples in. Moreover, during the period of increase MP counts due to sea pray (A8a), the wind speed is low (<1m/s), thus again this indicates entrainment of beach MPs are not influencing our results.

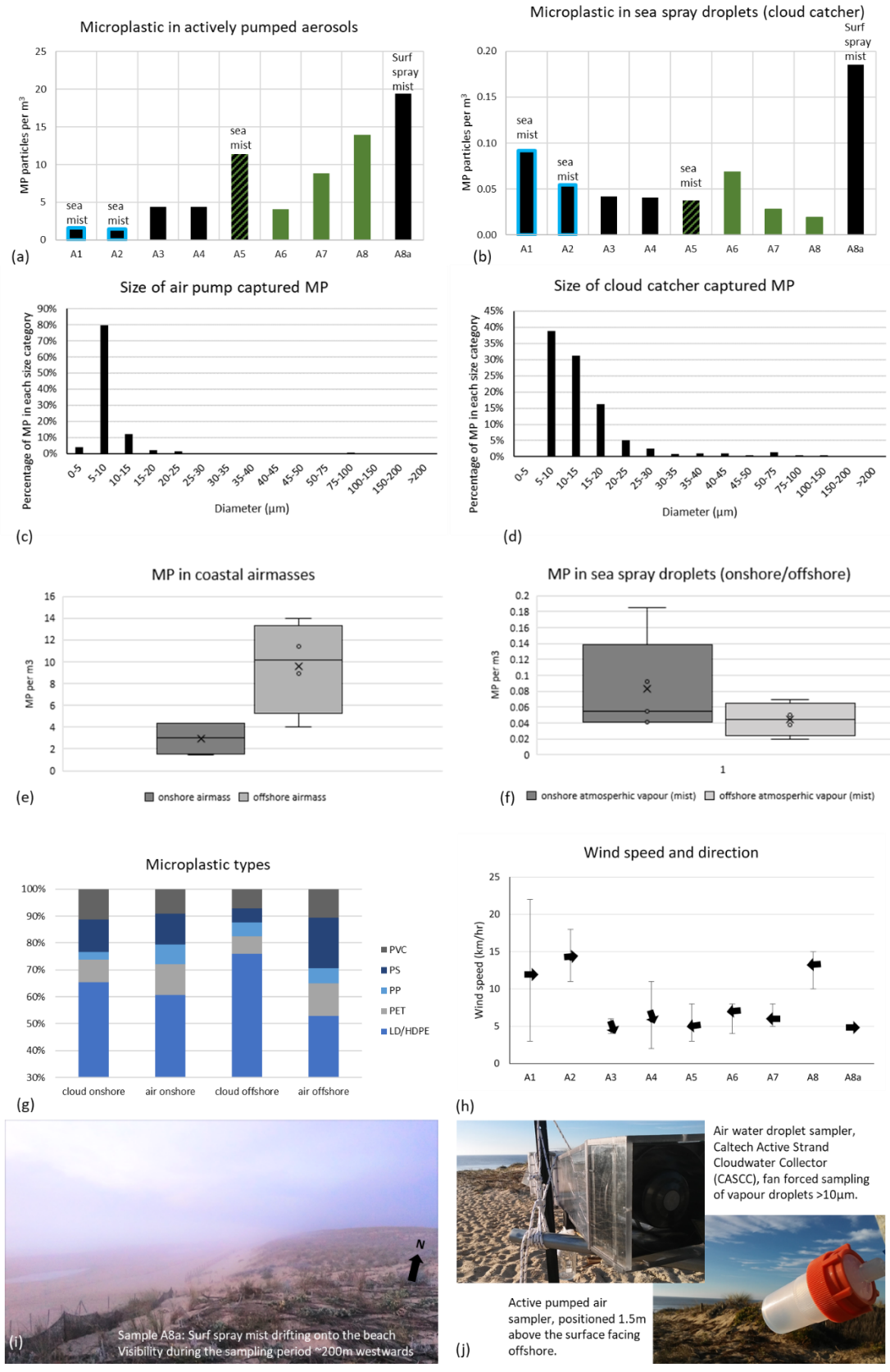

Figure 14. Sea mist and air mass microplastic counts for onshore and offshore wind and dense sea mist daily samples. Figure 15a and 16b highlights days with rain using a blue outline. Days with onshore wind are presented in black, offshore

wind samples are presented in green. The final sample A8a presented very low onshore wind, with sea mist annotated on the figure. Figure 17b and c present the MP particle size for the relative samples. Figure 18h illustrates recorded average wind speed and direction (arrows) and the maximum and minimum wind speeds (error bars). Figure 19e and f illustrate the onshore (ocean) sourced atmospheric MP compared to offshore (land-based) MP counts. The sample collectors, both standardised atmospheric sampling designs, are illustrated in 20j. Microplastic types and found represented in the samples (aerosol and droplet) are presented in 21g. MP per m^3 refer to the respective volume of air sampled.

Total for both pumped air and cloud catcher size ranges were average 20µm (+/- 13µm) ranged between 5µm to 140µm. Particle sizes recorded from pumped filters using ImageJ software ranged between 5µm to 38µm with an average of around 13µm (+/- 4µm). This is surprising when compared to other atmospheric MP studies however this study used pumped air and not total deposition collectors which may explain the difference. It is possible the pump rate was insufficient to hold the larger and heavier particles and fibres. The largest particle captured by the cloud catcher was 140µm with a minimum of 8µm and an average 24µm (+/- 14µm) which suggests that low volume pumped filters may be underestimating particles size.

The CASCC2 cloud catcher MP levels in sea spray droplets during onshore wind conditions were found to be at least an order of magnitude lower (0.06±0.05, mean, 1σ, n=9) than actively pumped total aerosols levels (7.7±6.1, mean, 1σ, n=9), on a per m^3 air basis. The design of the cloud sampler is to collect only material within atmospheric water droplets. Water droplets >10µm were collected by Teflon strings located ~50µm apart, with a collector efficiency (for water droplets) of 80%. As a result, the CASCC2 collected only MP that were within the water droplet fraction of the air mass. The quantities of MP found in the water droplet samples are therefore lower than the total airmass MP collected on the quartz filters. It is worth noting (as expected given CASCC2 designed function) that the CASCC2 retained more MP particles on days of high humidity (Figure 14c) and there is consequently a correlation between humidity and MP counts.

MP was found in all samples taken throughout the study with the sea spray mist event occurring on the last day having the highest count. Lowest air mass counts

were during the heavy rain on the first two days suggesting a potential for plastics to be rained out of the atmosphere (scoured) (Figure 14a). Air water droplet showed higher MP counts during high humidity periods (rainfall periods over the first 2 days and the heavy mist periods on the last day; A1, A2, A8a, Figure 14). The water droplet trend in MP counts appeared to be inverse to the air mass counts, with greater overall air mass MP counts occurring during offshore winds, but greater water droplet MP counts occurring with onshore winds and sea mist/spray. The exception occurred with the final sample, comprised primarily of dense sea spray, A8a, where both air mass and water droplet MP counts rose notably. It is however noted that replicate samples were not collected (not possible) during this pilot study and as such the variability within a day cannot be compared to the variability between days with different weather conditions.

5.6.2 Comparison of air mass, cloud droplet and sea surf MP counts

The quantity of MP found in the sea surf water, collected at high tide each of the monitoring days, was determined to allow simple comparison between the air mass findings and sea surf MP quantities. The MP in the air mass and droplets (cloudcatcher) is not necessarily expected to come solely from sea spray occurring directly in front of the monitoring location, it could also come from bubble burst ejection in turbulent sea states further out to sea-as far as the Atlantic Ocean. However, comparison of local sea surf conditions can provide an insight into the potential sea-sky link in sea spray aerosol MP.

Sea surf and air mass MP counts show a positive correlation, with elevated air mass MP counts occurring with higher sea surf counts ($r=0.66$, $p \leq 0.01$) (Figure 22). While correlation does not equal causation, this trend suggests air mass MP quantities may tentatively be influenced by local sea state conditions, where sea state is a predictor of sea surf MP content and bubble burst ejection activity.

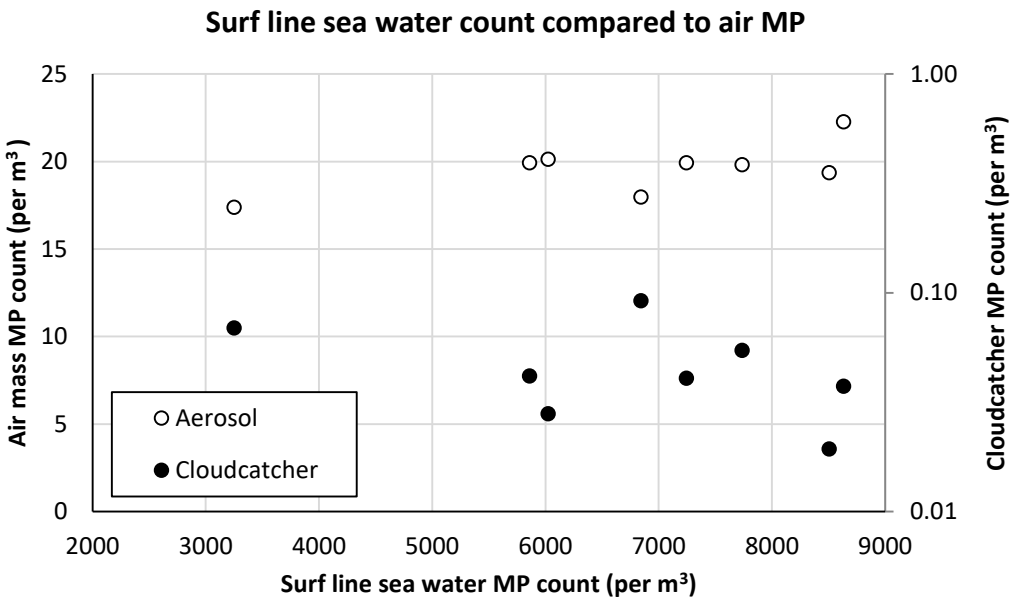

Figure 22. Sea mist and air mass microplastic counts compared to the MP found in the sea surf.

Sea surf MP counts show a low inverse correlation with cloudcatcher MP counts ($r=-0.41$, $p>0.1$) (Figure 22). This could open the discussion of MP lost to atmospheric droplets (cloudcatcher droplet samples) being represented or seen through the sea surf MP count decrease. It could also suggest that the MP in the aerosol droplets (rather than total air mass samples) could have been 'sourced' from sea masses more distal to the monitoring location (not from the coastal surf directly in front of the monitoring site) as well as locally.

The comparison suggests that air mass sampling is a more inclusive method of atmospheric MP analysis, and could be a useful future sea spray aerosol analysis method to further consider ocean-to-atmosphere MP transport. It also suggests a potential comparative trend between sea surf MP counts and aerosol MP counts in the sea spray influenced zone (monitored here). Significant further field monitoring and investigation is needed to advance these considerations, but there may be a, potentially logical, link between the MP quantities in sea surf and the quantity of MP in the sea spray arriving inland.

5.6.3 Comparison of sea surf MP counts to global water MP counts

Sea surf water has not yet been sampled and published to date. There are numerous sea water, lake water drinking and bottled water studies published

showing a wide range of MP counts, from inland low population rivers (e.g. St Louis River USA (<1MP/m^3)) up to highly contaminated sea waters (e.g. Jinhae Bay, South Korea (>50,000MP/m^3)) (*121*, *232*). A recent manuscript, published in 2020 (*233*), provides a comprehensive overview of MP content in the Bay of Biscay (water and sediment).

The quantity of MP particles found in the sea surf is relatively high compared to freshwater river reported values, some open coastal areas, and the reported surface and sub-surface (not surf) MP counts from previous Bay of Biscay surveys (~2MP/m^3) (Figure 23).It is noted that these previously published MP counts were collected through Manta or Neuston net drag surveys and therefore exclude the smaller MP (MP<300µm). This surf sample includes the full range of MP, analysing down to 5µm. This could partially account for the elevated MP values for sea surf spray. However, these results, when compared to previously published findings, suggest that the sea surf zone may be a concentration area for MP, similar to the mid-ocean gyres. This could result in significantly higher MP counts in the surf break and wave action areas of the coastal sea environment, potentially resulting in an effective bubble burst ejection region for MP ocean-to-atmosphere transfer due to the concentration of MP particles and turbulent sea conditions. This comment requires further study and field exploration as analysis of coastal sea surf, as opposed to coastal waters (out of the surf and turbulence zones) have not been highly monitored in a comparable manner, and an offshore to surf zone transect of MP content to illustrate zones of MP concentration (beyond gyres) is still needed.

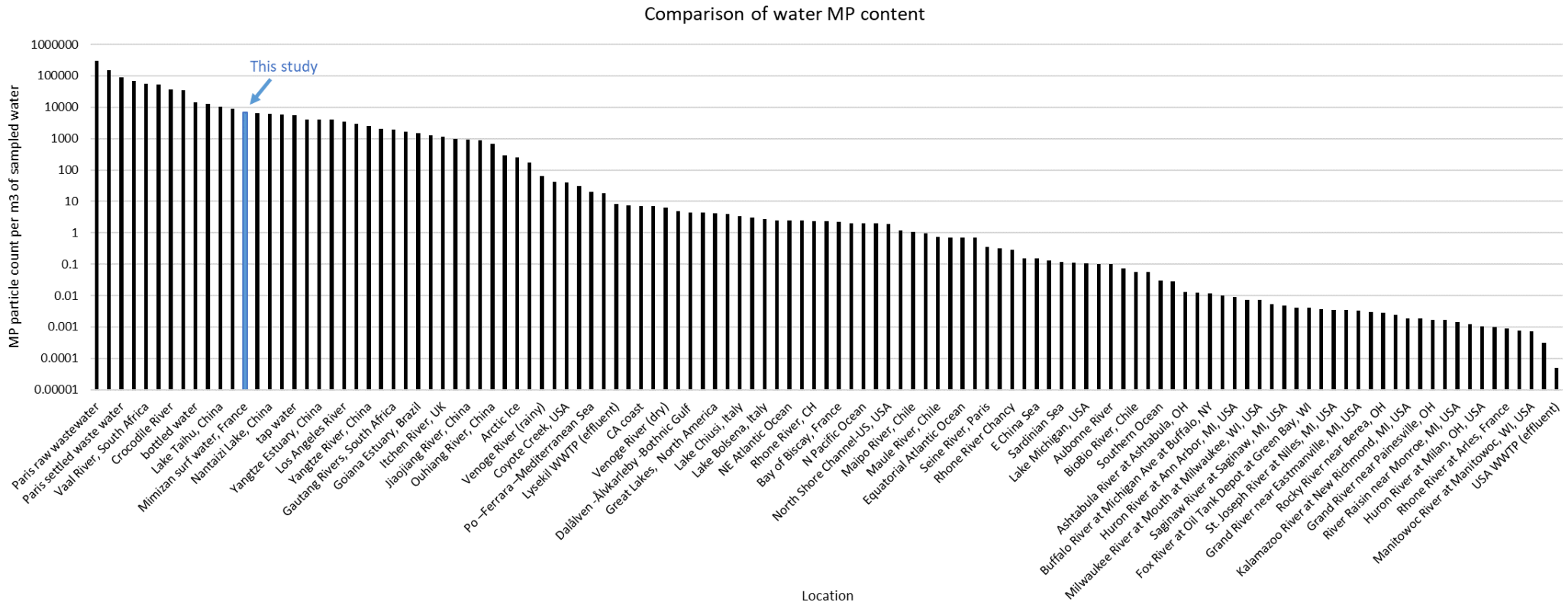

Figure 23. Sea surf MP counts compared to global water MP counts (from lakes, sea and municipal waters)

5.7 Exploratory modelling of onshore blown MP

The existing atmospheric transport and particle dispersal models have difficulty simulating particles that travel close to land or sea surface (i.e. <50 m above surface level) and do not yet include bubble burst ejection of matter from ocean to air processes. However, to help evidence the source of the onshore wind MP particles as occurring from a marine source, HYSPLIT back trajectory modelling was completed to estimate the possible 'starting point' of the collected particles.

To undertake backward trajectory modelling, an estimation of the approximate atmospheric transport duration is helpful (if free falling from an established inversion layer or atmospheric boundary, e.g. the marine boundary layer). To calculate the possible transport duration, particle size, density, shape and meteorological conditions were considered.

Using Stokes Law to estimate particle settling (deposition) velocity and analysed key particle sizes (Figure 14), an estimation of the potential time of flight and atmospheric transport distance can be completed. Stokes Law was used to calculate particle settling velocity following:

$$V = {gr^2(\rho_p - \rho_m)}\Big/{18\mu}$$

Where: Eqn. 5

g = acceleration of gravity (g) (9.80665 m/s)

ρ_p = particle density (1000kg/m^3)

ρ_m =medium density (density of air at ~20˚C, 1.21kg/m^3)

μ = medium viscosity (air viscosity at ~20˚C,1.8x10^{-5}kg/m-s)

r = particle diameter (m)

Settling velocities were calculated for average particle size of onshore blown MP (9μm, ±3), the smallest recorded particle and larger particle sizes (4μm, 35μm). Resultant settling velocity estimates for the 3 particle sizes were 0.0005m/s, 0.0024m/s, 0.0433m/s for the 4μm, 9μm and 35μm particles.

The resulting Stokes settling velocities were then used to estimate the potential duration of travel and possible distance travelled using the simplistic transport

equation described in (*234*) and equation 4 in the 'Atmospheric Transport and Deposition of Microplastics in a Remote Mountain Catchment Chapter.

$$distance = back - trajectory\ duration\ x\ wind\ direction$$

Where: Eqn. 6

distance = potential horizontal trajectory of MP (m)

back-trajectory duration = the duration MP is airborne (sec); calculated as h /V , h = maximum elevation defined as the marine boundary layer, 200m in this study, V settling velocity (m/s)

wind speed = average recorded wind speed (2 m/s).

The resulting potential transport distances and durations are tabulated below.

Table 4. Onshore MP duration and potential distance of atmospheric transport following the simplistic equations above.

Particle size	**4µm**	**9µm**	**35µm**
Time of flight (hrs)	110	22	1.2
(days)	46	0.9	<1
Distance travelled (km)	791	156	9

The durations of flight from MBL top elevation (200m ASL) to the sampling height (~10m ASL) were used in HYSPLIT trajectory modelling (HYSPLIT4). Models were created for the onshore wind periods, to consider the possible transport trajectory and possible source locations for onshore blown (ocean to atmosphere bubble burst ejection) particles. Models for the first 2 sample periods (A1, A2) were completed as these were the most direct onshore meteorological conditions. The models were run in backward mode for up to 22 hours (Table 4, 9µm average particle size), with individual backward trajectory analysis run for each hour of the monitoring period. The first 5 hours of each backward trajectory were analysed to identify the elevation above surface level (the Bay of Biscay) and distance from the monitoring location. The results are presented in Figure 24.

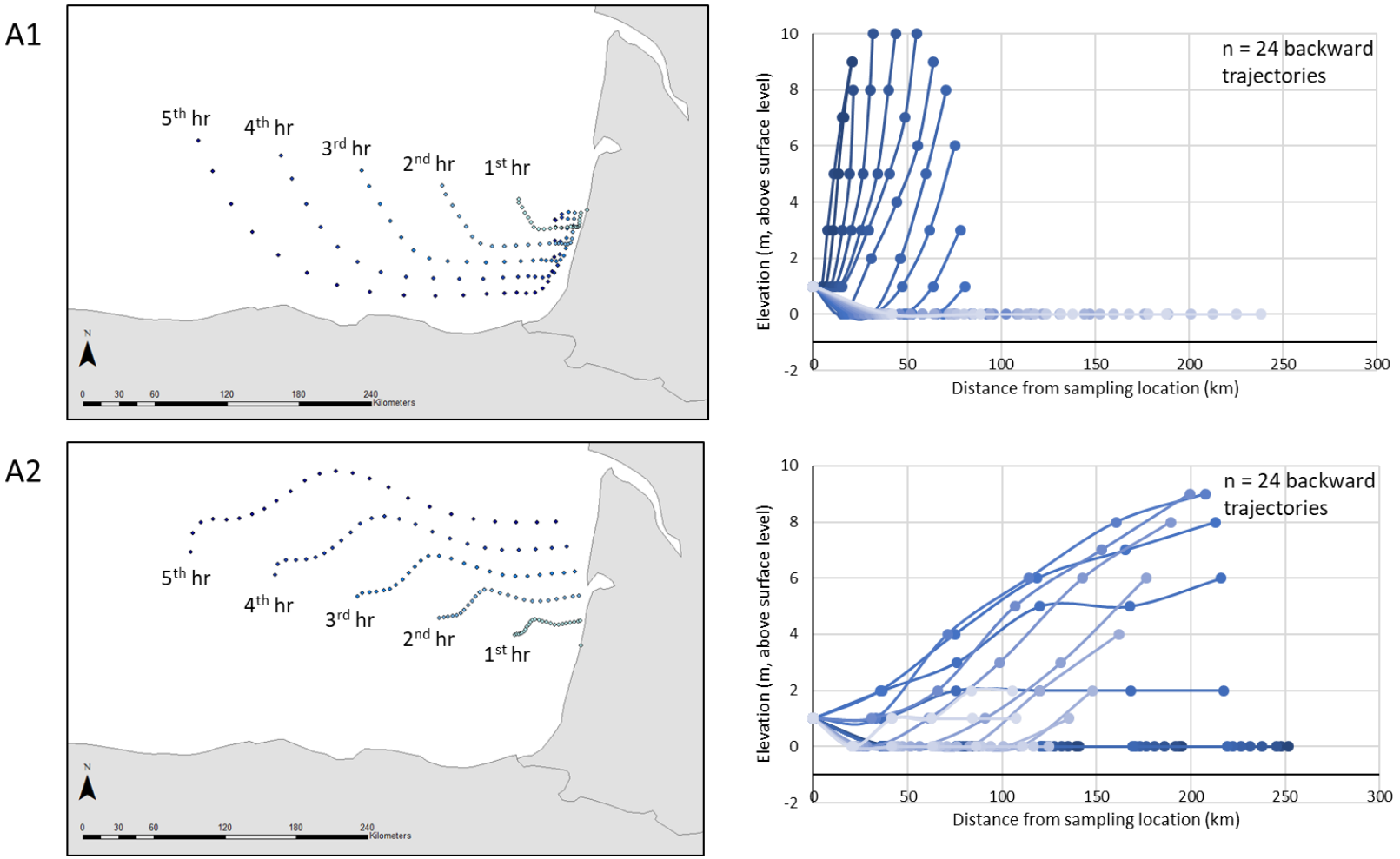

Figure 24. HYSPLIT backward trajectory analysis for onshore wind sample periods.

The simple backward trajectory analysis shows the direct A1 and A2 onshore wind trajectories to pass over the westwards Bay of Biscay marine area. The elevation of the trajectories is below 10 meters above surface (sea) level for the 5 hours prior to arriving at the sample location.

Sample A1 backward mode trajectory modelling suggests that 17 of the 24 trajectories move from the monitoring location down to sea level within a few hours (1-5 hours). The trajectories suggest short atmospheric transport durations of <5 hours and ~27km (16-42km). The other 7 trajectories present trajectories that remain close to surface level for the first 5 hours, ≤10m ASL, therefore within the bubble jet ejection elevation of influence within the marine boundary layer.

For A2, 19 of the 24 trajectories (one for each hour of the monitoring period of each sample) suggest localised marine source of MP, with trajectories passing sea level (<1m ASL) close to the sampling location. These particles are atmospherically transported ~1-5 hours and ~30km (20-41km). The remaining 5 backward modelled trajectories suggest longer distance transport of material to the monitoring location (and an elevated trajectory) from potentially distal marine sources.

It should be noted that accurate modelling at such a low altitude is extremely unreliable with Hysplit due to the large grid size and issues with pressures/altitude. This makes any analysis of wind along the beach inaccurate. Similarly, the last day with sea breeze convergence was impossible to model as according to reanalysis wind data, it did not occur. This is an area that needs a great deal of work to make the model accurate for this type of study.

5.8 Key pilot study MP findings and ocean to atmosphere exchange processes

This studies early findings provide tentative early evidence to support MP exchange between ocean to atmosphere.

The data from the beach air survey suggests the possibility of ocean to atmosphere transmission. Whilst there was clearly more MP coming off the land in offshore air masses, there were still significant MP numbers in onshore wind from the open Atlantic and the largest number in sea spray mist. From a review

of the literature on the process of particle ejection from sea water and the global transport of SSA, organic, biologic and mineral particulates, it appears that with the presence of oceanic MP/NP there exists a potential for subsequent ocean-atmosphere transmission.

As yet, nothing is known about how plastics might behave as an aerosol but in spite of its many differences (density, shape, charge and hygroscopicity) compared to MP, Saharan dust or SSA could perhaps provide analogues for the investigation of aeolian MP transport (*235*). This poses the question that with a lower density than either sand or SSA, and a greater surface area due to shape (films, fibres and irregularly shaped particles), could plastic be transported similar distances?

Whether the open ocean surface is a source of MP and NP or if the ocean acts as a line source from shoreline wave action, we suggest it is possible that plastic can be atmospherically entrained from bubble action/jet expulsion in a similar manner to SSA and other oceanic particulates. The sheer ocean surface area and length of ocean/land interface suggests that if MPs can escape the ocean and become entrained through ocean-atmospheric exchange, then this is an area that warrants future study.

6 Conclusions, limitations, and future research

Protocol development for this research whilst not perfect, has proved effective over a wide range of environmental samples including atmospheric, sea water and even soils and peat. At the time of development all facets of the protocols were in use however it had not been drawn together in a complete and coherent system. With slight variations the MP community is currently in agreeance with this protocol.

Findings in the French Pyrenees (Chapter 3) (*11*) showed for the first time that MP is not only present in the atmosphere in remote areas but importantly, that it was transported there by wind. This opens a new field of enquiry into the fate and transport of MP and although it was not possible to pinpoint the source of the MP, it was possible say with certainty it travelled at least 95km to deposit in the remote mountain study site. Deposition rates of around 365MP/m^2/day of films, fibres and fragments of size fractions compared to detection limits of other studies, are similar to city counts. Differences begin to standout when comparing fibre counts and fragments between studies. It is apparent that fibre numbers are higher in the city studies than the remote area Pyrenees. This suggests that either fibres do not travel as far or that meteorological conditions that entrain MP for transport to remote locations might be different to those in cities.

The Pic Du Midi research was the first to illustrate free tropospheric presence of MP and modelling showed long range transport for the first time. This means that atmospheric MP has the potential to reach everywhere and possibly be a global transport mechanism for bacteria and virus'.

Ocean to atmosphere transfer of microplastics has been illustrated through beach sampling on the French Atlantic coast. The findings suggest that the ocean and other aquatic environments may not only be a sink for microplastic but also a source. The potential impact of this is unknown but has implications especially for residents near highly polluted waterways.

6.1 Future research

This research has started the remote area microplastic search and is part of the new and emerging science of atmospheric microplastics. As such, this thesis and

the papers published therein present the tip of the iceberg with regards to atmospheric microplastic understanding. The novel research undertaken as part of this thesis has illustrated the presence of microplastic in the atmosphere outside and away from cities and expected or assumed MP sources. This research also looked to explain some of the atmospheric MP transport potentials and drivers (wind direction, velocity etc.). However, there is still much that is unknown, and a few of the future research areas are highlighted in the following discussion.

6.1.1 Advance the understanding of ocean-to-atmosphere MP transport

My work published in *Nature Geoscience* demonstrated the significance of atmospheric transport and deposition of microplastics (MPs), revealing over 10,000 microplastic particles/m^2/month deposited from the atmosphere in a remote region of the Pyrenees. This and work by others clearly demonstrates that atmospheric transport is an important part of global microplastics behaviour. The current position, however, is that these atmospheric microplastics are sourced directly from terrestrial environments, such as urban centres, landfills and industrial zones. However, my further research into the marine-atmospheric exchange has demonstrated a potentially hugely significant and radically different atmospheric MP source. Preliminary data from this research has illustrated that microplastics appear to be being released by the marine environment into the atmosphere, likely through the process of sea spray aerosol (SSA) generation. Due to the abundance of microplastics in the marine environment and the pervasiveness of SSA generation, this process has the potential to contribute massively to the atmospheric MP inventory, and subsequently to global MP transport and deposition. A focused study is needed to undertake detailed field sampling and laboratory simulations to demonstrate whether SSA release of marine MPs into the atmosphere is a viable and significant process.

Key research needs: Generation of greater and more detailed body of evidence that marine MPs are being released into the atmosphere by sea spray generation. This could be demonstrated through a focus on the following objectives:

1) To demonstrate that SSA generation entrains MPs within the atmosphere.

2) To enable sea spray aerosol generated MPs (SSAMPs) to be identified as a distinct end-member of the atmospheric inventory, providing further evidence for their production.

3) To explore whether MP size, shape, composition or biofilm attachment influences MP entrainment into the atmosphere by the SSA process.

4) To illustrate potential atmospheric transport pathways for MPs away from SSA source zones to illustrate distribution potential. This could be used to illustrate atmospheric input into known, monitored or modelled sites and thus mixing of different atmospheric end-members (marine and terrestrial sourced).

6.1.2 Create a global perspective of atmospheric MP through detailed field study

The majority of MP research has focused on oceanic transport, sources and sinks however recent publications are shifting the focus to terrestrial sinks such as freshwater lakes, rivers and soils. Aerosol MP has entirely evaded detection until now and as such, this enquiry opens a new arena for its study. There is a great deal we do not know and a pressing need to understand it and attempt to mitigate it. Key to advancing the global knowledge of atmospheric MP is an understanding of how far around the globe it has reached. It could be assumed to be everywhere, but evidence of trends and fluctuations relative to locations is needed. Furthermore, detailed analysis of the transport mechanisms and particle dynamics are needed to explain how it moves.

Key research needs: Generation of an evidenced based global scale assessment of atmospheric MP pollution and mechanisms for entrainment and transport. This could be demonstrated through a focus on the following objectives:

1) Analysis of a global spatial quantity and characteristics (type, shape) of atmospheric MP through extensive field sampling internationally

2) Using field sampling and laboratory-controlled studies, consider the temporal aspect of atmospheric MP pollution (can we create an archaeological record that show when it started and the trend in atmospheric MP over the past decades).

3) Examine, using detailed atmospheric particle transport modelling and field based atmospheric MP evidence, the time taken and transport dynamics of MP pollution reaching remote, uninhabited environments.

4) Examine in the field and laboratory-controlled environment what the transport dynamics of atmospheric MP are: settling velocities in air relative to a range of atmospheric conditions; influence of pH, humidity, dust, tribo electric effect on atmospheric MP entrainment, transport and deposition/settling.

6.1.3 Sources of atmospheric MP

To date, there is very limited evidence of the specific, the key and the most polluting sources of atmospheric MP. Detailed field studies are needed to start identifying and quantifying the atmospheric MP emissions of different human activities. It is assumed that cities, and their related transport and inhabitants' activities, landfills and waste disposal/management activities, plastic industries and other industrial activities in which plastic is used are the key atmospheric MP sources. However, the quantity, MP characteristics (types, shape, size) and the entrainment potential and therefore transport potential from these different activities across different countries is unknown and unexplored. To help manage or mitigate atmospheric MP pollution knowledge of atmospheric MP sources is imperative.

Key research needs: Generation of an evidenced based dataset, both spatial and activity based, that quantifies and characterises atmospheric MP emissions. This could be demonstrated through a focus on the following objectives:

1) Characterisation of the quantity and atmospheric MP type/size/shape of surf zone sea spray emissions, city, agricultural, industrial, rural and likely entrainment points (i.e. open landfill sites) to assist in determining the most abundant sources of atmospheric MP.

2) Examination of atmospheric MP emissions relative to activities, environmental conditions and location to identify if there are conditions that result in greater atmospheric MP emissions.

3) Consideration of potential mitigation actions that could decrease or prevent atmospheric MP release.

6.1.4 Other avenues of future research

There is a plethora of avenues for future atmospheric research beyond the three stated above. These extend from the impact of biodegradable plastics on atmospheric MP quantities and pollution through to human health impacts from

atmospheric MP inhalation and uptake and further to the consideration of atmospheric nanoplastic. This is just the beginning.

References

1. I. Baker, Fifty Materials That Make the World. *Springer Int. Publ. AG*. **Chapter**-**33**, 175–178 (2018).
2. Y. Liu, Z. Shao, P. Zhou, X. Chen, Thermal and crystalline behaviour of silk fiborin/nylon 66 blend films. *Polymer (Guildf).* **45**, 7705–7710 (2004).
3. S. Werner, A. Budziak, J. A. Van Fanneker, F. Galgani, G. Hanke, T. Maes, M. Matiddi, P. Nilsson, L. Oosterbaan, E. Priestland, R. C. Thompson, J. M. Veiga, T. Vlachogianni, *Harm caused by Marine Litter - European Commission* (2016; https://ec.europa.eu/jrc/en/publication/harm-caused-marine-litter).
4. K. w Kenyon, E. Kridler, Laysan Albatrosses Swallow Indigestible Matter. *AUK*. **86**, 339–343 (1969).
5. S. I. Rothstein, Plastic particle pollution of the surface of the Atlantic Ocean: evidence from a seabird. *Condor*. **75**, 344–345 (1973).
6. E. J. Carpenter, K. L. J. Smith, Plastics on the Sargasso Sea Surface. *Science*. **175**, 1240–1241 (1972).
7. R. Dris, thesis, Université Paris-Est (2016).
8. L. Cai, J. Wang, J. Peng, Z. Tan, Z. Zhan, X. Tan, Q. Chen, Characteristic of microplastics in the atmospheric fallout from Dongguan city, China: preliminary research and first evidence. *Environ. Sci. Pollut. Res.* **24**, 24928–24935 (2017).
9. S. Dehghani, F. Moore, R. Akhbarizadeh, Microplastic pollution in deposited urban dust, Tehran metropolis, Iran. *Environ. Sci. Pollut. Res.* **24**, 20360–20371 (2017).
10. K. Zhang, J. Su, X. Xiong, X. Wu, C. Wu, J. Liu, Microplastic pollution of lakeshore sediments from remote lakes in Tibet plateau, China. *Environ. Pollut.* **219**, 450–455 (2016).
11. S. Allen, D. Allen, V. R. Phoenix, G. Le Roux, P. Duranteza, A. Simonneau, B. Stéphane, D. Galop, Atmospheric transport and deposition of microplastics in a remote mountain catchment. *Nat. Geosci.* **12**, 339–344 (2019).

12. PlasticsEurope, “Plastics – the Facts 2018: An analysis of European plastics production, demand and waste data” (2018), (available at http://www.plasticseurope.org).

13. C. M. Rochman, C. Brookson, J. Bikker, N. Djuric, A. Earn, K. Bucci, S. Athey, A. Huntington, H. McIlwraith, K. Munno, H. De Frond, A. Kolomijeca, L. Erdle, J. Grbic, M. Bayoumi, S. B. Borrelle, T. Wu, S. Santoro, L. M. Werbowski, X. Zhu, R. K. Giles, B. M. Hamilton, C. Thaysen, A. Kaura, N. Klasios, L. Ead, J. Kim, C. Sherlock, A. Ho, C. Hung, Rethinking microplastics as a diverse contaminant suite. *Environ. Toxicol. Chem.* **38**, 703–711 (2019).

14. E. Y. Zeng, Ed., *Microplastic Contamination in Aquatic Environments - An Emerging Matter of Environmental Urgency* (Elsevier, 2018; https://www.sciencedirect.com/book/9780128137475/microplastic-contamination-in-aquatic-environments).

15. GESAMP, *Sources, Fate and Effects of Microplastics in the Marine Environment: Part 2 of a Global Assessment* (IMO/FAO/UNESCO-IOC/UNIDO/WMO/IAEA/UN/ UNEP/UNDP Joint Group of Experts on the Scientific Aspects of Marine Environmental Protection, 2016; file:///C:/Users/BACHEL~2/AppData/Local/Temp/sources-fate-and-effects-of-microplastics-in-the-marine-environment-part-2-of-a-global-assessment-en.pdf).

16. C. Masura, Julie, Baker, Joel, Foster, Gregory, Arthur, “Laboratory Methods for the Analysis of Microplastics in the Marine Environment” (2015), (available at https://marinedebris.noaa.gov/sites/default/files/publications-files/noaa_microplastics_methods_manual.pdf).

17. R. C. Thompson, Y. Olsen, R. P. Mitchell, A. Davis, S. J. Rowland, A. W. G. John, D. McGonigle, A. E. Russell, Lost at Sea: Where does all the plastic go? *Science (80-.).* **304**, 838 (2004).

18. N. B. Hartmann, T. Hüffer, R. C. Thompson, M. Hassellöv, A. Verschoor, A. E. Daugaard, S. Rist, T. Karlsson, N. Brennholt, M. Cole, M. P. Herrling, M. C. Hess, N. P. Ivleva, A. L. Lusher, M. Wagner, Are We Speaking the Same Language? Recommendations for a Definition and Categorization Framework for Plastic Debris. *Environ. Sci. Technol.* **53**, 1039–1047

(2019).

19. O. S. Alimi, J. Farner Budarz, L. M. Hernandez, N. Tufenkji, Microplastics and Nanoplastics in Aquatic Environments: Aggregation, Deposition, and Enhanced Contaminant Transport. *Environ. Sci. Technol.* **52**, 1704–1724 (2018).

20. M. G. J. Löder, G. Gerdts, in *Marine Anthropogenic Litter*, M. Bergmann, L. Gutow, M. Klages, Eds. (2015), pp. 201–227.

21. M. S. Bank, S. V. Hansson, *Environ. Sci. Technol.*, in press, doi:10.1021/acs.est.9b02942.

22. W. G. Kreyling, M. Semmler-Behnke, Q. Chaudhry, A complementary definition of nanomaterial. *Nano Today*. **5**, 165–168 (2010).

23. C. Joachim, To be nano or not to be nano? *Nat. Mater.* **4**, 107–109 (2005).

24. H. S. Auta, C. U. Emenike, S. H. Fauziah, Distribution and importance of microplastics in the marine environmentA review of the sources, fate, effects, and potential solutions. *Environ. Int.* **102**, 165–176 (2017).

25. J. Li, H. Liu, J. Paul Chen, Microplastics in freshwater systems: A review on occurrence, environmental effects, and methods for microplastics detection. *Water Res.* **137**, 362–374 (2018).

26. J. C. Prata, J. P. da Costa, A. V Girão, I. Lopes, A. C. Duarte, T. Rocha-Santos, Identifying a quick and efficient method of removing organic matter without damaging microplastic samples. *Sci. Total Environ.* **686**, 131–139 (2019).

27. P. Ribeiro-Claro, M. M. Nolasco, C. Araújo, Characterization of Microplastics by Raman Spectroscopy. *Compr. Anal. Chem.* **75**, 119–151 (2017).

28. C. M. Rochman, in *Marine Anthropogenic Litter*, M. Bergmann, L. Gutow, M. Klages, Eds. (Springer, Cham, 2015), pp. 117–140.

29. A. A. Horton, S. J. Dixon, Microplastics: An introduction to environmental transport processes. *Wiley Interdiscip. Rev. Water*. **5**, e1268 (2018).

30. L. Camarero, M. Bacardit, A. de Diego, G. Arana, Decadal trends in atmospheric deposition in a high elevation station: Effects of climate and pollution on the long-range flux of metals and trace elements over SW

Europe. *Atmos. Environ.* **167**, 542–552 (2017).

31. R. Ambrosini, R. S. Azzoni, F. Pittino, G. Diolaiuti, A. Franzetti, M. Parolini, First evidence of microplastic contamination in the supraglacial debris of an alpine glacier. *Environ. Pollut.* **253**, 297–301 (2019).

32. M. Klein, E. K. Fischer, Microplastic abundance in atmospheric deposition within the Metropolitan area of Hamburg, Germany. *Sci. Total Environ.* **685**, 96–103 (2019).

33. K. Liu, X. Wang, T. Fang, P. Xu, L. Zhu, D. Li, Source and potential risk assessment of suspended atmospheric microplastics in Shanghai. *Sci. Total Environ.* **675**, 462–471 (2019).

34. K. Liu, T. Wu, X. Wang, Z. Song, C. Zong, N. Wei, D. Li, Consistent transport of terrestrial microplastics to the ocean through atmosphere. *Environ. Sci. Technol.*, 1–12 (2019).

35. Y. Zhang, T. Gao, S. Kang, M. Sillanpaa, Microplastics intrude into the Tibetan Plateau. *Sci. Rep.* **in review** (2019).

36. L. G. A. Barboza, L. R. Vieira, V. Branco, N. Figueiredo, F. Carvalho, C. Carvalho, L. Guilhermino, Microplastics cause neurotoxicity, oxidative damage and energy-related changes and interact with the bioaccumulation of mercury in the European seabass, Dicentrarchus labrax (Linnaeus, 1758). *Aquat. Toxicol.* **195**, 49–57 (2018).

37. J. Gasperi, S. L. Wright, R. Dris, F. Collard, C. Mandin, M. Guerrouache, V. Langlois, F. J. Kelly, B. Tassin, Microplastics in air: Are we breathing it in? *Curr. Opin. Environ. Sci. Heal.* **1**, 1–5 (2018).

38. C. Liu, J. Li, Y. Zhang, L. Wang, J. Deng, Y. Gao, L. Yu, J. Zhang, H. Sun, Widespread distribution of PET and PC microplastics in dust in urban China and their estimated human exposure. *Environ. Int.* **128**, 116–124 (2019).

39. P. S. Tourinho, V. Kočí, S. Loureiro, C. A. M. van Gestel, Partitioning of chemical contaminants to microplastics: Sorption mechanisms, environmental distribution and effects on toxicity and bioaccumulation. *Environ. Pollut.* **252**, 1246–1256 (2019).

40. S. L. Wright, F. J. Kelly, Plastic and Human Health: A Micro Issue? *Environ. Sci. Technol.* **51**, 6634–6647 (2017).

41. C. G. Alimba, C. Faggio, Microplastics in the marine environment: Current trends in environmental pollution and mechanisms of toxicological profile. *Environ. Toxicol. Pharmacol.* **68**, 61–74 (2019).

42. R. Dris, C. J. Gasperi, A. V. Rocher, B. M. Saad, N. Renault, B. Tassin, Microplastic contamination in an urban area : a case study in Greater Paris. *Environ. Chem.* **12**, 592–599 (2015).

43. R. Dris, J. Gasperi, C. Mirande, C. Mandin, M. Guerrouache, V. Langlois, B. Tassin, A first overview of textile fibers, including microplastics, in indoor and outdoor environments. *Environ. Pollut.* **221**, 453–458 (2017).

44. S. Abbasi, B. Keshavarzi, F. Moore, H. Delshab, N. Soltani, A. Sorooshian, Investigation of microrubbers, microplastics and heavy metals in street dust: a study in Bushehr city, Iran. *Environ. Earth Sci.* **76** (2017), doi:10.1007/s12665-017-7137-0.

45. S. J. Hayward, T. Gouin, F. Wania, Comparison of four active and passive sampling techniques for pesticides in air. *Environ. Sci. Technol.* **44**, 3410–3416 (2010).

46. A. Dommergue, P. Amato, R. Tignat-perrier, O. Magand, A. Thollot, M. Joly, L. Bouvier, K. Sellegri, T. Vogel, J. Sonke, J. Jaffrezo, M. Andrade, I. Moreno, C. Labuschagne, L. Martin, Q. Zhang, C. Larose, D. A. Pearce, Methods to Investigate the Global Atmospheric Microbiome. *Front. Microbiol.* **10**, 1–12 (2019).

47. V. Hidalgo-Ruz, L. Gutow, R. C. Thompson, M. Thiel, Microplastics in the marine environment: A review of the methods used for identification and quantification. *Environ. Sci. Technol.* **46**, 3060–3075 (2012).

48. B. Nguyen, D. Claveau-Mallet, L. M. Hernandez, E. G. Xu, J. M. Farner, N. Tufenkji, Separation and Analysis of Microplastics and Nanoplastics in Complex Environmental Samples. *Acc. Chem. Res.* **52**, 858–866 (2019).

49. Q. Zhou, C. Tian, Y. Luo, Various forms and deposition fluxes of microplastics identified in the coastal urban atmosphere. *Chinese Sci. Bull.* **62**, 3902–3909 (2017).

50. Marine & Environmental Research Institute, *Guide to Microplastic Identification* (Marine & Environmental Research Instatite, 2015).

51. A. B. Silva, A. S. Bastos, C. I. L. Justino, J. P. da Costa, A. C. Duarte, T. A.

P. Rocha-Santos, Microplastics in the environment: Challenges in analytical chemistry - A review. *Anal. Chim. Acta*. **1017**, 1–19 (2018).

52. M. G. J. Löder, H. K. Imhof, M. Ladehoff, L. A. Löschel, C. Lorenz, S. Mintenig, S. Piehl, S. Primpke, I. Schrank, C. Laforsch, G. Gerdts, Enzymatic Purification of Microplastics in Environmental Samples. *Environ. Sci. Technol.* **51**, 14283–14292 (2017).

53. J. S. Hanvey, P. J. Lewis, J. L. Lavers, N. D. Crosbie, K. Pozo, B. O. Clarke, A review of analytical techniques for quantifying microplastics in sediments. *Anal. Methods*. **9**, 1369–1383 (2017).

54. G. Renner, T. C. Schmidt, J. Schram, Analytical methodologies for monitoring micro(nano)plastics: Which are fit for purpose? *Curr. Opin. Environ. Sci. Heal.* **1**, 55–61 (2018).

55. T. Stanton, M. Johnson, P. Nathanail, W. MacNaughtan, R. L. Gomes, Freshwater and airborne textile fibre populations are dominated by 'natural', not microplastic, fibres. *Sci. Total Environ.* **666**, 377–389 (2019).

56. R. Hurley, A. L. Lusher, M. Olsen, L. Nizzetto, Validation of a Method for Extracting Microplastics from Complex, Organic-Rich, Environmental Matrices. *Environ. Sci. Technol.* **52**, 7409–7417 (2018).

57. A. S. Tagg, J. P. Harrison, Y. Ju-Nam, M. Sapp, E. L. Bradley, C. J. Sinclair, J. J. Ojeda, Fenton's reagent for the rapid and efficient isolation of microplastics from wastewater. *Chem. Commun.* **53**, 372–375 (2017).

58. B. Quinn, F. Murphy, C. Ewins, Validation of density separation for the rapid recovery of microplastics from sediment. *Anal. Methods*. **9**, 1491–1498 (2017).

59. A. Käppler, D. Fischer, S. Oberbeckmann, G. Schernewski, M. Labrenz, K.-J. Eichhorn, B. Voit, Analysis of environmental microplastics by vibrational microspectroscopy: FTIR, Raman or both? *Anal Bioanal Chem*. **408**, 8377–8391 (2016).

60. C. Araujo, M. M. Nolasco, A. M. P. Ribeiro, P. J. A. Ribeiro-Claro, Identification of microplastics using Raman spectroscopy: Latest developments and future prospects. *Water Res.* **142**, 426–440 (2018).

61. E. Hendrickson, E. C. Minor, K. Schreiner, Microplastic Abundance and Composition in Western Lake Superior As Determined via Microscopy, Pyr-

GC/MS, and FTIR. *Environ. Sci. Technol.* **52**, 1787–1796 (2018).

62. D. Materić, A. Kasper-Giebl, D. Kau, M. Anten, M. Greilinger, E. Ludewig, E. van Sebille, T. Röckmann, R. Holzinger, Micro- and nanoplastics in Alpine snow – a new method for chemical identification and quantification in the nanogram range. *Environ. Sci. Technol.* **54**, 2353–2359 (2020).

63. R. Gillibert, G. Balakrishnan, Q. Deshoules, M. Tardivel, A. Magazzù, M. G. Donato, O. M. Maragò, M. Lamy de La Chapelle, F. Colas, F. Lagarde, P. G. Gucciardi, Raman Tweezers for Small Microplastics and Nanoplastics Identification in Seawater. *Environ. Sci. Technol.* **53**, 9003–9013 (2019).

64. E. Fries, J. H. Dekiff, J. Willmeyer, M.-T. Nuelle, M. Ebert, D. Remy, Identification of polymer types and additives in marine microplastic particles using pyrolysis-GC/MS and scanning electron microscopy. *Environ. Sci. Process. Impacts*. **15**, 1949 (2013).

65. D. Materić, E. Ludewig, K. Xu, T. Röckmann, R. Holzinger, Brief communication: Analysis of organic matter in surface snow by PTR-MS - Implications for dry deposition dynamics in the Alps. *Cryosphere*. **13**, 297–307 (2019).

66. D. Materić, M. Peacock, M. Kent, S. Cook, V. Gauci, T. Röckmann, R. Holzinger, Characterisation of the semi-volatile component of Dissolved Organic Matter by Thermal Desorption - Proton Transfer Reaction - Mass Spectrometry. *Sci. Rep.* **7**, 1–8 (2017).

67. M. Fischer, B. M. Scholz-Böttcher, Simultaneous Trace Identification and Quantification of Common Types of Microplastics in Environmental Samples by Pyrolysis-Gas Chromatography-Mass Spectrometry. *Environ. Sci. Technol.* **51**, 5052–5060 (2017).

68. A. Käppler, M. Fischer, B. M. Scholz-Böttcher, S. Oberbeckmann, M. Labrenz, D. Fischer, K. J. Eichhorn, B. Voit, Comparison of µ-ATR-FTIR spectroscopy and py-GCMS as identification tools for microplastic particles and fibers isolated from river sediments. *Anal. Bioanal. Chem.* **410**, 5313–5327 (2018).

69. E. Dümichen, A. K. Barthel, U. Braun, C. G. Bannick, K. Brand, M. Jekel, R. Senz, Analysis of polyethylene microplastics in environmental samples,

using a thermal decomposition method. *Water Res.* **85**, 451–457 (2015).

70. E. Dümichen, P. Eisentraut, C. G. Bannick, A. K. Barthel, R. Senz, U. Braun, Fast identification of microplastics in complex environmental samples by a thermal degradation method. *Chemosphere*. **174**, 572–584 (2017).

71. J. David, Z. Steinmetz, J. Kučerík, G. E. Schaumann, Quantitative Analysis of Poly(ethylene terephthalate) Microplastics in Soil via Thermogravimetry-Mass Spectrometry. *Anal. Chem.* **90**, 8793–8799 (2018).

72. A. Centrone, Infrared Imaging and Spectroscopy Beyond the Diffraction Limit. *Annu. Rev. Anal. Chem.* **8**, 101–126 (2015).

73. M. Bergmann, S. Mützel, S. Primpke, M. B. Tekman, J. Trachsel, G. Gerdts, White and wonderful? Microplastics prevail in snow from the Alps to the Arctic. *Sci. Adv.* **5**, eaax1157 (2019).

74. S. Primpke, C. Lorenz, R. Rascher-Friesenhausen, G. Gerdts, An automated approach for microplastics analysis using focal plane array (FPA) FTIR microscopy and image analysis. *Anal. Methods*. **9**, 1499–1511 (2017).

75. N. Everall, P. Griffiths, J. Chamlers, *Vibrational Spectroscopy of Polymers: Principles and Practice* (Wiley, 2007; https://www.wiley.com/en-us/Vibrational+Spectroscopy+of+Polymers%3A+Principles+and+Practice-p-9780470016626).

76. A. Vianello, R. L. Jensen, L. Liu, J. Vollertsen, Simulating human exposure to indoor airborne microplastics using a Breathing Thermal Manikin. *Sci. Rep.* **9**, 1–11 (2019).

77. F. Huth, A. Govyadinov, S. Amarie, W. Nuansing, F. Keilmann, R. Hillenbrand, Nano-FTIR absorption spectroscopy of molecular fingerprints at 20 nm spatial resolution. *Nano Lett.* **12**, 3973–3978 (2012).

78. M. Meyns, S. Primpke, G. Gerdts, “Library based identification and characterisation of polymers with nano-FTIR and IR-sSNOM imaging” (2019), , doi:arXiv:1906.10243.

79. R. Dris, J. Gasperi, M. Saad, C. Mirande, B. Tassin, Synthetic fibers in atmospheric fallout: A source of microplastics in the environment? *Mar. Pollut. Bull.* **104**, 290–293 (2016).

80. M. Ganguly, P. A. Ariya, Ice Nucleation of Model Nano-Micro Plastics: A Novel Synthetic Protocol and the Influence of Particle Capping at Diverse Atmospheric Environments. *ACS Earth Sp. Chem.* (2019), doi:10.1021/acsearthspacechem.9b00132.

81. A. C. Rocha-Santos, Teresa Duarte, *Characterization and Analysis of Microplastics* (Elsevier, 2017; https://books.google.co.uk/books?hl=en&lr=&id=DqCpDQAAQBAJ&oi=fnd&pg=PP1&dq=Rocha-Santos+and+Duarte,+2017.+Characterization+and+analysis+of+microplastics.&ots=tHW_iRapBc&sig=GcxB39KZu1IszvGvXjJv5pG1M6Q#v=onepage&q=Rocha-Santos and Duarte%2C 2017. Characte), vol. 75.

82. A. Klein, F. Ravetta, J. L. Thomas, G. Ancellet, P. Augustin, R. Wilson, E. Dieudonné, M. Fourmentin, H. Delbarre, J. Pelon, Influence of vertical mixing and nighttime transport on surface ozone variability in the morning in Paris and the surrounding region. *Atmos. Environ.* **197**, 92–102 (2019).

83. S. Abbasi, B. Keshavarzi, F. Moore, A. Turner, F. J. Kelly, A. O. Dominguez, N. Jaafarzadeh, Distribution and potential health impacts of microplastics and microrubbers in air and street dusts from Asaluyeh County, Iran. *Environ. Pollut.* **244**, 153–164 (2019).

84. P. A. Helm, Improving microplastics source apportionment: A role for microplastic morphology and taxonomy? *Anal. Methods*. **9**, 1328–1331 (2017).

85. I. E. Napper, R. C. Thompson, Release of synthetic microplastic plastic fibres from domestic washing machines: Effects of fabric type and washing conditions. *Mar. Pollut. Bull.* **112**, 39–45 (2016).

86. A. Jemec, P. Horvat, U. Kunej, M. Bele, A. Kržan, Uptake and effects of microplastic textile fibers on freshwater crustacean Daphnia magna. *Environ. Pollut.* **219**, 201–209 (2016).

87. M. Cole, A novel method for preparing microplastic fibers. *Sci. Rep.* **6**, 1–7 (2016).

88. T. Hüffer, A. Praetorius, S. Wagner, F. Von Der Kammer, T. Hofmann, Microplastic Exposure Assessment in Aquatic Environments: Learning from Similarities and Differences to Engineered Nanoparticles. *Environ.*

Sci. Technol. **51**, 2499–2507 (2017).

89. E. Besseling, J. T. K. Quik, M. Sun, A. A. Koelmans, Fate of nano- and microplastic in freshwater systems: A modeling study. *Environ. Pollut.* **220**, 540–548 (2017).

90. A. Isobe, K. Uchida, T. Tokai, S. Iwasaki, East Asian seas: A hot spot of pelagic microplastics. *Mar. Pollut. Bull.* **101**, 618–623 (2015).

91. Z. Fu, J. Wang, Current practices and future perspectives of microplastic pollution in freshwater ecosystems in China. *Sci. Total Environ.* **691**, 697–712 (2019).

92. M. A. Browne, P. Crump, S. J. Niven, E. Teuten, A. Tonkin, T. Galloway, R. C. Thompson, Accumulation of Microplastic on Shorelines Woldwide : Sources and Sinks, 9175–9179 (2011).

93. B. Kuczenski, R. Geyer, Material flow analysis of polyethylene terephthalate in the US, 1996-2007. *Resour. Conserv. Recycl.* **54**, 1161–1169 (2010).

94. L. Hermabessiere, A. Dehaut, I. Paul-Pont, C. Lacroix, R. Jezequel, P. Soudant, G. Duflos, Occurrence and effects of plastic additives on marine environments and organisms: A review. *Chemosphere*. **182** (2017), pp. 781–793.

95. F. M. Windsor, I. Durance, A. A. Horton, R. C. Thompson, C. R. Tyler, S. J. Ormerod, A catchment-scale perspective of plastic pollution. *Glob. Chang. Biol.* **25**, 1207–1221 (2019).

96. S. Turner, A. A. Horton, N. L. Rose, C. Hall, A temporal sediment record of microplastics in an urban lake, London, UK. *J. Paleolimnol.* **61**, 449–462 (2019).

97. D. Allen, S. Allen, J. Sonke, V. Phoenix, in *International Conference on Microplastic Pollution inthe Mediterranean Sea*, M. Cocca, E. Di Pace, M. Errico, G. Gentile, A. Montarsolo, R. Mossotti, Eds. (Springer Water. Springer, Cham, Capri, 2019), pp. 1–8.

98. M. van der Does, P. Knippertz, P. Zschenderlein, R. Giles Harrison, J.-B. W. Stuut, The mysterious long-range transport of giant mineral dust particles. *Sci. Adv.* **4** (2018), doi:10.1126/sciadv.aau2768.

99. J. R. Jambeck, R. Geyer, C. Wilcox, T. R. Siegler, M. Perryman, A. Andrady, R. Narayan, K. L. Law, Plastic waste inputs from land into the Ocean. *Science (80-.).* **347**, 768–771 (2015).

100. J. C. Prata, Airborne microplastics: Consequences to human health? *Environ. Pollut.* **234**, 115–126 (2018).

101. C. M. Rochman, A. Tahir, S. L. Williams, D. V. Baxa, R. Lam, J. T. Miller, F. C. Teh, S. Werorilangi, S. J. Teh, Anthropogenic debris in seafood: Plastic debris and fibers from textiles in fish and bivalves sold for human consumption. *Sci. Rep.* **5**, 1–10 (2015).

102. A. Churg, M. Brauer, Ambient atmospheric particles in the airways of human lungs. *Ultrastruct. Pathol.* **24**, 353–361 (2000).

103. J. L. Pauly, S. J. Stegmeier, H. A. Allaart, R. T. Cheney, P. J. Zhang, A. G. Mayer, R. J. Streck, Inhaled cellulosic and plastic fibers found in human lung tissue. *Cancer Epidemiol. Biomarkers Prev.* **7**, 419–428 (1998).

104. A. M. Kremer, T. M. Pal, J. S. M. Boleij, J. P. Schouten, B. Rijcken, Airway hyperresponsiveness, prevalence of chronic respiratory symptoms, and lung function in workers exposed to irritants. *Occup. Environ. Med.* **51**, 3–13 (1994).

105. N. Laskar, U. Kumar, Plastics and microplastics: A threat to environment. *Environ. Technol. Innov.* **14**, 100352 (2019).

106. G. Latini, C. De Felice, G. Presta, A. Del Vecchio, I. Paris, F. Ruggieri, P. Mzzeo, In utero exposure to di-(2-ethylhexyl)phthalate and duration of human pregnancy. *Environ. Health Perspect.* **111**, 1783–1785 (2003).

107. J. J. Wirth, M. Rossano, R. Potter, E. Puscheck, D. Daly, N. Paneth, S. Krawetz, B. Protas, M. Diamond, A Pilot Study Associating Urinary Concentrations of Phthalate Metabolites and Semen Quality. *Syst. Biol. Reprod. Med.* **54**, 143–154 (2008).

108. J. Drummond, S. Krause, L. Nel, S. Allen, D. Allen, L. Simon, C. Doaudy, “Gathering at the top? Environmental controls of microplastic uptake and biomagnification in aquatic food webs” (2019).

109. T. C. Nardelli, H. C. Erythropel, B. Robaire, Toxicogenomic screening of replacements for Di(2-Ethylhexyl) phthalate (DEHP) using the immortalized TM4 sertoli cell line. *PLoS One*. **10**, 1–17 (2015).

110. J. Peretz, L. Vrooman, W. A. Ricke, P. A. Hunt, S. Ehrlich, R. Hauser, V. Padmanabhan, H. S. Taylor, S. H. Swan, C. A. Vandevoort, J. A. Flaws, Bisphenol A and reproductive health: Update of experimental and human evidence, 2007-2013. *Environ. Health Perspect.* **122**, 775–786 (2014).

111. R. A. Bhat, D. Kumar, S. M. Bhat, I. R. Sofi, in *Handbook of Research on Environmental and Human Health Impacts of Plastic Pollution* (IGI Global, 2020), pp. 246–262.

112. P. Fu, K. Kawamura, Ubiquity of bisphenol A in the atmosphere. *Environ. Pollut.* **158**, 3138–3143 (2010).

113. R. Lehner, C. Weder, A. Petri-Fink, B. Rothen-Rutishauser, Emergence of Nanoplastic in the Environment and Possible Impact on Human Health. *Environ. Sci. Technol.* (2019), doi:10.1021/acs.est.8b05512.

114. C. Rosevelt, M. Los Huertos, C. Garza, H. M. Nevins, Marine debris in central California: Quantifying type and abundance of beach litter in Monterey Bay, CA. *Mar. Pollut. Bull.* **71**, 299–306 (2013).

115. PlasticsEurope, *Plastics – the Facts 2014 / 2015 An analysis of European plastics production , demand and waste data* (Plastic Recycling and Recovery Organisations (EPRO), Belgium, 2015; https://www.plasticseurope.org/application/files/5515/1689/9220/2014plastics_the_facts_PubFeb2015.pdf).

116. PlasticsEurope, *Plastics – the Facts 2017, An analysis of the European plastics production, demand and waste data* (PlasticsEurope, European Association of Plastics Recycling and Recovery Organisations, Belgium, 2017; https://www.plasticseurope.org/application/files/5715/1717/4180/Plastics_the_facts_2017_FINAL_for_website_one_page.pdf).

117. Y. K. Song, S. H. Hong, M. Jang, G. M. Han, S. W. Jung, W. J. Shim, Combined Effects of UV Exposure Duration and Mechanical Abrasion on Microplastic Fragmentation by Polymer Type. *Environ. Sci. Technol.* **51**, 4368–4376 (2017).

118. J. P. da Costa, Micro- and nanoplastics in the environment: Research and policymaking. *Curr. Opin. Environ. Sci. Heal.* **1**, 12–16 (2018).

119. K. Mattsson, L.-A. Hansson, T. Cedervall, Nano-plastics in the aquatic

environment. *Environ. Sci. Process. Impacts*. **17**, 1712–1721 (2015).

120. M. Scheurer, M. Bigalke, Microplastics in Swiss floodplain soils (2018), doi:10.1021/acs.est.7b06003.

121. R. Hurley, J. Woodward, J. J. Rothwell, Microplastic contamination of river beds significantly reduced by catchment-wide flooding. *Nat. Geosci.* **11**, 251–257 (2018).

122. P. L. Corcoran, Benthic plastic debris in marine and fresh water environments. *Environ. Sci. Process. Impacts*. **17**, 1363–1369 (2015).

123. M. Zbyszewski, P. L. Corcoran, A. Hockin, Comparison of the distribution and degradation of plastic debris along shorelines of the Great Lakes , North America. *J. Great Lakes Res.* **40**, 288–299 (2014).

124. L. Watkins, S. McGrattan, P. J. Sullivan, M. T. Walter, The effect of dams on river transport of microplastic pollution. *Sci. Total Environ.* (2019), doi:https://doi.org/10.1016/j.scitotenv.2019.02.028.

125. Centre d'Etudes Spatiales de la BIOsphere (CESBIO), Donnees meteorologiques – Sud Ouest Bernadouze (2018), (available at http://www.cesbio.ups-tlse.fr/data_meteo/index.php?perma=1319145390).

126. INSEE, Institut national de la statistique et des etudes economiques (2018), (available at https://www.insee.fr/fr/statistiques/3293086?geo=COM-09334).

127. G. Erni-Cassola, M. I. Gibson, R. C. Thompson, J. A. Christie-Oleza, Lost, but Found with Nile Red: A Novel Method for Detecting and Quantifying Small Microplastics (1 mm to 20 μm) in Environmental Samples. *Environ. Sci. Technol.* **51**, 13641–13648 (2017).

128. N. Digka, C. Tsangaris, H. Kaberi, A. Adamopoulou, C. Zeri, in *Proceedings of the International Conference on Microplastic Pollution in the Mediterranean Sea*, M. Cocca, E. Di Pace, M. Errico, G. Gentile, A. Montarsolo, R. Mossotti, Eds. (Springer Water. Springer, Cham, 2018; http://link.springer.com/10.1007/978-3-319-71279-6), pp. 17–24.

129. W. Wang, A. W. Ndungu, Z. Li, J. Wang, Microplastics pollution in inland freshwaters of China: A case study in urban surface waters of Wuhan, China. *Sci. Total Environ.* **575**, 1369–1374 (2017).

130. R. Klein, in *Laser Welding of Plastics: Materials, Processes and Industrial Applications* (John Wiley & Sons, ed. 1, 2012), pp. 3–69.

131. M. Löder, G. Gerdts, in *Marine Anthropogenic Litter*, M. Bergmann, L. Gutow, M. Klages, Eds. (Springer, Cham, 2015; https://link.springer.com/chapter/10.1007%2F978-3-319-16510-3_8#citeas).

132. F. Noren, “Small plastic particles in Coastal Swedish waters” (2007).

133. W. J. Shim, S. H. Hong, S. E. Eo, Identification methods in microplastic analysis: a review. *Anal. Methods*. **9**, 1384–1391 (2017).

134. I. Peeken, S. Primpke, B. Beyer, J. Gütermann, C. Katlein, T. Krumpen, M. Bergmann, L. Hehemann, G. Gerdts, Arctic sea ice is an important temporal sink and means of transport for microplastic. *Nat. Commun.* **9**, 1505 (2018).

135. H. K. Imhof, C. Laforsch, A. C. Wiesheu, J. Schmid, P. M. Anger, R. Niessner, N. P. Ivleva, Pigments and plastic in limnetic ecosystems: A qualitative and quantitative study on microparticles of different size classes. *Water Res.* **98**, 64–74 (2016).

136. R. Lenz, K. Enders, C. A. Stedmon, D. M. A. MacKenzie, T. G. Nielsen, A critical assessment of visual identification of marine microplastic using Raman spectroscopy for analysis improvement. *Mar. Pollut. Bull.* **100**, 82–91 (2015).

137. K. Enders, R. Lenz, C. A. Stedmon, T. G. Nielsen, Abundance, size and polymer composition of marine microplastics ≥10μm in the Atlantic Ocean and their modelled vertical distribution. *Mar. Pollut. Bull.* **100**, 70–81 (2015).

138. Y. K. Song, S. H. Hong, M. Jang, G. M. Han, M. Rani, J. Lee, W. J. Shim, A comparison of microscopic and spectroscopic identification methods for analysis of microplastics in environmental samples. *Mar. Pollut. Bull.* **93**, 202–209 (2015).

139. F. Menges, Spectragryph – optical imaging software (2016), (available at https://www.effemm2.de/spectragryph/).

140. P. Y. Khashaba, H. R. H. Ali, M. M. El-Wekil, A rapid Fourier transform infrared spectroscopic method for analysis of certain proton pump inhibitors in binary and ternary mixtures. *Spectrochim. Acta Part A Mol. Biomol.*

Spectrosc. **190**, 10–14 (2018).

141. R. Ševčík, P. Mácová, Localized quantification of anhydrous calcium carbonate polymorphs using micro-Raman spectroscopy. *Vib. Spectrosc.* **95**, 1–6 (2018).

142. J. M. Lagaron, N. M. Dixon, W. Reed, J. M. Pastor, B. J. Kip, Morphological characterisation of the crystalline structure of cold-drawn HDPE used as a model material for the environmental stress cracking (ESC) phenomenon. *Polymer (Guildf).* **40**, 2569–2586 (1999).

143. E. Sanchez, C. Yague, M. A. Gazetner, Planetary boundary layer energetics simulated from a regional climate model over Europe for present climate and climate change conditions. *Geophys. Res. Lett.* **34** (2007), doi:10.1029/2006gL028340.

144. C. S. Zender, Mineral Dust Entrainment and Deposition (DEAD) model: Description and 1990s dust climatology. *J. Geophys. Res.* **108**, 4416 (2003).

145. R. R. Draxler, D. Hess, G, “Description of the Hysplit4 modeling system” (Maryland, 2018), (available at https://www.researchgate.net/publication/255682850_Description_of_the_HYSPLIT_4_modelling_system).

146. A. Stein, R. Draxler, G. Rolph, B. Stunder, M. Dohen, F. Ngqn, NOAA’s HYSPLIT atmospheric transport and dispersion modeling system. *Bull. Am. Meteorol. Soc.* **96**, 2059–2077 (2015).

147. L. Su, Z. Yuan, J. C. H. Fung, A. K. H. Lau, A comparison of HYSPLIT backward trajectories generated from two GDAS datasets. *Sci. Total Environ.* **506**–**507**, 527–537 (2015).

148. K. Ashrafi, M. Shafiepour-Motlagh, A. Aslemand, S. Ghader, Dust storm simulation over Iran using HYSPLIT. *J. Environ. Heal. Sci. Eng.* **12**, 9 (2014).

149. I. Reche, G. D’Orta, N. Mladenov, D. M. Winget, C. A. Suttle, Deposition rates of viruses and bacteria above the atmospheric boundary layer. *ISME J.* **12**, 1154–1162 (2018).

150. C. D. G. Zwaaftink, Ó. Arnalds, P. Dagsson-waldhauserova, S. Eckhardt, J. Prospero, A. Stohl, Temporal and spatial variability of Icelandic dust

emissions and atmospheric transport. *Atmos. Chem. Phys.*, 10865–10878 (2017).

151. B. Marticorena, B. Chatenet, J. L. Rajot, G. Bergametti, A. Deroubaix, J. Vincent, A. Kouoi, C. Schmechtig, M. Coulibaly, A. Diallo, I. Koné, A. Maman, T. NDiaye, A. Zakou, Mineral dust over west and central Sahel: Seasonal patterns of dry and wet deposition fluxes from a pluriannual sampling (2006-2012). *J. Geophys. Res. Atmos.* **122**, 1338–1364 (2017).

152. R. Morales-Baquero, E. Pulido-Villen, I. Reche, Chemical signature of Saharan dust on dry and wet atmospheric deposition in the south-western Mediterranean region. *Tellus Ser. B*. **1**, 1–12 (2013).

153. M. Schwikowski, P. Seibert, U. Baltensperger, H. W. Gaggeler, A study of an outstanding Saharan dust event at the high-alpine site Jungfraujoch, Switzerland. *Atmos. Environ.* **29**, 1829–1842 (1995).

154. J. Dessens, P. Van Dinh, Frequent Saharan Dust Outbreaks North of the Pyrenees: A sign of a climatic change? *Weather*. **45**, 327–333 (1990).

155. J. Schindelin, I. Arganda-Carreras, E. Frise, V. Kaynig, M. Longair, T. Pietzsch, S. Preibisch, C. Rueden, S. Saalfeld, B. Schmid, J.-Y. Tinevez, D. J. White, V. Hartenstein, K. Eliceiri, P. Tomancak, A. Cardona, Fiji: an open-source platform for biological image analysis. *Nat. Methods*. **9**, 676–682 (2012).

156. D. Schymanski, C. Goldbeck, H. U. Humpf, P. Fürst, Analysis of microplastics in water by micro-Raman spectroscopy: Release of plastic particles from different packaging into mineral water. *Water Res.* **129**, 154–162 (2018).

157. European Comission, A European Strategy for Plastics in a Circular Economy. *Eur. Com.*, 24 (2018).

158. K. Magnusson, K. Eliasson, A. Fråne, K. Haikonen, J. Hultén, M. Olshammar, J. Stadmark, A. Voisin, Swedish sources and pathways for microplastics to the marine environment. A review of existing data. *IVL Rep.*, 1–89 (2016).

159. R. Dris, H. Imhof, W. Sanchez, J. Gasperi, F. Galgani, B. Tassin, C. Laforsch, Beyond the ocean: Contamination of freshwater ecosystems with (micro-) plastic particles. *Environ. Chem.* **12**, 539–550 (2015).

160. W. J. Shim, S. H. Hong, S. Eo, in *Microplastic Contamination in Aquatic Environments*, E. Y. Zeng, Ed. (Elsevier, 2018; http://www.sciencedirect.com/science/article/pii/B9780128137475000011), pp. 1–26.

161. R. Dris, J. Gasperi, B. Tassin, in *Freshwater Microplastics The Handbook of Environmental Chemistry*, S. Lambert, M. Wagber, Eds. (2018; http://link.springer.com/10.1007/978-3-319-61615-5), pp. 69–83.

162. S. L. Wright, J. Ulke, A. Font, K. L. . Chan, F. J. Kelly, Atmospheric microplastic deposition in an urban environment and an evaluation of transport. *Environ. Int.* (2019), doi:10.1016/j.envint.2019.105411.

163. X. Wang, C. Li, K. Liu, L. Zhu, Z. Song, D. Li, Atmospheric microplastic over the South China Sea and East Indian Ocean : abundance , distribution and source. *J. Hazard. Mater.* (2019), doi:10.1016/j.jhazmat.2019.121846.

164. M. Bergmann, S. Mützel, S. Primpke, M. B. Tekman, G. Gerdts, in *Arctic Frontiers* (Alfred-Wegener-Institut andd Helmholtz Gemeinschaft, Tromso, 2019; https://epic.awi.de/id/eprint/48975/), p. 1.

165. D. Durnford, A. Dastoor, D. Figueras-Nieto, A. Ryjkov, Long range transport of mercury to the Arctic and across Canada. *Atmos. Chem. Phys.* **10**, 6063–6086 (2010).

166. D. Hirdman, K. Aspmo, J. F. Burkhart, S. Eckhardt, H. Sodemann, A. Stohl, Transport of mercury in the Arctic atmosphere: Evidence for a springtime net sink and summer-time source. *Geophys. Res. Lett.* **36**, 1–5 (2009).

167. I. Uno, K. Eguchi, K. Yumimoto, T. Takemura, A. Shimizu, M. Uematsu, Z. Liu, Z. Wang, Y. Hara, N. Sugimoto, Asian dust transported one full circuit around the globe. *Nat. Geosci.* **2**, 557–560 (2009).

168. P. Ricaud, R. Zbinden, V. Catoire, V. Brocchi, F. Dulac, E. Hamonou, J. Canonici, L. ElAmraoui, S. Massart, U. Piguet, U. Dayan, P. Nabat, J. Sciare, M. Ramonet, M. Delmotte, A. di Sarra, D. Sferlazzo, T. di Iorio, S. Piacentino, P. Cristofanelli, N. Mihalopoulos, G. Kouvarakis, M. Pikridas, C. Savvides, R. Mamouri, A. Nisantzi, D. Hadjimitsis, J. Attié, H. Ferré, Y. Kangah, N. Jaidan, J. Guth, P. Jacquet, S. Chevrier, C. Robert, A. Bourdon, J. Bourdinot, J. Etienne, K. Gisèle, T. Pierre, The GLAM airborne campaign across the Mediterranean Basin. *Bull. Am. Meteorol. Soc.* **99**, 361–380

(2017).

169. X. Fu, N. Marusczak, L. E. Heimbürger, B. Sauvage, F. Gheusi, E. M. Prestbo, J. Sonke, Atmospheric mercury speciation dynamics at the high-altitude Pic du Midi Observatory, southern France. *Atmos. Chem. Phys.* **16**, 5623–5639 (2016).

170. A. Marenco, H. Gouget, P. Nedelec, J. P. Pages, F. Karcher, Evidence of a long-term increase in tropospheric ozone from Pic du Midi data series: consequences: positive radiative forcing. *J. Geophys. Res.* **99**, 617–632 (1994).

171. A. Chevalier, F. Gheusi, J.-L. Attié, R. Delmas, R. Zbinden, G. Athier, J.-M. Cousin, Carbon monoxide observations from ground stations in France and Europe and long trends in the free troposphere. *Atmos. Chem. Phys. Discuss.* **8**, 3313–3356 (2008).

172. G. Erni-cassola, M. I. Gibson, R. C. Thompson, J. A. Christie-oleza, Lost , but found with Nile red ; a novel method to detect and quantify small microplastics (20 µm – 1 mm) in environmental samples, 1–9 (2017).

173. R. R. Draxler, D. Hess, G, An Overview of the HYSPLIT_4 Modelling System for Trajectories, Dispersion, and Deposition. *Aust. Meteorolofical Mag.* **47**, 295–308 (1998).

174. M. Kooi, A. A. Koelmans, Simplifying Microplastic via Continuous Probability Distributions for Size, Shape,and Density. *Environ. Sci. Technol. Lett.* **6**, 551–557 (2019).

175. F. Gheusi, F. Ravetta, H. Delbarre, C. Tsamalis, A. Chevalier-Rosso, C. Leroy, P. Augustin, R. Delmas, G. Ancellet, G. Athier, P. Bouchou, B. Campistron, J. M. Cousin, M. Fourmentin, Y. Meyerfeld, Pic 2005, a field campaign to investigate low-tropospheric ozone variability in the Pyrenees. *Atmos. Res.* **101**, 640–665 (2011).

176. A. F. Stein, R. R. Draxler, G. D. Rolph, B. J. B. Stunder, M. D. Cohen, F. Ngan, NOAA’s HYSPLIT Atmospheric Transport and Dispersion Modeling System. *Bull. Am. Meteorol. Soc.* **96**, 2059–2077 (2015).

177. A. F. Stein, Y. Wang, J. D. de la Rosa, A. M. Sanchez de la Campa, N. Castell, R. R. Draxler, Modeling PM10 Originating from Dust Intrusions in the Southern Iberian Peninsula Using HYSPLIT. *Weather Forecast.* **26**,

236–242 (2011).

178. Y. Li, L. Shao, W. Wang, M. Zhang, X. Feng, W. Li, D. Zhang, Airborne fiber particles: Types, size and concentration observed in Beijing. *Sci. Total Environ.* **705** (2020), doi:10.1016/j.scitotenv.2019.135967.

179. S. Allen, D. Allen, K. Moss, G. Le Roux, V. R. Phoenix, J. Sonke, Examination of the ocean as a source for atmospheric microplastics. *PLoS One*. **15** (2020), doi:10.1371/journal.pone.0232746.

180. M. Yurtsever, A. Kaya, C. Bayraktar, in *International Conference on Microplastic Pollution in the Mediterranean Sea*, M. Cocca, Ed. (Springer International Publishing, 2018; http://link.springer.com/10.1007/978-3-319-71279-6), vol. 22, p. 238.

181. N. Asrin, A. Dipareza, Microplastics in Ambient Air (Case Study : Urip Sumoharjo Street and Mayjend Sungkono Street of Surabaya City , Indonesia). *IAETSD J. Adv. Res. Appl. Sci.* **6**, 54–57 (2019).

182. N. Evangeliou, H. Grythe, Z. Klimont, C. Heyes, S. Eckhardt, S. Lopez-Aparicio, A. Stohl, Atmospheric transport, a major pathway of microplastics to remote regions. *Preprints*, 1–32 (2020).

183. M. L. Moser, D. S. Lee, A Fourteen-Year Survey of Plastic Ingestion by Western North Atlantic Seabirds. *Colon. Waterbirds*. **15**, 883–94 (1992).

184. PlasticsEurope, “Plastics – the Facts 2019” (2019).

185. W. J. Shim, R. C. Thomposon, Microplastics in the Ocean. *Arch. Environ. Contam. Toxicol.* **69**, 265–268 (2015).

186. R. Geyer, J. R. Jambeck, K. L. Law, Production, use, and fate of all plastics ever made. *Sci. Adv.* **3**, e1700782 (2017).

187. Z. Akdogan, B. Guven, Microplastics in the environment: A critical review of current understanding and identification of future research needs. *Environ. Pollut.* **254**, 113011 (2019).

188. E. Van Sebille, C. Wilcox, L. Lebreton, N. Maximenko, B. D. Hardesty, J. A. Van Franeker, M. Eriksen, D. Siegel, F. Galgani, K. L. Law, A global inventory of small floating plastic debris. *Environ. Res. Lett.* **10**, 124006 (2015).

189. A. A. Koelmans, M. Kooi, K. L. Law, E. Van Sebille, All is not lost: Deriving

a top-down mass budget of plastic at sea. *Environ. Res. Lett.* **12**, 1–23 (2017).

190. N. Maximenko, J. Hafner, P. Niiler, Pathways of marine debris derived from trajectories of Lagrangian drifters. *Mar. Pollut. Bull.* **65**, 51–62 (2012).

191. D. Wichmann, P. Delandmeter, E. van Sebille, Influence of near-surface currents on the global dispersal of marine microplastic. *JGR Ocean.*, 1–18 (2018).

192. N. Sharma, A. Rai, *Algal Particles in the Atmosphere* (Elsevier, 2011).

193. M. Sofiev, J. Soares, M. Prank, G. De Leeuw, J. Kukkonen, A regional-to-global model of emission and transport of sea salt particles in the atmosphere. *J. Geophys. Res. Atmos.* **116** (2011), doi:10.1029/2010JD014713.

194. M. A. Erinin, S. D. Wang, R. Liu, D. Towle, X. Liu, J. H. Duncan, Spray Generation by a Plunging Breaker. *Geophys. Res. Lett.* **46** (2019), doi:10.1029/2019GL082831.

195. E. Lewis, S. Schwartz, *Sea salt aerosol production: mechanisms, methods, measurements and models* (American Geophysical Union, Washington, USA, 2004).

196. W. A. Hoppel, G. M. Frick, J. W. Fitzgerald, Surface source function for sea-salt aerosol and aerosol dry deposition to the ocean surface. *J. Geophys. Res. Atmos.* **107**, 1–17 (2002).

197. D. Richer, F. Veron, Ocean Spray:an outsized influence on weather and climate. *Phys. Today*. **69**, 35–39 (2016).

198. C. D. O'Dowd, G. de Leeuw, Marine aerosol production: a review of the current knowledge. *Philos. Trans. R. Soc. A Math. Phys. Eng. Sci.* **365**, 1753–1774 (2007).

199. J. A. Quinn, R. A. Steinbrook, J. L. Anderson, Breaking bubbles and the water-to-air transport of particulate matter. *Chem. Eng. Sci.* **30**, 1177–1184 (1975).

200. M. Pósfai, J. Li, J. R. Anderson, P. R. Buseck, Aerosol bacteria over the Southern Ocean during ACE-1. *Atmos. Res.* **66**, 231–240 (2003).

201. I. Reche, G. D'Orta, N. Mladenov, D. M. Winget, C. A. Suttle, Deposition

rates of viruses and bacteria above the atmospheric boundary layer. *ISME J.* (2018), doi:10.1038/s41396-017-0042-4.

202. J. C. McWilliams, P. P. Sullivan, C.-H. Moeng, Langmuir turbulence in the ocean. *J. Fluid Mech.* **334**, S0022112096004375 (1997).

203. C. A. Choy, B. H. Robison, T. O. Gagne, B. Erwin, E. Firl, R. U. Halden, J. A. Hamilton, K. Katija, S. E. Lisin, C. Rolsky, K. S. Van Houtan, The vertical distribution and biological transport of marine microplastics across the epipelagic and mesopelagic water column. *Sci. Rep.* **9**, 1–9 (2019).

204. T. Kukulka, R. R. Harcourt, Influence of Stokes Drift Decay Scale on Langmuir Turbulence. *J. Phys. Oceanogr.* **47**, 1637–1656 (2017).

205. Y. Zhang, T. Gao, S. Kang, M. Sillanpää, Importance of atmospheric transport for microplastics deposited in remote areas. *Environ. Pollut.* **254** (2019), doi:10.1016/j.envpol.2019.07.121.

206. C. E. Enyoh, A. W. Verla, E. N. Verla, F. C. Ibe, C. E. Amaobi, Airborne microplastics: a review study on method for analysis, occurrence, movement and risks. *Environ. Monit. Assess.* **191**, 1–17 (2019).

207. Y. Zhang, S. Kang, S. Allen, D. Allen, T. Gao, M. Sillanpaa, Atmospheric microplastics: A review on current status and perspectives. *Earth-Science Rev.* **203**, 103118 (2020).

208. P. L. Corcoran, M. C. Biesinger, M. Grifi, Plastics and beaches: A degrading relationship. *Mar. Pollut. Bull.* **58**, 80–84 (2009).

209. S. Lambert, M. Wagner, Characterisation of nanoplastics during the degradation of polystyrene. *Chemosphere*. **145**, 265–268 (2016).

210. A. Jahnke, H. P. H. Arp, B. I. Escher, B. Gewert, E. Gorokhova, D. Kühnel, M. Ogonowski, A. Potthoff, C. Rummel, M. Schmitt-Jansen, E. Toorman, M. MacLeod, Reducing Uncertainty and Confronting Ignorance about the Possible Impacts of Weathering Plastic in the Marine Environment. *Environ. Sci. Technol. Lett.* **4**, 85–90 (2017).

211. F. Julienne, N. Delorme, F. Lagarde, From macroplastics to microplastics: Role of water in the fragmentation of polyethylene. *Chemosphere*. **236**, 124409 (2019).

212. A. L. Dawson, S. Kawaguchi, C. K. King, K. A. Townsend, R. King, W. M.

Huston, S. M. Bengtson Nash, Turning microplastics into nanoplastics through digestive fragmentation by Antarctic krill. *Nat. Commun.* **9**, 1–8 (2018).

213. Hong Kong Observatory, The Weather of October 2016, 1–9 (2018).

214. Hong Kong Observatory, The Weather of November 2016 Warnings and Signals issued in November 2016, 1–6 (2018).

215. Hong Kong Observatory, The Weather of December 2016 Warnings and Signals issued in December 2016, 1–6 (2018).

216. E. Athanasopoulou, M. Tombrou, S. N. Pandis, A. G. Russell, The role of sea-salt emissions and heterogeneous chemistry in the air quality of polluted coastal areas. *Atmos. Chem. Phys.* **8**, 5755–5769 (2008).

217. J. Yan, L. Chen, Q. Lin, S. Zhao, M. Zhang, Effect of typhoon on atmospheric aerosol particle pollutants accumulation over Xiamen, China. *Chemosphere*. **159**, 244–255 (2016).

218. V. C. Slonosky, Wet winters, dry summers? Three centuries of precipitation data from Paris. *Geophys. Res. Lett.* **29**, 34-1-34–4 (2002).

219. G. S. Fanourgakis, M. Kanakidou, A. Nenes, S. E. Bauer, T. Bergman, K. S. Carslaw, A. Grini, D. S. Hamilton, J. S. Johnson, V. A. Karydis, A. Kirkevåg, J. K. Kodros, U. Lohmann, G. Luo, R. Makkonen, H. Matsui, D. Neubauer, J. R. Pierce, J. Schmale, P. Stier, K. Tsigaridis, T. van Noije, H. Wang, D. Watson-Parris, D. M. Westervelt, Y. Yang, M. Yoshioka, N. Daskalakis, S. Decesari, M. Gysel Beer, N. Kalivitis, X. Liu, N. M. Mahowald, S. Myriokefalitakis, R. Schrödner, M. Sfakianaki, A. P. Tsimpidi, M. Wu, F. Yu, Evaluation of global simulations of aerosol particle number and cloud condensation nuclei, and implications for cloud droplet formation. *Atmos. Chem. Phys. Discuss.*, 1–40 (2019).

220. M. O. Andreae, D. Rosenfeld, Aerosol-cloud-precipitation interactions. Part 1. The nature and sources of cloud-active aerosols. *Earth-Science Rev.* **89**, 13–41 (2008).

221. M. Van Der Does, A. Pourmand, A. Sharifi, J.-B. W. Stuut, North African mineral dust across the tropical Atlantic Ocean: Insights from dust particle size, radiogenic Sr-Nd-Hf isotopes and rare earth elements (REE). *Aeolian Res.* **33**, 106–116 (2018).

222. R. L. Modini, B. Harris, Z. Ristovski, The organic fraction of bubble-generated, accumulation mode Sea Spray Aerosol (SSA). *Atmos. Chem. Phys.* **10**, 2867–2877 (2010).

223. E. Fuentes, H. Coe, D. Green, G. De Leeuw, G. McFiggans, Laboratory-generated primary marine aerosol via bubble-bursting and atomization. *Atmos. Meas. Tech.* **3**, 141–162 (2010).

224. W. R. Ke, Y. M. Kuo, C. W. Lin, S. H. Huang, C. C. Chen, *Characterization of aerosol emissions from single bubble bursting* (Elsevier Ltd, 2017; http://dx.doi.org/10.1016/j.jaerosci.2017.03.006), vol. 109.

225. D. B. J. Demoz.B.B, Coller JL. Jr, on the Caltech Active Strand Cloudwater collectors. *Atmos. Res.* **41**, 46672 (1995).

226. T. Wrzesinsky, O. Klemm, Summertime fog chemistry at a mountainous site in central Europe. *Atmos. Environ.* **34**, 1487–1496 (2000).

227. P. Roman, Z. Polkowska, J. Namieśnik, Sampling procedures in studies of cloud water composition: A review. *Crit. Rev. Environ. Sci. Technol.* **43**, 1517–1555 (2013).

228. P. Herckes, M. P. Hannigan, L. Trenary, T. Lee, J. L. Collett, Organic compounds in radiation fogs in Davis (California). *Atmos. Res.* **64**, 99–108 (2002).

229. MeteoFrance, Météo et climat: Mimizan (2018), (available at http://www.meteofrance.com/previsions-meteo-france/mimizan/40200).

230. S. Zhao, M. Danley, J. E. Ward, D. Li, T. J. Mincer, An approach for extraction, characterization and quantitation of microplastic in natural marine snow using Raman microscopy. *Anal. Methods*. **9**, 1470–1478 (2017).

231. D. Koračin, C. E. Dorman, J. M. Lewis, J. G. Hudson, E. M. Wilcox, A. Torregrosa, Marine fog: A review. *Atmos. Res.* **143**, 142–175 (2014).

232. A. K. Baldwin, S. R. Corsi, S. A. Mason, Plastic Debris in 29 Great Lakes Tributaries: Relations to Watershed Attributes and Hydrology. *Environ. Sci. Technol.* **50**, 10377–10385 (2016).

233. A. Mendoza, J. L. Osa, O. C. Basurko, A. Rubio, M. Santos, J. Gago, F. Galgani, C. Peña-Rodriguez, Microplastics in the Bay of Biscay: An

overview. *Mar. Pollut. Bull.* **153** (2020), doi:10.1016/j.marpolbul.2020.110996.

234. S. Allen, D. Allen, V. R. Phoenix, G. Le Roux, P. Durantez, Atmospheric deposition of microplastics found on a remote mountain catchment. *Nat. Geosci.* (2018).

235. B. Marticorena, G. Bergametti, B. Aumont, M. Legrand, Modeling the atmospheric dust cycle: 2. Simulation of Saharan dust sources. *J. Geophys. Res.* **102**, 4387–4404 (1997).

236. C. Szczypta, S. Gascoin, T. Houet, O. Hagolle, J. F. Dejoux, C. Vigneau, P. Fanise, Impact of climate and land cover changes on snow cover in a small Pyrenean catchment. *J. Hydrol.* **521**, 84–99 (2015).

237. S. M. Rhind, Anthropogenic pollutants: a threat to ecosystem sustainability? *Philos Trans R Soc L. B Biol Sci*. **364**, 3391–3401 (2009).

238. N. Pirrone, S. Cinnirella, X. Feng, R. B. Finkelman, H. R. Friedli, J. Leaner, R. Mason, A. B. Mukherjee, G. B. Stracher, D. G. Streets, K. Telmer, Global mercury emissions to the atmosphere from anthropogenic and natural sources. *Atmos. Chem. Phys.* **10**, 5951–5964 (2010).

239. J. O. Nriagu, Global inventory of natural and anthropogenic emissions of trace metals to the atmosphere. *Nature*. **279**, 409 (1979).

240. J. Catalan, L. Camarero, M. Felip, S. Pla, M. Ventura, T. Buchaca, F. Bartumeus, G. De Mendoza, A. Miró, E. O. Casamayor, J. M. Medina-Sánchez, M. Bacardit, M. Altuna, M. Bartrons, D. D. De Quijano, High mountain lakes: Extreme habitats and witnesses of environmental changes. *Limnetica*. **25**, 551–584 (2006).

241. P. Fernández, R. M. Vilanova, C. Martínez, P. Appleby, J. O. Grimalt, The historical record of atmospheric pyrolytic pollution over Europe registered in the sedimentary PAH from remote mountain lakes. *Environ. Sci. Technol.* **34**, 1906–1913 (2000).

242. M. Bacardit, L. Camarero, Atmospherically deposited major and trace elements in the winter snowpack along a gradient of altitude in the Central Pyrenees: The seasonal record of long-range fluxes over SW Europe. *Atmos. Environ.* **44**, 582–595 (2010).

243. S. V. Hansson, A. Claustres, A. Probst, F. De Vleeschouwer, S. Baron, D.

Galop, F. Mazier, G. Le Roux, Atmospheric and terrigenous metal accumulation over 3000 years in a French mountain catchment: Local vs distal influences. *Anthropocene*. **19**, 45–54 (2017).

244. A. Hervàs, L. Camarero, I. Reche, E. O. Casamayor, Viability and potential for immigration of airborne bacteria from Africa that reach high mountain lakes in Europe. *Environ. Microbiol.* **11**, 1612–1623 (2009).

245. F. E. Grousset, P. Ginoux, A. Bory, P. E. Biscaye, Case study of a Chinese dust plume reaching the French Alps. *Geophys. Res. Lett.* **30**, 23–26 (2003).

246. J. Gago, O. Carretero, A. V Filgueiras, L. Viñas, Synthetic microfibers in the marine environment: A review on their occurrence in seawater and sediments. *Mar. Pollut. Bull.* **127**, 365–376 (2018).

247. R. Dris, J. Gasperi, B. Tassin, M. Wagner, S. Lambert, Eds. (Springer International Publishing, Cham, 2018; https://doi.org/10.1007/978-3-319-61615-5_4), pp. 69–83.

248. M. Filella, Questions of size and numbers in environmental research on microplastics: Methodological and conceptual aspects. *Environ. Chem.* **12**, 527–538 (2015).

249. R. Hurley, J. Woodward, J. J. Rothwell, Supplementary Information - Microplastic contamination of river beds significantly reduced by catchment-wide flooding. *Nat. Geosci.* **11**, 251–257 (2018).

250. M. T. Nuelle, J. H. Dekiff, D. Remy, E. Fries, A new analytical approach for monitoring microplastics in marine sediments. *Environ. Pollut.* **184**, 161–169 (2014).

Appendices

Appendix 1: Summary of characteristics of atmospheric microplastics from the literature.

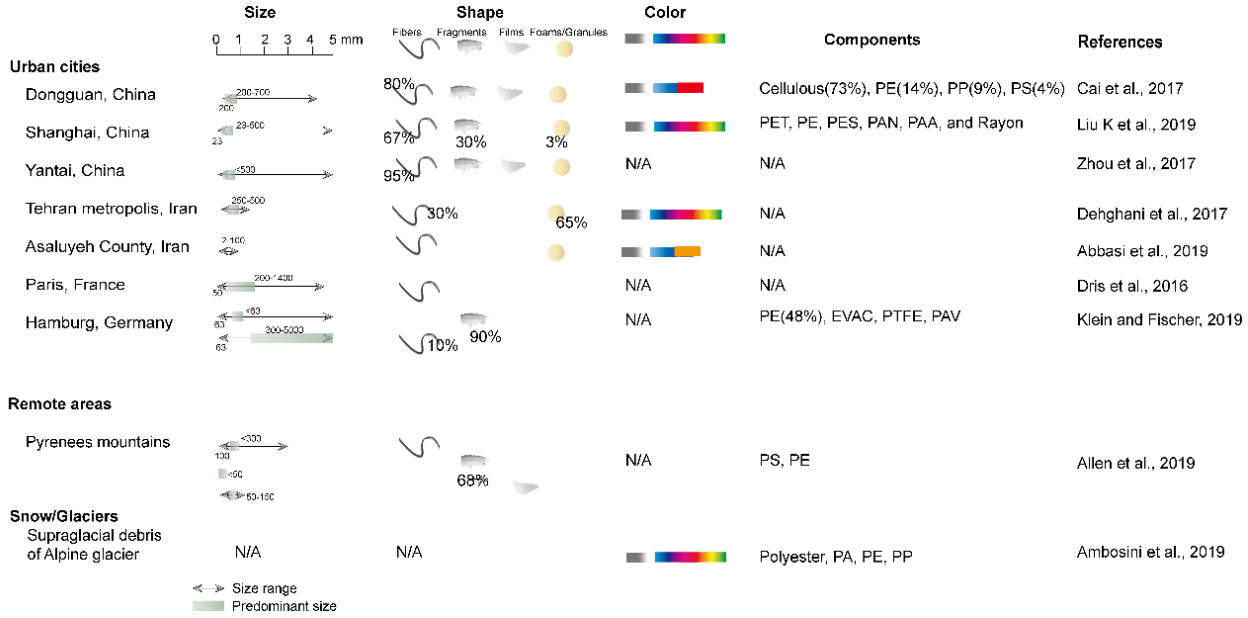

Appendix 2: Detailed site description for Bernadouze, French Pyrenees field site.

The study site is located at the Bernadouze meteorological station (OHM Haut Vicdessos Labex-DRIIHM station run by CESBIO and ENSAT INP University of Toulouse(*125*, *236*)) (Figure 1). The meteorological station is situated 42°48'14.6"N 1°25'06.8"E, at 1425m a.s.l. within the Vicdessos catchment, in the mountain range of Mid-Pyrenees mountains in south-west of France.

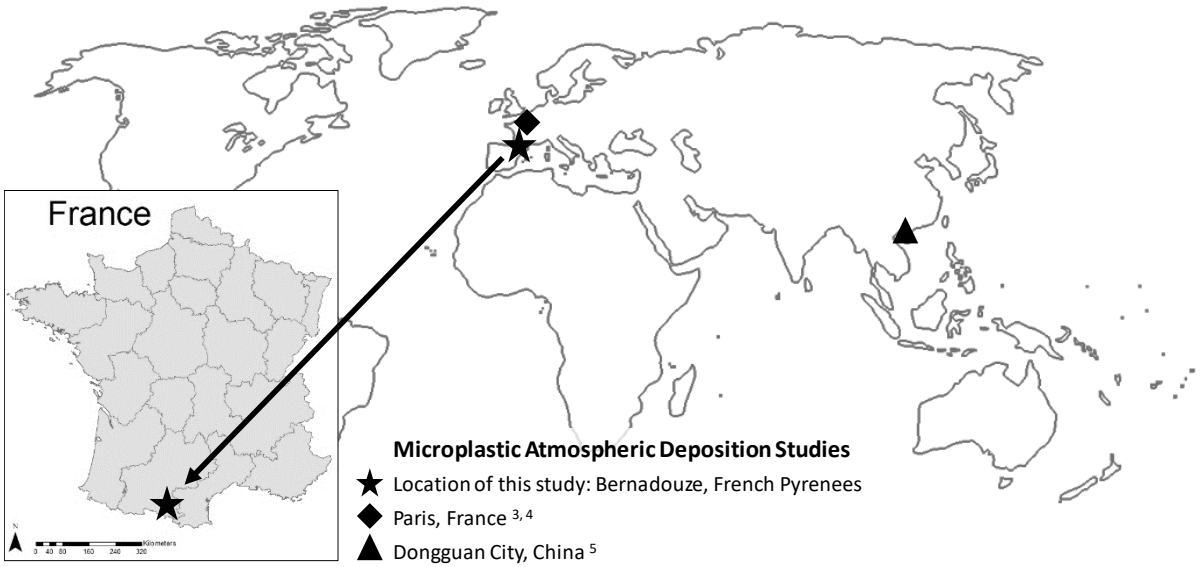

Figure 1. Study site location and previous atmospheric deposition MP studies ((*8*, *43*, *79*)).

The mountainous regions of the Pyrenees are anecdotally considered a pristine wilderness area due to limited development, difficulty of human access (primarily recreation and agriculture use) and distance from major populations or industrial centres. A review of the literature however shows that the Pyrenees Mountains have been the sentinels of anthropogenic pollution(*237–239*) as far back as 685AD with lake cores illustrating high levels of lead and remarkable levels of arsenic(*240*) from mining and industrial activities(*241*, *242*). Pyrenean peat archives illustrate both local and distal pollutant influences; from the Roman Period influence is suggested to occur from the Iberic Peninsula or/and local Bronze Age pollution(*243*). The Pyrenees have also been shown to receive bacteria and virus' from airborne deposits of dust from Africa (*242*, *244*, *245*).

The station is located in the saddle of the pass running East-West and is 214m to the south of the only road that traverses through the pass (the road was closed to normal

traffic throughout the study period due to standard Winter traffic regulations). The local vicinity is sparsely populated and without industrial, commercial or large agricultural activities and is primarily used for recreational activities (hiking, skiing, environmental education and scientific research). The closest local residential area is a village ~6km to the east in the Vicdessos valley (Vicdessos village, population ~540 (*126*)) with a moderately sized town located ~25km to the north-east (Foix, population ~9,720 (*126*)). The field site is approximately 100km south of Toulouse, 120km west of Perpignan (and the Mediterranean coast), approximately 24km north of the metropolitan area of Andorra and approximately 12km north west of the French-Spanish border.

The meteorological station is located in a clearing, free from road access and tree cover. The monitoring location is within a saddle pass that faces east south-east with the Pyrenean mountain range stretching around the site and to the north-west and south-east. The 'Pic de Trois Seigneurs' (2199m a.s.l.) is located 3km to the north north-east, at the top of the adjacent Arbu catchment.

This field site is a location of continuous monitoring for climate and environmental analysis, primarily used in analysis of atmospheric pollution such as Pb, Hg, Sb, CO_2 in conjunction with local peat and mountain lake pollution repositories (studies undertaken by EcoLab, Observatoire Homme-Milieu Pyrénées Haut Vicdessos and Observatoire Midi Pyrenees). For this reason, this location was selected as the preliminary case study site, due to the history of atmospheric pollution research undertaken at this location, the availability of meteorological data and physical sample acquisition.

References

1. I. Baker, Fifty Materials That Make the World. *Springer Int. Publ. AG*. **Chapter**-**33**, 175–178 (2018).
2. Y. Liu, Z. Shao, P. Zhou, X. Chen, Thermal and crystalline behaviour of silk fiborin/nylon 66 blend films. *Polymer (Guildf).* **45**, 7705–7710 (2004).
3. S. Werner, A. Budziak, J. A. Van Fanneker, F. Galgani, G. Hanke, T. Maes, M. Matiddi, P. Nilsson, L. Oosterbaan, E. Priestland, R. C. Thompson, J. M. Veiga, T. Vlachogianni, *Harm caused by Marine Litter - European Commission* (2016; https://ec.europa.eu/jrc/en/publication/harm-caused-marine-litter).
4. K. w Kenyon, E. Kridler, Laysan Albatrosses Swallow Indigestible Matter. *AUK*. **86**, 339–343 (1969).

5. S. I. Rothstein, Plastic particle pollution of the surface of the Atlantic Ocean: evidence from a seabird. *Condor*. **75**, 344–345 (1973).

6. E. J. Carpenter, K. L. J. Smith, Plastics on the Sargasso Sea Surface. *Science*. **175**, 1240–1241 (1972).

7. R. Dris, thesis, Université Paris-Est (2016).

8. L. Cai, J. Wang, J. Peng, Z. Tan, Z. Zhan, X. Tan, Q. Chen, Characteristic of microplastics in the atmospheric fallout from Dongguan city, China: preliminary research and first evidence. *Environ. Sci. Pollut. Res.* **24**, 24928–24935 (2017).

9. S. Dehghani, F. Moore, R. Akhbarizadeh, Microplastic pollution in deposited urban dust, Tehran metropolis, Iran. *Environ. Sci. Pollut. Res.* **24**, 20360–20371 (2017).

10. K. Zhang, J. Su, X. Xiong, X. Wu, C. Wu, J. Liu, Microplastic pollution of lakeshore sediments from remote lakes in Tibet plateau, China. *Environ. Pollut.* **219**, 450–455 (2016).

11. S. Allen, D. Allen, V. R. Phoenix, G. Le Roux, P. Duranteza, A. Simonneau, B. Stéphane, D. Galop, Atmospheric transport and deposition of microplastics in a remote mountain catchment. *Nat. Geosci.* **12**, 339–344 (2019).

12. PlasticsEurope, "Plastics – the Facts 2018: An analysis of European plastics production, demand and waste data" (2018), (available at http://www.plasticseurope.org).

13. C. M. Rochman, C. Brookson, J. Bikker, N. Djuric, A. Earn, K. Bucci, S. Athey, A. Huntington, H. McIlwraith, K. Munno, H. De Frond, A. Kolomijeca, L. Erdle, J. Grbic, M. Bayoumi, S. B. Borrelle, T. Wu, S. Santoro, L. M. Werbowski, X. Zhu, R. K. Giles, B. M. Hamilton, C. Thaysen, A. Kaura, N. Klasios, L. Ead, J. Kim, C. Sherlock, A. Ho, C. Hung, Rethinking microplastics as a diverse contaminant suite. *Environ. Toxicol. Chem.* **38**, 703–711 (2019).

14. E. Y. Zeng, Ed., *Microplastic Contamination in Aquatic Environments - An Emerging Matter of Environmental Urgency* (Elsevier, 2018; https://www.sciencedirect.com/book/9780128137475/microplastic-contamination-in-aquatic-environments).

15. GESAMP, *Sources, Fate and Effects of Microplastics in the Marine Environment: Part 2 of a Global Assessment* (IMO/FAO/UNESCO-IOC/UNIDO/WMO/IAEA/UN/ UNEP/UNDP Joint Group of Experts on the Scientific Aspects of Marine Environmental Protection, 2016; file:///C:/Users/BACHEL~2/AppData/Local/Temp/sources-fate-and-effects-of-microplastics-in-the-marine-environment-part-2-of-a-global-assessment-en.pdf).

16. C. Masura, Julie, Baker, Joel, Foster, Gregory, Arthur, "Laboratory Methods for the Analysis of Microplastics in the Marine Environment" (2015), (available at https://marinedebris.noaa.gov/sites/default/files/publications-files/noaa_microplastics_methods_manual.pdf).

17. R. C. Thompson, Y. Olsen, R. P. Mitchell, A. Davis, S. J. Rowland, A. W. G. John, D. McGonigle, A. E. Russell, Lost at Sea: Where does all the plastic go? *Science (80-.).* **304**, 838 (2004).

18. N. B. Hartmann, T. Hüffer, R. C. Thompson, M. Hassellöv, A. Verschoor, A. E. Daugaard, S. Rist, T. Karlsson, N. Brennholt, M. Cole, M. P. Herrling, M. C. Hess, N. P. Ivleva, A. L.

Lusher, M. Wagner, Are We Speaking the Same Language? Recommendations for a Definition and Categorization Framework for Plastic Debris. *Environ. Sci. Technol.* **53**, 1039–1047 (2019).

19. O. S. Alimi, J. Farner Budarz, L. M. Hernandez, N. Tufenkji, Microplastics and Nanoplastics in Aquatic Environments: Aggregation, Deposition, and Enhanced Contaminant Transport. *Environ. Sci. Technol.* **52**, 1704–1724 (2018).

20. M. G. J. Löder, G. Gerdts, in *Marine Anthropogenic Litter*, M. Bergmann, L. Gutow, M. Klages, Eds. (2015), pp. 201–227.

21. M. S. Bank, S. V. Hansson, *Environ. Sci. Technol.*, in press, doi:10.1021/acs.est.9b02942.

22. W. G. Kreyling, M. Semmler-Behnke, Q. Chaudhry, A complementary definition of nanomaterial. *Nano Today*. **5**, 165–168 (2010).

23. C. Joachim, To be nano or not to be nano? *Nat. Mater.* **4**, 107–109 (2005).

24. H. S. Auta, C. U. Emenike, S. H. Fauziah, Distribution and importance of microplastics in the marine environmentA review of the sources, fate, effects, and potential solutions. *Environ. Int.* **102**, 165–176 (2017).

25. J. Li, H. Liu, J. Paul Chen, Microplastics in freshwater systems: A review on occurrence, environmental effects, and methods for microplastics detection. *Water Res.* **137**, 362–374 (2018).

26. J. C. Prata, J. P. da Costa, A. V Girão, I. Lopes, A. C. Duarte, T. Rocha-Santos, Identifying a quick and efficient method of removing organic matter without damaging microplastic samples. *Sci. Total Environ.* **686**, 131–139 (2019).

27. P. Ribeiro-Claro, M. M. Nolasco, C. Araújo, Characterization of Microplastics by Raman Spectroscopy. *Compr. Anal. Chem.* **75**, 119–151 (2017).

28. C. M. Rochman, in *Marine Anthropogenic Litter*, M. Bergmann, L. Gutow, M. Klages, Eds. (Springer, Cham, 2015), pp. 117–140.

29. A. A. Horton, S. J. Dixon, Microplastics: An introduction to environmental transport processes. *Wiley Interdiscip. Rev. Water*. **5**, e1268 (2018).

30. L. Camarero, M. Bacardit, A. de Diego, G. Arana, Decadal trends in atmospheric deposition in a high elevation station: Effects of climate and pollution on the long-range flux of metals and trace elements over SW Europe. *Atmos. Environ.* **167**, 542–552 (2017).

31. R. Ambrosini, R. S. Azzoni, F. Pittino, G. Diolaiuti, A. Franzetti, M. Parolini, First evidence of microplastic contamination in the supraglacial debris of an alpine glacier. *Environ. Pollut.* **253**, 297–301 (2019).

32. M. Klein, E. K. Fischer, Microplastic abundance in atmospheric deposition within the Metropolitan area of Hamburg, Germany. *Sci. Total Environ.* **685**, 96–103 (2019).

33. K. Liu, X. Wang, T. Fang, P. Xu, L. Zhu, D. Li, Source and potential risk assessment of suspended atmospheric microplastics in Shanghai. *Sci. Total Environ.* **675**, 462–471 (2019).

34. K. Liu, T. Wu, X. Wang, Z. Song, C. Zong, N. Wei, D. Li, Consistent transport of terrestrial

microplastics to the ocean through atmosphere. *Environ. Sci. Technol.*, 1–12 (2019).

35. Y. Zhang, T. Gao, S. Kang, M. Sillanpaa, Microplastics intrude into the Tibetan Plateau. *Sci. Rep.* **in review** (2019).

36. L. G. A. Barboza, L. R. Vieira, V. Branco, N. Figueiredo, F. Carvalho, C. Carvalho, L. Guilhermino, Microplastics cause neurotoxicity, oxidative damage and energy-related changes and interact with the bioaccumulation of mercury in the European seabass, Dicentrarchus labrax (Linnaeus, 1758). *Aquat. Toxicol.* **195**, 49–57 (2018).

37. J. Gasperi, S. L. Wright, R. Dris, F. Collard, C. Mandin, M. Guerrouache, V. Langlois, F. J. Kelly, B. Tassin, Microplastics in air: Are we breathing it in? *Curr. Opin. Environ. Sci. Heal.* **1**, 1–5 (2018).

38. C. Liu, J. Li, Y. Zhang, L. Wang, J. Deng, Y. Gao, L. Yu, J. Zhang, H. Sun, Widespread distribution of PET and PC microplastics in dust in urban China and their estimated human exposure. *Environ. Int.* **128**, 116–124 (2019).

39. P. S. Tourinho, V. Kočí, S. Loureiro, C. A. M. van Gestel, Partitioning of chemical contaminants to microplastics: Sorption mechanisms, environmental distribution and effects on toxicity and bioaccumulation. *Environ. Pollut.* **252**, 1246–1256 (2019).

40. S. L. Wright, F. J. Kelly, Plastic and Human Health: A Micro Issue? *Environ. Sci. Technol.* **51**, 6634–6647 (2017).

41. C. G. Alimba, C. Faggio, Microplastics in the marine environment: Current trends in environmental pollution and mechanisms of toxicological profile. *Environ. Toxicol. Pharmacol.* **68**, 61–74 (2019).

42. R. Dris, C. J. Gasperi, A. V. Rocher, B. M. Saad, N. Renault, B. Tassin, Microplastic contamination in an urban area : a case study in Greater Paris. *Environ. Chem.* **12**, 592–599 (2015).

43. R. Dris, J. Gasperi, C. Mirande, C. Mandin, M. Guerrouache, V. Langlois, B. Tassin, A first overview of textile fibers, including microplastics, in indoor and outdoor environments. *Environ. Pollut.* **221**, 453–458 (2017).

44. S. Abbasi, B. Keshavarzi, F. Moore, H. Delshab, N. Soltani, A. Sorooshian, Investigation of microrubbers, microplastics and heavy metals in street dust: a study in Bushehr city, Iran. *Environ. Earth Sci.* **76** (2017), doi:10.1007/s12665-017-7137-0.

45. S. J. Hayward, T. Gouin, F. Wania, Comparison of four active and passive sampling techniques for pesticides in air. *Environ. Sci. Technol.* **44**, 3410–3416 (2010).

46. A. Dommergue, P. Amato, R. Tignat-perrier, O. Magand, A. Thollot, M. Joly, L. Bouvier, K. Sellegri, T. Vogel, J. Sonke, J. Jaffrezo, M. Andrade, I. Moreno, C. Labuschagne, L. Martin, Q. Zhang, C. Larose, D. A. Pearce, Methods to Investigate the Global Atmospheric Microbiome. *Front. Microbiol.* **10**, 1–12 (2019).

47. V. Hidalgo-Ruz, L. Gutow, R. C. Thompson, M. Thiel, Microplastics in the marine environment: A review of the methods used for identification and quantification. *Environ. Sci. Technol.* **46**, 3060–3075 (2012).

48. B. Nguyen, D. Claveau-Mallet, L. M. Hernandez, E. G. Xu, J. M. Farner, N. Tufenkji, Separation and Analysis of Microplastics and Nanoplastics in Complex Environmental

Samples. *Acc. Chem. Res.* **52**, 858–866 (2019).

49. Q. Zhou, C. Tian, Y. Luo, Various forms and deposition fluxes of microplastics identified in the coastal urban atmosphere. *Chinese Sci. Bull.* **62**, 3902–3909 (2017).

50. Marine & Environmental Research Institute, *Guide to Microplastic Identification* (Marine & Environmental Research Instatite, 2015).

51. A. B. Silva, A. S. Bastos, C. I. L. Justino, J. P. da Costa, A. C. Duarte, T. A. P. Rocha-Santos, Microplastics in the environment: Challenges in analytical chemistry - A review. *Anal. Chim. Acta*. **1017**, 1–19 (2018).

52. M. G. J. Löder, H. K. Imhof, M. Ladehoff, L. A. Löschel, C. Lorenz, S. Mintenig, S. Piehl, S. Primpke, I. Schrank, C. Laforsch, G. Gerdts, Enzymatic Purification of Microplastics in Environmental Samples. *Environ. Sci. Technol.* **51**, 14283–14292 (2017).

53. J. S. Hanvey, P. J. Lewis, J. L. Lavers, N. D. Crosbie, K. Pozo, B. O. Clarke, A review of analytical techniques for quantifying microplastics in sediments. *Anal. Methods*. **9**, 1369–1383 (2017).

54. G. Renner, T. C. Schmidt, J. Schram, Analytical methodologies for monitoring micro(nano)plastics: Which are fit for purpose? *Curr. Opin. Environ. Sci. Heal.* **1**, 55–61 (2018).

55. T. Stanton, M. Johnson, P. Nathanail, W. MacNaughtan, R. L. Gomes, Freshwater and airborne textile fibre populations are dominated by 'natural', not microplastic, fibres. *Sci. Total Environ.* **666**, 377–389 (2019).

56. R. Hurley, A. L. Lusher, M. Olsen, L. Nizzetto, Validation of a Method for Extracting Microplastics from Complex, Organic-Rich, Environmental Matrices. *Environ. Sci. Technol.* **52**, 7409–7417 (2018).

57. A. S. Tagg, J. P. Harrison, Y. Ju-Nam, M. Sapp, E. L. Bradley, C. J. Sinclair, J. J. Ojeda, Fenton's reagent for the rapid and efficient isolation of microplastics from wastewater. *Chem. Commun.* **53**, 372–375 (2017).

58. B. Quinn, F. Murphy, C. Ewins, Validation of density separation for the rapid recovery of microplastics from sediment. *Anal. Methods*. **9**, 1491–1498 (2017).

59. A. Käppler, D. Fischer, S. Oberbeckmann, G. Schernewski, M. Labrenz, K.-J. Eichhorn, B. Voit, Analysis of environmental microplastics by vibrational microspectroscopy: FTIR, Raman or both? *Anal Bioanal Chem*. **408**, 8377–8391 (2016).

60. C. Araujo, M. M. Nolasco, A. M. P. Ribeiro, P. J. A. Ribeiro-Claro, Identification of microplastics using Raman spectroscopy: Latest developments and future prospects. *Water Res.* **142**, 426–440 (2018).

61. E. Hendrickson, E. C. Minor, K. Schreiner, Microplastic Abundance and Composition in Western Lake Superior As Determined via Microscopy, Pyr-GC/MS, and FTIR. *Environ. Sci. Technol.* **52**, 1787–1796 (2018).

62. D. Materić, A. Kasper-Giebl, D. Kau, M. Anten, M. Greilinger, E. Ludewig, E. van Sebille, T. Röckmann, R. Holzinger, Micro- and nanoplastics in Alpine snow – a new method for chemical identification and quantification in the nanogram range. *Environ. Sci. Technol.* **54**, 2353–2359 (2020).

63. R. Gillibert, G. Balakrishnan, Q. Deshoules, M. Tardivel, A. Magazzù, M. G. Donato, O. M. Maragò, M. Lamy de La Chapelle, F. Colas, F. Lagarde, P. G. Gucciardi, Raman Tweezers for Small Microplastics and Nanoplastics Identification in Seawater. *Environ. Sci. Technol.* **53**, 9003–9013 (2019).

64. E. Fries, J. H. Dekiff, J. Willmeyer, M.-T. Nuelle, M. Ebert, D. Remy, Identification of polymer types and additives in marine microplastic particles using pyrolysis-GC/MS and scanning electron microscopy. *Environ. Sci. Process. Impacts*. **15**, 1949 (2013).

65. D. Materić, E. Ludewig, K. Xu, T. Röckmann, R. Holzinger, Brief communication: Analysis of organic matter in surface snow by PTR-MS - Implications for dry deposition dynamics in the Alps. *Cryosphere*. **13**, 297–307 (2019).

66. D. Materić, M. Peacock, M. Kent, S. Cook, V. Gauci, T. Röckmann, R. Holzinger, Characterisation of the semi-volatile component of Dissolved Organic Matter by Thermal Desorption - Proton Transfer Reaction - Mass Spectrometry. *Sci. Rep.* **7**, 1–8 (2017).

67. M. Fischer, B. M. Scholz-Böttcher, Simultaneous Trace Identification and Quantification of Common Types of Microplastics in Environmental Samples by Pyrolysis-Gas Chromatography-Mass Spectrometry. *Environ. Sci. Technol.* **51**, 5052–5060 (2017).

68. A. Käppler, M. Fischer, B. M. Scholz-Böttcher, S. Oberbeckmann, M. Labrenz, D. Fischer, K. J. Eichhorn, B. Voit, Comparison of µ-ATR-FTIR spectroscopy and py-GCMS as identification tools for microplastic particles and fibers isolated from river sediments. *Anal. Bioanal. Chem.* **410**, 5313–5327 (2018).

69. E. Dümichen, A. K. Barthel, U. Braun, C. G. Bannick, K. Brand, M. Jekel, R. Senz, Analysis of polyethylene microplastics in environmental samples, using a thermal decomposition method. *Water Res.* **85**, 451–457 (2015).

70. E. Dümichen, P. Eisentraut, C. G. Bannick, A. K. Barthel, R. Senz, U. Braun, Fast identification of microplastics in complex environmental samples by a thermal degradation method. *Chemosphere*. **174**, 572–584 (2017).

71. J. David, Z. Steinmetz, J. Kučerík, G. E. Schaumann, Quantitative Analysis of Poly(ethylene terephthalate) Microplastics in Soil via Thermogravimetry-Mass Spectrometry. *Anal. Chem.* **90**, 8793–8799 (2018).

72. A. Centrone, Infrared Imaging and Spectroscopy Beyond the Diffraction Limit. *Annu. Rev. Anal. Chem.* **8**, 101–126 (2015).

73. M. Bergmann, S. Mützel, S. Primpke, M. B. Tekman, J. Trachsel, G. Gerdts, White and wonderful? Microplastics prevail in snow from the Alps to the Arctic. *Sci. Adv.* **5**, eaax1157 (2019).

74. S. Primpke, C. Lorenz, R. Rascher-Friesenhausen, G. Gerdts, An automated approach for microplastics analysis using focal plane array (FPA) FTIR microscopy and image analysis. *Anal. Methods*. **9**, 1499–1511 (2017).

75. N. Everall, P. Griffiths, J. Chamlers, *Vibrational Spectroscopy of Polymers: Principles and Practice* (Wiley, 2007; https://www.wiley.com/en-us/Vibrational+Spectroscopy+of+Polymers%3A+Principles+and+Practice-p-9780470016626).

76. A. Vianello, R. L. Jensen, L. Liu, J. Vollertsen, Simulating human exposure to indoor airborne microplastics using a Breathing Thermal Manikin. *Sci. Rep.* **9**, 1–11 (2019).

77. F. Huth, A. Govyadinov, S. Amarie, W. Nuansing, F. Keilmann, R. Hillenbrand, Nano-FTIR absorption spectroscopy of molecular fingerprints at 20 nm spatial resolution. *Nano Lett.* **12**, 3973–3978 (2012).

78. M. Meyns, S. Primpke, G. Gerdts, "Library based identification and characterisation of polymers with nano-FTIR and IR-sSNOM imaging" (2019), , doi:arXiv:1906.10243.

79. R. Dris, J. Gasperi, M. Saad, C. Mirande, B. Tassin, Synthetic fibers in atmospheric fallout: A source of microplastics in the environment? *Mar. Pollut. Bull.* **104**, 290–293 (2016).

80. M. Ganguly, P. A. Ariya, Ice Nucleation of Model Nano-Micro Plastics: A Novel Synthetic Protocol and the Influence of Particle Capping at Diverse Atmospheric Environments. *ACS Earth Sp. Chem.* (2019), doi:10.1021/acsearthspacechem.9b00132.

81. A. C. Rocha-Santos, Teresa Duarte, *Characterization and Analysis of Microplastics* (Elsevier, 2017; https://books.google.co.uk/books?hl=en&lr=&id=DqCpDQAAQBAJ&oi=fnd&pg=PP1&dq=Rocha-Santos+and+Duarte,+2017.+Characterization+and+analysis+of+microplastics.&ots=tHW_iRapBc&sig=GcxB39KZu1IszvGvXjJv5pG1M6Q#v=onepage&q=Rocha-Santos and Duarte%2C 2017. Characte), vol. 75.

82. A. Klein, F. Ravetta, J. L. Thomas, G. Ancellet, P. Augustin, R. Wilson, E. Dieudonné, M. Fourmentin, H. Delbarre, J. Pelon, Influence of vertical mixing and nighttime transport on surface ozone variability in the morning in Paris and the surrounding region. *Atmos. Environ.* **197**, 92–102 (2019).

83. S. Abbasi, B. Keshavarzi, F. Moore, A. Turner, F. J. Kelly, A. O. Dominguez, N. Jaafarzadeh, Distribution and potential health impacts of microplastics and microrubbers in air and street dusts from Asaluyeh County, Iran. *Environ. Pollut.* **244**, 153–164 (2019).

84. P. A. Helm, Improving microplastics source apportionment: A role for microplastic morphology and taxonomy? *Anal. Methods*. **9**, 1328–1331 (2017).

85. I. E. Napper, R. C. Thompson, Release of synthetic microplastic plastic fibres from domestic washing machines: Effects of fabric type and washing conditions. *Mar. Pollut. Bull.* **112**, 39–45 (2016).

86. A. Jemec, P. Horvat, U. Kunej, M. Bele, A. Kržan, Uptake and effects of microplastic textile fibers on freshwater crustacean Daphnia magna. *Environ. Pollut.* **219**, 201–209 (2016).

87. M. Cole, A novel method for preparing microplastic fibers. *Sci. Rep.* **6**, 1–7 (2016).

88. T. Hüffer, A. Praetorius, S. Wagner, F. Von Der Kammer, T. Hofmann, Microplastic Exposure Assessment in Aquatic Environments: Learning from Similarities and Differences to Engineered Nanoparticles. *Environ. Sci. Technol.* **51**, 2499–2507 (2017).

89. E. Besseling, J. T. K. Quik, M. Sun, A. A. Koelmans, Fate of nano- and microplastic in freshwater systems: A modeling study. *Environ. Pollut.* **220**, 540–548 (2017).

90. A. Isobe, K. Uchida, T. Tokai, S. Iwasaki, East Asian seas: A hot spot of pelagic microplastics. *Mar. Pollut. Bull.* **101**, 618–623 (2015).

91. Z. Fu, J. Wang, Current practices and future perspectives of microplastic pollution in freshwater ecosystems in China. *Sci. Total Environ.* **691**, 697–712 (2019).

92. M. A. Browne, P. Crump, S. J. Niven, E. Teuten, A. Tonkin, T. Galloway, R. C. Thompson, Accumulation of Microplastic on Shorelines Woldwide : Sources and Sinks, 9175–9179 (2011).

93. B. Kuczenski, R. Geyer, Material flow analysis of polyethylene terephthalate in the US, 1996-2007. *Resour. Conserv. Recycl.* **54**, 1161–1169 (2010).

94. L. Hermabessiere, A. Dehaut, I. Paul-Pont, C. Lacroix, R. Jezequel, P. Soudant, G. Duflos, Occurrence and effects of plastic additives on marine environments and organisms: A review. *Chemosphere*. **182** (2017), pp. 781–793.

95. F. M. Windsor, I. Durance, A. A. Horton, R. C. Thompson, C. R. Tyler, S. J. Ormerod, A catchment-scale perspective of plastic pollution. *Glob. Chang. Biol.* **25**, 1207–1221 (2019).

96. S. Turner, A. A. Horton, N. L. Rose, C. Hall, A temporal sediment record of microplastics in an urban lake, London, UK. *J. Paleolimnol.* **61**, 449–462 (2019).

97. D. Allen, S. Allen, J. Sonke, V. Phoenix, in *International Conference on Microplastic Pollution inthe Mediterranean Sea*, M. Cocca, E. Di Pace, M. Errico, G. Gentile, A. Montarsolo, R. Mossotti, Eds. (Springer Water. Springer, Cham, Capri, 2019), pp. 1–8.

98. M. van der Does, P. Knippertz, P. Zschenderlein, R. Giles Harrison, J.-B. W. Stuut, The mysterious long-range transport of giant mineral dust particles. *Sci. Adv.* **4** (2018), doi:10.1126/sciadv.aau2768.

99. J. R. Jambeck, R. Geyer, C. Wilcox, T. R. Siegler, M. Perryman, A. Andrady, R. Narayan, K. L. Law, Plastic waste inputs from land into the Ocean. *Science (80-.).* **347**, 768–771 (2015).

100. J. C. Prata, Airborne microplastics: Consequences to human health? *Environ. Pollut.* **234**, 115–126 (2018).

101. C. M. Rochman, A. Tahir, S. L. Williams, D. V. Baxa, R. Lam, J. T. Miller, F. C. Teh, S. Werorilangi, S. J. Teh, Anthropogenic debris in seafood: Plastic debris and fibers from textiles in fish and bivalves sold for human consumption. *Sci. Rep.* **5**, 1–10 (2015).

102. A. Churg, M. Brauer, Ambient atmospheric particles in the airways of human lungs. *Ultrastruct. Pathol.* **24**, 353–361 (2000).

103. J. L. Pauly, S. J. Stegmeier, H. A. Allaart, R. T. Cheney, P. J. Zhang, A. G. Mayer, R. J. Streck, Inhaled cellulosic and plastic fibers found in human lung tissue. *Cancer Epidemiol. Biomarkers Prev.* **7**, 419–428 (1998).

104. A. M. Kremer, T. M. Pal, J. S. M. Boleij, J. P. Schouten, B. Rijcken, Airway hyperresponsiveness, prevalence of chronic respiratory symptoms, and lung function in workers exposed to irritants. *Occup. Environ. Med.* **51**, 3–13 (1994).

105. N. Laskar, U. Kumar, Plastics and microplastics: A threat to environment. *Environ. Technol. Innov.* **14**, 100352 (2019).

106. G. Latini, C. De Felice, G. Presta, A. Del Vecchio, I. Paris, F. Ruggieri, P. Mzzeo, In utero exposure to di-(2-ethylhexyl)phthalate and duration of human pregnancy. *Environ. Health Perspect.* **111**, 1783–1785 (2003).

107. J. J. Wirth, M. Rossano, R. Potter, E. Puscheck, D. Daly, N. Paneth, S. Krawetz, B. Protas, M. Diamond, A Pilot Study Associating Urinary Concentrations of Phthalate Metabolites and Semen Quality. *Syst. Biol. Reprod. Med.* **54**, 143–154 (2008).

108. J. Drummond, S. Krause, L. Nel, S. Allen, D. Allen, L. Simon, C. Doaudy, "Gathering at the top? Environmental controls of microplastic uptake and biomagnification in aquatic food webs" (2019).

109. T. C. Nardelli, H. C. Erythropel, B. Robaire, Toxicogenomic screening of replacements for Di(2-Ethylhexyl) phthalate (DEHP) using the immortalized TM4 sertoli cell line. *PLoS One*. **10**, 1–17 (2015).

110. J. Peretz, L. Vrooman, W. A. Ricke, P. A. Hunt, S. Ehrlich, R. Hauser, V. Padmanabhan, H. S. Taylor, S. H. Swan, C. A. Vandevoort, J. A. Flaws, Bisphenol A and reproductive health: Update of experimental and human evidence, 2007-2013. *Environ. Health Perspect.* **122**, 775–786 (2014).

111. R. A. Bhat, D. Kumar, S. M. Bhat, I. R. Sofi, in *Handbook of Research on Environmental and Human Health Impacts of Plastic Pollution* (IGI Global, 2020), pp. 246–262.

112. P. Fu, K. Kawamura, Ubiquity of bisphenol A in the atmosphere. *Environ. Pollut.* **158**, 3138–3143 (2010).

113. R. Lehner, C. Weder, A. Petri-Fink, B. Rothen-Rutishauser, Emergence of Nanoplastic in the Environment and Possible Impact on Human Health. *Environ. Sci. Technol.* (2019), doi:10.1021/acs.est.8b05512.

114. C. Rosevelt, M. Los Huertos, C. Garza, H. M. Nevins, Marine debris in central California: Quantifying type and abundance of beach litter in Monterey Bay, CA. *Mar. Pollut. Bull.* **71**, 299–306 (2013).

115. PlasticsEurope, *Plastics – the Facts 2014 / 2015 An analysis of European plastics production , demand and waste data* (Plastic Recycling and Recovery Organisations (EPRO), Belgium, 2015; https://www.plasticseurope.org/application/files/5515/1689/9220/2014plastics_the_facts_PubFeb2015.pdf).

116. PlasticsEurope, *Plastics – the Facts 2017, An analysis of the European plastics production, demand and waste data* (PlasticsEurope, European Association of Plastics Recycling and Recovery Organisations, Belgium, 2017; https://www.plasticseurope.org/application/files/5715/1717/4180/Plastics_the_facts_2017_FINAL_for_website_one_page.pdf).

117. Y. K. Song, S. H. Hong, M. Jang, G. M. Han, S. W. Jung, W. J. Shim, Combined Effects of UV Exposure Duration and Mechanical Abrasion on Microplastic Fragmentation by Polymer Type. *Environ. Sci. Technol.* **51**, 4368–4376 (2017).

118. J. P. da Costa, Micro- and nanoplastics in the environment: Research and policymaking. *Curr. Opin. Environ. Sci. Heal.* **1**, 12–16 (2018).

119. K. Mattsson, L.-A. Hansson, T. Cedervall, Nano-plastics in the aquatic environment.

Environ. Sci. Process. Impacts. **17**, 1712–1721 (2015).

120. M. Scheurer, M. Bigalke, Microplastics in Swiss floodplain soils (2018), doi:10.1021/acs.est.7b06003.

121. R. Hurley, J. Woodward, J. J. Rothwell, Microplastic contamination of river beds significantly reduced by catchment-wide flooding. *Nat. Geosci.* **11**, 251–257 (2018).

122. P. L. Corcoran, Benthic plastic debris in marine and fresh water environments. *Environ. Sci. Process. Impacts*. **17**, 1363–1369 (2015).

123. M. Zbyszewski, P. L. Corcoran, A. Hockin, Comparison of the distribution and degradation of plastic debris along shorelines of the Great Lakes , North America. *J. Great Lakes Res.* **40**, 288–299 (2014).

124. L. Watkins, S. McGrattan, P. J. Sullivan, M. T. Walter, The effect of dams on river transport of microplastic pollution. *Sci. Total Environ.* (2019), doi:https://doi.org/10.1016/j.scitotenv.2019.02.028.

125. Centre d'Etudes Spatiales de la BIOsphere (CESBIO), Donnees meteorologiques – Sud Ouest Bernadouze (2018), (available at http://www.cesbio.ups-tlse.fr/data_meteo/index.php?perma=1319145390).

126. INSEE, Institut national de la statistique et des etudes economiques (2018), (available at https://www.insee.fr/fr/statistiques/3293086?geo=COM-09334).

127. G. Erni-Cassola, M. I. Gibson, R. C. Thompson, J. A. Christie-Oleza, Lost, but Found with Nile Red: A Novel Method for Detecting and Quantifying Small Microplastics (1 mm to 20 µm) in Environmental Samples. *Environ. Sci. Technol.* **51**, 13641–13648 (2017).

128. N. Digka, C. Tsangaris, H. Kaberi, A. Adamopoulou, C. Zeri, in *Proceedings of the International Conference on Microplastic Pollution in the Mediterranean Sea*, M. Cocca, E. Di Pace, M. Errico, G. Gentile, A. Montarsolo, R. Mossotti, Eds. (Springer Water. Springer, Cham, 2018; http://link.springer.com/10.1007/978-3-319-71279-6), pp. 17–24.

129. W. Wang, A. W. Ndungu, Z. Li, J. Wang, Microplastics pollution in inland freshwaters of China: A case study in urban surface waters of Wuhan, China. *Sci. Total Environ.* **575**, 1369–1374 (2017).

130. R. Klein, in *Laser Welding of Plastics: Materials, Processes and Industrial Applications* (John Wiley & Sons, ed. 1, 2012), pp. 3–69.

131. M. Löder, G. Gerdts, in *Marine Anthropogenic Litter*, M. Bergmann, L. Gutow, M. Klages, Eds. (Springer, Cham, 2015; https://link.springer.com/chapter/10.1007%2F978-3-319-16510-3_8#citeas).

132. F. Noren, "Small plastic particles in Coastal Swedish waters" (2007).

133. W. J. Shim, S. H. Hong, S. E. Eo, Identification methods in microplastic analysis: a review. *Anal. Methods*. **9**, 1384–1391 (2017).

134. I. Peeken, S. Primpke, B. Beyer, J. Gütermann, C. Katlein, T. Krumpen, M. Bergmann, L. Hehemann, G. Gerdts, Arctic sea ice is an important temporal sink and means of transport for microplastic. *Nat. Commun.* **9**, 1505 (2018).

135. H. K. Imhof, C. Laforsch, A. C. Wiesheu, J. Schmid, P. M. Anger, R. Niessner, N. P. Ivleva, Pigments and plastic in limnetic ecosystems: A qualitative and quantitative study on microparticles of different size classes. *Water Res.* **98**, 64–74 (2016).

136. R. Lenz, K. Enders, C. A. Stedmon, D. M. A. MacKenzie, T. G. Nielsen, A critical assessment of visual identification of marine microplastic using Raman spectroscopy for analysis improvement. *Mar. Pollut. Bull.* **100**, 82–91 (2015).

137. K. Enders, R. Lenz, C. A. Stedmon, T. G. Nielsen, Abundance, size and polymer composition of marine microplastics ≥10μm in the Atlantic Ocean and their modelled vertical distribution. *Mar. Pollut. Bull.* **100**, 70–81 (2015).

138. Y. K. Song, S. H. Hong, M. Jang, G. M. Han, M. Rani, J. Lee, W. J. Shim, A comparison of microscopic and spectroscopic identification methods for analysis of microplastics in environmental samples. *Mar. Pollut. Bull.* **93**, 202–209 (2015).

139. F. Menges, Spectragryph – optical imaging software (2016), (available at https://www.effemm2.de/spectragryph/).

140. P. Y. Khashaba, H. R. H. Ali, M. M. El-Wekil, A rapid Fourier transform infrared spectroscopic method for analysis of certain proton pump inhibitors in binary and ternary mixtures. *Spectrochim. Acta Part A Mol. Biomol. Spectrosc.* **190**, 10–14 (2018).

141. R. Ševčík, P. Mácová, Localized quantification of anhydrous calcium carbonate polymorphs using micro-Raman spectroscopy. *Vib. Spectrosc.* **95**, 1–6 (2018).

142. J. M. Lagaron, N. M. Dixon, W. Reed, J. M. Pastor, B. J. Kip, Morphological characterisation of the crystalline structure of cold-drawn HDPE used as a model material for the environmental stress cracking (ESC) phenomenon. *Polymer (Guildf).* **40**, 2569–2586 (1999).

143. E. Sanchez, C. Yague, M. A. Gazetner, Planetary boundary layer energetics simulated from a regional climate model over Europe for present climate and climate change conditions. *Geophys. Res. Lett.* **34** (2007), doi:10.1029/2006gL028340.

144. C. S. Zender, Mineral Dust Entrainment and Deposition (DEAD) model: Description and 1990s dust climatology. *J. Geophys. Res.* **108**, 4416 (2003).

145. R. R. Draxler, D. Hess, G, "Description of the Hysplit4 modeling system" (Maryland, 2018), (available at https://www.researchgate.net/publication/255682850_Description_of_the_HYSPLIT_4_modelling_system).

146. A. Stein, R. Draxler, G. Rolph, B. Stunder, M. Dohen, F. Ngqn, NOAA's HYSPLIT atmospheric transport and dispersion modeling system. *Bull. Am. Meteorol. Soc.* **96**, 2059–2077 (2015).

147. L. Su, Z. Yuan, J. C. H. Fung, A. K. H. Lau, A comparison of HYSPLIT backward trajectories generated from two GDAS datasets. *Sci. Total Environ.* **506**–**507**, 527–537 (2015).

148. K. Ashrafi, M. Shafiepour-Motlagh, A. Aslemand, S. Ghader, Dust storm simulation over Iran using HYSPLIT. *J. Environ. Heal. Sci. Eng.* **12**, 9 (2014).

149. I. Reche, G. D'Orta, N. Mladenov, D. M. Winget, C. A. Suttle, Deposition rates of viruses and bacteria above the atmospheric boundary layer. *ISME J.* **12**, 1154–1162 (2018).

150. C. D. G. Zwaaftink, Ó. Arnalds, P. Dagsson-waldhauserova, S. Eckhardt, J. Prospero, A. Stohl, Temporal and spatial variability of Icelandic dust emissions and atmospheric transport. *Atmos. Chem. Phys.*, 10865–10878 (2017).

151. B. Marticorena, B. Chatenet, J. L. Rajot, G. Bergametti, A. Deroubaix, J. Vincent, A. Kouoi, C. Schmechtig, M. Coulibaly, A. Diallo, I. Koné, A. Maman, T. NDiaye, A. Zakou, Mineral dust over west and central Sahel: Seasonal patterns of dry and wet deposition fluxes from a pluriannual sampling (2006-2012). *J. Geophys. Res. Atmos.* **122**, 1338–1364 (2017).

152. R. Morales-Baquero, E. Pulido-Villen, I. Reche, Chemical signature of Saharan dust on dry and wet atmospheric deposition in the south-western Mediterranean region. *Tellus Ser. B*. **1**, 1–12 (2013).

153. M. Schwikowski, P. Seibert, U. Baltensperger, H. W. Gaggeler, A study of an outstanding Saharan dust event at the high-alpine site Jungfraujoch, Switzerland. *Atmos. Environ.* **29**, 1829–1842 (1995).

154. J. Dessens, P. Van Dinh, Frequent Saharan Dust Outbreaks North of the Pyrenees: A sign of a climatic change? *Weather*. **45**, 327–333 (1990).

155. J. Schindelin, I. Arganda-Carreras, E. Frise, V. Kaynig, M. Longair, T. Pietzsch, S. Preibisch, C. Rueden, S. Saalfeld, B. Schmid, J.-Y. Tinevez, D. J. White, V. Hartenstein, K. Eliceiri, P. Tomancak, A. Cardona, Fiji: an open-source platform for biological image analysis. *Nat. Methods*. **9**, 676–682 (2012).

156. D. Schymanski, C. Goldbeck, H. U. Humpf, P. Fürst, Analysis of microplastics in water by micro-Raman spectroscopy: Release of plastic particles from different packaging into mineral water. *Water Res.* **129**, 154–162 (2018).

157. European Comission, A European Strategy for Plastics in a Circular Economy. *Eur. Com.*, 24 (2018).

158. K. Magnusson, K. Eliasson, A. Fråne, K. Haikonen, J. Hultén, M. Olshammar, J. Stadmark, A. Voisin, Swedish sources and pathways for microplastics to the marine environment. A review of existing data. *IVL Rep.*, 1–89 (2016).

159. R. Dris, H. Imhof, W. Sanchez, J. Gasperi, F. Galgani, B. Tassin, C. Laforsch, Beyond the ocean: Contamination of freshwater ecosystems with (micro-) plastic particles. *Environ. Chem.* **12**, 539–550 (2015).

160. W. J. Shim, S. H. Hong, S. Eo, in *Microplastic Contamination in Aquatic Environments*, E. Y. Zeng, Ed. (Elsevier, 2018; http://www.sciencedirect.com/science/article/pii/B9780128137475000011), pp. 1–26.

161. R. Dris, J. Gasperi, B. Tassin, in *Freshwater Microplastics The Handbook of Environmental Chemistry*, S. Lambert, M. Wagber, Eds. (2018; http://link.springer.com/10.1007/978-3-319-61615-5), pp. 69–83.

162. S. L. Wright, J. Ulke, A. Font, K. L. . Chan, F. J. Kelly, Atmospheric microplastic deposition in an urban environment and an evaluation of transport. *Environ. Int.* (2019), doi:10.1016/j.envint.2019.105411.

163. X. Wang, C. Li, K. Liu, L. Zhu, Z. Song, D. Li, Atmospheric microplastic over the South

China Sea and East Indian Ocean : abundance , distribution and source. *J. Hazard. Mater.* (2019), doi:10.1016/j.jhazmat.2019.121846.

164. M. Bergmann, S. Mützel, S. Primpke, M. B. Tekman, G. Gerdts, in *Arctic Frontiers* (Alfred-Wegener-Institut andd Helmholtz Gemeinschaft, Tromso, 2019; https://epic.awi.de/id/eprint/48975/), p. 1.

165. D. Durnford, A. Dastoor, D. Figueras-Nieto, A. Ryjkov, Long range transport of mercury to the Arctic and across Canada. *Atmos. Chem. Phys.* **10**, 6063–6086 (2010).

166. D. Hirdman, K. Aspmo, J. F. Burkhart, S. Eckhardt, H. Sodemann, A. Stohl, Transport of mercury in the Arctic atmosphere: Evidence for a springtime net sink and summer-time source. *Geophys. Res. Lett.* **36**, 1–5 (2009).

167. I. Uno, K. Eguchi, K. Yumimoto, T. Takemura, A. Shimizu, M. Uematsu, Z. Liu, Z. Wang, Y. Hara, N. Sugimoto, Asian dust transported one full circuit around the globe. *Nat. Geosci.* **2**, 557–560 (2009).

168. P. Ricaud, R. Zbinden, V. Catoire, V. Brocchi, F. Dulac, E. Hamonou, J. Canonici, L. ElAmraoui, S. Massart, U. Piguet, U. Dayan, P. Nabat, J. Sciare, M. Ramonet, M. Delmotte, A. di Sarra, D. Sferlazzo, T. di Iorio, S. Piacentino, P. Cristofanelli, N. Mihalopoulos, G. Kouvarakis, M. Pikridas, C. Savvides, R. Mamouri, A. Nisantzi, D. Hadjimitsis, J. Attié, H. Ferré, Y. Kangah, N. Jaidan, J. Guth, P. Jacquet, S. Chevrier, C. Robert, A. Bourdon, J. Bourdinot, J. Etienne, K. Gisèle, T. Pierre, The GLAM airborne campaign across the Mediterranean Basin. *Bull. Am. Meteorol. Soc.* **99**, 361–380 (2017).

169. X. Fu, N. Marusczak, L. E. Heimbürger, B. Sauvage, F. Gheusi, E. M. Prestbo, J. Sonke, Atmospheric mercury speciation dynamics at the high-altitude Pic du Midi Observatory, southern France. *Atmos. Chem. Phys.* **16**, 5623–5639 (2016).

170. A. Marenco, H. Gouget, P. Nedelec, J. P. Pages, F. Karcher, Evidence of a long-term increase in tropospheric ozone from Pic du Midi data series: consequences: positive radiative forcing. *J. Geophys. Res.* **99**, 617–632 (1994).

171. A. Chevalier, F. Gheusi, J.-L. Attié, R. Delmas, R. Zbinden, G. Athier, J.-M. Cousin, Carbon monoxide observations from ground stations in France and Europe and long trends in the free troposphere. *Atmos. Chem. Phys. Discuss.* **8**, 3313–3356 (2008).

172. G. Erni-cassola, M. I. Gibson, R. C. Thompson, J. A. Christie-oleza, Lost , but found with Nile red ; a novel method to detect and quantify small microplastics (20 µm – 1 mm) in environmental samples, 1–9 (2017).

173. R. R. Draxler, D. Hess, G, An Overview of the HYSPLIT_4 Modelling System for Trajectories, Dispersion, and Deposition. *Aust. Meteorolofical Mag.* **47**, 295–308 (1998).

174. M. Kooi, A. A. Koelmans, Simplifying Microplastic via Continuous Probability Distributions for Size, Shape,and Density. *Environ. Sci. Technol. Lett.* **6**, 551–557 (2019).

175. F. Gheusi, F. Ravetta, H. Delbarre, C. Tsamalis, A. Chevalier-Rosso, C. Leroy, P. Augustin, R. Delmas, G. Ancellet, G. Athier, P. Bouchou, B. Campistron, J. M. Cousin, M. Fourmentin, Y. Meyerfeld, Pic 2005, a field campaign to investigate low-tropospheric ozone variability in the Pyrenees. *Atmos. Res.* **101**, 640–665 (2011).

176. A. F. Stein, R. R. Draxler, G. D. Rolph, B. J. B. Stunder, M. D. Cohen, F. Ngan, NOAA's

HYSPLIT Atmospheric Transport and Dispersion Modeling System. *Bull. Am. Meteorol. Soc.* **96**, 2059–2077 (2015).

177. A. F. Stein, Y. Wang, J. D. de la Rosa, A. M. Sanchez de la Campa, N. Castell, R. R. Draxler, Modeling PM10 Originating from Dust Intrusions in the Southern Iberian Peninsula Using HYSPLIT. *Weather Forecast.* **26**, 236–242 (2011).

178. Y. Li, L. Shao, W. Wang, M. Zhang, X. Feng, W. Li, D. Zhang, Airborne fiber particles: Types, size and concentration observed in Beijing. *Sci. Total Environ.* **705** (2020), doi:10.1016/j.scitotenv.2019.135967.

179. S. Allen, D. Allen, K. Moss, G. Le Roux, V. R. Phoenix, J. Sonke, Examination of the ocean as a source for atmospheric microplastics. *PLoS One*. **15** (2020), doi:10.1371/journal.pone.0232746.

180. M. Yurtsever, A. Kaya, C. Bayraktar, in *International Conference on Microplastic Pollution in the Mediterranean Sea*, M. Cocca, Ed. (Springer International Publishing, 2018; http://link.springer.com/10.1007/978-3-319-71279-6), vol. 22, p. 238.

181. N. Asrin, A. Dipareza, Microplastics in Ambient Air (Case Study : Urip Sumoharjo Street and Mayjend Sungkono Street of Surabaya City , Indonesia). *IAETSD J. Adv. Res. Appl. Sci.* **6**, 54–57 (2019).

182. N. Evangeliou, H. Grythe, Z. Klimont, C. Heyes, S. Eckhardt, S. Lopez-Aparicio, A. Stohl, Atmospheric transport, a major pathway of microplastics to remote regions. *Preprints*, 1–32 (2020).

183. M. L. Moser, D. S. Lee, A Fourteen-Year Survey of Plastic Ingestion by Western North Atlantic Seabirds. *Colon. Waterbirds*. **15**, 883–94 (1992).

184. PlasticsEurope, “Plastics – the Facts 2019” (2019).

185. W. J. Shim, R. C. Thomposon, Microplastics in the Ocean. *Arch. Environ. Contam. Toxicol.* **69**, 265–268 (2015).

186. R. Geyer, J. R. Jambeck, K. L. Law, Production, use, and fate of all plastics ever made. *Sci. Adv.* **3**, e1700782 (2017).

187. Z. Akdogan, B. Guven, Microplastics in the environment: A critical review of current understanding and identification of future research needs. *Environ. Pollut.* **254**, 113011 (2019).

188. E. Van Sebille, C. Wilcox, L. Lebreton, N. Maximenko, B. D. Hardesty, J. A. Van Franeker, M. Eriksen, D. Siegel, F. Galgani, K. L. Law, A global inventory of small floating plastic debris. *Environ. Res. Lett.* **10**, 124006 (2015).

189. A. A. Koelmans, M. Kooi, K. L. Law, E. Van Sebille, All is not lost: Deriving a top-down mass budget of plastic at sea. *Environ. Res. Lett.* **12**, 1–23 (2017).

190. N. Maximenko, J. Hafner, P. Niiler, Pathways of marine debris derived from trajectories of Lagrangian drifters. *Mar. Pollut. Bull.* **65**, 51–62 (2012).

191. D. Wichmann, P. Delandmeter, E. van Sebille, Influence of near-surface currents on the global dispersal of marine microplastic. *JGR Ocean.*, 1–18 (2018).

192. N. Sharma, A. Rai, *Algal Particles in the Atmosphere* (Elsevier, 2011).

193. M. Sofiev, J. Soares, M. Prank, G. De Leeuw, J. Kukkonen, A regional-to-global model of emission and transport of sea salt particles in the atmosphere. *J. Geophys. Res. Atmos.* **116** (2011), doi:10.1029/2010JD014713.

194. M. A. Erinin, S. D. Wang, R. Liu, D. Towle, X. Liu, J. H. Duncan, Spray Generation by a Plunging Breaker. *Geophys. Res. Lett.* **46** (2019), doi:10.1029/2019GL082831.

195. E. Lewis, S. Schwartz, *Sea salt aerosol production: mechanisms, methods, measurements and models* (American Geophysical Union, Washington, USA, 2004).

196. W. A. Hoppel, G. M. Frick, J. W. Fitzgerald, Surface source function for sea-salt aerosol and aerosol dry deposition to the ocean surface. *J. Geophys. Res. Atmos.* **107**, 1–17 (2002).

197. D. Richer, F. Veron, Ocean Spray:an outsized influence on weather and climate. *Phys. Today*. **69**, 35–39 (2016).

198. C. D. O'Dowd, G. de Leeuw, Marine aerosol production: a review of the current knowledge. *Philos. Trans. R. Soc. A Math. Phys. Eng. Sci.* **365**, 1753–1774 (2007).

199. J. A. Quinn, R. A. Steinbrook, J. L. Anderson, Breaking bubbles and the water-to-air transport of particulate matter. *Chem. Eng. Sci.* **30**, 1177–1184 (1975).

200. M. Pósfai, J. Li, J. R. Anderson, P. R. Buseck, Aerosol bacteria over the Southern Ocean during ACE-1. *Atmos. Res.* **66**, 231–240 (2003).

201. I. Reche, G. D'Orta, N. Mladenov, D. M. Winget, C. A. Suttle, Deposition rates of viruses and bacteria above the atmospheric boundary layer. *ISME J.* (2018), doi:10.1038/s41396-017-0042-4.

202. J. C. McWilliams, P. P. Sullivan, C.-H. Moeng, Langmuir turbulence in the ocean. *J. Fluid Mech.* **334**, S0022112096004375 (1997).

203. C. A. Choy, B. H. Robison, T. O. Gagne, B. Erwin, E. Firl, R. U. Halden, J. A. Hamilton, K. Katija, S. E. Lisin, C. Rolsky, K. S. Van Houtan, The vertical distribution and biological transport of marine microplastics across the epipelagic and mesopelagic water column. *Sci. Rep.* **9**, 1–9 (2019).

204. T. Kukulka, R. R. Harcourt, Influence of Stokes Drift Decay Scale on Langmuir Turbulence. *J. Phys. Oceanogr.* **47**, 1637–1656 (2017).

205. Y. Zhang, T. Gao, S. Kang, M. Sillanpää, Importance of atmospheric transport for microplastics deposited in remote areas. *Environ. Pollut.* **254** (2019), doi:10.1016/j.envpol.2019.07.121.

206. C. E. Enyoh, A. W. Verla, E. N. Verla, F. C. Ibe, C. E. Amaobi, Airborne microplastics: a review study on method for analysis, occurrence, movement and risks. *Environ. Monit. Assess.* **191**, 1–17 (2019).

207. Y. Zhang, S. Kang, S. Allen, D. Allen, T. Gao, M. Sillanpaa, Atmospheric microplastics: A review on current status and perspectives. *Earth-Science Rev.* **203**, 103118 (2020).

208. P. L. Corcoran, M. C. Biesinger, M. Grifi, Plastics and beaches: A degrading relationship. *Mar. Pollut. Bull.* **58**, 80–84 (2009).

209. S. Lambert, M. Wagner, Characterisation of nanoplastics during the degradation of

polystyrene. *Chemosphere*. **145**, 265–268 (2016).

210. A. Jahnke, H. P. H. Arp, B. I. Escher, B. Gewert, E. Gorokhova, D. Kühnel, M. Ogonowski, A. Potthoff, C. Rummel, M. Schmitt-Jansen, E. Toorman, M. MacLeod, Reducing Uncertainty and Confronting Ignorance about the Possible Impacts of Weathering Plastic in the Marine Environment. *Environ. Sci. Technol. Lett.* **4**, 85–90 (2017).

211. F. Julienne, N. Delorme, F. Lagarde, From macroplastics to microplastics: Role of water in the fragmentation of polyethylene. *Chemosphere*. **236**, 124409 (2019).

212. A. L. Dawson, S. Kawaguchi, C. K. King, K. A. Townsend, R. King, W. M. Huston, S. M. Bengtson Nash, Turning microplastics into nanoplastics through digestive fragmentation by Antarctic krill. *Nat. Commun.* **9**, 1–8 (2018).

213. Hong Kong Observatory, The Weather of October 2016, 1–9 (2018).

214. Hong Kong Observatory, The Weather of November 2016 Warnings and Signals issued in November 2016, 1–6 (2018).

215. Hong Kong Observatory, The Weather of December 2016 Warnings and Signals issued in December 2016, 1–6 (2018).

216. E. Athanasopoulou, M. Tombrou, S. N. Pandis, A. G. Russell, The role of sea-salt emissions and heterogeneous chemistry in the air quality of polluted coastal areas. *Atmos. Chem. Phys.* **8**, 5755–5769 (2008).

217. J. Yan, L. Chen, Q. Lin, S. Zhao, M. Zhang, Effect of typhoon on atmospheric aerosol particle pollutants accumulation over Xiamen, China. *Chemosphere*. **159**, 244–255 (2016).

218. V. C. Slonosky, Wet winters, dry summers? Three centuries of precipitation data from Paris. *Geophys. Res. Lett.* **29**, 34-1-34–4 (2002).

219. G. S. Fanourgakis, M. Kanakidou, A. Nenes, S. E. Bauer, T. Bergman, K. S. Carslaw, A. Grini, D. S. Hamilton, J. S. Johnson, V. A. Karydis, A. Kirkevåg, J. K. Kodros, U. Lohmann, G. Luo, R. Makkonen, H. Matsui, D. Neubauer, J. R. Pierce, J. Schmale, P. Stier, K. Tsigaridis, T. van Noije, H. Wang, D. Watson-Parris, D. M. Westervelt, Y. Yang, M. Yoshioka, N. Daskalakis, S. Decesari, M. Gysel Beer, N. Kalivitis, X. Liu, N. M. Mahowald, S. Myriokefalitakis, R. Schrödner, M. Sfakianaki, A. P. Tsimpidi, M. Wu, F. Yu, Evaluation of global simulations of aerosol particle number and cloud condensation nuclei, and implications for cloud droplet formation. *Atmos. Chem. Phys. Discuss.*, 1–40 (2019).

220. M. O. Andreae, D. Rosenfeld, Aerosol-cloud-precipitation interactions. Part 1. The nature and sources of cloud-active aerosols. *Earth-Science Rev.* **89**, 13–41 (2008).

221. M. Van Der Does, A. Pourmand, A. Sharifi, J.-B. W. Stuut, North African mineral dust across the tropical Atlantic Ocean: Insights from dust particle size, radiogenic Sr-Nd-Hf isotopes and rare earth elements (REE). *Aeolian Res.* **33**, 106–116 (2018).

222. R. L. Modini, B. Harris, Z. Ristovski, The organic fraction of bubble-generated, accumulation mode Sea Spray Aerosol (SSA). *Atmos. Chem. Phys.* **10**, 2867–2877 (2010).

223. E. Fuentes, H. Coe, D. Green, G. De Leeuw, G. McFiggans, Laboratory-generated primary marine aerosol via bubble-bursting and atomization. *Atmos. Meas. Tech.* **3**, 141–162 (2010).

224. W. R. Ke, Y. M. Kuo, C. W. Lin, S. H. Huang, C. C. Chen, *Characterization of aerosol emissions from single bubble bursting* (Elsevier Ltd, 2017; http://dx.doi.org/10.1016/j.jaerosci.2017.03.006), vol. 109.

225. D. B. J. Demoz.B.B, Coller JL. Jr, on the Caltech Active Strand Cloudwater collectors. *Atmos. Res.* **41**, 46672 (1995).

226. T. Wrzesinsky, O. Klemm, Summertime fog chemistry at a mountainous site in central Europe. *Atmos. Environ.* **34**, 1487–1496 (2000).

227. P. Roman, Z. Polkowska, J. Namieśnik, Sampling procedures in studies of cloud water composition: A review. *Crit. Rev. Environ. Sci. Technol.* **43**, 1517–1555 (2013).

228. P. Herckes, M. P. Hannigan, L. Trenary, T. Lee, J. L. Collett, Organic compounds in radiation fogs in Davis (California). *Atmos. Res.* **64**, 99–108 (2002).

229. MeteoFrance, Météo et climat: Mimizan (2018), (available at http://www.meteofrance.com/previsions-meteo-france/mimizan/40200).

230. S. Zhao, M. Danley, J. E. Ward, D. Li, T. J. Mincer, An approach for extraction, characterization and quantitation of microplastic in natural marine snow using Raman microscopy. *Anal. Methods*. **9**, 1470–1478 (2017).

231. D. Koračin, C. E. Dorman, J. M. Lewis, J. G. Hudson, E. M. Wilcox, A. Torregrosa, Marine fog: A review. *Atmos. Res.* **143**, 142–175 (2014).

232. A. K. Baldwin, S. R. Corsi, S. A. Mason, Plastic Debris in 29 Great Lakes Tributaries: Relations to Watershed Attributes and Hydrology. *Environ. Sci. Technol.* **50**, 10377–10385 (2016).

233. A. Mendoza, J. L. Osa, O. C. Basurko, A. Rubio, M. Santos, J. Gago, F. Galgani, C. Peña-Rodriguez, Microplastics in the Bay of Biscay: An overview. *Mar. Pollut. Bull.* **153** (2020), doi:10.1016/j.marpolbul.2020.110996.

234. S. Allen, D. Allen, V. R. Phoenix, G. Le Roux, P. Durantez, Atmospheric deposition of microplastics found on a remote mountain catchment. *Nat. Geosci.* (2018).

235. B. Marticorena, G. Bergametti, B. Aumont, M. Legrand, Modeling the atmospheric dust cycle: 2. Simulation of Saharan dust sources. *J. Geophys. Res.* **102**, 4387–4404 (1997).

236. C. Szczypta, S. Gascoin, T. Houet, O. Hagolle, J. F. Dejoux, C. Vigneau, P. Fanise, Impact of climate and land cover changes on snow cover in a small Pyrenean catchment. *J. Hydrol.* **521**, 84–99 (2015).

237. S. M. Rhind, Anthropogenic pollutants: a threat to ecosystem sustainability? *Philos Trans R Soc L. B Biol Sci*. **364**, 3391–3401 (2009).

238. N. Pirrone, S. Cinnirella, X. Feng, R. B. Finkelman, H. R. Friedli, J. Leaner, R. Mason, A. B. Mukherjee, G. B. Stracher, D. G. Streets, K. Telmer, Global mercury emissions to the atmosphere from anthropogenic and natural sources. *Atmos. Chem. Phys.* **10**, 5951–5964 (2010).

239. J. O. Nriagu, Global inventory of natural and anthropogenic emissions of trace metals to the atmosphere. *Nature*. **279**, 409 (1979).

240. J. Catalan, L. Camarero, M. Felip, S. Pla, M. Ventura, T. Buchaca, F. Bartumeus, G. De

Mendoza, A. Miró, E. O. Casamayor, J. M. Medina-Sánchez, M. Bacardit, M. Altuna, M. Bartrons, D. D. De Quijano, High mountain lakes: Extreme habitats and witnesses of environmental changes. *Limnetica*. **25**, 551–584 (2006).

241. P. Fernández, R. M. Vilanova, C. Martínez, P. Appleby, J. O. Grimalt, The historical record of atmospheric pyrolytic pollution over Europe registered in the sedimentary PAH from remote mountain lakes. *Environ. Sci. Technol.* **34**, 1906–1913 (2000).

242. M. Bacardit, L. Camarero, Atmospherically deposited major and trace elements in the winter snowpack along a gradient of altitude in the Central Pyrenees: The seasonal record of long-range fluxes over SW Europe. *Atmos. Environ.* **44**, 582–595 (2010).

243. S. V. Hansson, A. Claustres, A. Probst, F. De Vleeschouwer, S. Baron, D. Galop, F. Mazier, G. Le Roux, Atmospheric and terrigenous metal accumulation over 3000 years in a French mountain catchment: Local vs distal influences. *Anthropocene*. **19**, 45–54 (2017).

244. A. Hervàs, L. Camarero, I. Reche, E. O. Casamayor, Viability and potential for immigration of airborne bacteria from Africa that reach high mountain lakes in Europe. *Environ. Microbiol.* **11**, 1612–1623 (2009).

245. F. E. Grousset, P. Ginoux, A. Bory, P. E. Biscaye, Case study of a Chinese dust plume reaching the French Alps. *Geophys. Res. Lett.* **30**, 23–26 (2003).

246. J. Gago, O. Carretero, A. V Filgueiras, L. Viñas, Synthetic microfibers in the marine environment: A review on their occurrence in seawater and sediments. *Mar. Pollut. Bull.* **127**, 365–376 (2018).

247. R. Dris, J. Gasperi, B. Tassin, M. Wagner, S. Lambert, Eds. (Springer International Publishing, Cham, 2018; https://doi.org/10.1007/978-3-319-61615-5_4), pp. 69–83.

248. M. Filella, Questions of size and numbers in environmental research on microplastics: Methodological and conceptual aspects. *Environ. Chem.* **12**, 527–538 (2015).

249. R. Hurley, J. Woodward, J. J. Rothwell, Supplementary Information -Microplastic contamination of river beds significantly reduced by catchment-wide flooding. *Nat. Geosci.* **11**, 251–257 (2018).

250. M. T. Nuelle, J. H. Dekiff, D. Remy, E. Fries, A new analytical approach for monitoring microplastics in marine sediments. *Environ. Pollut.* **184**, 161–169 (2014).

Appendix: 3: Rainfall, snowfall, temperature and wind data relative to microplastic monitoring periods.

						Wind					
	Sampling start date	Sampling end date	Duration of sampling period	Total microP / m2/ day	Average wind speed (m/s)	Predominant wind direction	Maximum recorded wind speed (m/s)	Frequency of wind speeds greater than 1m/s	Frequency of wind speeds greater than 2m/s	Frequency of wind speeds greater than 3m/s	Frequency of wind speeds greater than 5m/s
Meteorological data normalised to daily time-step											
November	16/11/2017	28/11/2017	12	462	0.9	WSW	2.4	4.1	0.2	0	0
December	29/11/2017	18/12/2017	19	359	1.2	W	7.1	3.8	1.6	0.1	0.2
January	19/12/2017	22/01/2018	34	306	1.2	WSW/W	4.3	3.5	1.4	0.5	0
February	23/01/2018	05/03/2018	41	297	0.9	SW	4.5	2.6	0.9	0.1	0
March	06/03/2018	09/04/2018	34	402	1.1	WSW	4.8	4.3	2.4	0.8	0
Meteorological data relative to the monitored period											
November	16/11/2017	28/11/2017	12	5544*	0.9	WSW	2.4	49	2	0	0
December	29/11/2017	18/12/2017	19	6819*	1.2	W	7.1	73	31	2	3
January	19/12/2017	22/01/2018	34	10401*	1.2	WSW/W	4.3	118	49	16	0
February	23/01/2018	05/03/2018	41	12188*	0.9	SW	4.5	108	35	5	0
March	06/03/2018	09/04/2018	34	13680*	1.1	WSW	4.8	146	80	28	0
Total dataset	16/11/2017	09/04/2018	140	58358*	1.1	WSW	7.1	494	197	51	3

Rainfall												
	Sampling start date	Sampling end date	Duration of sampling period	Total microP / m2/ day	Total rainfall (mm)	Average daily rainfall (mm/day)	Average rainfall event intensity (mm/hr)	Maximum event intensity (mm/hr)	Number of rainfall events >1mm	Number of rainfall events >2mm	Number of rainfall events >5mm	Number of rainfall events >10mm
Meteorological data normalised to daily time-step												
November	16/11/2017	28/11/2017	12	462		1.5	0.9	11.5	0.2	0.2	0.1	0.1
December	29/11/2017	18/12/2017	19	359		6.5	0.8	8.8	0.7	0.6	0.4	0.3
January	19/12/2017	22/01/2018	34	306		11.6	0.9	6.4	0.8	0.6	0.3	0.2
February	23/01/2018	05/03/2018	41	297		6.1	1.5	6	0.3	0.2	0.2	0.1
March	06/03/2018	09/04/2018	34	402		5.7	1.5	9.2	0.5	0.4	0.2	0.2
Meteorological data relative to the monitored period												
November	16/11/2017	28/11/2017	12	5544*	18	1.5	0.9	11.5	2	2	1	1
December	29/11/2017	18/12/2017	19	6819*	124	6.5	0.8	8.8	13	11	8	5
January	19/12/2017	22/01/2018	34	10401*	394	11.6	0.9	6.4	27	22	10	6
February	23/01/2018	05/03/2018	41	12188*	250	6.1	1.5	6	12	10	7	6
March	06/03/2018	09/04/2018	34	13680*	193	5.7	1.5	9.2	18	13	8	7
Total dataset	16/11/2017	09/04/2018	140	58358*	980				72	58	34	25

	Snowfall											
	Sampling start date	Sampling end date	Duration of sampling period	Total microP / m2/ day	Total snowfall (mm)	Average daily snowfall (mm/day)	Average snowfall event intensity (mm/hr)	Maximum event intensity (mm/hr)	Number of rainfall events >1mm	Number of rainfall events >2mm	Number of rainfall events >5mm	Number of rainfall events >10mm
Meteorological data normalised to daily time-step												
November	16/11/2017	28/11/2017	12	462		1.1	0	0	0	0	0	0
December	29/11/2017	18/12/2017	19	359		15.7	0.5	1.3	0.6	0.5	0.4	0.2
January	19/12/2017	22/01/2018	34	306		21.9	1	1.9	0.6	0.6	0.5	0.3
February	23/01/2018	05/03/2018	41	297		33.1	1.2	2.6	1.2	1	0.6	0.3
March	06/03/2018	09/04/2018	34	402		40.7	2	3.7	2.5	2.5	1.5	0.7
Meteorological data relative to the monitored period												
November	16/11/2017	28/11/2017	12	5544*	14	1.1	0	0	0	0	0	0
December	29/11/2017	18/12/2017	19	6819*	298	15.7	0.5	1.3	12	10	7	3
January	19/12/2017	22/01/2018	34	10401*	745	21.9	1	1.9	22	22	16	9
February	23/01/2018	05/03/2018	41	12188*	1356	33.1	1.2	2.6	51	40	23	12
March	06/03/2018	09/04/2018	34	13680*	1385	40.7	2	3.7	85	85	50	23
Total dataset	16/11/2017	09/04/2018	140	58358*	3799				170	157	96	47

* For the dataset presented relative to the monitored period the MP count is the total MP/m^2 for the total monitored period (i.e. cumulative MP count over the total 34 days for the January sample).

For the purposes of this assessment a wind event is defined as an instantaneous wind speed greater than a given threshold. All wind, rainfall and snowfall values are presented *per day* for the 'Meteorological data normalised to daily time-step' and *per monitored period* (i.e. 19 days in November) for the 'Meteorological data relative to monitored period'.

Appendix 4: Images of Raman laser impact on plastic

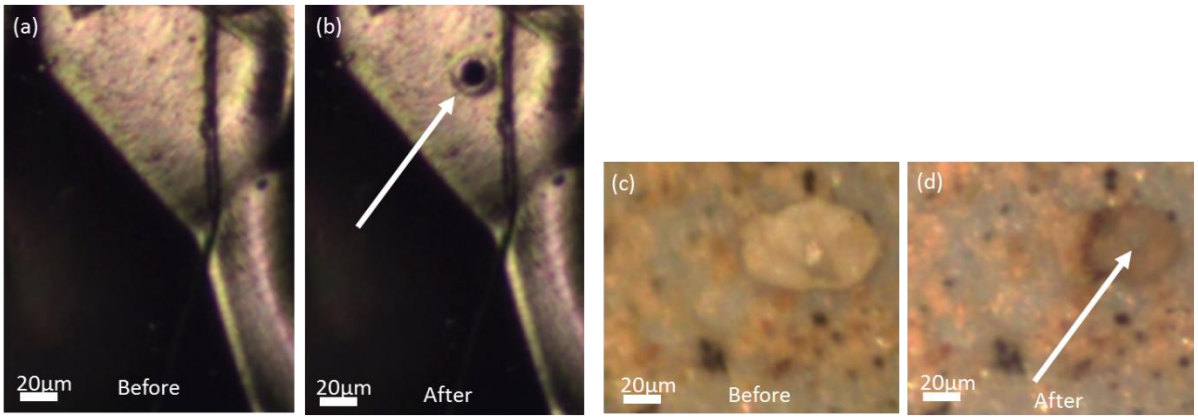

Methodology Figure 1. Images of Raman laser impact on plastic at 50% (a, b) and 100% (c, d) laser power (a and b is a control plastic particle, c and d is a sample fragment). Plastic becomes vaporised (burns) leaving a hole at the focal point of the laser when high laser power is used for analysis.

Appendix 5: Fragment- fibre- film ratio in the mountain atmospheric deposition samples

The composition of MP particles (fragment, fibre, film) is interesting compared to other studies published, generally illustrating lower fibre counts than in previously published city atmospheric deposition studies. There are several possible reasons for the smaller proportion of fibres compared to particles in the deposition samples. These include:

(1) Early MP studies and field sampling campaigns presented plastic fibre counts in environmental samples. There are several studies that present only fibre counts, without corresponding particle or film counts. In early studies this may be partly due to the ease of fibre identification. There may be a resulting expectation of high plastic fibre findings due to the earlier published slight bias towards plastic fibre analysis in environmental samples (*8*, *43*, *159*, *246*, *247*). A Scopus search to identify the number of published articles ("microplastic" AND "environment" AND fibre/film/particle/fragment) identified a total of 525 articles on microplastic and environment, 169 discussed fibres or microfibres specifically (322 - particles, 101 - fragments, 31 – films). It is also noted that Shim et al.(*160*) presents several studies of sea water and sediment that show fibre counts similar and smaller than that found in this study (with acknowledgement that these are different environmental compartments).

(2) It is potentially possible that in microplastic analysis to date there is a limited identification and description of the very small particles in previous studies due to particle size analysis limitations (for example, studies may consider plastic greater than 50 or 100 µm). It has been suggested through several studies(*137*, *248*) that the particle count increases exponentially with decreasing size. Therefore, potentially, the ratio of fragments to fibres may be different in this study due to the analysis of MP particles down to a lower size limit than some previous studies. When only >200µm MP particles are considered in this remote mountain field analysis, the proportion of fibres in the sample rises to 70%, comparable to the higher fibre counts presented in the mega-city studies (Paris and Dongguan)(*8*, *79*).

(3) The deposition collection method is open to the atmosphere for the duration of the sample period. While films and fragments may become and remain deposited in the standard field rainfall samples the fibres are potentially lighter

and more easily entrained and therefore if dry deposition occurs the potential for resuspension may be greater for these MPs than for films or fragments. However, the entrainment potential of fibres vs films vs fragments has not been tested (in the field or laboratory) and so this potential field fibre re-entrainment cannot be evidenced.

(4) The sample preparation methods follow standard protocols previously used and published. It is noted however that the use of H_2O_2, even when diluted, can results in 'loss' of fibres through acid dissolution. This could potentially affect aged or degraded fibres or fibres of Rayon or similar composition(*249*, *250*), resulting in a lower fibre count in comparison to fragment numbers. It is noted that the Fenton's reagent method(*249*) may assist in limiting sample fibre loss during organic material removal.

References

1. I. Baker, Fifty Materials That Make the World. *Springer Int. Publ. AG*. **Chapter-33**, 175–178 (2018).
2. Y. Liu, Z. Shao, P. Zhou, X. Chen, Thermal and crystalline behaviour of silk fiborin/nylon 66 blend films. *Polymer (Guildf).* **45**, 7705–7710 (2004).
3. S. Werner, A. Budziak, J. A. Van Fanneker, F. Galgani, G. Hanke, T. Maes, M. Matiddi, P. Nilsson, L. Oosterbaan, E. Priestland, R. C. Thompson, J. M. Veiga, T. Vlachogianni, *Harm caused by Marine Litter - European Commission* (2016; https://ec.europa.eu/jrc/en/publication/harm-caused-marine-litter).
4. K. w Kenyon, E. Kridler, Laysan Albatrosses Swallow Indigestible Matter. *AUK*. **86**, 339–343 (1969).
5. S. I. Rothstein, Plastic particle pollution of the surface of the Atlantic Ocean: evidence from a seabird. *Condor*. **75**, 344–345 (1973).
6. E. J. Carpenter, K. L. J. Smith, Plastics on the Sargasso Sea Surface. *Science*. **175**, 1240–1241 (1972).
7. R. Dris, thesis, Université Paris-Est (2016).
8. L. Cai, J. Wang, J. Peng, Z. Tan, Z. Zhan, X. Tan, Q. Chen, Characteristic of microplastics in the atmospheric fallout from Dongguan city, China: preliminary research and first evidence. *Environ. Sci. Pollut. Res.* **24**, 24928–24935 (2017).
9. S. Dehghani, F. Moore, R. Akhbarizadeh, Microplastic pollution in deposited urban dust, Tehran metropolis, Iran. *Environ. Sci. Pollut. Res.* **24**, 20360–20371 (2017).
10. K. Zhang, J. Su, X. Xiong, X. Wu, C. Wu, J. Liu, Microplastic pollution of lakeshore sediments from remote lakes in Tibet plateau, China. *Environ. Pollut.* **219**, 450–455 (2016).

11. S. Allen, D. Allen, V. R. Phoenix, G. Le Roux, P. Duranteza, A. Simonneau, B. Stéphane, D. Galop, Atmospheric transport and deposition of microplastics in a remote mountain catchment. *Nat. Geosci.* **12**, 339–344 (2019).

12. PlasticsEurope, “Plastics – the Facts 2018: An analysis of European plastics production, demand and waste data” (2018), (available at http://www.plasticseurope.org).

13. C. M. Rochman, C. Brookson, J. Bikker, N. Djuric, A. Earn, K. Bucci, S. Athey, A. Huntington, H. McIlwraith, K. Munno, H. De Frond, A. Kolomijeca, L. Erdle, J. Grbic, M. Bayoumi, S. B. Borrelle, T. Wu, S. Santoro, L. M. Werbowski, X. Zhu, R. K. Giles, B. M. Hamilton, C. Thaysen, A. Kaura, N. Klasios, L. Ead, J. Kim, C. Sherlock, A. Ho, C. Hung, Rethinking microplastics as a diverse contaminant suite. *Environ. Toxicol. Chem.* **38**, 703–711 (2019).

14. E. Y. Zeng, Ed., *Microplastic Contamination in Aquatic Environments - An Emerging Matter of Environmental Urgency* (Elsevier, 2018; https://www.sciencedirect.com/book/9780128137475/microplastic-contamination-in-aquatic-environments).

15. GESAMP, *Sources, Fate and Effects of Microplastics in the Marine Environment: Part 2 of a Global Assessment* (IMO/FAO/UNESCO-IOC/UNIDO/WMO/IAEA/UN/ UNEP/UNDP Joint Group of Experts on the Scientific Aspects of Marine Environmental Protection, 2016; file:///C:/Users/BACHEL~2/AppData/Local/Temp/sources-fate-and-effects-of-microplastics-in-the-marine-environment-part-2-of-a-global-assessment-en.pdf).

16. C. Masura, Julie, Baker, Joel, Foster, Gregory, Arthur, “Laboratory Methods for the Analysis of Microplastics in the Marine Environment” (2015), (available at https://marinedebris.noaa.gov/sites/default/files/publications-files/noaa_microplastics_methods_manual.pdf).

17. R. C. Thompson, Y. Olsen, R. P. Mitchell, A. Davis, S. J. Rowland, A. W. G. John, D. McGonigle, A. E. Russell, Lost at Sea: Where does all the plastic go? *Science (80-.).* **304**, 838 (2004).

18. N. B. Hartmann, T. Hüffer, R. C. Thompson, M. Hassellöv, A. Verschoor, A. E. Daugaard, S. Rist, T. Karlsson, N. Brennholt, M. Cole, M. P. Herrling, M. C. Hess, N. P. Ivleva, A. L. Lusher, M. Wagner, Are We Speaking the Same Language? Recommendations for a Definition and Categorization Framework for Plastic Debris. *Environ. Sci. Technol.* **53**, 1039–1047 (2019).

19. O. S. Alimi, J. Farner Budarz, L. M. Hernandez, N. Tufenkji, Microplastics and Nanoplastics in Aquatic Environments: Aggregation, Deposition, and Enhanced Contaminant Transport. *Environ. Sci. Technol.* **52**, 1704–1724 (2018).

20. M. G. J. Löder, G. Gerdts, in *Marine Anthropogenic Litter*, M. Bergmann, L. Gutow, M. Klages, Eds. (2015), pp. 201–227.

21. M. S. Bank, S. V. Hansson, *Environ. Sci. Technol.*, in press, doi:10.1021/acs.est.9b02942.

22. W. G. Kreyling, M. Semmler-Behnke, Q. Chaudhry, A complementary definition of nanomaterial. *Nano Today*. **5**, 165–168 (2010).

23. C. Joachim, To be nano or not to be nano? *Nat. Mater.* **4**, 107–109 (2005).

24. H. S. Auta, C. U. Emenike, S. H. Fauziah, Distribution and importance of microplastics in the marine environmentA review of the sources, fate, effects, and potential solutions. *Environ. Int.* **102**, 165–176 (2017).

25. J. Li, H. Liu, J. Paul Chen, Microplastics in freshwater systems: A review on occurrence, environmental effects, and methods for microplastics detection. *Water Res.* **137**, 362–374 (2018).

26. J. C. Prata, J. P. da Costa, A. V Girão, I. Lopes, A. C. Duarte, T. Rocha-Santos, Identifying a quick and efficient method of removing organic matter without damaging microplastic samples. *Sci. Total Environ.* **686**, 131–139 (2019).

27. P. Ribeiro-Claro, M. M. Nolasco, C. Araújo, Characterization of Microplastics by Raman Spectroscopy. *Compr. Anal. Chem.* **75**, 119–151 (2017).

28. C. M. Rochman, in *Marine Anthropogenic Litter*, M. Bergmann, L. Gutow, M. Klages, Eds. (Springer, Cham, 2015), pp. 117–140.

29. A. A. Horton, S. J. Dixon, Microplastics: An introduction to environmental transport processes. *Wiley Interdiscip. Rev. Water*. **5**, e1268 (2018).

30. L. Camarero, M. Bacardit, A. de Diego, G. Arana, Decadal trends in atmospheric deposition in a high elevation station: Effects of climate and pollution on the long-range flux of metals and trace elements over SW Europe. *Atmos. Environ.* **167**, 542–552 (2017).

31. R. Ambrosini, R. S. Azzoni, F. Pittino, G. Diolaiuti, A. Franzetti, M. Parolini, First evidence of microplastic contamination in the supraglacial debris of an alpine glacier. *Environ. Pollut.* **253**, 297–301 (2019).

32. M. Klein, E. K. Fischer, Microplastic abundance in atmospheric deposition within the Metropolitan area of Hamburg, Germany. *Sci. Total Environ.* **685**, 96–103 (2019).

33. K. Liu, X. Wang, T. Fang, P. Xu, L. Zhu, D. Li, Source and potential risk assessment of suspended atmospheric microplastics in Shanghai. *Sci. Total Environ.* **675**, 462–471 (2019).

34. K. Liu, T. Wu, X. Wang, Z. Song, C. Zong, N. Wei, D. Li, Consistent transport of terrestrial microplastics to the ocean through atmosphere. *Environ. Sci. Technol.*, 1–12 (2019).

35. Y. Zhang, T. Gao, S. Kang, M. Sillanpaa, Microplastics intrude into the Tibetan Plateau. *Sci. Rep.* **in review** (2019).

36. L. G. A. Barboza, L. R. Vieira, V. Branco, N. Figueiredo, F. Carvalho, C. Carvalho, L. Guilhermino, Microplastics cause neurotoxicity, oxidative damage and energy-related changes and interact with the bioaccumulation of mercury in the European seabass, Dicentrarchus labrax (Linnaeus, 1758). *Aquat. Toxicol.* **195**, 49–57 (2018).

37. J. Gasperi, S. L. Wright, R. Dris, F. Collard, C. Mandin, M. Guerrouache, V. Langlois, F. J. Kelly, B. Tassin, Microplastics in air: Are we breathing it in? *Curr. Opin. Environ. Sci. Heal.* **1**, 1–5 (2018).

38. C. Liu, J. Li, Y. Zhang, L. Wang, J. Deng, Y. Gao, L. Yu, J. Zhang, H. Sun, Widespread distribution of PET and PC microplastics in dust in urban China and their estimated human exposure. *Environ. Int.* **128**, 116–124 (2019).

39. P. S. Tourinho, V. Kočí, S. Loureiro, C. A. M. van Gestel, Partitioning of chemical contaminants to microplastics: Sorption mechanisms, environmental distribution and effects on toxicity and bioaccumulation. *Environ. Pollut.* **252**, 1246–1256 (2019).

40. S. L. Wright, F. J. Kelly, Plastic and Human Health: A Micro Issue? *Environ. Sci. Technol.* **51**, 6634–6647 (2017).

41. C. G. Alimba, C. Faggio, Microplastics in the marine environment: Current trends in environmental pollution and mechanisms of toxicological profile. *Environ. Toxicol. Pharmacol.* **68**, 61–74 (2019).

42. R. Dris, C. J. Gasperi, A. V. Rocher, B. M. Saad, N. Renault, B. Tassin, Microplastic contamination in an urban area : a case study in Greater Paris. *Environ. Chem.* **12**, 592–599 (2015).

43. R. Dris, J. Gasperi, C. Mirande, C. Mandin, M. Guerrouache, V. Langlois, B. Tassin, A first overview of textile fibers, including microplastics, in indoor and outdoor environments. *Environ. Pollut.* **221**, 453–458 (2017).

44. S. Abbasi, B. Keshavarzi, F. Moore, H. Delshab, N. Soltani, A. Sorooshian, Investigation of microrubbers, microplastics and heavy metals in street dust: a study in Bushehr city, Iran. *Environ. Earth Sci.* **76** (2017), doi:10.1007/s12665-017-7137-0.

45. S. J. Hayward, T. Gouin, F. Wania, Comparison of four active and passive sampling techniques for pesticides in air. *Environ. Sci. Technol.* **44**, 3410–3416 (2010).

46. A. Dommergue, P. Amato, R. Tignat-perrier, O. Magand, A. Thollot, M. Joly, L. Bouvier, K. Sellegri, T. Vogel, J. Sonke, J. Jaffrezo, M. Andrade, I. Moreno, C. Labuschagne, L. Martin, Q. Zhang, C. Larose, D. A. Pearce, Methods to Investigate the Global Atmospheric Microbiome. *Front. Microbiol.* **10**, 1–12 (2019).

47. V. Hidalgo-Ruz, L. Gutow, R. C. Thompson, M. Thiel, Microplastics in the marine environment: A review of the methods used for identification and quantification. *Environ. Sci. Technol.* **46**, 3060–3075 (2012).

48. B. Nguyen, D. Claveau-Mallet, L. M. Hernandez, E. G. Xu, J. M. Farner, N. Tufenkji, Separation and Analysis of Microplastics and Nanoplastics in Complex Environmental Samples. *Acc. Chem. Res.* **52**, 858–866 (2019).

49. Q. Zhou, C. Tian, Y. Luo, Various forms and deposition fluxes of microplastics identified in the coastal urban atmosphere. *Chinese Sci. Bull.* **62**, 3902–3909 (2017).

50. Marine & Environmental Research Institute, *Guide to Microplastic Identification* (Marine & Environmental Research Instatite, 2015).

51. A. B. Silva, A. S. Bastos, C. I. L. Justino, J. P. da Costa, A. C. Duarte, T. A. P. Rocha-Santos, Microplastics in the environment: Challenges in analytical chemistry - A review. *Anal. Chim. Acta*. **1017**, 1–19 (2018).

52. M. G. J. Löder, H. K. Imhof, M. Ladehoff, L. A. Löschel, C. Lorenz, S. Mintenig, S. Piehl, S. Primpke, I. Schrank, C. Laforsch, G. Gerdts, Enzymatic Purification of Microplastics in Environmental Samples. *Environ. Sci. Technol.* **51**, 14283–

14292 (2017).

53. J. S. Hanvey, P. J. Lewis, J. L. Lavers, N. D. Crosbie, K. Pozo, B. O. Clarke, A review of analytical techniques for quantifying microplastics in sediments. *Anal. Methods*. **9**, 1369–1383 (2017).

54. G. Renner, T. C. Schmidt, J. Schram, Analytical methodologies for monitoring micro(nano)plastics: Which are fit for purpose? *Curr. Opin. Environ. Sci. Heal.* **1**, 55–61 (2018).

55. T. Stanton, M. Johnson, P. Nathanail, W. MacNaughtan, R. L. Gomes, Freshwater and airborne textile fibre populations are dominated by 'natural', not microplastic, fibres. *Sci. Total Environ.* **666**, 377–389 (2019).

56. R. Hurley, A. L. Lusher, M. Olsen, L. Nizzetto, Validation of a Method for Extracting Microplastics from Complex, Organic-Rich, Environmental Matrices. *Environ. Sci. Technol.* **52**, 7409–7417 (2018).

57. A. S. Tagg, J. P. Harrison, Y. Ju-Nam, M. Sapp, E. L. Bradley, C. J. Sinclair, J. J. Ojeda, Fenton's reagent for the rapid and efficient isolation of microplastics from wastewater. *Chem. Commun.* **53**, 372–375 (2017).

58. B. Quinn, F. Murphy, C. Ewins, Validation of density separation for the rapid recovery of microplastics from sediment. *Anal. Methods*. **9**, 1491–1498 (2017).

59. A. Käppler, D. Fischer, S. Oberbeckmann, G. Schernewski, M. Labrenz, K.-J. Eichhorn, B. Voit, Analysis of environmental microplastics by vibrational microspectroscopy: FTIR, Raman or both? *Anal Bioanal Chem*. **408**, 8377–8391 (2016).

60. C. Araujo, M. M. Nolasco, A. M. P. Ribeiro, P. J. A. Ribeiro-Claro, Identification of microplastics using Raman spectroscopy: Latest developments and future prospects. *Water Res.* **142**, 426–440 (2018).

61. E. Hendrickson, E. C. Minor, K. Schreiner, Microplastic Abundance and Composition in Western Lake Superior As Determined via Microscopy, Pyr-GC/MS, and FTIR. *Environ. Sci. Technol.* **52**, 1787–1796 (2018).

62. D. Materić, A. Kasper-Giebl, D. Kau, M. Anten, M. Greilinger, E. Ludewig, E. van Sebille, T. Röckmann, R. Holzinger, Micro- and nanoplastics in Alpine snow – a new method for chemical identification and quantification in the nanogram range. *Environ. Sci. Technol.* **54**, 2353–2359 (2020).

63. R. Gillibert, G. Balakrishnan, Q. Deshoules, M. Tardivel, A. Magazzù, M. G. Donato, O. M. Maragò, M. Lamy de La Chapelle, F. Colas, F. Lagarde, P. G. Gucciardi, Raman Tweezers for Small Microplastics and Nanoplastics Identification in Seawater. *Environ. Sci. Technol.* **53**, 9003–9013 (2019).

64. E. Fries, J. H. Dekiff, J. Willmeyer, M.-T. Nuelle, M. Ebert, D. Remy, Identification of polymer types and additives in marine microplastic particles using pyrolysis-GC/MS and scanning electron microscopy. *Environ. Sci. Process. Impacts*. **15**, 1949 (2013).

65. D. Materić, E. Ludewig, K. Xu, T. Röckmann, R. Holzinger, Brief communication: Analysis of organic matter in surface snow by PTR-MS - Implications for dry deposition dynamics in the Alps. *Cryosphere*. **13**, 297–307 (2019).

66. D. Materić, M. Peacock, M. Kent, S. Cook, V. Gauci, T. Röckmann, R. Holzinger,

Characterisation of the semi-volatile component of Dissolved Organic Matter by Thermal Desorption - Proton Transfer Reaction - Mass Spectrometry. *Sci. Rep.* **7**, 1–8 (2017).

67. M. Fischer, B. M. Scholz-Böttcher, Simultaneous Trace Identification and Quantification of Common Types of Microplastics in Environmental Samples by Pyrolysis-Gas Chromatography-Mass Spectrometry. *Environ. Sci. Technol.* **51**, 5052–5060 (2017).

68. A. Käppler, M. Fischer, B. M. Scholz-Böttcher, S. Oberbeckmann, M. Labrenz, D. Fischer, K. J. Eichhorn, B. Voit, Comparison of µ-ATR-FTIR spectroscopy and py-GCMS as identification tools for microplastic particles and fibers isolated from river sediments. *Anal. Bioanal. Chem.* **410**, 5313–5327 (2018).

69. E. Dümichen, A. K. Barthel, U. Braun, C. G. Bannick, K. Brand, M. Jekel, R. Senz, Analysis of polyethylene microplastics in environmental samples, using a thermal decomposition method. *Water Res.* **85**, 451–457 (2015).

70. E. Dümichen, P. Eisentraut, C. G. Bannick, A. K. Barthel, R. Senz, U. Braun, Fast identification of microplastics in complex environmental samples by a thermal degradation method. *Chemosphere*. **174**, 572–584 (2017).

71. J. David, Z. Steinmetz, J. Kučerík, G. E. Schaumann, Quantitative Analysis of Poly(ethylene terephthalate) Microplastics in Soil via Thermogravimetry-Mass Spectrometry. *Anal. Chem.* **90**, 8793–8799 (2018).

72. A. Centrone, Infrared Imaging and Spectroscopy Beyond the Diffraction Limit. *Annu. Rev. Anal. Chem.* **8**, 101–126 (2015).

73. M. Bergmann, S. Mützel, S. Primpke, M. B. Tekman, J. Trachsel, G. Gerdts, White and wonderful? Microplastics prevail in snow from the Alps to the Arctic. *Sci. Adv.* **5**, eaax1157 (2019).

74. S. Primpke, C. Lorenz, R. Rascher-Friesenhausen, G. Gerdts, An automated approach for microplastics analysis using focal plane array (FPA) FTIR microscopy and image analysis. *Anal. Methods*. **9**, 1499–1511 (2017).

75. N. Everall, P. Griffiths, J. Chamlers, *Vibrational Spectroscopy of Polymers: Principles and Practice* (Wiley, 2007; https://www.wiley.com/en-us/Vibrational+Spectroscopy+of+Polymers%3A+Principles+and+Practice-p-9780470016626).

76. A. Vianello, R. L. Jensen, L. Liu, J. Vollertsen, Simulating human exposure to indoor airborne microplastics using a Breathing Thermal Manikin. *Sci. Rep.* **9**, 1–11 (2019).

77. F. Huth, A. Govyadinov, S. Amarie, W. Nuansing, F. Keilmann, R. Hillenbrand, Nano-FTIR absorption spectroscopy of molecular fingerprints at 20 nm spatial resolution. *Nano Lett.* **12**, 3973–3978 (2012).

78. M. Meyns, S. Primpke, G. Gerdts, “Library based identification and characterisation of polymers with nano-FTIR and IR-sSNOM imaging” (2019), , doi:arXiv:1906.10243.

79. R. Dris, J. Gasperi, M. Saad, C. Mirande, B. Tassin, Synthetic fibers in atmospheric fallout: A source of microplastics in the environment? *Mar. Pollut. Bull.* **104**, 290–293 (2016).

80. M. Ganguly, P. A. Ariya, Ice Nucleation of Model Nano-Micro Plastics: A Novel Synthetic Protocol and the Influence of Particle Capping at Diverse Atmospheric Environments. *ACS Earth Sp. Chem.* (2019), doi:10.1021/acsearthspacechem.9b00132.

81. A. C. Rocha-Santos, Teresa Duarte, *Characterization and Analysis of Microplastics* (Elsevier, 2017; https://books.google.co.uk/books?hl=en&lr=&id=DqCpDQAAQBAJ&oi=fnd&pg=PP1&dq=Rocha-Santos+and+Duarte,+2017.+Characterization+and+analysis+of+microplastics.&ots=tHW_iRapBc&sig=GcxB39KZu1IszvGvXjJv5pG1M6Q#v=onepage&q=Rocha-Santos and Duarte%2C 2017. Characte), vol. 75.

82. A. Klein, F. Ravetta, J. L. Thomas, G. Ancellet, P. Augustin, R. Wilson, E. Dieudonné, M. Fourmentin, H. Delbarre, J. Pelon, Influence of vertical mixing and nighttime transport on surface ozone variability in the morning in Paris and the surrounding region. *Atmos. Environ.* **197**, 92–102 (2019).

83. S. Abbasi, B. Keshavarzi, F. Moore, A. Turner, F. J. Kelly, A. O. Dominguez, N. Jaafarzadeh, Distribution and potential health impacts of microplastics and microrubbers in air and street dusts from Asaluyeh County, Iran. *Environ. Pollut.* **244**, 153–164 (2019).

84. P. A. Helm, Improving microplastics source apportionment: A role for microplastic morphology and taxonomy? *Anal. Methods*. **9**, 1328–1331 (2017).

85. I. E. Napper, R. C. Thompson, Release of synthetic microplastic plastic fibres from domestic washing machines: Effects of fabric type and washing conditions. *Mar. Pollut. Bull.* **112**, 39–45 (2016).

86. A. Jemec, P. Horvat, U. Kunej, M. Bele, A. Kržan, Uptake and effects of microplastic textile fibers on freshwater crustacean Daphnia magna. *Environ. Pollut.* **219**, 201–209 (2016).

87. M. Cole, A novel method for preparing microplastic fibers. *Sci. Rep.* **6**, 1–7 (2016).

88. T. Hüffer, A. Praetorius, S. Wagner, F. Von Der Kammer, T. Hofmann, Microplastic Exposure Assessment in Aquatic Environments: Learning from Similarities and Differences to Engineered Nanoparticles. *Environ. Sci. Technol.* **51**, 2499–2507 (2017).

89. E. Besseling, J. T. K. Quik, M. Sun, A. A. Koelmans, Fate of nano- and microplastic in freshwater systems: A modeling study. *Environ. Pollut.* **220**, 540–548 (2017).

90. A. Isobe, K. Uchida, T. Tokai, S. Iwasaki, East Asian seas: A hot spot of pelagic microplastics. *Mar. Pollut. Bull.* **101**, 618–623 (2015).

91. Z. Fu, J. Wang, Current practices and future perspectives of microplastic pollution in freshwater ecosystems in China. *Sci. Total Environ.* **691**, 697–712 (2019).

92. M. A. Browne, P. Crump, S. J. Niven, E. Teuten, A. Tonkin, T. Galloway, R. C. Thompson, Accumulation of Microplastic on Shorelines Woldwide : Sources and Sinks, 9175–9179 (2011).

93. B. Kuczenski, R. Geyer, Material flow analysis of polyethylene terephthalate in the US, 1996-2007. *Resour. Conserv. Recycl.* **54**, 1161–1169 (2010).

94. L. Hermabessiere, A. Dehaut, I. Paul-Pont, C. Lacroix, R. Jezequel, P. Soudant, G. Duflos, Occurrence and effects of plastic additives on marine environments and organisms: A review. *Chemosphere*. **182** (2017), pp. 781–793.

95. F. M. Windsor, I. Durance, A. A. Horton, R. C. Thompson, C. R. Tyler, S. J. Ormerod, A catchment-scale perspective of plastic pollution. *Glob. Chang. Biol.* **25**, 1207–1221 (2019).

96. S. Turner, A. A. Horton, N. L. Rose, C. Hall, A temporal sediment record of microplastics in an urban lake, London, UK. *J. Paleolimnol.* **61**, 449–462 (2019).

97. D. Allen, S. Allen, J. Sonke, V. Phoenix, in *International Conference on Microplastic Pollution inthe Mediterranean Sea*, M. Cocca, E. Di Pace, M. Errico, G. Gentile, A. Montarsolo, R. Mossotti, Eds. (Springer Water. Springer, Cham, Capri, 2019), pp. 1–8.

98. M. van der Does, P. Knippertz, P. Zschenderlein, R. Giles Harrison, J.-B. W. Stuut, The mysterious long-range transport of giant mineral dust particles. *Sci. Adv.* **4** (2018), doi:10.1126/sciadv.aau2768.

99. J. R. Jambeck, R. Geyer, C. Wilcox, T. R. Siegler, M. Perryman, A. Andrady, R. Narayan, K. L. Law, Plastic waste inputs from land into the Ocean. *Science (80-.).* **347**, 768–771 (2015).

100. J. C. Prata, Airborne microplastics: Consequences to human health? *Environ. Pollut.* **234**, 115–126 (2018).

101. C. M. Rochman, A. Tahir, S. L. Williams, D. V. Baxa, R. Lam, J. T. Miller, F. C. Teh, S. Werorilangi, S. J. Teh, Anthropogenic debris in seafood: Plastic debris and fibers from textiles in fish and bivalves sold for human consumption. *Sci. Rep.* **5**, 1–10 (2015).

102. A. Churg, M. Brauer, Ambient atmospheric particles in the airways of human lungs. *Ultrastruct. Pathol.* **24**, 353–361 (2000).

103. J. L. Pauly, S. J. Stegmeier, H. A. Allaart, R. T. Cheney, P. J. Zhang, A. G. Mayer, R. J. Streck, Inhaled cellulosic and plastic fibers found in human lung tissue. *Cancer Epidemiol. Biomarkers Prev.* **7**, 419–428 (1998).

104. A. M. Kremer, T. M. Pal, J. S. M. Boleij, J. P. Schouten, B. Rijcken, Airway hyperresponsiveness, prevalence of chronic respiratory symptoms, and lung function in workers exposed to irritants. *Occup. Environ. Med.* **51**, 3–13 (1994).

105. N. Laskar, U. Kumar, Plastics and microplastics: A threat to environment. *Environ. Technol. Innov.* **14**, 100352 (2019).

106. G. Latini, C. De Felice, G. Presta, A. Del Vecchio, I. Paris, F. Ruggieri, P. Mzzeo, In utero exposure to di-(2-ethylhexyl)phthalate and duration of human pregnancy. *Environ. Health Perspect.* **111**, 1783–1785 (2003).

107. J. J. Wirth, M. Rossano, R. Potter, E. Puscheck, D. Daly, N. Paneth, S. Krawetz, B. Protas, M. Diamond, A Pilot Study Associating Urinary Concentrations of Phthalate Metabolites and Semen Quality. *Syst. Biol. Reprod. Med.* **54**, 143–154 (2008).

108. J. Drummond, S. Krause, L. Nel, S. Allen, D. Allen, L. Simon, C. Doaudy, “Gathering at the top? Environmental controls of microplastic uptake and biomagnification in aquatic food webs” (2019).

109. T. C. Nardelli, H. C. Erythropel, B. Robaire, Toxicogenomic screening of replacements for Di(2-Ethylhexyl) phthalate (DEHP) using the immortalized TM4 sertoli cell line. *PLoS One*. **10**, 1–17 (2015).

110. J. Peretz, L. Vrooman, W. A. Ricke, P. A. Hunt, S. Ehrlich, R. Hauser, V. Padmanabhan, H. S. Taylor, S. H. Swan, C. A. Vandevoort, J. A. Flaws, Bisphenol A and reproductive health: Update of experimental and human evidence, 2007-2013. *Environ. Health Perspect.* **122**, 775–786 (2014).

111. R. A. Bhat, D. Kumar, S. M. Bhat, I. R. Sofi, in *Handbook of Research on Environmental and Human Health Impacts of Plastic Pollution* (IGI Global, 2020), pp. 246–262.

112. P. Fu, K. Kawamura, Ubiquity of bisphenol A in the atmosphere. *Environ. Pollut.* **158**, 3138–3143 (2010).

113. R. Lehner, C. Weder, A. Petri-Fink, B. Rothen-Rutishauser, Emergence of Nanoplastic in the Environment and Possible Impact on Human Health. *Environ. Sci. Technol.* (2019), doi:10.1021/acs.est.8b05512.

114. C. Rosevelt, M. Los Huertos, C. Garza, H. M. Nevins, Marine debris in central California: Quantifying type and abundance of beach litter in Monterey Bay, CA. *Mar. Pollut. Bull.* **71**, 299–306 (2013).

115. PlasticsEurope, *Plastics – the Facts 2014 / 2015 An analysis of European plastics production , demand and waste data* (Plastic Recycling and Recovery Organisations (EPRO), Belgium, 2015; https://www.plasticseurope.org/application/files/5515/1689/9220/2014plastics_the_facts_PubFeb2015.pdf).

116. PlasticsEurope, *Plastics – the Facts 2017, An analysis of the European plastics production, demand and waste data* (PlasticsEurope, European Association of Plastics Recycling and Recovery Organisations, Belgium, 2017; https://www.plasticseurope.org/application/files/5715/1717/4180/Plastics_the_facts_2017_FINAL_for_website_one_page.pdf).

117. Y. K. Song, S. H. Hong, M. Jang, G. M. Han, S. W. Jung, W. J. Shim, Combined Effects of UV Exposure Duration and Mechanical Abrasion on Microplastic Fragmentation by Polymer Type. *Environ. Sci. Technol.* **51**, 4368–4376 (2017).

118. J. P. da Costa, Micro- and nanoplastics in the environment: Research and policymaking. *Curr. Opin. Environ. Sci. Heal.* **1**, 12–16 (2018).

119. K. Mattsson, L.-A. Hansson, T. Cedervall, Nano-plastics in the aquatic environment. *Environ. Sci. Process. Impacts*. **17**, 1712–1721 (2015).

120. M. Scheurer, M. Bigalke, Microplastics in Swiss floodplain soils (2018), doi:10.1021/acs.est.7b06003.

121. R. Hurley, J. Woodward, J. J. Rothwell, Microplastic contamination of river beds significantly reduced by catchment-wide flooding. *Nat. Geosci.* **11**, 251–257 (2018).

122. P. L. Corcoran, Benthic plastic debris in marine and fresh water environments.

Environ. Sci. Process. Impacts. **17**, 1363–1369 (2015).

123. M. Zbyszewski, P. L. Corcoran, A. Hockin, Comparison of the distribution and degradation of plastic debris along shorelines of the Great Lakes , North America. *J. Great Lakes Res.* **40**, 288–299 (2014).

124. L. Watkins, S. McGrattan, P. J. Sullivan, M. T. Walter, The effect of dams on river transport of microplastic pollution. *Sci. Total Environ.* (2019), doi:https://doi.org/10.1016/j.scitotenv.2019.02.028.

125. Centre d'Etudes Spatiales de la BIOsphere (CESBIO), Donnees meteorologiques – Sud Ouest Bernadouze (2018), (available at http://www.cesbio.ups-tlse.fr/data_meteo/index.php?perma=1319145390).

126. INSEE, Institut national de la statistique et des etudes economiques (2018), (available at https://www.insee.fr/fr/statistiques/3293086?geo=COM-09334).

127. G. Erni-Cassola, M. I. Gibson, R. C. Thompson, J. A. Christie-Oleza, Lost, but Found with Nile Red: A Novel Method for Detecting and Quantifying Small Microplastics (1 mm to 20 μm) in Environmental Samples. *Environ. Sci. Technol.* **51**, 13641–13648 (2017).

128. N. Digka, C. Tsangaris, H. Kaberi, A. Adamopoulou, C. Zeri, in *Proceedings of the International Conference on Microplastic Pollution in the Mediterranean Sea*, M. Cocca, E. Di Pace, M. Errico, G. Gentile, A. Montarsolo, R. Mossotti, Eds. (Springer Water. Springer, Cham, 2018; http://link.springer.com/10.1007/978-3-319-71279-6), pp. 17–24.

129. W. Wang, A. W. Ndungu, Z. Li, J. Wang, Microplastics pollution in inland freshwaters of China: A case study in urban surface waters of Wuhan, China. *Sci. Total Environ.* **575**, 1369–1374 (2017).

130. R. Klein, in *Laser Welding of Plastics: Materials, Processes and Industrial Applications* (John Wiley & Sons, ed. 1, 2012), pp. 3–69.

131. M. Löder, G. Gerdts, in *Marine Anthropogenic Litter*, M. Bergmann, L. Gutow, M. Klages, Eds. (Springer, Cham, 2015; https://link.springer.com/chapter/10.1007%2F978-3-319-16510-3_8#citeas).

132. F. Noren, "Small plastic particles in Coastal Swedish waters" (2007).

133. W. J. Shim, S. H. Hong, S. E. Eo, Identification methods in microplastic analysis: a review. *Anal. Methods*. **9**, 1384–1391 (2017).

134. I. Peeken, S. Primpke, B. Beyer, J. Gütermann, C. Katlein, T. Krumpen, M. Bergmann, L. Hehemann, G. Gerdts, Arctic sea ice is an important temporal sink and means of transport for microplastic. *Nat. Commun.* **9**, 1505 (2018).

135. H. K. Imhof, C. Laforsch, A. C. Wiesheu, J. Schmid, P. M. Anger, R. Niessner, N. P. Ivleva, Pigments and plastic in limnetic ecosystems: A qualitative and quantitative study on microparticles of different size classes. *Water Res.* **98**, 64–74 (2016).

136. R. Lenz, K. Enders, C. A. Stedmon, D. M. A. MacKenzie, T. G. Nielsen, A critical assessment of visual identification of marine microplastic using Raman spectroscopy for analysis improvement. *Mar. Pollut. Bull.* **100**, 82–91 (2015).

137. K. Enders, R. Lenz, C. A. Stedmon, T. G. Nielsen, Abundance, size and polymer

composition of marine microplastics ≥10μm in the Atlantic Ocean and their modelled vertical distribution. *Mar. Pollut. Bull.* **100**, 70–81 (2015).

138. Y. K. Song, S. H. Hong, M. Jang, G. M. Han, M. Rani, J. Lee, W. J. Shim, A comparison of microscopic and spectroscopic identification methods for analysis of microplastics in environmental samples. *Mar. Pollut. Bull.* **93**, 202–209 (2015).

139. F. Menges, Spectragryph – optical imaging software (2016), (available at https://www.effemm2.de/spectragryph/).

140. P. Y. Khashaba, H. R. H. Ali, M. M. El-Wekil, A rapid Fourier transform infrared spectroscopic method for analysis of certain proton pump inhibitors in binary and ternary mixtures. *Spectrochim. Acta Part A Mol. Biomol. Spectrosc.* **190**, 10–14 (2018).

141. R. Ševčík, P. Mácová, Localized quantification of anhydrous calcium carbonate polymorphs using micro-Raman spectroscopy. *Vib. Spectrosc.* **95**, 1–6 (2018).

142. J. M. Lagaron, N. M. Dixon, W. Reed, J. M. Pastor, B. J. Kip, Morphological characterisation of the crystalline structure of cold-drawn HDPE used as a model material for the environmental stress cracking (ESC) phenomenon. *Polymer (Guildf).* **40**, 2569–2586 (1999).

143. E. Sanchez, C. Yague, M. A. Gazetner, Planetary boundary layer energetics simulated from a regional climate model over Europe for present climate and climate change conditions. *Geophys. Res. Lett.* **34** (2007), doi:10.1029/2006gL028340.

144. C. S. Zender, Mineral Dust Entrainment and Deposition (DEAD) model: Description and 1990s dust climatology. *J. Geophys. Res.* **108**, 4416 (2003).

145. R. R. Draxler, D. Hess, G, “Description of the Hysplit4 modeling system” (Maryland, 2018), (available at https://www.researchgate.net/publication/255682850_Description_of_the_HYSPLIT_4_modelling_system).

146. A. Stein, R. Draxler, G. Rolph, B. Stunder, M. Dohen, F. Ngqn, NOAA’s HYSPLIT atmospheric transport and dispersion modeling system. *Bull. Am. Meteorol. Soc.* **96**, 2059–2077 (2015).

147. L. Su, Z. Yuan, J. C. H. Fung, A. K. H. Lau, A comparison of HYSPLIT backward trajectories generated from two GDAS datasets. *Sci. Total Environ.* **506**–**507**, 527–537 (2015).

148. K. Ashrafi, M. Shafiepour-Motlagh, A. Aslemand, S. Ghader, Dust storm simulation over Iran using HYSPLIT. *J. Environ. Heal. Sci. Eng.* **12**, 9 (2014).

149. I. Reche, G. D’Orta, N. Mladenov, D. M. Winget, C. A. Suttle, Deposition rates of viruses and bacteria above the atmospheric boundary layer. *ISME J.* **12**, 1154–1162 (2018).

150. C. D. G. Zwaaftink, Ó. Arnalds, P. Dagsson-waldhauserova, S. Eckhardt, J. Prospero, A. Stohl, Temporal and spatial variability of Icelandic dust emissions and atmospheric transport. *Atmos. Chem. Phys.*, 10865–10878 (2017).

151. B. Marticorena, B. Chatenet, J. L. Rajot, G. Bergametti, A. Deroubaix, J. Vincent, A. Kouoi, C. Schmechtig, M. Coulibaly, A. Diallo, I. Koné, A. Maman, T. NDiaye, A. Zakou, Mineral dust over west and central Sahel: Seasonal patterns of dry

and wet deposition fluxes from a pluriannual sampling (2006-2012). *J. Geophys. Res. Atmos.* **122**, 1338–1364 (2017).

152. R. Morales-Baquero, E. Pulido-Villen, I. Reche, Chemical signature of Saharan dust on dry and wet atmospheric deposition in the south-western Mediterranean region. *Tellus Ser. B*. **1**, 1–12 (2013).

153. M. Schwikowski, P. Seibert, U. Baltensperger, H. W. Gaggeler, A study of an outstanding Saharan dust event at the high-alpine site Jungfraujoch, Switzerland. *Atmos. Environ.* **29**, 1829–1842 (1995).

154. J. Dessens, P. Van Dinh, Frequent Saharan Dust Outbreaks North of the Pyrenees: A sign of a climatic change? *Weather*. **45**, 327–333 (1990).

155. J. Schindelin, I. Arganda-Carreras, E. Frise, V. Kaynig, M. Longair, T. Pietzsch, S. Preibisch, C. Rueden, S. Saalfeld, B. Schmid, J.-Y. Tinevez, D. J. White, V. Hartenstein, K. Eliceiri, P. Tomancak, A. Cardona, Fiji: an open-source platform for biological image analysis. *Nat. Methods*. **9**, 676–682 (2012).

156. D. Schymanski, C. Goldbeck, H. U. Humpf, P. Fürst, Analysis of microplastics in water by micro-Raman spectroscopy: Release of plastic particles from different packaging into mineral water. *Water Res.* **129**, 154–162 (2018).

157. European Comission, A European Strategy for Plastics in a Circular Economy. *Eur. Com.*, 24 (2018).

158. K. Magnusson, K. Eliasson, A. Fråne, K. Haikonen, J. Hultén, M. Olshammar, J. Stadmark, A. Voisin, Swedish sources and pathways for microplastics to the marine environment. A review of existing data. *IVL Rep.*, 1–89 (2016).

159. R. Dris, H. Imhof, W. Sanchez, J. Gasperi, F. Galgani, B. Tassin, C. Laforsch, Beyond the ocean: Contamination of freshwater ecosystems with (micro-) plastic particles. *Environ. Chem.* **12**, 539–550 (2015).

160. W. J. Shim, S. H. Hong, S. Eo, in *Microplastic Contamination in Aquatic Environments*, E. Y. Zeng, Ed. (Elsevier, 2018; http://www.sciencedirect.com/science/article/pii/B9780128137475000011), pp. 1–26.

161. R. Dris, J. Gasperi, B. Tassin, in *Freshwater Microplastics The Handbook of Environmental Chemistry*, S. Lambert, M. Wagber, Eds. (2018; http://link.springer.com/10.1007/978-3-319-61615-5), pp. 69–83.

162. S. L. Wright, J. Ulke, A. Font, K. L. . Chan, F. J. Kelly, Atmospheric microplastic deposition in an urban environment and an evaluation of transport. *Environ. Int.* (2019), doi:10.1016/j.envint.2019.105411.

163. X. Wang, C. Li, K. Liu, L. Zhu, Z. Song, D. Li, Atmospheric microplastic over the South China Sea and East Indian Ocean : abundance , distribution and source. *J. Hazard. Mater.* (2019), doi:10.1016/j.jhazmat.2019.121846.

164. M. Bergmann, S. Mützel, S. Primpke, M. B. Tekman, G. Gerdts, in *Arctic Frontiers* (Alfred-Wegener-Institut andd Helmholtz Gemeinschaft, Tromso, 2019; https://epic.awi.de/id/eprint/48975/), p. 1.

165. D. Durnford, A. Dastoor, D. Figueras-Nieto, A. Ryjkov, Long range transport of mercury to the Arctic and across Canada. *Atmos. Chem. Phys.* **10**, 6063–6086 (2010).

166. D. Hirdman, K. Aspmo, J. F. Burkhart, S. Eckhardt, H. Sodemann, A. Stohl, Transport of mercury in the Arctic atmosphere: Evidence for a springtime net sink and summer-time source. *Geophys. Res. Lett.* **36**, 1–5 (2009).

167. I. Uno, K. Eguchi, K. Yumimoto, T. Takemura, A. Shimizu, M. Uematsu, Z. Liu, Z. Wang, Y. Hara, N. Sugimoto, Asian dust transported one full circuit around the globe. *Nat. Geosci.* **2**, 557–560 (2009).

168. P. Ricaud, R. Zbinden, V. Catoire, V. Brocchi, F. Dulac, E. Hamonou, J. Canonici, L. ElAmraoui, S. Massart, U. Piguet, U. Dayan, P. Nabat, J. Sciare, M. Ramonet, M. Delmotte, A. di Sarra, D. Sferlazzo, T. di Iorio, S. Piacentino, P. Cristofanelli, N. Mihalopoulos, G. Kouvarakis, M. Pikridas, C. Savvides, R. Mamouri, A. Nisantzi, D. Hadjimitsis, J. Attié, H. Ferré, Y. Kangah, N. Jaidan, J. Guth, P. Jacquet, S. Chevrier, C. Robert, A. Bourdon, J. Bourdinot, J. Etienne, K. Gisèle, T. Pierre, The GLAM airborne campaign across the Mediterranean Basin. *Bull. Am. Meteorol. Soc.* **99**, 361–380 (2017).

169. X. Fu, N. Marusczak, L. E. Heimbürger, B. Sauvage, F. Gheusi, E. M. Prestbo, J. Sonke, Atmospheric mercury speciation dynamics at the high-altitude Pic du Midi Observatory, southern France. *Atmos. Chem. Phys.* **16**, 5623–5639 (2016).

170. A. Marenco, H. Gouget, P. Nedelec, J. P. Pages, F. Karcher, Evidence of a long-term increase in tropospheric ozone from Pic du Midi data series: consequences: positive radiative forcing. *J. Geophys. Res.* **99**, 617–632 (1994).

171. A. Chevalier, F. Gheusi, J.-L. Attié, R. Delmas, R. Zbinden, G. Athier, J.-M. Cousin, Carbon monoxide observations from ground stations in France and Europe and long trends in the free troposphere. *Atmos. Chem. Phys. Discuss.* **8**, 3313–3356 (2008).

172. G. Erni-cassola, M. I. Gibson, R. C. Thompson, J. A. Christie-oleza, Lost , but found with Nile red ; a novel method to detect and quantify small microplastics (20 µm – 1 mm) in environmental samples, 1–9 (2017).

173. R. R. Draxler, D. Hess, G, An Overview of the HYSPLIT_4 Modelling System for Trajectories, Dispersion, and Deposition. *Aust. Meteorolofical Mag.* **47**, 295–308 (1998).

174. M. Kooi, A. A. Koelmans, Simplifying Microplastic via Continuous Probability Distributions for Size, Shape,and Density. *Environ. Sci. Technol. Lett.* **6**, 551–557 (2019).

175. F. Gheusi, F. Ravetta, H. Delbarre, C. Tsamalis, A. Chevalier-Rosso, C. Leroy, P. Augustin, R. Delmas, G. Ancellet, G. Athier, P. Bouchou, B. Campistron, J. M. Cousin, M. Fourmentin, Y. Meyerfeld, Pic 2005, a field campaign to investigate low-tropospheric ozone variability in the Pyrenees. *Atmos. Res.* **101**, 640–665 (2011).

176. A. F. Stein, R. R. Draxler, G. D. Rolph, B. J. B. Stunder, M. D. Cohen, F. Ngan, NOAA's HYSPLIT Atmospheric Transport and Dispersion Modeling System. *Bull. Am. Meteorol. Soc.* **96**, 2059–2077 (2015).

177. A. F. Stein, Y. Wang, J. D. de la Rosa, A. M. Sanchez de la Campa, N. Castell, R. R. Draxler, Modeling PM10 Originating from Dust Intrusions in the Southern Iberian Peninsula Using HYSPLIT. *Weather Forecast.* **26**, 236–242 (2011).

178. Y. Li, L. Shao, W. Wang, M. Zhang, X. Feng, W. Li, D. Zhang, Airborne fiber

particles: Types, size and concentration observed in Beijing. *Sci. Total Environ.* **705** (2020), doi:10.1016/j.scitotenv.2019.135967.

179. S. Allen, D. Allen, K. Moss, G. Le Roux, V. R. Phoenix, J. Sonke, Examination of the ocean as a source for atmospheric microplastics. *PLoS One*. **15** (2020), doi:10.1371/journal.pone.0232746.

180. M. Yurtsever, A. Kaya, C. Bayraktar, in *International Conference on Microplastic Pollution in the Mediterranean Sea*, M. Cocca, Ed. (Springer International Publishing, 2018; http://link.springer.com/10.1007/978-3-319-71279-6), vol. 22, p. 238.

181. N. Asrin, A. Dipareza, Microplastics in Ambient Air (Case Study : Urip Sumoharjo Street and Mayjend Sungkono Street of Surabaya City , Indonesia). *IAETSD J. Adv. Res. Appl. Sci.* **6**, 54–57 (2019).

182. N. Evangeliou, H. Grythe, Z. Klimont, C. Heyes, S. Eckhardt, S. Lopez-Aparicio, A. Stohl, Atmospheric transport, a major pathway of microplastics to remote regions. *Preprints*, 1–32 (2020).

183. M. L. Moser, D. S. Lee, A Fourteen-Year Survey of Plastic Ingestion by Western North Atlantic Seabirds. *Colon. Waterbirds*. **15**, 883–94 (1992).

184. PlasticsEurope, “Plastics – the Facts 2019” (2019).

185. W. J. Shim, R. C. Thomposon, Microplastics in the Ocean. *Arch. Environ. Contam. Toxicol.* **69**, 265–268 (2015).

186. R. Geyer, J. R. Jambeck, K. L. Law, Production, use, and fate of all plastics ever made. *Sci. Adv.* **3**, e1700782 (2017).

187. Z. Akdogan, B. Guven, Microplastics in the environment: A critical review of current understanding and identification of future research needs. *Environ. Pollut.* **254**, 113011 (2019).

188. E. Van Sebille, C. Wilcox, L. Lebreton, N. Maximenko, B. D. Hardesty, J. A. Van Franeker, M. Eriksen, D. Siegel, F. Galgani, K. L. Law, A global inventory of small floating plastic debris. *Environ. Res. Lett.* **10**, 124006 (2015).

189. A. A. Koelmans, M. Kooi, K. L. Law, E. Van Sebille, All is not lost: Deriving a top-down mass budget of plastic at sea. *Environ. Res. Lett.* **12**, 1–23 (2017).

190. N. Maximenko, J. Hafner, P. Niiler, Pathways of marine debris derived from trajectories of Lagrangian drifters. *Mar. Pollut. Bull.* **65**, 51–62 (2012).

191. D. Wichmann, P. Delandmeter, E. van Sebille, Influence of near-surface currents on the global dispersal of marine microplastic. *JGR Ocean.*, 1–18 (2018).

192. N. Sharma, A. Rai, *Algal Particles in the Atmosphere* (Elsevier, 2011).

193. M. Sofiev, J. Soares, M. Prank, G. De Leeuw, J. Kukkonen, A regional-to-global model of emission and transport of sea salt particles in the atmosphere. *J. Geophys. Res. Atmos.* **116** (2011), doi:10.1029/2010JD014713.

194. M. A. Erinin, S. D. Wang, R. Liu, D. Towle, X. Liu, J. H. Duncan, Spray Generation by a Plunging Breaker. *Geophys. Res. Lett.* **46** (2019), doi:10.1029/2019GL082831.

195. E. Lewis, S. Schwartz, *Sea salt aerosol production: mechanisms, methods, measurements and models* (American Geophysical Union, Washington, USA,

2004).

196. W. A. Hoppel, G. M. Frick, J. W. Fitzgerald, Surface source function for sea-salt aerosol and aerosol dry deposition to the ocean surface. *J. Geophys. Res. Atmos.* **107**, 1–17 (2002).

197. D. Richer, F. Veron, Ocean Spray:an outsized influence on weather and climate. *Phys. Today*. **69**, 35–39 (2016).

198. C. D. O'Dowd, G. de Leeuw, Marine aerosol production: a review of the current knowledge. *Philos. Trans. R. Soc. A Math. Phys. Eng. Sci.* **365**, 1753–1774 (2007).

199. J. A. Quinn, R. A. Steinbrook, J. L. Anderson, Breaking bubbles and the water-to-air transport of particulate matter. *Chem. Eng. Sci.* **30**, 1177–1184 (1975).

200. M. Pósfai, J. Li, J. R. Anderson, P. R. Buseck, Aerosol bacteria over the Southern Ocean during ACE-1. *Atmos. Res.* **66**, 231–240 (2003).

201. I. Reche, G. D'Orta, N. Mladenov, D. M. Winget, C. A. Suttle, Deposition rates of viruses and bacteria above the atmospheric boundary layer. *ISME J.* (2018), doi:10.1038/s41396-017-0042-4.

202. J. C. McWilliams, P. P. Sullivan, C.-H. Moeng, Langmuir turbulence in the ocean. *J. Fluid Mech.* **334**, S0022112096004375 (1997).

203. C. A. Choy, B. H. Robison, T. O. Gagne, B. Erwin, E. Firl, R. U. Halden, J. A. Hamilton, K. Katija, S. E. Lisin, C. Rolsky, K. S. Van Houtan, The vertical distribution and biological transport of marine microplastics across the epipelagic and mesopelagic water column. *Sci. Rep.* **9**, 1–9 (2019).

204. T. Kukulka, R. R. Harcourt, Influence of Stokes Drift Decay Scale on Langmuir Turbulence. *J. Phys. Oceanogr.* **47**, 1637–1656 (2017).

205. Y. Zhang, T. Gao, S. Kang, M. Sillanpää, Importance of atmospheric transport for microplastics deposited in remote areas. *Environ. Pollut.* **254** (2019), doi:10.1016/j.envpol.2019.07.121.

206. C. E. Enyoh, A. W. Verla, E. N. Verla, F. C. Ibe, C. E. Amaobi, Airborne microplastics: a review study on method for analysis, occurrence, movement and risks. *Environ. Monit. Assess.* **191**, 1–17 (2019).

207. Y. Zhang, S. Kang, S. Allen, D. Allen, T. Gao, M. Sillanpaa, Atmospheric microplastics: A review on current status and perspectives. *Earth-Science Rev.* **203**, 103118 (2020).

208. P. L. Corcoran, M. C. Biesinger, M. Grifi, Plastics and beaches: A degrading relationship. *Mar. Pollut. Bull.* **58**, 80–84 (2009).

209. S. Lambert, M. Wagner, Characterisation of nanoplastics during the degradation of polystyrene. *Chemosphere*. **145**, 265–268 (2016).

210. A. Jahnke, H. P. H. Arp, B. I. Escher, B. Gewert, E. Gorokhova, D. Kühnel, M. Ogonowski, A. Potthoff, C. Rummel, M. Schmitt-Jansen, E. Toorman, M. MacLeod, Reducing Uncertainty and Confronting Ignorance about the Possible Impacts of Weathering Plastic in the Marine Environment. *Environ. Sci. Technol. Lett.* **4**, 85–90 (2017).

211. F. Julienne, N. Delorme, F. Lagarde, From macroplastics to microplastics: Role

of water in the fragmentation of polyethylene. *Chemosphere*. **236**, 124409 (2019).

212. A. L. Dawson, S. Kawaguchi, C. K. King, K. A. Townsend, R. King, W. M. Huston, S. M. Bengtson Nash, Turning microplastics into nanoplastics through digestive fragmentation by Antarctic krill. *Nat. Commun.* **9**, 1–8 (2018).
213. Hong Kong Observatory, The Weather of October 2016, 1–9 (2018).
214. Hong Kong Observatory, The Weather of November 2016 Warnings and Signals issued in November 2016, 1–6 (2018).
215. Hong Kong Observatory, The Weather of December 2016 Warnings and Signals issued in December 2016, 1–6 (2018).
216. E. Athanasopoulou, M. Tombrou, S. N. Pandis, A. G. Russell, The role of sea-salt emissions and heterogeneous chemistry in the air quality of polluted coastal areas. *Atmos. Chem. Phys.* **8**, 5755–5769 (2008).
217. J. Yan, L. Chen, Q. Lin, S. Zhao, M. Zhang, Effect of typhoon on atmospheric aerosol particle pollutants accumulation over Xiamen, China. *Chemosphere*. **159**, 244–255 (2016).
218. V. C. Slonosky, Wet winters, dry summers? Three centuries of precipitation data from Paris. *Geophys. Res. Lett.* **29**, 34-1-34–4 (2002).
219. G. S. Fanourgakis, M. Kanakidou, A. Nenes, S. E. Bauer, T. Bergman, K. S. Carslaw, A. Grini, D. S. Hamilton, J. S. Johnson, V. A. Karydis, A. Kirkevåg, J. K. Kodros, U. Lohmann, G. Luo, R. Makkonen, H. Matsui, D. Neubauer, J. R. Pierce, J. Schmale, P. Stier, K. Tsigaridis, T. van Noije, H. Wang, D. Watson-Parris, D. M. Westervelt, Y. Yang, M. Yoshioka, N. Daskalakis, S. Decesari, M. Gysel Beer, N. Kalivitis, X. Liu, N. M. Mahowald, S. Myriokefalitakis, R. Schrödner, M. Sfakianaki, A. P. Tsimpidi, M. Wu, F. Yu, Evaluation of global simulations of aerosol particle number and cloud condensation nuclei, and implications for cloud droplet formation. *Atmos. Chem. Phys. Discuss.*, 1–40 (2019).
220. M. O. Andreae, D. Rosenfeld, Aerosol-cloud-precipitation interactions. Part 1. The nature and sources of cloud-active aerosols. *Earth-Science Rev.* **89**, 13–41 (2008).
221. M. Van Der Does, A. Pourmand, A. Sharifi, J.-B. W. Stuut, North African mineral dust across the tropical Atlantic Ocean: Insights from dust particle size, radiogenic Sr-Nd-Hf isotopes and rare earth elements (REE). *Aeolian Res.* **33**, 106–116 (2018).
222. R. L. Modini, B. Harris, Z. Ristovski, The organic fraction of bubble-generated, accumulation mode Sea Spray Aerosol (SSA). *Atmos. Chem. Phys.* **10**, 2867–2877 (2010).
223. E. Fuentes, H. Coe, D. Green, G. De Leeuw, G. McFiggans, Laboratory-generated primary marine aerosol via bubble-bursting and atomization. *Atmos. Meas. Tech.* **3**, 141–162 (2010).
224. W. R. Ke, Y. M. Kuo, C. W. Lin, S. H. Huang, C. C. Chen, *Characterization of aerosol emissions from single bubble bursting* (Elsevier Ltd, 2017; http://dx.doi.org/10.1016/j.jaerosci.2017.03.006), vol. 109.

225. D. B. J. Demoz.B.B, Coller JL. Jr, on the Caltech Active Strand Cloudwater collectors. *Atmos. Res.* **41**, 46672 (1995).

226. T. Wrzesinsky, O. Klemm, Summertime fog chemistry at a mountainous site in central Europe. *Atmos. Environ.* **34**, 1487–1496 (2000).

227. P. Roman, Z. Polkowska, J. Namieśnik, Sampling procedures in studies of cloud water composition: A review. *Crit. Rev. Environ. Sci. Technol.* **43**, 1517–1555 (2013).

228. P. Herckes, M. P. Hannigan, L. Trenary, T. Lee, J. L. Collett, Organic compounds in radiation fogs in Davis (California). *Atmos. Res.* **64**, 99–108 (2002).

229. MeteoFrance, Météo et climat: Mimizan (2018), (available at http://www.meteofrance.com/previsions-meteo-france/mimizan/40200).

230. S. Zhao, M. Danley, J. E. Ward, D. Li, T. J. Mincer, An approach for extraction, characterization and quantitation of microplastic in natural marine snow using Raman microscopy. *Anal. Methods*. **9**, 1470–1478 (2017).

231. D. Koračin, C. E. Dorman, J. M. Lewis, J. G. Hudson, E. M. Wilcox, A. Torregrosa, Marine fog: A review. *Atmos. Res.* **143**, 142–175 (2014).

232. A. K. Baldwin, S. R. Corsi, S. A. Mason, Plastic Debris in 29 Great Lakes Tributaries: Relations to Watershed Attributes and Hydrology. *Environ. Sci. Technol.* **50**, 10377–10385 (2016).

233. A. Mendoza, J. L. Osa, O. C. Basurko, A. Rubio, M. Santos, J. Gago, F. Galgani, C. Peña-Rodriguez, Microplastics in the Bay of Biscay: An overview. *Mar. Pollut. Bull.* **153** (2020), doi:10.1016/j.marpolbul.2020.110996.

234. S. Allen, D. Allen, V. R. Phoenix, G. Le Roux, P. Durantez, Atmospheric deposition of microplastics found on a remote mountain catchment. *Nat. Geosci.* (2018).

235. B. Marticorena, G. Bergametti, B. Aumont, M. Legrand, Modeling the atmospheric dust cycle: 2. Simulation of Saharan dust sources. *J. Geophys. Res.* **102**, 4387–4404 (1997).

236. C. Szczypta, S. Gascoin, T. Houet, O. Hagolle, J. F. Dejoux, C. Vigneau, P. Fanise, Impact of climate and land cover changes on snow cover in a small Pyrenean catchment. *J. Hydrol.* **521**, 84–99 (2015).

237. S. M. Rhind, Anthropogenic pollutants: a threat to ecosystem sustainability? *Philos Trans R Soc L. B Biol Sci*. **364**, 3391–3401 (2009).

238. N. Pirrone, S. Cinnirella, X. Feng, R. B. Finkelman, H. R. Friedli, J. Leaner, R. Mason, A. B. Mukherjee, G. B. Stracher, D. G. Streets, K. Telmer, Global mercury emissions to the atmosphere from anthropogenic and natural sources. *Atmos. Chem. Phys.* **10**, 5951–5964 (2010).

239. J. O. Nriagu, Global inventory of natural and anthropogenic emissions of trace metals to the atmosphere. *Nature*. **279**, 409 (1979).

240. J. Catalan, L. Camarero, M. Felip, S. Pla, M. Ventura, T. Buchaca, F. Bartumeus, G. De Mendoza, A. Miró, E. O. Casamayor, J. M. Medina-Sánchez, M. Bacardit, M. Altuna, M. Bartrons, D. D. De Quijano, High mountain lakes: Extreme habitats and witnesses of environmental changes. *Limnetica*. **25**, 551–584 (2006).

241. P. Fernández, R. M. Vilanova, C. Martínez, P. Appleby, J. O. Grimalt, The historical record of atmospheric pyrolytic pollution over Europe registered in the sedimentary PAH from remote mountain lakes. *Environ. Sci. Technol.* **34**, 1906–1913 (2000).

242. M. Bacardit, L. Camarero, Atmospherically deposited major and trace elements in the winter snowpack along a gradient of altitude in the Central Pyrenees: The seasonal record of long-range fluxes over SW Europe. *Atmos. Environ.* **44**, 582–595 (2010).

243. S. V. Hansson, A. Claustres, A. Probst, F. De Vleeschouwer, S. Baron, D. Galop, F. Mazier, G. Le Roux, Atmospheric and terrigenous metal accumulation over 3000 years in a French mountain catchment: Local vs distal influences. *Anthropocene*. **19**, 45–54 (2017).

244. A. Hervàs, L. Camarero, I. Reche, E. O. Casamayor, Viability and potential for immigration of airborne bacteria from Africa that reach high mountain lakes in Europe. *Environ. Microbiol.* **11**, 1612–1623 (2009).

245. F. E. Grousset, P. Ginoux, A. Bory, P. E. Biscaye, Case study of a Chinese dust plume reaching the French Alps. *Geophys. Res. Lett.* **30**, 23–26 (2003).

246. J. Gago, O. Carretero, A. V Filgueiras, L. Viñas, Synthetic microfibers in the marine environment: A review on their occurrence in seawater and sediments. *Mar. Pollut. Bull.* **127**, 365–376 (2018).

247. R. Dris, J. Gasperi, B. Tassin, M. Wagner, S. Lambert, Eds. (Springer International Publishing, Cham, 2018; https://doi.org/10.1007/978-3-319-61615-5_4), pp. 69–83.

248. M. Filella, Questions of size and numbers in environmental research on microplastics: Methodological and conceptual aspects. *Environ. Chem.* **12**, 527–538 (2015).

249. R. Hurley, J. Woodward, J. J. Rothwell, Supplementary Information -Microplastic contamination of river beds significantly reduced by catchment-wide flooding. *Nat. Geosci.* **11**, 251–257 (2018).

250. M. T. Nuelle, J. H. Dekiff, D. Remy, E. Fries, A new analytical approach for monitoring microplastics in marine sediments. *Environ. Pollut.* **184**, 161–169 (2014).

Appendix 6: Bernadouze, French Pyrenees dataset

Form and particle size characterisation																	
three photographs (of 58mm2 at consistent locations and areas on each slide) were analysed for each filter, two filters per monitoring period (month) resulting in six photograph areas viewed for eac																	
total n =	1147	51%	of total Raman estimated microP particulates														
PSD of fragments in the atmospheric collectors					PSD of fragments in the atmospheric collectors by month									Standard Deviations				
particle si	# of partic	% of parti	Standard deviation			Nov	Dec	Jan	Feb	Mar	Overall			Nov	Dec	Jan	Feb	Mar
<25um	418	53%	3%		0um	0%	0%	0%	0%	0%	0%		0um	0%	0%	0%	0%	0%
25-50um	250	32%	1%		25um	58%	67%	59%	39%	38%	53%		25um	3%	2%	19%	5%	15%
50-75um	68	9%	1%		50µm	94%	93%	83%	76%	76%	85%		50µm	2%	4%	16%	5%	16%
75-100um	34	4%	0%		75µm	99%	98%	92%	88%	90%	94%		75µm	1%	0%	13%	2%	5%
100-125un	11	1%	0%		100µm	100%	100%	99%	94%	96%	98%		100µm	0%	0%	3%	0%	0%
125-150un	2	0%	0%		125µm	100%	100%	99%	98%	99%	99%		125µm	0%	0%	1%	2%	0%
150-175un	2	0%	0%		150µm	100%	100%	99%	100%	99%	100%		150µm	0%	0%	1%	0%	0%
175-200un	0	0%	0%		175µm	100%	100%	99%	100%	100%	100%		175µm	0%	0%	1%	0%	0%
200-225µn	1	0%	0%		200µm	100%	100%	99%	100%	100%	100%		200µm	0%	0%	1%	0%	0%
225-250un	0	0%	0%		225µm	100%	100%	100%	100%	100%	100%		225µm	0%	0%	0%	0%	0%
250-275µn	0	0%	0%		250µm	100%	100%	100%	100%	100%	100%		250µm	0%	0%	0%	0%	0%
275-300un	0	0%	0%		275µm	100%	100%	100%	100%	100%	100%		275µm	0%	0%	0%	0%	0%
>300µm	0	0%	0%		300µm	100%	100%	100%	100%	100%	100%		300µm	0%	0%	0%	0%	0%
n = 786																		
786 particles sized and checked					Total	124	213	155	127	167								

PSD of films in the atmospheric deposition						# of particles within this particle size range					
	# of partic	% of parti	Standard deviation			Nov	Dec	Jan	Feb	Mar	Total
<50um	12	5%	2%		>50um				3	9	12
50-100um	97	41%	10%		50-100um	2	1	31	9	54	97
100-150un	74	31%	5%		100-150un	1	7	16	28	22	74
150-200un	28	12%	3%		150-200un	1	3	4	17	3	28
200-250un	13	5%	1%		200-250um		3	5	4	1	13
250-300un	5	2%	0%		250-300um		1	2	2		5
300-350un	6	3%	0%		300-350um		2	2	2		6
350-400un	1	0%	0%		350-400um		1				1
450-500un	1	0%	0%		450-500um			1			1
500µm-55	0	0%	0%		500µm-550µm						0
550µm-60	1	0%	0%		550µm-600µm			1			1
n = 238					Total	4	18	62	65	89	238

Length of fibres in the atmospheric deposition						# of particles within this particle size range					
	# of fibres	% of fibre	Standard deviation			Nov	Dec	Jan	Feb	Mar	Total
<100um	18	14%	4%		<100um	3	12	1	1	1	18
100-200un	21	17%	2%		100-200un	6	4	1	5	5	21
200-300un	21	17%	1%		200-300un	6	5	3	3	4	21
300-400un	12	10%	1%		300-400un	2		5	1	4	12
400-500un	9	7%	1%		400-500un	1	2	3	1	2	9
500-600un	10	8%	1%		500-600un	3		3	3	1	10
600-700un	6	5%	0%		600-700un	2	1	1	1	1	6
700-800un	8	6%	0%		700-800um		2	3		3	8
800-900un	7	6%	1%		800-900um		1	2		4	7
900-1000u	0	0%	0%		900-1000um						0
1000-1100	1	1%	0%		1000-1100µm					1	1
1100-1200	2	2%	0%		1100-1200	1				1	2
1200-1300	4	3%	1%		1200-1300µm			3		1	4
1300-1400	0	0%	0%		1300-1400µm						0
1400-1500	1	1%	0%		1400-1500µm					1	1
1500-1600	0	0%	0%		1500-1600µm						0
1600-1700	1	1%	0%		1600-1700	1					1
1700-1800	0	0%	0%		1700-1800µm						0
1800-1900	1	1%	0%		1800-1900µm			1			1
1900-2000	0	0%	0%		1900-2000µm						0
2000-2100	0	0%	0%		2000-2100µm						0
2100-2200	0	0%	0%		2100-2200µm						0
2200-2300	1	1%	0%		2200-2300µm			1			1
2300-2400	0	0%	0%		2300-2400µm						0
2400-2500	1	1%	0%		2400-2500µm		1				1
2500-2600	1	1%	0%		2500-2600µm					1	1
>2600µm	1	1%	0%		>2600µm			1			1
n = 126					Total	25	28	28	15	30	126

period	sampler	Sampling start date	Sampling end date	days	# particles per inspected area (3x13mm2)	# fibres per inspected area (3x13mm2)	#films per inspected area (3x13mm2)	microP per inspection area (13mm2)	total filter area inspected (6 x 13 mm2)	# particles on the filter	# fibres on the filter	#films on the filter	microP per filter	# particles on the filter - ε	# fibres on the filter - ε	#films on the filter - ε	microP per filter - ε	Collector sample area (m2)	# particles / m2 / monitoring period	# fibres / m2 / monitoring period	#films / m2 / monitoring period	microP / m2 / monitoring period	particles / m2 / day	fibres / m2 / day	films /m2/ day	Total microP / m2/ day	particles / m2 / day	fibres / m2/ day	films /m2/ day	Total microP / m2/ day		
Nov	Palmex	16/11/2017	28/11/2017	12	9	2	1	12	39	80	18	9	107	72	15	8	95	0.014	5051	1037	554	6642	421	86	46	554	354	75	34	462	Nov	91.4830248
Dec	Palmex	29/11/2017	18/12/2017	19	12	3	2	17	39	107	27	18	152	99	24	17	140	0.014	6922	1661	1177	9759	364	87	62	514	258	56	45	359	Dec	154.755164
Jan	Palmex	19/12/2017	22/01/2018	34	9	3	1	13	39	80	27	9	116	72	24	8	104	0.014	5051	1661	554	7265	149	49	16	214	183	31	91	306	Jan	92.2095469
Feb	Palmex	23/01/2018	03/05/2018	41	9	3	4	16	39	80	27	36	143	72	24	35	131	0.014	5051	1661	2424	9136	123	41	59	223	183	29	85	297	Feb	74.4422875
March	Palmex	03/06/2018	04/09/2018	34	23	2	9	34	39	205	18	80	303	197	15	79	291	0.014	13779	1037	5541	20357	405	31	163	599	266	26	110	402	March	196.384632
Nov	NILU	16/11/2017	28/11/2017	12	13	3	1	17	39	116	27	9	152	108	24	8	140	0.0314	3438	757	252	4446	286	63	21	371	249	44	73	365	Daily average	
Dec	NILU	29/11/2017	18/12/2017	19	11	2	2	15	39	98	18	18	134	90	15	17	122	0.0314	2870	473	536	3878	151	25	28	204	68%	12%	20%			
Jan	NILU	19/12/2017	22/01/2018	34	27	2	20	49	39	241	18	178	437	233	15	177	425	0.0314	7414	473	5649	13536	218	14	166	398						
Feb	NILU	23/01/2018	03/05/2018	41	36	3	16	55	39	321	27	143	491	313	24	142	479	0.0314	9971	757	4513	15240	243	18	110	372						
March	NILU	03/06/2018	04/09/2018	34	16	3	7	26	39	143	27	62	232	135	24	61	220	0.0314	4290	757	1956	7003	126	22	58	206					StDev	
																												Sum	1826	103	
Total							254					2265				2145					97263			3653				Daily averag	365	69	
individual inspection area		13	mm2				11%																								
area of 1 filtre		346	mm2																												
filtre area/inspected area		9																													
number of microP found in the blank filters (354 mm2) (ε)																															
partiles	8																														
fibres	3																														
films	1																														
Individual sample counts																		Total					StDev							
period	sampler	Sampling start date	Sampling end date	days	# fragments per inspected area (13mm2)	# fibres per inspected area (13mm2)	#films per inspected area (13mm2)			# fragments per inspected area (13mm2)	# fibres per inspected area (13mm2)	#films per inspected area (13mm2)		# fragments per inspected area (13mm2)	# fibres per inspected area (13mm2)	#films per inspected area (13mm2)		# fragments per inspected area (3x13mm2)	# fibres per inspected area (3x13mm2)	#films per inspected area (3x13mm2)			# fragments per inspected area (13mm2)	# fibres per inspected area (13mm2)	#films per inspected area (13mm2)							
Nov	Palmex	16/11/2017	28/11/2017	12	3	0	0			2	1	0		4	1	1		9	2	1			1	1	1							
Dec	Palmex	29/11/2017	18/12/2017	19	4	1	1			3	1	1		5	1	0		12	3	2			1	0	1							
Jan	Palmex	19/12/2017	22/01/2018	34	2	1	0			2	1	1		5	1	0		9	3	1			2	0	1							
Feb	Palmex	23/01/2018	03/05/2018	41	2	1	1			3	0	2		4	2	1		9	3	4			1	1	1							
March	Palmex	03/06/2018	04/09/2018	34	8	2	3			7	0	3		8	0	3		23	2	9			1	1	0							
Nov	NILU	16/11/2017	28/11/2017	12	4	2	1			5	1	0		4	0	0		13	3	1			1	1	1							
Dec	NILU	29/11/2017	18/12/2017	19	3	0	0			4	1	2		4	1	0		11	2	2			1	1	1							
Jan	NILU	19/12/2017	22/01/2018	34	9	0	6			8	1	8		10	1	6		27	2	20			1	1	1							
Feb	NILU	23/01/2018	03/05/2018	41	11	2	4			12	1	6		13	0	6		36	3	16			1	1	1							
March	NILU	03/06/2018	04/09/2018	34	5	1	3			6	2	2		5	0	2		16	3	7			1	1	1							

Types of plastics found in the atmospheric fallout																		
	Number of particles analysed						Percentage							Standard deviation				
Plastic type	Nov	Dec	Jan	Feb	March		Nov	Dec	Jan	Feb	March	Average for monitoring period		Nov total	Dec total	Jan total	Feb total	March total
PS	13	13	31	22	22		45%	41%	50%	31%	37%	41%		2.4%	2.2%	1.1%	2.0%	0.0%
PE	7	12	15	17	31		24%	38%	24%	24%	52%	32%		2.4%	0.0%	1.1%	1.0%	1.2%
PP	7	3	9	23	5		24%	9%	15%	32%	8%	18%		2.4%	2.2%	1.1%	1.0%	1.2%
PVC	1	3	4	8	2		3%	9%	6%	11%	3%	7%		2.4%	2.2%	0.0%	2.0%	0.0%
PET	0	1	3	1	0		0%	3%	5%	1%	0%	2%		0.0%	2.2%	1.1%	1.0%	0.0%
other	1	0	0	0	0		3%	0%	0%	0%	0%	1%		2.4%	0.0%	0.0%	0.0%	0.0%
Number of plastic particles a	29	32	62	71	60		100%	100%	100%	100%	100%	100%						
					254													
period	Nov	Nov	Dec	Dec	Jan	Jan	Feb	Feb	March	March		St Dev						
sampler	Palmex	NILU	Palmex	NILU	Palmex	NILU	Palmex	NILU	Palmex	NILU		Nov	Dec	Jan	Feb	March		
PS	7	6	6	7	15	16	12	10	11	11		0.71	0.71	0.71	1.41	0.00		
PE	4	3	6	6	7	8	9	8	16	15		0.71	0.00	0.71	0.71	0.71		
PP	3	4	2	1	5	4	12	11	2	3		0.71	0.71	0.71	0.71	0.71		
PVC	0	1	1	2	2	2	5	3	1	1		0.71	0.71	0.00	1.41	0.00		
PET	0	0	1	0	1	2	0	1	0	0		0.00	0.71	0.71	0.71	0.00		
other	1	0	0	0	0	0	0	0	0	0		0.71	0.00	0.00	0.00	0.00		
Sum	15	14	16	16	30	32	38	33	30	30		0.71	0.00	1.41	3.54	0.00		

MicroP count per filter area								
	Blank 1	Blank 2	Blank 3	Blank 4	Field blank 1	Field blank 2	Average	StDev
fibers	2	4	3	2	5	4	3	1
films	0	1	1	1	0	1	1	1
particles	7	8	7	6	9	10	8	1
Total	9	13	11	9	14	15	11	

period	Na / 23 [#3]	Mg / 24 [#3]	Al / 27 [#3]	K / 39 [#3]	Ca / 44 [#3]	Ti / 49 [#2]	V / 51 [#2]	Cr / 52 [#2]	Mn / 55 [#2]	Fe / 56 [#2]	Co / 59 [#2]	Ni / 60 [#3]	Cu / 63 [#3]	Zn / 66 [#2]	Ga / 71 [#2]		
Nov	277.2	23.49	0.3968	153.2	176.4	0.029	0.05499	0.03652	0.2749	0.6812	0.003584	0.05078	0.052	1.496	0.005309	As / 75 [#2]	
Dec	312.5	27.4	0.3323	148.1	139.6	0.02417	0.02605	0.02452	0.2697	0.7111	0.003584	0.0358	0.04734	0.5747	0.00637	0.01643	
Jan	414.5	53.48	3.172	151.7	456.9	0.05317	0.0492	0.03039	1.404	1.958	0.007436	0.04037	0.03758	0.164	0.004601	0.01859	
Feb	179.4	12.16	0.3602	137.5	128.9	0.029	0.02392	0.0283	0.1993	0.7021	0.002329	0.07503	0.05439	0.5169	0.007432	0.01095	
March	194.8	48.12	4	152.9	996.7	0.058	0.1056	0.03665	2.999	2.778	0.02768	0.06119	0.06595	0.3345	0.006724	0.016	
																0.02508	
period	Rb / 85 [#3]	Sr / 88 [#3]	Y / 89 [#3]	Zr / 90 [#3]	Nb / 93 [#3]	Mo / 97 [#3]	Cd / 111 [#3]	Sb / 121 [#3]	Cs / 133 [#3]	Ba / 138 [#3]	La / 139 [#3]	Ta / 181 [#3]	W / 184 [#3]	Pb / 208 [#3]	Bi / 209 [#3]	Th / 232 [#3]	U / 238 [#3]
Nov	0.03499	0.2378	0.0003611	0.001091	0.0001199	0.006826	0.004243	0.0154	0.0005934	0.1331	0.0001449	0.000214	0.001179	0.007904	0.0008701	0.0004717	0.0006464
Dec	0.01932	0.1718	0.0002669	0.0005012	0.0001399	0.003754	0.003664	0.008406	0.000541	0.04224	0.0002029	0.0002304	0.0008714	0.01861	0.0008217	0.000511	0.0005838
Jan	0.04183	0.9448	0.004369	0.001887	0.0003997	0.004608	0.0027	0.003757	0.0004538	0.4156	0.002203	0.0002469	0.0008201	0.006069	0.0005801	0.00173	0.0006255
Feb	0.01764	0.09492	0.0002669	0.0006486	0.0001998	0.00529	0.004243	0.008077	0.0007156	0.05211	0.0002898	0.0002304	0.001025	0.02654	0.0008701	0.0002162	0.000563
March	0.04857	2.109	0.00504	0.002978	0.0007995	0.0145	0.005979	0.05955	0.001082	0.8842	0.004941	0.0003786	0.002102	0.0206	0.0005317	0.001553	0.0009592

Appendix 7: Total MP deposition relative to monitoring periods (MP counts without normalisation)

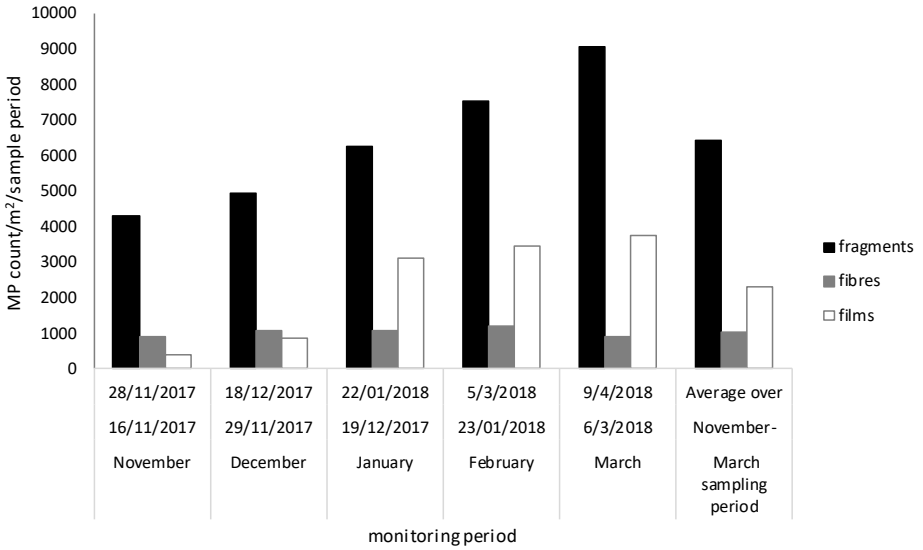

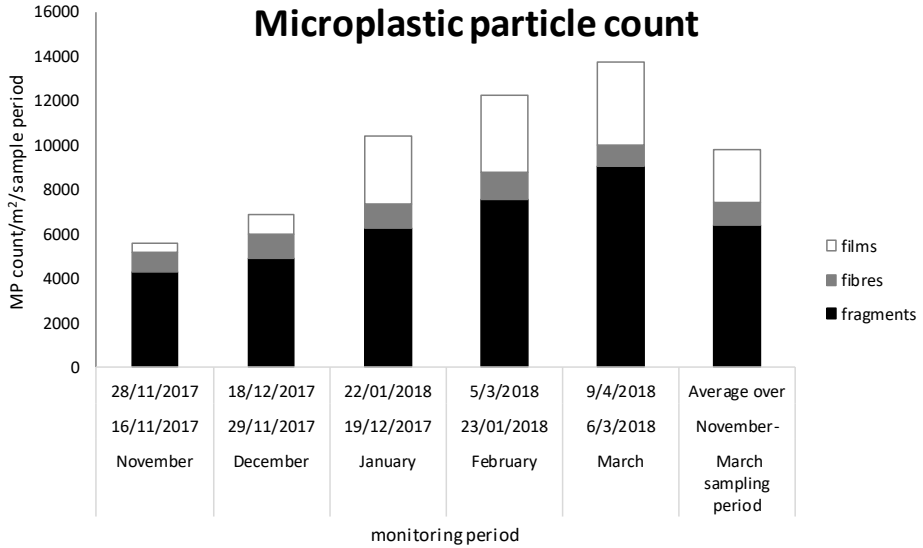

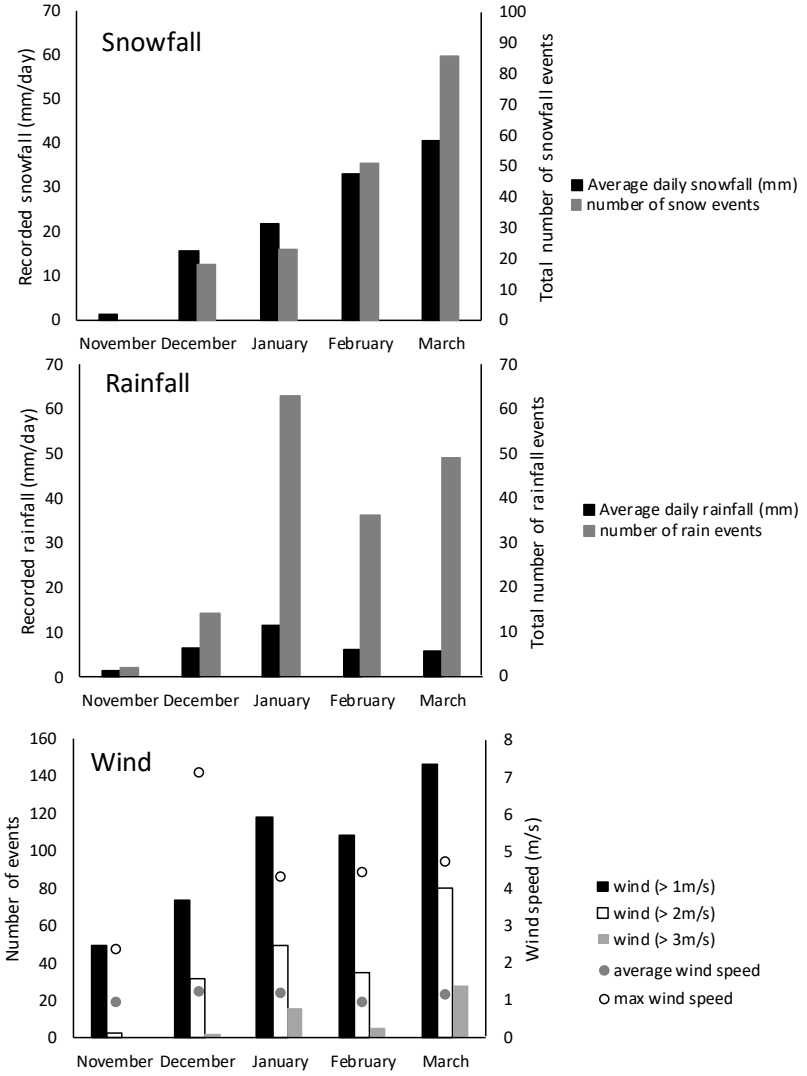

MP deposition for the total monitored periods of November (12 days, 16/11/2017-28/11/2017), December (19 days, 29/11/2017-18/12/20170, January (34 days, 19/12/2017-22/01/2018), February (41 days, 22/01/2018-05/03/2018) and March (34 days, 006/03/2018-09/04/2018).

The non-normalised dataset has been considered and the MP/m^2/monitoring period correlated to actual meteorological conditions specific and recorded for the known monitored durations. Both rainfall and snowfall show moderate to strong significant correlations to MP count in the original (non-normalised) dataset ($r \geq 0.8$, $p < 0.05$). This dataset also presents a strong, positive correlation between the monitoring duration (days) and MP deposition (MP/m^2/monitoring period). The original dataset illustrates a stronger correlation between snowfall (total and number of events) and MP deposition compared to rainfall, suggesting effective snowfall scavenging of atmospheric MP. There is also a trend of increasing daily snow deposition (mm/day) during the total monitoring period (November – March) that corresponds to the (non-normalised) increase in MP deposition trend, while daily rainfall rises to a maximum in January then declines. The frequency of wind speeds >2 m/s and >3 m/s also show positive strong correlations to MP deposition, with higher MP counts for periods recording a greater number of elevated wind speeds.

Appendix 8: Pic du Midi Biggore MP counts

Sample ID	start date	end date	sample volume (m3)	count per µRaman filter	MP particles quartz filter	MP particles per m3	Standard Deviation	monitored hours	days of sampling
A1	23/06/2017	04/07/2017	11799	37	2052	0.17	0.08	171	12
A2	04/07/2017	11/07/2017	7728	81	5130	0.66	0.08	112	8
A3	12/07/2017	18/07/2017	7728	33	1759	0.23	0.09	112	8
A4	19/07/2017	22/07/2017	7728	21	879	0.11	0.07	112	9
A5	01/08/2017	08/08/2017	7728	25	1173	0.15	0.07	112	8
A6	09/08/2017	15/08/2017	7728	19	733	0.09	0.01	112	8
A7	16/08/2017	22/08/2017	7728	19	733	0.09	0.01	112	8
A8	23/08/2017	28/08/2017	6624	46	2638	0.40	0.04	96	7
A9	29/08/2017	06/09/2017	8832	25	1173	0.13	0.07	128	9
A10	06/09/2017	12/09/2017	6624	27	1319	0.20	0.14	96	7
A11	20/09/2017	26/09/2017	7728	25	1173	0.15	0.08	112	8
A12	27/09/2017	03/10/2017	7728	33	1759	0.23	0.18	112	8
A13	03/10/2017	10/10/2017	7728	29	1466	0.19	0.11	112	8
A14	10/10/2017	17/10/2017	7728	46	2638	0.34	0.04	112	8
A15	17/10/2017	23/10/2017	7038	42	2345	0.33	0.13	102	7
blanks				8	average	0.23			
					St. Dev	0.15			
					min	0.09			
					max	0.66			

Pic du Midi Biggore MP polymer type

Sample ID	LD/HDPE	PET	PP	PS	PVC	% fibres	% fragments
A1	49%	17%	7%	15%	13%	45%	55%
A2	49%	10%	6%	17%	17%	46%	54%
A3	46%	23%	4%	15%	12%	54%	46%
A4	46%	13%	9%	15%	16%	25%	75%
A5	46%	10%	13%	21%	11%	37%	63%
A6	54%	5%	9%	12%	20%	27%	73%
A7	51%	8%	13%	14%	15%	35%	65%
A8	42%	8%	13%	18%	18%	31%	69%
A9	31%	29%	8%	18%	14%	53%	47%
A10	37%	14%	8%	23%	17%	47%	53%
A11	53%	12%	11%	14%	10%	46%	54%
A12	31%	19%	12%	20%	18%	59%	41%
A13	34%	12%	12%	26%	16%	49%	51%
A14	45%	12%	10%	20%	13%	25%	75%
A15	42%	14%	17%	16%	10%	45%	55%
Average	44%	14%	10%	18%	15%	42%	58%

Pic du Midi Biggore MP characteristics

length or diameter		fragments, films, foam			fibers		
min (µm)	max (µm)	count	frequency as % of fragments	frequency as % of all particles	count	frequency as % of fibers	frequency as %
5	10	114	39%	22%	0	0%	0%
10	15	117	40%	23%	30	14%	6%
15	20	37	13%	7%	27	13%	5%
20	25	13	5%	3%	13	6%	3%
25	30	7	2%	1%	27	13%	5%
30	35	3	1%	1%	23	11%	5%
35	40	3	1%	1%	8	4%	2%
40	45	0	0%	0%	23	11%	5%
45	50	0	0%	0%	0	0%	0%
50	55	0	0%	0%	10	5%	2%
55	60	0	0%	0%	7	3%	1%
60	65	0	0%	0%	3	1%	1%
65	70	0	0%	0%	13	6%	3%
70	75	0	0%	0%	3	1%	1%

75	80	0	0%	0%	0	0%	0%
80	85	0	0%	0%	0	0%	0%
85	90	0	0%	0%	7	3%	1%
90	95	0	0%	0%	0	0%	0%
95	100	0	0%	0%	0	0%	0%
100	105	0	0%	0%	7	3%	1%
105	110	0	0%	0%	0	0%	0%
110	115	0	0%	0%	3	1%	1%
115	120	0	0%	0%	4	2%	1%
120	125	0	0%	0%	0	0%	0%
125	130	0	0%	0%	3	1%	1%
130	135	0	0%	0%	0	0%	0%
135	140	0	0%	0%	0	0%	0%
140	145	0	0%	0%	0	0%	0%
145	150	0	0%	0%	0	0%	0%
150	155	0	0%	0%	0	0%	0%
155	160	0	0%	0%	0	0%	0%
160	165	0	0%	0%	3	1%	1%

Appendix 9: Meteorological conditions monitored at Pic du Midi Biggore for the sampling period

Sample ID	start date	start time	end date	end time	monitored hours	flow rate (m3/min)	sample volume (m3)
A1	23/06/2017	23:00:00	04/07/2017	10:00:00	171	1.15	11799
A2	04/07/2017	10:00:00	11/07/2017	10:00:00	112	1.15	7728
A3	11/07/2017	10:00:00	18/07/2017	10:00:00	112	1.15	7728
A4 (sampler stopped from 23/7 to 30/7 due to electricity work)	18/07/2017	10:00:00	01/08/2017	10:00:00	112	1.15	7728
A5	01/08/2017	10:00:00	08/08/2017	10:00:00	112	1.15	7728
A6	08/08/2017	10:00:00	15/08/2017	10:00:00	112	1.15	7728
A7	15/08/2017	10:00:00	22/08/2017	10:00:00	112	1.15	7728
A8	22/08/2017	10:00:00	28/08/2017	10:00:00	96	1.15	6624
Oven Blank	28/08/2017						0
A9	29/08/2017	10:00:00	06/09/2017	10:00:00	128	1.15	8832
A10 (stopped on 12/9/2017 for 1 week due to work on telescope)	06/09/2017	10:00:00	12/09/2017	10:00:00	96	1.15	6624
A11	19/09/2017	10:00:00	26/09/2017	10:00:00	112	1.15	7728
A12	26/09/2017	10:00:00	03/10/2017	10:00:00	112	1.15	7728
A13	03/10/2017	10:00:00	10/10/2017	10:00:00	112	1.15	7728
A14	10/10/2017	10:00:00	17/10/2017	10:00:00	112	1.15	7728
A15	17/10/2017	10:00:00	23/10/2017	16:00:00	102	1.15	7038
Field Blank	23/10/2017						

Air Temperature (degrees C)

PM10 (count)

Sample ID	# reported values	Average	Max	Min	StdDev	Var	total	# reported values	Average	Max	Min	StdDev	Var	total
A1	48	6.15	13.94	-1.57	4.59	21.09	295.12	48	907.39	4256.50	81.08	980.44	961260.91	43554.59
A2	119	9.19	15.09	4.09	3.01	9.07	1094.04	119	1297.42	2992.17	142.08	662.41	438786.67	154392.5
A3	119	11.63	15.09	8.14	1.95	3.79	1383.94	75	1726.10	4518.08	429.25	938.21	880235.99	129457.2
A4	120	9.49	16.83	4.52	3.04	9.27	1139.02							
A5	119	11.17	15.32	3.34	2.75	7.55	1329.77							
A6	119	4.07	13.83	-6.45	5.15	26.51	484.52	No data available						
A7	120	10.99	15.54	6.06	2.19	4.79	1319.25							
A8	102	10.89	16.64	7.63	2.13	4.52	1110.56							
A9	136	4.31	10.9	-4.44	3.73	13.92	586.07	27	1428.76	6347.00	305.58	1713.10	2934723.61	38576.5
A10	103	2.20	8.86	-4.74	3.88	15.06	226.27	103	495.15	1246.92	21.42	314.18	98706.99	51000.29
A11	119	3.43	7.55	-2.56	2.48	6.13	408.26	119	1102.14	11175.75	165.50	1161.75	1349665.94	131154.7
A12	119	5.07	9.25	1.34	1.79	3.22	602.78	59	1336.58	5091.50	63.14	1152.40	1328018.97	78857.97
A13	119	5.39	12.99	0.88	2.75	7.54	640.85	114	790.10	7288.50	156.33	1077.83	1161719.19	90071.26
A14	119	5.93	9.96	3.28	1.65	2.71	705.59	70	1861.59	14622.92	31.60	2583.25	6673160.54	130311.1
A15	109	0.90	7.36	-5.72	3.42	11.67	98.55	109	978.32	9649.17	0.00	1611.76	2597757.65	106636.6

Sample ID	Wind Direction (degrees) # reported values	Average	Max	Min	StdDev	Var	total	Wind Velocity (m/s) # reported values	Average	Max	Min	StdDev	Var	total	Rainfall mm
A1	48	129	319	9	105	10960	6215	48	6.29	12.23	1.42	3.11	9.67	302.13	79.8
A2	119	193	273	61	49	2353	22946	119	8.56	19.37	1.95	3.77	14.25	1018.42	23.2
A3	119	208	311	10	79	6318	24717	119	8.18	16.00	2.27	4.18	17.44	974.01	ND
A4	120	210	251	184	10	104	25211	120	10.23	18.76	4.70	3.21	10.28	1227.42	ND
A5	119	217	282	175	19	361	25821	119	9.02	17.04	4.14	2.67	7.11	1072.92	20.1
A6	119	197	325	41	65	4236	23398	119	7.12	14.76	2.42	2.58	6.66	847.12	12.8

A7	120	197	304	39	72	5211	23694	120	7.17	13.00	2.31	2.66	7.08	860.15	ND
A8	102	203	276	64	33	1119	20710	102	8.69	16.61	2.40	3.62	13.08	886.10	23.4
A9	136	216	318	40	50	2518	29439	136	7.59	15.60	3.18	2.90	8.39	1031.72	37.0
A10	103	206	311	7	81	6487	21204	103	9.98	21.70	2.40	4.74	22.45	1028.04	27.8
A11	119	201	301	24	71	4974	23929	119	6.45	14.24	2.39	2.71	7.37	767.99	ND
A12	119	197	301	18	82	6657	23441	119	7.56	13.95	2.36	2.84	8.04	900.20	32.8
A13	119	108	305	6	77	5881	12873	119	5.04	11.08	1.75	2.05	4.20	599.69	ND
A14	119	202	294	47	66	4391	24086	119	6.62	13.87	2.09	3.36	11.29	787.75	ND
A15	109	202	347	40	60	3602	22039	109	8.01	18.63	2.15	3.39	11.47	872.85	21.9

Appendix 10: Air mass trajectories elevation per sample collected from Pic du Midi Biggore. Trajectories are presented in metres above mean sea level.

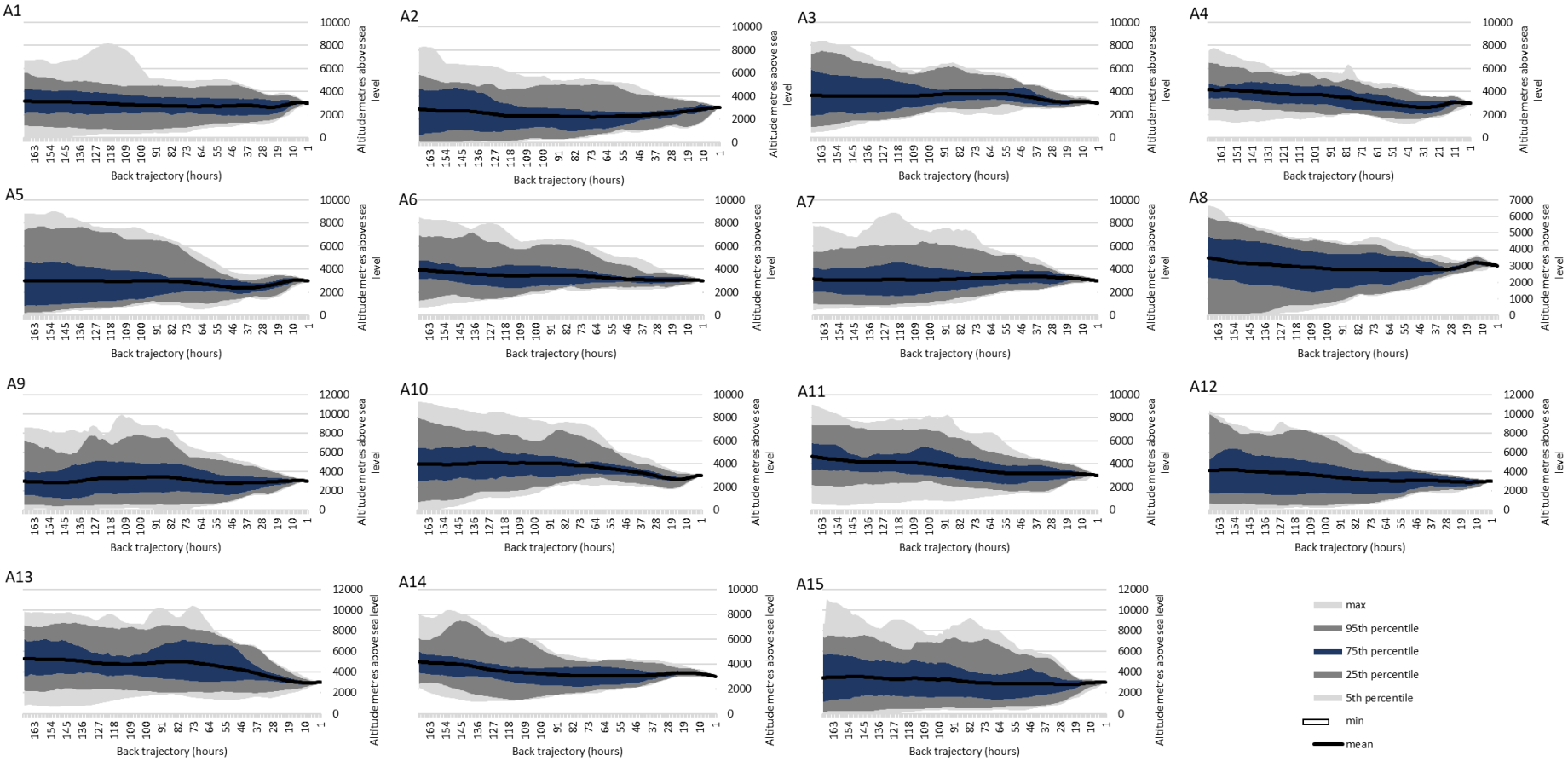

Appendix 11: Air mass trajectories per sample collected from Pic du Midi Biggore. Trajectories are presented in metres above surface level.

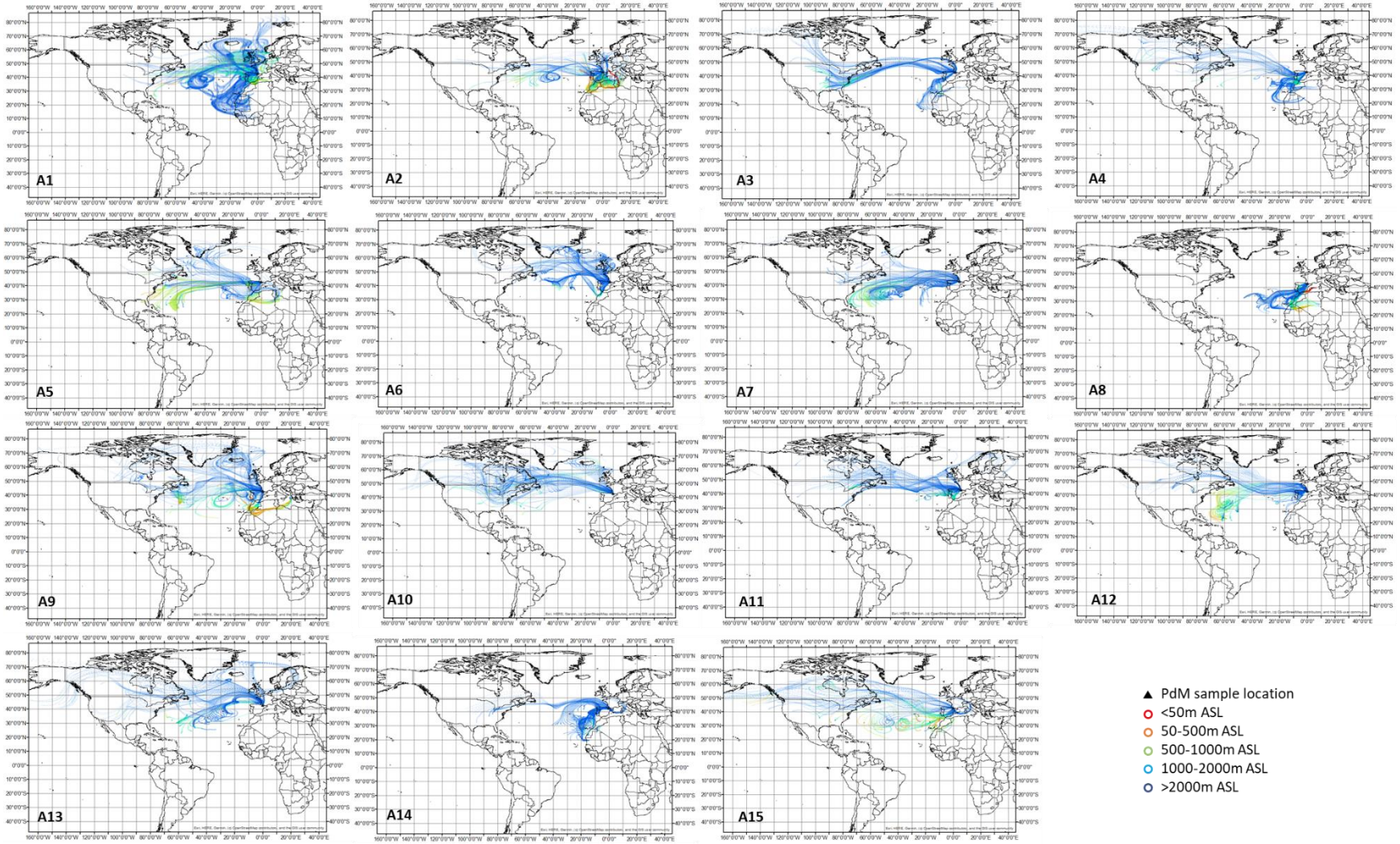

Air mass back trajectories frequency plots for hourly back trajectories extending 169 hours backwards for samples with MP<0.3MP/m^3. This plot illustrated the extensive area over which the air mass reaching Pic du Midi Biggore has travelled.

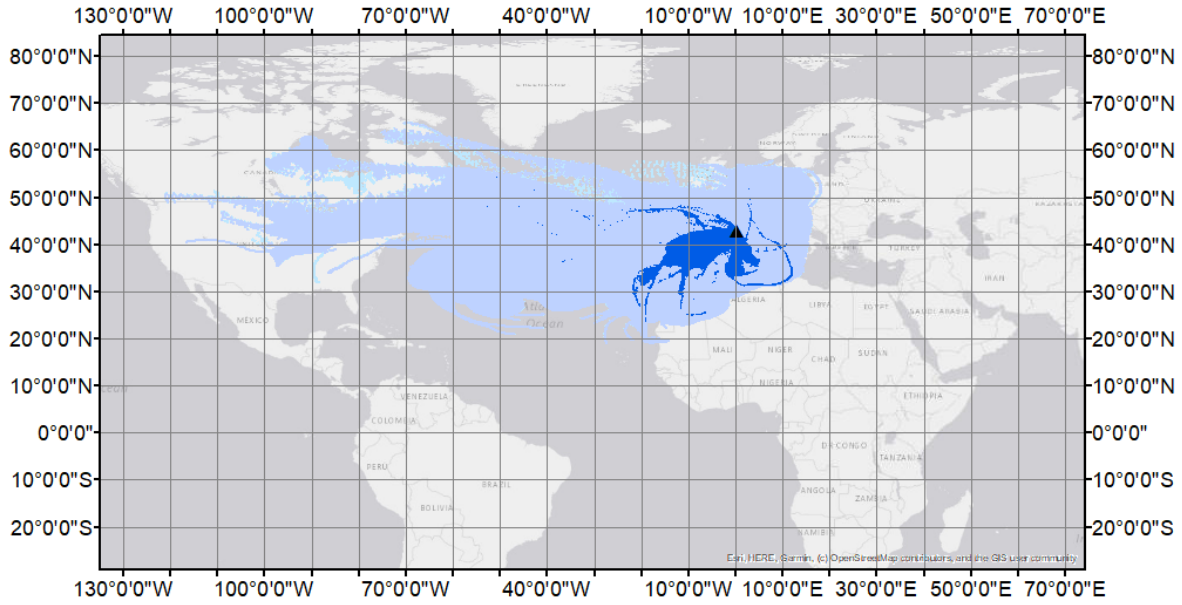

Air mass back trajectories frequency plots for hourly back trajectories extending 74 hours backwards for samples with MP<0.3MP/m^3. This plot illustrated the potential area where the air mass was close to mean sea level.

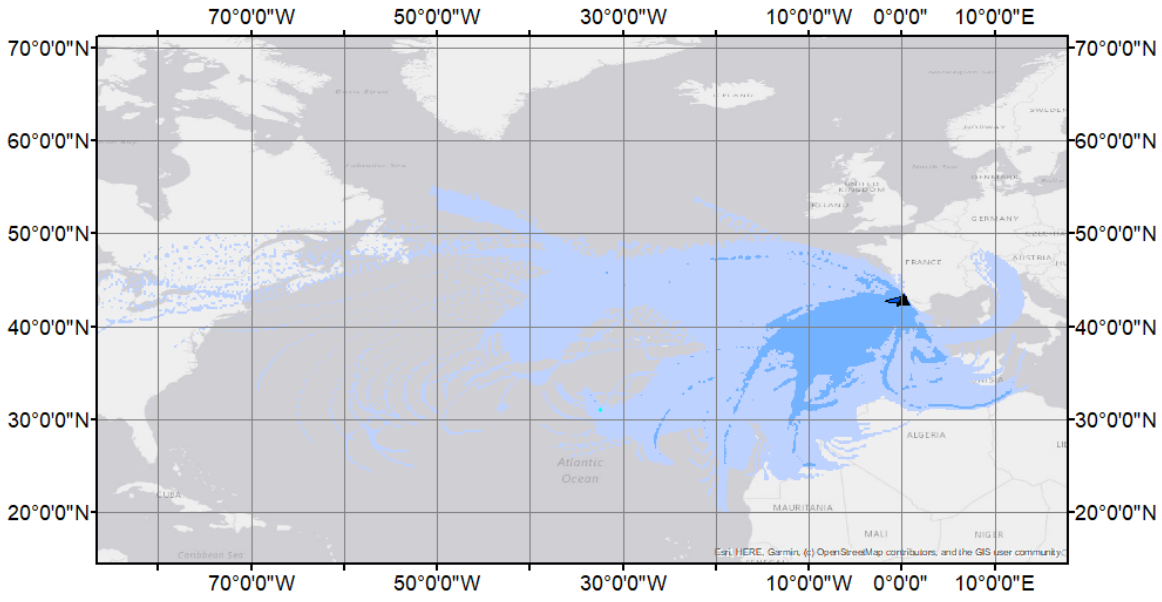

Air mass back trajectories frequency plots for hourly back trajectories extending 169 hours backwards for samples with MP>0.3MP/m^3. This plot illustrated the extensive area over which the air mass reaching Pic du Midi Biggore has travelled.

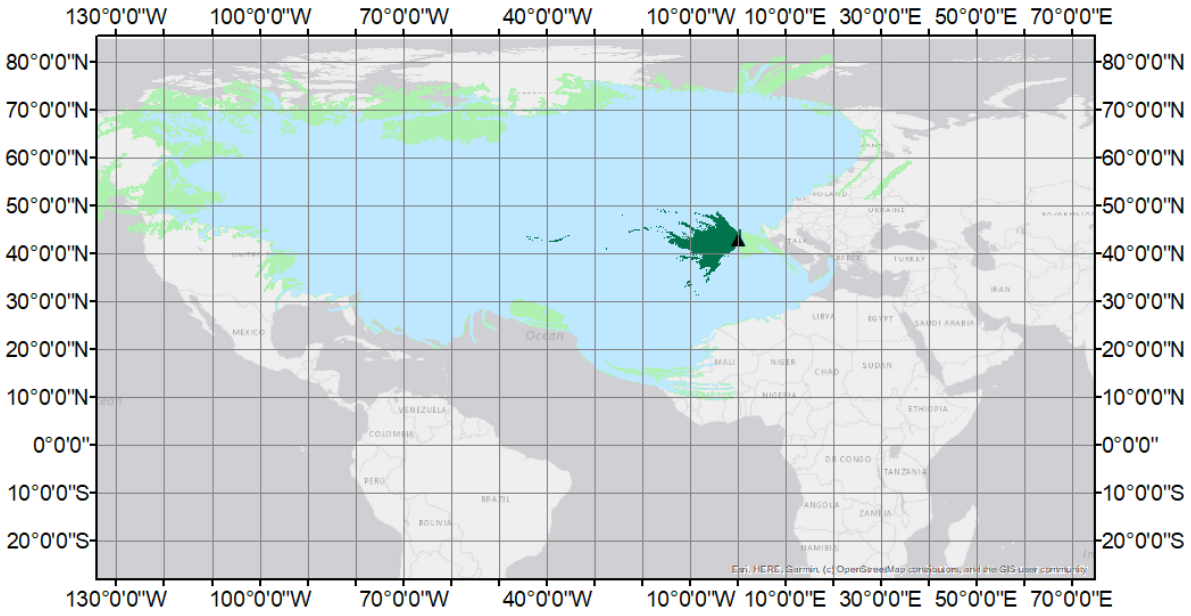

Air mass back trajectories frequency plots for hourly back trajectories extending 113 hours backwards for samples with MP>0.3MP/m^3. This plot illustrated the potential area where the air mass was close to mean sea level.

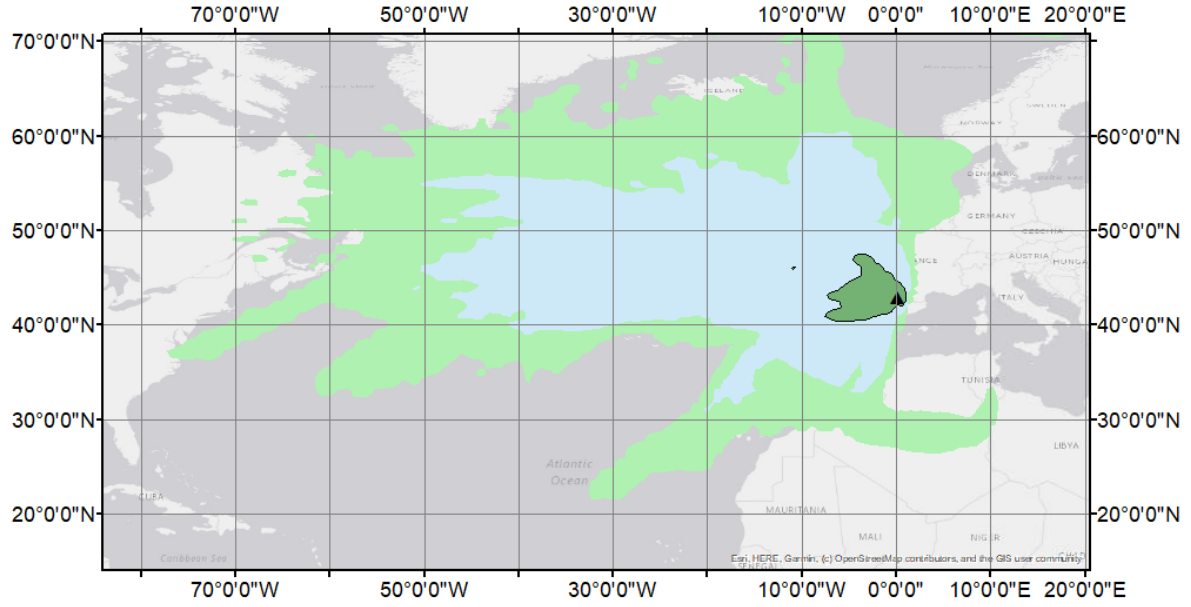

Appendix 12: HYSPLIT air mas back trajectories: tabulated data for MP>0.3 MP/m^3 and MP>0.3 MP/m^3 at elevation above mean sea level and above the HYSPLIT modelled ground level

HYSPLIT air mass trajectory elevation
Trajectory elevations above mean sea level (m AMSL)
for trajectory runs relative to samples with **MP < 0.3 MP/m^3**

Time step	min	5th percentile	25th percentile	mean	75th percentile	95th percentile	max	Mode
1	2998	2999	2999	2999.087	2999	3000	3000	2999
2	2923	2969.5	3004	3020.113	3038	3067	3108	3021
3	2777	2929.5	2998	3031.972	3069	3123.25	3188	3029
4	2656	2881.5	2989	3039.304	3094	3173	3274	3061
5	2561	2840	2977	3044.268	3114	3224	3375	3108
6	2487	2778.5	2957.75	3046.27	3135.25	3272	3480	3117
7	2413	2702.75	2935.75	3046.837	3160	3322.25	3555	3063
8	2359	2647.25	2913.75	3046.874	3182	3360.25	3606	3134
9	2308	2585	2898	3045.408	3201.25	3405.25	3658	3170
10	2238	2532.25	2880.75	3040.376	3219.25	3431.25	3701	3092
11	2109	2470.75	2849	3033.477	3230	3471.25	3738	3075
12	2000	2407.5	2823.75	3025.242	3244	3499.25	3780	3214
13	1933	2330.5	2799.75	3015.565	3251	3520.5	3842	3016
14	1876	2267.75	2773	3006.882	3263	3540.25	3935	3176
15	1811	2220	2737.25	2999.253	3273	3558.25	4015	3215
16	1696	2163.75	2713	2992.231	3287	3576.5	4070	3225
17	1586	2105.75	2682	2984.605	3301	3589.25	4122	2987
18	1545	2061.75	2673	2977.017	3322	3614.75	4178	2878
19	1504	2006.5	2652	2969.994	3337	3636.25	4247	3191
20	1418	1948.75	2635	2964.461	3351	3667.25	4332	3166
21	1364	1916.5	2627.25	2961.896	3363.25	3707.75	4416	3180
22	1325	1868	2611.75	2961.254	3384.75	3746.75	4509	3487
23	1269	1850.25	2601.75	2961.572	3407.25	3800.25	4590	2818
24	1180	1834.75	2594	2964.334	3422	3857.5	4676	3260
25	1101	1810.25	2580	2968.735	3428.25	3910.5	4782	3150
26	1023	1780.5	2572	2974.458	3442.25	3964.25	4890	3581
27	951	1749	2553.75	2979.827	3451	4021.5	5005	3324
28	901	1725.5	2553	2985.638	3456.5	4077.75	5114	3009
29	864	1706.75	2545.5	2992.713	3480	4139.75	5222	3095
30	829	1692.5	2544.75	3000.948	3500	4184.25	5338	3580
31	801	1674	2538.25	3009.586	3519.25	4232	5482	3517
32	767	1670.5	2530.75	3018.661	3542	4272.75	5642	3098
33	733	1657.75	2535	3028.034	3546	4321.5	5803	2799
34	703	1641	2530.25	3037.867	3564.25	4382.25	5973	3075
35	671	1609	2526.75	3047.154	3580.25	4435	6148	2807
36	641	1585.75	2521	3056.393	3585.5	4496	6309	2939

37	607	1573.75	2514.5	3065.13	3608.25	4536	6451	2964
38	584	1547.5	2503.75	3073.287	3627.5	4562.25	6551	2952
39	576	1526.75	2490.75	3080.964	3640.5	4598.25	6613	2950
40	569	1513.5	2488.75	3088.039	3658.25	4641.25	6652	3069
41	561	1510	2477.75	3094.378	3669.25	4721.5	6666	2947
42	550	1496.25	2460	3100.575	3680.25	4767.25	6659	2878
43	520	1471.5	2440.75	3106.237	3701.5	4791.25	6659	2028
44	491	1453.25	2447.5	3113.096	3730.5	4806.25	6669	3312
45	463	1420	2445	3118.902	3741.5	4830.5	6694	3275
46	432	1394	2436.5	3124.974	3756.5	4842	6709	3870
47	399	1380.5	2427.75	3129.971	3767.25	4913	6756	3003
48	362	1357.5	2415.75	3135.542	3774	4974.5	6888	2982
49	336	1348.5	2414.5	3141.334	3782	5020.5	6987	2951
50	313	1335.5	2407.5	3147.048	3784.25	5063.5	7072	2466
51	297	1316	2404	3153.78	3798.25	5098.25	7152	2945
52	290	1299.25	2394	3161.072	3807.5	5170	7216	3297
53	290	1298	2384.75	3167.881	3809.75	5230.75	7273	2317
54	296	1289	2379.75	3176.118	3804	5269.5	7342	2998
55	301	1284.5	2378	3184.44	3823	5297.75	7427	3248
56	310	1267	2381.5	3192.817	3837.5	5316	7517	3018
57	324	1253.25	2381	3201.973	3848.75	5323.75	7646	3424
58	340	1234.5	2374.75	3211.027	3873.5	5404.5	7757	2997
59	362	1210.25	2371	3220.755	3888	5451.5	7859	3331
60	380	1197.75	2376.5	3230.106	3904	5516	7934	2254
61	396	1181.5	2377.75	3241.179	3917	5572.75	8004	3683
62	384	1178.25	2381.5	3251.134	3922.25	5611.25	8274	2957
63	367	1175	2375	3261.666	3937.5	5644.75	8492	3250
64	353	1178.75	2378	3271.773	3955	5691.25	8698	2991
65	337	1168	2381.75	3281.947	3974.5	5741	8888	3198
66	323	1163	2380.5	3291.519	3978.5	5795.75	9066	2993
67	310	1136.75	2381.75	3300.509	3985	5848.5	9313	1968
68	284	1128	2376.25	3310.554	3993.25	5894.5	9594	2896
69	212	1131.25	2364.75	3320.123	4011.25	5905.5	9858	3307
70	154	1136.25	2362.5	3329.649	4002.25	5984.25	10092	3686
71	114	1135	2361.75	3338.654	4010.5	6003.75	10243	3176
72	83	1145.75	2351	3348.299	4016	6082.5	10354	3620
73	60	1152.75	2357.75	3357.695	4026	6165.75	10421	3218
74	44	1148	2354.75	3367.167	4044.25	6228.75	10384	2263
75	35	1147.25	2369.75	3378.35	4059.5	6310.75	10285	3867
76	42	1140.75	2387.75	3388.439	4087.75	6383	10118	2747
77	36	1131.25	2394	3399.765	4098.75	6414.25	9945	3564
78	34	1138	2400.75	3409.202	4120.75	6439	9757	2416
79	33	1138.75	2402	3418.674	4138	6470	9576	2514
80	34	1142	2401.5	3427.616	4165.25	6500.5	9388	3279
81	38	1148	2400.75	3435.069	4186.5	6532.75	9317	2603
82	46	1152.75	2414	3442.746	4193.75	6572	9315	3231

83	57	1137.25	2400.75	3449.034	4216.25	6584.5	9303	2060
84	70	1115	2391.5	3456.44	4253	6606	9452	3668
85	88	1100.75	2379.5	3462.479	4276.5	6634	9594	3643
86	98	1083	2379	3467.833	4286.5	6631.5	9737	3405
87	102	1074.75	2398.75	3472.563	4288.75	6609	9858	3023
88	103	1068.75	2402.25	3477.382	4301	6638.75	9970	3193
89	107	1062.75	2399	3481.594	4336.25	6657.25	10061	3268
90	112	1051.25	2393.25	3486.351	4340.25	6637	10137	4658
91	118	1054.25	2398.75	3488.929	4353.25	6655.25	10182	2888
92	124	1055.5	2413.75	3492.057	4372.75	6628.25	10204	2663
93	132	1074.5	2428.5	3495.47	4374.75	6631.25	10192	3216
94	146	1069	2432	3497.281	4378.5	6588	10136	2268
95	155	1078.25	2428	3499.834	4399.5	6596.75	10053	3488
96	164	1093.25	2423	3500.334	4405.75	6643	9910	2476
97	174	1093.25	2404.75	3501.793	4423.25	6603	9729	4221
98	185	1082.5	2390.25	3501.797	4449	6632.75	9509	3879
99	192	1068	2366	3501.907	4466.25	6619	9254	3228
100	201	1064.75	2351.5	3503.52	4480.5	6577	8978	4951
101	210	1057.25	2341.5	3503.248	4495.75	6560.25	9009	2759
102	215	1047.5	2330.5	3505.408	4507.5	6581.75	9114	4055
103	219	1025	2314.5	3506.576	4517.25	6592.25	9174	3019
104	220	1010.25	2300.75	3508.622	4520.25	6652.5	9320	2760
105	222	982.5	2301	3511.324	4522.75	6648.75	9506	3177
106	221	964.75	2295.75	3513.034	4537.25	6656.5	9633	2240
107	221	954.75	2296.75	3515.102	4550.25	6636	9694	2379
108	216	941.5	2291.5	3517.175	4563.25	6619	9608	3035
109	208	934.25	2294.75	3519.447	4575.75	6605.25	9662	3739
110	196	939	2292.25	3521.162	4585.5	6607.5	9811	2589
111	180	958	2303	3523.757	4597.25	6598.5	9897	2343
112	161	944.5	2300.25	3527.839	4596.5	6652	9872	4473
113	151	950.75	2313.25	3530.825	4597.5	6706.5	9768	4784
114	149	956	2316	3532.238	4608.25	6742.5	9579	2357
115	152	965.25	2327.75	3535.259	4602.25	6729.5	9291	2374
116	155	985	2330.5	3539.431	4608.25	6763.25	9276	3666
117	161	965.75	2317.25	3542.71	4623	6775.5	9401	2399
118	153	957.25	2315.5	3547.362	4621	6796	9513	2465
119	137	954.75	2313.75	3550.921	4636.25	6821.25	9563	722
120	115	953.25	2307.5	3556.818	4635.75	6818.25	9571	3155
121	95	946	2307.5	3561.359	4648.5	6814.75	9572	3437
122	82	946	2310.5	3565.117	4634.25	6896.25	9545	2704
123	70	939	2316.25	3568.935	4644.75	6951.25	9475	3242
124	60	937.75	2292.75	3571.946	4638	7010	9397	3560
125	53	930	2270	3574.297	4651.25	6963.25	9293	3278
126	48	917.75	2244.5	3577.706	4681.25	6956.75	9192	4055
127	43	913.75	2238.5	3582.025	4718.75	6998.5	9190	4873
128	34	907.25	2224.5	3585.708	4706.75	6996.5	9046	4270

129	31	895	2226.5	3588.928	4711.25	6958.75	9057	1374
130	30	889	2225.25	3595.178	4702.75	6947.75	9140	3178
131	30	896	2210.75	3600.499	4715	6967	9218	3497
132	31	896.5	2221.5	3607.096	4718	7005.75	9282	6393
133	31	853	2230.5	3609.766	4739.25	7009.5	9346	3747
134	36	846.5	2227.5	3613.447	4732.25	7005	9395	3930
135	36	832.75	2234.5	3616.307	4715.5	7029.25	9435	3220
136	35	818.5	2245.5	3618.725	4693	7066.75	9469	1535
137	34	805.5	2268	3623.734	4698.5	7082.5	9491	4128
138	32	796.5	2267.75	3627.634	4722	7128	9504	4224
139	29	797.75	2270.75	3631.936	4714.75	7159.5	9516	4445
140	32	798.25	2263.5	3636.197	4708.25	7200.25	9608	4088
141	28	795.5	2248.5	3640.784	4713.5	7187	9682	3926
142	27	795.25	2239.5	3644.49	4715	7232	9742	3002
143	23	780.5	2239	3649.074	4731.25	7222.5	9778	3441
144	20	756.75	2245.75	3652.728	4727.75	7261.5	9791	2323
145	18	752.5	2230.75	3657.7	4722.75	7260	9769	3268
146	17	758.75	2248.5	3661.25	4734.75	7290.75	9709	1494
147	18	754	2243.5	3667.435	4741	7307.25	9694	3604
148	18	751.25	2243.75	3673.177	4751	7342.75	9706	4275
149	18	764.75	2240.5	3679.543	4767.5	7339.75	9725	5344
150	18	768	2241.75	3684.513	4771.25	7322.5	9748	3823
151	18	758.75	2252	3690.681	4785.75	7346	9695	4006
152	16	753.25	2239	3696.888	4796.25	7382.75	9680	3478
153	12	752.5	2244.5	3703.189	4815.5	7408.75	9898	2681
154	9	744	2227.25	3709.094	4824.25	7429.5	10050	1715
155	5	729.5	2234.75	3716.16	4822	7405.5	10125	4028
156	7	709.75	2241	3720.825	4852.5	7462.75	10141	3501
157	6	710.5	2239.75	3725.911	4873.5	7451.5	10251	3858
158	4	705	2226.75	3730.936	4887	7426.75	10389	4092
159	2	690	2213.25	3733.963	4886.75	7453.75	10560	1057
160	3	697.25	2218	3740.27	4903.75	7459.25	10638	3742
161	6	693.75	2211	3745.625	4929.25	7467.5	10654	5240
162	-3	688.25	2222.5	3749.331	4921.5	7480.75	10661	4246
163	0	697	2222.75	3752.054	4929	7487.75	10679	2128
164	4	700	2255.75	3756.534	4939	7481.5	10727	3015
165	5	705	2246	3760.132	4939.75	7477	10846	1297
166	5	701.75	2265.75	3766.282	4964	7480.75	10963	3434
167	10	703.25	2271.5	3772.397	4993.5	7474.75	11068	5007
168	7	693.5	2291.5	3771.399	5007.5	7478	10238	2532
169	6	704	2297	3777.631	5018.5	7491.7	10344	3605

Trajectory elevations above mean sea level (m AMSL)

for trajectory runs relative to samples with **MP > 0.3 MP/m^3**

Time step	min	5th percentile	25th percentile	mean	75th percentile	95th percentile	max	mode
1	2998	2999	2999	2999.059	2999	3000	3000	2999
2	2934	2962.7	3013	3026.162	3045	3065	3104	3049
3	2800	2884.4	3019.5	3041.394	3082	3122.6	3188	3095
4	2653	2811.8	3020	3044.236	3104	3161	3271	3051
5	2505	2725.1	3009	3045.491	3123.5	3201.3	3343	3097
6	2360	2677.2	2997	3045.912	3148	3242.6	3406	3143
7	2217	2638.2	2986.5	3047.217	3175	3290	3460	3100
8	2074	2573.6	2978.5	3050.905	3200.5	3338	3496	3112
9	1937	2498.7	2965.5	3054.989	3220	3387.9	3523	3132
10	1805	2436.1	2945.5	3057.537	3245.5	3436.3	3556	3041
11	1705	2384.9	2932	3057.794	3271	3477.2	3607	3216
12	1619	2347.1	2922.5	3053.503	3282	3488.5	3641	3140
13	1543	2291.9	2903	3046.156	3288	3513	3663	2922
14	1477	2231.3	2893.5	3035.602	3289.5	3541.3	3651	3141
15	1417	2123.3	2887.5	3022.566	3289.5	3547	3681	3222
16	1363	2021.2	2859.5	3006.926	3282.5	3550.6	3722	3180
17	1315	1965.4	2812	2989.217	3287.5	3550.6	3766	3052
18	1267	1912.9	2754	2973.779	3272.5	3560.3	3814	3083
19	1223	1825	2740	2959.714	3259	3583.6	3864	3026
20	1194	1781.8	2720	2945.04	3242.5	3619.9	3906	3218
21	1191	1732.2	2713	2930.307	3232.5	3662	3940	2964
22	1221	1665	2693.5	2914.964	3225.5	3694	3987	2728
23	1236	1629	2671	2899.368	3218.5	3755.2	4161	3301
24	1180	1592.9	2638	2884.52	3210.5	3807.5	4325	2796
25	1101	1568.8	2629	2871.229	3202	3849.2	4483	2972
26	1023	1541.4	2613.5	2859.261	3198.5	3886.7	4651	2966
27	951	1508.2	2605.5	2848.676	3199	3955.7	4796	2963
28	901	1476.6	2589.5	2839.251	3186	4009.7	4934	3009
29	864	1463.5	2578.5	2831.779	3171.5	4050.9	5080	2746
30	829	1434	2560	2825.848	3162	4083.6	5227	2806
31	801	1401.9	2550.5	2821.194	3150	4123.4	5378	2712
32	767	1355.1	2518	2817.004	3136	4155.5	5507	2924
33	733	1319.3	2504	2812.434	3122.5	4188.5	5613	2717
34	703	1291.6	2484.5	2807.444	3102	4247.8	5690	2609
35	671	1273.4	2437.5	2801.707	3092	4260.7	5738	2630
36	641	1246.1	2393	2796.038	3109.5	4333.9	5771	3057
37	607	1227.6	2358.5	2790.693	3142	4426.5	5799	3127
38	584	1192.7	2304	2785.309	3181.5	4514.8	5826	2638
39	576	1159.7	2285	2779.973	3212	4606.6	5861	2630
40	569	1130.3	2263.5	2773.798	3233.5	4677.7	5882	2617
41	561	1112.8	2242	2766.971	3259.5	4741.4	5894	2624
42	550	1088.8	2228.5	2760.785	3268.5	4777.3	5967	2614

43	520	1070.7	2205	2756.042	3300.5	4744.3	6059	2057
44	491	1057.1	2173.5	2752.678	3327	4682.3	6140	2488
45	463	1054.7	2138.5	2749.56	3356.5	4663.5	6204	2533
46	432	1052.7	2121.5	2746.057	3379.5	4711.8	6223	2477
47	399	1050.7	2096.5	2741.84	3415	4742.6	6220	1715
48	362	1057.7	2090	2737.973	3449.5	4727.5	6233	2343
49	336	1074.7	2075.5	2734.366	3468.5	4718.8	6208	2023
50	313	1091.8	2058.5	2730.947	3491	4736.3	6174	2993
51	297	1104.8	2034.5	2727.556	3509	4818.3	6163	2094
52	290	1120.5	2020	2724.594	3530	4798.9	6225	2588
53	290	1126.7	1999	2722.002	3551.5	4818.6	6338	2318
54	296	1120.3	1976.5	2720.116	3565	4762.3	6524	1345
55	301	1115.3	1958	2718.585	3581	4757	6713	2291
56	310	1097.1	1939.5	2717.844	3589.5	4769.1	6880	2291
57	324	1083.1	1920	2717.922	3597.5	4838.7	6976	2427
58	340	1054.4	1903.5	2718.019	3605	4886.5	7041	2398
59	362	1013.8	1889.5	2717.846	3613.5	4955.3	7166	2019
60	380	974.5	1884.5	2717.076	3612	5041.3	7301	2367
61	396	945.8	1874.5	2716.322	3618	5072	7465	2189
62	407	929	1871.5	2716.059	3619	5078.4	7632	2182
63	415	921.5	1849	2715.811	3626	5071.8	7763	3695
64	417	893.4	1821	2715.617	3642	5068.9	7890	966
65	414	865.2	1802.5	2715.8	3652	5067.7	8024	5223
66	417	848.2	1791	2715.935	3665	5062.3	8055	4038
67	405	818.9	1783.5	2716.703	3686	5059.3	8068	2079
68	385	777.7	1760.5	2717.455	3708.5	5058	8068	3731
69	352	757.8	1744.5	2717.867	3690	5057.6	8081	2890
70	322	727.2	1720.5	2718.364	3684.5	5057.3	8116	2056
71	325	711.6	1717	2719.095	3692	5055.4	8150	3811
72	310	705	1701.5	2720.406	3685.5	5054.1	8169	3852
73	297	705.4	1695.5	2721.964	3678	5037.1	8216	2346
74	290	694	1706	2723.893	3678	5014.3	8290	1887
75	299	686.4	1720	2726.078	3674	5022.9	8414	2673
76	298	668	1732.5	2728.76	3664	5039.6	8554	2985
77	300	633.7	1735.5	2731.996	3655	5036.6	8680	2146
78	314	613.3	1742	2736.261	3660.5	5093	8814	4919
79	315	601.1	1731.5	2741.171	3646.5	5084.2	8969	2970
80	305	594.8	1742	2746.703	3653.5	5077.3	9132	3460
81	295	577.2	1735	2752.253	3647	5079.3	9251	868
82	286	561.6	1749	2757.531	3658	5069.6	9233	799
83	276	546.6	1758	2762.541	3677	5085.4	9140	1988
84	268	534.4	1761	2767.842	3670.5	5157	9033	1691
85	262	526.4	1747	2773.52	3669.5	5208.8	8923	1711
86	258	524	1749	2779.634	3672	5271.2	8812	2011
87	254	524.3	1745	2786.857	3684.5	5293.4	8701	3723
88	244	532.1	1731	2794.562	3685.5	5335	8619	1880

89	244	546.2	1725.5	2801.968	3677.5	5355.3	8579	1646
90	240	547.2	1716.5	2809.263	3664.5	5360.4	8551	2767
91	239	556.1	1700	2816.065	3665	5420.1	8577	3517
92	233	559.2	1694.5	2822.076	3663.5	5372.1	8551	1171
93	228	549.6	1682	2827.196	3666	5337.1	8421	2844
94	220	550.9	1669	2831.606	3680	5382	8161	4760
95	212	553.3	1661	2835.305	3676.5	5341.5	8173	3587
96	220	537.2	1651	2838.181	3669.5	5271.7	8136	3700
97	229	532.3	1638	2839.48	3672	5326.1	8050	3550
98	228	523.5	1638	2840.501	3662	5304.8	7675	2597
99	237	518	1621.5	2842.032	3656	5310	7751	3415
100	251	520	1605	2844.754	3647.5	5316.3	7721	1347
101	263	503.6	1587	2848.442	3655	5350.1	7548	2662
102	249	492.8	1580	2852.825	3665.5	5454.4	7532	3607
103	240	472.7	1583	2857.817	3680	5535.6	7589	3509
104	234	461.1	1579.5	2863.219	3704.5	5484.8	7608	3291
105	235	475.4	1566	2869.204	3729	5542.5	7620	1213
106	226	461.4	1567	2875.32	3745	5630.9	7608	4781
107	212	444	1565.5	2881.015	3773.5	5660.8	7595	4499
108	192	427.4	1554.5	2885.945	3788	5678.9	7702	3688
109	164	423.9	1546	2890.663	3789	5714.9	7801	4524
110	136	413.8	1550	2896.011	3788	5726.1	7900	2704
111	99	404.3	1544	2901.943	3782.5	5780.9	8007	4257
112	66	390.3	1554	2907.817	3787	5824.1	8124	3530
113	31	372.5	1552.5	2913.657	3814	5829.1	8230	4611
114	0	356	1555.5	2918.796	3836.5	5864.3	8339	3566
115	0	346.7	1555	2922.657	3859	5850.8	8464	3446
116	0	320.6	1553.5	2925.171	3882	5773.1	8594	1038
117	0	303.1	1571	2926.474	3949	5741.6	8697	2399
118	0	313	1584.5	2928.021	3988	5691.9	8777	3583
119	0	320.2	1585.5	2930.074	4015.5	5656.9	8846	1159
120	0	289.2	1604.5	2932.697	4032.5	5632.9	8927	1023
121	0	261.1	1623	2936.684	4038	5623.7	9019	4597
122	0	247.4	1642	2941.939	4036.5	5600.2	9084	4556
123	0	243.3	1655.5	2948.48	4040	5597	9127	898
124	0	229.7	1666	2956.684	4047	5580.7	9126	3254
125	0	277	1667.5	2967.063	4055.5	5563.1	9119	4441
126	0	283.4	1683	2979.497	4083.5	5545	9112	4041
127	1	253	1675.5	2993.615	4093.5	5564.6	9095	3559
128	6	219.5	1674	3008.276	4096	5603.2	9046	1695
129	31	227.2	1660.5	3023.714	4106.5	5641.3	8947	83
130	30	228.7	1655	3039.855	4145	5661.6	8814	3733
131	30	192.1	1660	3056.497	4189	5730.7	8670	4177
132	31	165.7	1662	3073.215	4247	5806.4	8541	3958
133	31	188.6	1679.5	3088.869	4298.5	5862.8	8394	416
134	36	168.3	1661	3104.24	4340	5907.1	8264	3172

135	30	148	1698.5	3119.752	4372.5	5955.6	8230	95
136	33	148.5	1733.5	3135.535	4379.5	5963.7	8250	4195
137	32	150.6	1726	3150.787	4421.5	5977.4	8298	4483
138	31	151.5	1754	3165.634	4477.5	5983.5	8359	4517
139	29	148.9	1768	3180.046	4477	5917.7	8432	132
140	25	148.9	1758.5	3193.983	4481.5	5967.9	8515	4355
141	21	152.1	1780	3206.844	4507.5	6019.9	8596	4308
142	14	149.7	1805	3218.653	4529.5	6053.8	8663	4310
143	0	143.1	1838	3230.072	4577.5	6020.6	8776	4317
144	0	134.8	1846	3240.958	4609	5970.8	8958	4285
145	0	125.5	1879	3251.4	4642.5	5925.1	9136	23
146	0	116.1	1879.5	3260.766	4659.5	5907.6	9249	0
147	0	104.1	1832	3269.076	4681	5995.5	9329	4503
148	0	95	1830.5	3276.312	4684.5	6071.5	9444	0
149	0	87.7	1870.5	3282.259	4693	6000.8	9543	4383
150	0	80.4	1851.5	3287.347	4697	5895.3	9552	0
151	0	79.1	1842.5	3291.724	4683.5	5943.1	9536	0
152	0	72.3	1833	3297.038	4677	6162.7	9662	2756
153	0	74.4	1843.5	3302.413	4635.5	6397	9898	0
154	0	68.7	1831	3308.038	4658	6434.8	10050	0
155	0	69.2	1820	3313.124	4676.5	6371.2	10125	0
156	0	57.8	1826	3318.596	4675.5	6331.1	10141	0
157	0	60.4	1840.5	3325.501	4656.5	6189	10251	0
158	0	61.7	1846	3334.253	4654	6134	10389	0
159	0	72.1	1856.5	3343.672	4665.5	6114.2	10560	0
160	0	83	1867.5	3354.084	4668	6053.9	10638	0
161	0	91.2	1871.5	3364.524	4684.5	6032.2	10654	0
162	0	99.4	1884.5	3375	4691	6036.8	10661	0
163	0	111.7	1881	3385.013	4702.5	6057.2	10679	0
164	0	128	1846	3395.398	4711	6054.6	10727	0
165	0	143.2	1835	3406.566	4714	6048.1	10846	0
166	0	163.5	1875	3418.76	4772	6056.7	10963	0
167	0	172.7	1908.5	3430.754	4807.5	6082.8	11068	0
168	0	183.2	1903.75	3426.266	4825	6103.2	8698	0
169	0	185.5	1912	3437.947	4845	6134.05	8692	0

Trajectory elevations above modelled ground level (above surface level, m ASL)

for trajectory runs relative to samples with **MP < 0.3 MP/m^3**

Time step	min	5th percentile	25th percentile	mean	75th percentile	95th percentile	max
1							
2			Pyrenean mountain range				
3							
4	2055	2300.5	2403	2478.304	2554	2677	2840
5	1961	2257.5	2389	2491.601	2588	2751	2959

6	1875	2217.5	2376	2504.395	2625	2816	3074
7	1799	2174.5	2368	2516.893	2656.5	2882	3180
8	1724	2138	2355.5	2528.24	2692	2955	3286
9	1647	2102.5	2344.5	2538.998	2720	3016	3385
10	1568	2078	2335	2549.313	2753.5	3081	3470
11	1499	2039	2318.5	2558.939	2784	3142.5	3544
12	1446	2003	2301.5	2568.074	2817.5	3201	3634
13	1406	1968	2292.5	2577.45	2855	3257	3737
14	1376	1929.5	2282	2586.496	2886.5	3309.5	3824
15	1341	1894.5	2271.5	2596.561	2920.5	3346	3894
16	1277	1862	2264	2606.448	2954	3392.5	3954
17	1215	1829	2261	2616.466	2987	3449	4011
18	1157	1794.5	2260	2627.539	3013.5	3500	4075
19	1101	1769.5	2251	2639.4	3045.5	3544.5	4148
20	1049	1745	2244.5	2652.1	3084.5	3590.5	4220
21	997	1717.5	2247.5	2665.179	3114.5	3627	4297
22	947	1699.5	2246.5	2679.824	3146	3669.5	4374
23	902	1677.5	2252.5	2694.86	3187.5	3727	4450
24	863	1651.5	2255	2711.785	3213	3784.5	4552
25	829	1612	2256.5	2728.566	3245.5	3825.5	4660
26	802	1580.5	2269.5	2746.544	3273	3876.5	4765
27	783	1569	2281.5	2765.099	3294	3930.5	4878
28	772	1542	2295	2782.575	3322.5	3986.5	5004
29	769	1513.5	2303	2801.834	3359.5	4034	5150
30	768	1474.5	2310	2819.528	3385.5	4092.5	5312
31	763	1447	2315	2837.914	3411	4141	5476
32	752	1435.5	2313.5	2854.833	3421.5	4186.5	5639
33	739	1425.5	2325	2872.227	3443.5	4229	5803
34	723	1406	2344.5	2889.7	3458.5	4285.5	5966
35	673	1374	2351.5	2905.908	3471.5	4340	6123
36	625	1344	2362	2922.156	3481	4405.5	6256
37	583	1310	2381	2937.624	3510.5	4466	6374
38	547	1292.5	2390	2952.305	3532	4507	6482
39	503	1281.5	2402	2966.555	3537.5	4527.5	6569
40	459	1254.5	2408.5	2979.316	3555	4569	6632
41	412	1266.5	2398.5	2991.636	3576.5	4584.5	6683
42	368	1292	2397	3003.612	3593.5	4615.5	6716
43	330	1319	2391.5	3014.796	3597.5	4652.5	6741
44	299	1325	2395	3026.174	3588.5	4691.5	6756
45	272	1348	2405.5	3036.227	3615.5	4744	6762
46	250	1356.5	2411	3046.868	3614.5	4805	6761
47	230	1348.5	2405	3057.037	3636.5	4873	6758
48	212	1325.5	2388	3067.471	3652	4937.5	6804
49	196	1316	2395.5	3077.528	3678	4979.5	6937
50	181	1312.5	2398	3088.147	3692	5024	7053
51	168	1297.5	2404.5	3098.871	3700	5069.5	7158

52	156	1289.5	2397	3109.842	3723	5137	7253
53	147	1293.5	2400.5	3121.27	3736.5	5177	7338
54	138	1268.5	2392	3132.631	3767.5	5265.5	7456
55	130	1245	2385.5	3144.333	3785	5293	7560
56	121	1233	2399.5	3156.791	3796	5295	7638
57	113	1217	2389	3167.522	3793.5	5334	7699
58	105	1205	2392	3179.376	3816	5394.5	7753
59	99	1189	2379	3191.334	3846	5440.5	7809
60	92	1154	2390	3203.437	3869.5	5496	7866
61	87	1126.5	2390	3215.403	3894.5	5537	7932
62	82	1119.5	2389	3227.954	3909.5	5588.5	7989
63	77	1106	2391	3239.924	3928	5616	8041
64	73	1093	2401	3250.389	3940.5	5658.5	8086
65	68	1076.5	2403	3262.508	3971	5674	8127
66	62	1064.5	2403	3273.512	3985	5722.5	8166
67	56	1062.5	2390.5	3283.725	4000	5778	8206
68	51	1064.5	2383.5	3294.096	4020	5826.5	8234
69	47	1056.5	2382.5	3304.566	4018	5876	8256
70	44	1050.5	2393.5	3314.535	4005	5941.5	8270
71	42	1058.5	2391	3324.281	4024.5	6002	8276
72	40	1069	2397.5	3334.523	4023.5	6079.5	8278
73	38	1065	2406	3343.267	4043	6111.5	8278
74	38	1049.5	2417	3353.062	4061	6204	8268
75	37	1019	2435	3363.022	4069	6224.5	8254
76	35	1004.5	2439.5	3371.935	4097.5	6233.5	8248
77	34	992	2435.5	3379.664	4129	6267.5	8290
78	34	1008.5	2441.5	3388.659	4155.5	6299	8331
79	33	999	2447.5	3396.74	4170.5	6340	8364
80	32	991.5	2450	3404.213	4192.5	6382	8404
81	32	985	2442.5	3410.558	4214	6421	8444
82	31	979	2435.5	3417.356	4249	6460.5	8478
83	29	982	2436	3422.486	4245	6469	8511
84	27	987.5	2434.5	3427.168	4246.5	6475.5	8569
85	25	971	2429	3431.927	4257.5	6514.5	8616
86	22	953.5	2419.5	3434.028	4271	6504.5	8658
87	19	960	2415.5	3438.513	4290.5	6554.5	8685
88	17	998	2425.5	3440.292	4296	6548	8682
89	15	1009.5	2421.5	3442.166	4302.5	6545	8653
90	13	996	2423.5	3444.058	4312	6545.5	8661
91	12	987	2407	3445.352	4311.5	6542.5	8665
92	12	973	2418.5	3446.699	4320	6459.5	8666
93	11	951	2439	3448.826	4320.5	6465.5	8664
94	9	932	2428	3448.219	4328	6448	8670
95	6	915.5	2417.5	3448.706	4332	6429.5	8664
96	2	899.5	2405	3448.277	4338	6429	8659
97	0	884	2383.5	3448.928	4355	6427	8652

98	0	872.5	2370	3448.793	4384	6437	8644
99	0	875.5	2347.5	3447.519	4395.5	6456	8661
100	0	875	2328	3447.523	4411.5	6454	8690
101	0	864	2306.5	3446.617	4430.5	6470	8715
102	0	859	2285	3445.967	4442	6493.5	8719
103	0	859	2273	3445.353	4469	6497.5	8713
104	0	861	2264.5	3444.867	4476.5	6534	8687
105	0	871	2262	3444.958	4508	6557	8655
106	0	882.5	2262	3445.19	4517	6531.5	8617
107	0	896.5	2262.5	3446.798	4535.5	6574	8590
108	0	876.5	2260	3444.976	4532	6608.5	8561
109	0	875	2260	3447.166	4532.5	6583	8521
110	0	881.5	2258	3447.506	4530	6590.5	8518
111	0	875	2254	3449.773	4538.5	6606.5	8587
112	0	870	2255.5	3449.852	4539.5	6623	8677
113	0	858	2242	3449.803	4540.5	6611.5	8771
114	0	839	2241	3450.521	4556	6581.5	8866
115	0	840	2232.5	3450.524	4552.5	6585	8934
116	0	817	2204	3451.048	4555	6589	8983
117	0	819	2187.5	3451.835	4570	6580	9012
118	0	828	2175	3452.85	4572.5	6598.5	9020
119	0	836	2161.5	3453.036	4583	6624.5	9034
120	0	831.5	2162	3453.781	4590.5	6594.5	9042
121	0	825	2157.5	3453.014	4591.5	6541.5	9034
122	0	826	2153.5	3453.434	4587	6525.5	9025
123	0	834.5	2151.5	3450.67	4590.5	6480.5	9029
124	0	829	2115	3447.754	4591.5	6455	9020
125	2	870	2100.5	3448.793	4591	6424	8995
126	4	866.5	2076	3446.434	4603.5	6441	8952
127	7	863.5	2073	3447.903	4592.5	6430.5	8867
128	11	861	2053.5	3448.116	4591.5	6468	8744
129	16	857	2051	3448.581	4606	6530.5	8722
130	21	846	2046	3447.129	4604	6515.5	8737
131	25	832	2059	3448.564	4599.5	6536.5	8754
132	27	828	2053.5	3450.325	4595	6564	8804
133	27	817	2055.5	3450.692	4607	6585	8922
134	24	801	2058.5	3451.355	4610.5	6587	9033
135	20	789.5	2051	3451.907	4609	6605	9136
136	15	785.5	2049	3452.646	4584	6613.5	9236
137	11	771	2043	3454	4583	6647	9338
138	7	756.5	2033	3455.922	4575	6669	9422
139	2	748	2027.5	3456.166	4567	6725	9501
140	0	734	2023.5	3460.704	4563.5	6769	9587
141	0	734.5	2011	3464.551	4573.5	6803	9667
142	0	740	2015	3466.282	4578	6850.5	9730
143	0	745	2021	3469.151	4593.5	6832.5	9774

144	0	740	2012	3470.997	4596.5	6927	9794
145	0	730.5	1998.5	3474.078	4577	7003	9790
146	0	728	2001	3477.949	4575	6997	9759
147	0	721	2007	3480.57	4574	6950.5	9675
148	0	718	2004.5	3481.746	4594	6934	9583
149	0	716	2005	3484.158	4599.5	6992.5	9559
150	0	710.5	1997	3486.029	4610	7024.5	9517
151	2	702	2014.5	3488.86	4613	7082	9554
152	3	689.5	2029	3493.277	4619	7064	9601
153	4	681	2037.5	3497.817	4629	7097	9637
154	6	670.5	2022.5	3501.911	4619.5	7118.5	9652
155	7	659.5	2026.5	3504.487	4626	7159	9658
156	7	656.5	2017	3510.818	4645	7168.5	9654
157	8	640	2015	3512.432	4674	7177	9637
158	8	644.5	2033	3517.817	4712	7186.5	9633
159	8	644	2031.5	3519.65	4690	7222	9644
160	8	646.5	2041	3523.27	4692	7230	9671
161	8	646	2046	3526.619	4698.5	7248.5	9712
162	8	651.5	2038.5	3529.826	4719.5	7247.5	9752
163	8	656	2047.5	3531.893	4717	7255.5	9788
164	8	657	2046.5	3534.592	4736.5	7280.5	9794
165	7	655	2026	3537.157	4740.5	7285	9777
166	7	661.5	2019	3540.441	4744.5	7301	9738
167	6	656.5	2011	3542.324	4742	7333	9755
168	6	658	2029	3546.548	4740.5	7351.5	9787
169	5	658.5	2025	3549.154	4734.5	7331.5	9848

Trajectory elevations above modelled ground level (above surface level, m ASL)

for trajectory runs relative to samples with **MP > 0.3 MP/m^3**

Time step	min	5th percentile	25th percentile	mean	75th percentile	95th percentile	max
1							
2				Pyrenean mountain range			
3							
4	2110	2224.05	2389	2442.325	2507	2572	2721
5	2013	2163.35	2378.25	2445.641	2534.25	2610.35	2788
6	1921	2100.95	2365	2448.996	2557	2652.9	2849
7	1835	2043.55	2354.5	2452.12	2584.25	2692.25	2903
8	1754	2002.25	2345.5	2454.363	2605	2736.9	2950
9	1677	1956.6	2339	2456.903	2620.75	2768.5	2993
10	1607	1900.35	2331	2458.761	2643	2806.25	3032
11	1540	1868.6	2328	2460.574	2657.5	2844	3067
12	1477	1825	2312.5	2462.722	2676.5	2883.45	3099
13	1421	1775.8	2298.25	2464.36	2691	2940	3127
14	1370	1746.1	2287.75	2465.732	2703	3011.35	3164

15	1322	1720.85	2272.5	2467.578	2710	3083.7	3236
16	1272	1685.1	2259	2470.709	2718.5	3138.05	3314
17	1218	1657.15	2240.5	2473.232	2731.25	3184.45	3402
18	1164	1627.25	2218.5	2475.984	2746	3227.6	3493
19	1115	1581.8	2203	2478.783	2756.25	3272.15	3586
20	1070	1542.65	2191.75	2481.966	2759.75	3324.05	3680
21	1017	1497.75	2171.75	2485.527	2767.25	3383	3827
22	964	1448.75	2169.25	2489.215	2788.5	3436.9	4008
23	914	1419.7	2150.5	2493.155	2807.5	3499.7	4181
24	871	1383.6	2139.5	2497.059	2819.75	3550.4	4336
25	836	1348.55	2136	2501.252	2831.25	3587.8	4478
26	808	1300.55	2125.5	2505.59	2858.25	3612.25	4618
27	787	1275.75	2103.25	2509.982	2887.25	3637.35	4774
28	772	1231.4	2076.75	2514.821	2913.75	3663.9	4938
29	755	1206.1	2058.5	2520.406	2936.25	3701.75	5096
30	722	1176.5	2034	2525.762	2953.25	3795.6	5246
31	657	1145.05	2007	2532.832	2966	3875.35	5379
32	595	1117.5	1977.25	2538.169	2986.5	3960.85	5496
33	539	1081.4	1951.5	2545.632	3010.5	4077.75	5595
34	489	1062.5	1943.5	2551.163	3032	4166.45	5671
35	445	1026.75	1931.5	2556.352	3071.25	4236.8	5727
36	406	1005.55	1922.75	2562.05	3104	4332.75	5766
37	372	991.75	1913.5	2566.669	3126.25	4406.6	5794
38	344	949.25	1909.5	2571.582	3143	4477.35	5821
39	320	895	1895	2575.379	3175	4561.7	5854
40	302	885.1	1888	2576.136	3204.5	4630.05	5890
41	288	849.15	1868	2579.687	3215.5	4706.75	5932
42	278	823.75	1853.25	2578.686	3237	4754.55	5956
43	268	786.95	1835.25	2578.29	3265	4769.35	5980
44	257	756.55	1828.75	2579.937	3297	4748.75	6007
45	244	748.15	1811.25	2576.936	3326.5	4757.7	6045
46	231	741.3	1803.75	2579.548	3364.25	4765.15	6104
47	217	721.25	1784.75	2575.253	3382	4814.8	6163
48	204	702.3	1787.75	2577.538	3409.25	4839.35	6211
49	190	687.2	1774.25	2576.026	3425	4840.8	6249
50	177	677.3	1759.75	2573.806	3437.5	4897.85	6277
51	165	672.15	1758.5	2567.836	3460.25	4887.3	6315
52	153	676.15	1761.5	2567.749	3481.25	4892.05	6360
53	141	670.8	1750.5	2564.889	3500.25	4898.25	6440
54	131	647.1	1731.5	2561.907	3523.5	4921.9	6533
55	121	626.8	1709.25	2559.974	3537.25	4946.3	6632
56	112	614.55	1696.5	2562.71	3548.75	4943.65	6711
57	104	608.5	1683.25	2562.913	3560.75	4971.45	6787
58	97	604.15	1674.25	2563.367	3573.25	4973.5	6875
59	90	596.4	1657.5	2564.041	3583	4956.35	6994
60	84	585.65	1639.5	2564.973	3591.75	5017.95	7095

61	79	566.3	1628.75	2563.498	3599.75	5038.55	7177
62	75	548.6	1612.75	2564.322	3597.75	5037.65	7250
63	71	531.6	1592.75	2566.59	3602	5035.45	7330
64	68	517.75	1570	2567.457	3606.5	5029.6	7408
65	66	481.4	1534	2565.817	3604	5020.95	7475
66	63	478.2	1524.25	2572.451	3618.25	5012.6	7571
67	59	460.35	1513.5	2572.298	3626	5006.7	7656
68	55	447.95	1490.75	2578.321	3657	5002.15	7741
69	52	438.55	1469.5	2579.816	3664	4997.6	7826
70	50	425.25	1460.75	2581.37	3679.5	4992.4	7904
71	47	414.35	1480.5	2580.935	3676.5	4980.9	7991
72	45	403.65	1495.25	2577.826	3666.5	4965.6	8099
73	43	411.2	1507.5	2584.314	3664.5	4947.05	8213
74	41	401.2	1509.5	2582.874	3651.5	4950	8320
75	39	411.25	1525	2595.246	3664.5	4964.05	8409
76	37	419.15	1538.75	2591.661	3658.25	4969.65	8509
77	36	430.55	1541.75	2598.635	3654.25	5015.35	8637
78	34	443.1	1547.75	2606.851	3670	5011.35	8760
79	33	440.95	1544.75	2601.858	3666.5	5003.15	8840
80	32	450.1	1545.75	2609.145	3664	4996.35	8857
81	30	455.4	1545.75	2620.561	3673.5	5017.35	8837
82	29	452.1	1533	2618.089	3675	5039.2	8828
83	28	454.1	1515.25	2623.806	3679.5	5068.1	8796
84	27	449	1504	2636.548	3688	5140.4	8717
85	26	445.1	1485.5	2640.674	3685.25	5174.05	8585
86	25	445.55	1454.25	2640.626	3684	5176.95	8416
87	25	448.55	1440.25	2642.13	3688.25	5181.3	8236
88	24	448.55	1436.5	2652.952	3698.25	5184.3	8046
89	24	430.6	1414.75	2658.153	3689	5185	7853
90	24	394.45	1399.75	2652.728	3676.75	5164.65	7660
91	24	357.2	1385.25	2663.844	3679.25	5171.65	7453
92	24	325.95	1402.75	2664.28	3684.75	5082.55	7355
93	24	320.55	1393.5	2668.513	3682.25	5076.45	7358
94	24	305.75	1370.75	2670.556	3684.75	5128.75	7373
95	25	290.85	1345.25	2670.291	3681.75	4953.5	7373
96	25	274.1	1327.25	2662.005	3673.75	4902.5	7367
97	26	260.55	1328	2668.825	3667.75	4935	7357
98	27	240.1	1310.75	2662.244	3654.5	4951.4	7339
99	28	228.2	1303.5	2663.307	3637.75	4907.8	7310
100	30	232.45	1293.5	2671.83	3646.25	4910.35	7274
101	31	225	1277	2672.403	3652	4899.15	7236
102	32	216.75	1251.25	2675.83	3642.5	4900.45	7195
103	33	211.4	1232.5	2680.816	3662	4930.9	7186
104	34	209.3	1231.25	2685.628	3675	4957.65	7302
105	35	200.6	1232	2689.656	3708.25	4968.1	7418
106	35	186.95	1213.5	2688.435	3728.5	4921.65	7519

107	35	173.85	1214.5	2692.157	3758.25	4880.95	7617
108	35	165.2	1228	2701.929	3779.5	4940.7	7722
109	34	157.65	1217	2705.519	3792	4935.85	7848
110	34	129.75	1195.75	2698.03	3802.5	4906.25	7974
111	30	126.85	1223.75	2708.417	3794	4953.1	8076
112	20	113.6	1231.5	2713.921	3814.75	4995.4	8168
113	14	102.25	1246.25	2717.058	3808.5	5040.9	8263
114	5	95.25	1265.75	2722.228	3821.5	5059.45	8364
115	0	88.25	1268.25	2730.898	3826.75	5093.05	8476
116	0	84.7	1271.75	2735.628	3837.25	5126.45	8579
117	0	83.6	1276.75	2745.266	3860.25	5169	8670
118	0	85.6	1278.25	2754.902	3895.5	5185.05	8762
119	0	73.2	1259	2752.701	3931	5216	8858
120	0	70.2	1268.5	2760.571	3969.75	5258.65	8947
121	0	80.75	1292.75	2777.609	3969.25	5294.6	9031
122	0	66.1	1293	2775.905	3968	5309.9	9088
123	0	61.7	1303.75	2783.85	3998	5347.25	9104
124	0	68.45	1324.25	2801.215	4020	5410.45	9119
125	0	57.65	1332.75	2804.006	4049.25	5418.3	9136
126	0	40.4	1345.75	2811.408	4026.25	5429.95	9156
127	0	37.65	1343	2821.954	4007.75	5467.45	9164
128	0	36	1350.25	2833.14	4008.5	5512.4	9115
129	0	36	1330.75	2845.003	3992.25	5543.15	9018
130	0	36	1361.5	2857.832	4012.25	5579.8	8894
131	0	31.85	1364	2871.399	4031.75	5577.5	8757
132	0	28.65	1361.25	2885.266	4057.5	5585.4	8608
133	0	26	1356.5	2899.203	4080.5	5581.15	8467
134	0	25.55	1367.75	2913.081	4115.25	5602.45	8382
135	0	22.3	1381	2926.731	4145.25	5627.85	8337
136	0	21.3	1405.25	2939.927	4193.25	5664.25	8327
137	0	21.65	1413.25	2952.607	4239.5	5738.6	8349
138	0	21.55	1417	2964.57	4264	5724.3	8398
139	0	21.75	1436.5	2975.827	4270.25	5703.05	8471
140	0	21.4	1432	2986.292	4300.5	5722.25	8541
141	0	21.5	1455	2996.33	4325.25	5688.2	8605
142	0	21.6	1467.75	3006.288	4356.5	5715.45	8679
143	0	21.15	1450.75	3016.206	4363.75	5717.35	8762
144	0	20.15	1444.75	3026.039	4392.5	5730.95	8841
145	0	19.6	1450.25	3035.699	4448.25	5712.9	8911
146	0	20.5	1460.75	3045.412	4462.75	5693.8	8987
147	0	21.3	1478	3055.127	4471.25	5674.15	9086
148	0	22.55	1486.5	3064.463	4501.5	5654	9166
149	0	21.55	1505.25	3073.233	4519.5	5659.8	9207
150	0	16.95	1513.25	3081.531	4524	5644.6	9284
151	0	15.85	1517.5	3089.162	4543.75	5633.1	9358
152	0	14.65	1523.5	3095.812	4556.5	5633.7	9351

153	0	14	1529.5	3102.187	4554.5	5657.8	9290
154	0	14	1539.75	3108.702	4557.75	5716.65	9232
155	0	15.55	1544.75	3116.252	4558.5	5800.1	9251
156	0	16	1537.5	3124.386	4560.5	5870.55	9301
157	0	15.1	1539	3132.784	4581.5	5853.25	9320
158	0	16.1	1548.25	3141.059	4591.25	5812.25	9283
159	0	15.1	1559	3149.397	4592.25	5758.4	9233
160	0	17.1	1554.5	3157.804	4604	5760.65	9199
161	0	17.55	1541	3166.859	4615.75	5739.65	9263
162	0	18	1535.5	3176.595	4633.5	5755.6	9350
163	0	19.55	1527.5	3187.09	4642.75	5782.7	9446
164	0	22.1	1525	3197.961	4663	5815.2	9557
165	0	26.1	1524	3208.52	4673.25	5833.95	9632
166	0	31.1	1526	3218.548	4677.75	5838.9	9686
167	0	36	1532.75	3228.489	4701.5	5875.45	9742
168	0	40.75	1542	3238.306	4725.5	5906.45	9830
169	0	37.85	1525	3216.116	4713.25	5918.5	7939

Appendix 13: Ocean to atmosphere field sampling dataset

Cumulative MP counts relative to wind direction and sampler (MP/m3)					
	LD/HDPE	PET	PP	PS	PVC
cloud onshore	0.10913073	0.014035	0.0047924	0.019836596	0.018952143
air onshore	7.18852591	1.351289	0.8758347	1.351172037	1.078217792
cloud offshore	0.3464462	0.029456	0.0237375	0.023537431	0.032353507

start date	stop date	hours	ID	Air Mass Sampler particles per m3	Atmospheric Water Vap particles per m3	wind
05.10.2018	06.10.2018	22	A1	1.62	0.09	v light onshore breeze
06.10.2018	07.10.2018	24	A2	1.47	0.05	20kts, windy, onshore
07.10.2018	08.10.2018	24	A3	4.38	0.04	20kts, windy, onshore
08.10.2018	09.10.2018	24	A4	4.38	0.04	onshore moderate breeze
09.10.2018	10.10.2018	26.5	A5	11.38	0.04	offshore, light wind
10.10.2018	11.10.2018	22.5	A6	4.06	0.07	offshore, light wind
11.10.2018	12.10.2018	24	A7	8.88	0.03	offshore, light wind
12.10.2018	13.10.2018	23	A8	13.96	0.02	offshore, light to no wind
13.10.2018	13.10.2018	2.5	A8a	19.38	0.19	calm, sea fog

Blanks				
cloudcatcher blanks			5	MP/filter
aerosol pump blanks			7	MP/filter
surf zone sea water blanks			8	MP/filter
laboratory blank			3	MP/filter

Cloudcatcher summary				
ID	MP Count	MP per filter	m3 air sampled	particles per m3
A1	77	606	6584	0.092
A2	51	393	7183	0.055
A3	41	300	7183	0.042
A4	40	293	7183	0.041
A5	40	297	7931	0.037
A6	60	465	6734	0.069
A7	29	202	7183	0.028
A8	21	133	6883	0.019
A8a	21	139	748	0.185
	mean		6401	0.063
	StDev		2154	0.051
	field filters (n)			9
	µRaman samples (n)			27

Aerosol summary				
ID	MP Count	MP per filter	m3 air sampled	particles per m3
A1	11	29	18	1.62
A2	11	29	20	1.47
A3	18	87	20	4.38
A4	18	87	20	4.38
A5	37	254	22	11.38
A6	16	71	17	4.06
A7	29	179	20	8.88
A8	40	270	19	13.96
A8a	12	37	2	19.38
	mean		18	7.72
	StDev		6	6.14
	field filters (n)			9
	µRaman samples (n)			27

Surf zone sea water summary*								
ID	MP Count	MP per filter	L water sampled	particles per m3	tide height	tide state		
A1	5	34	5	6842	3.987	1 hr before high tide		
A2	6	39	5	7737	3.76	2 hrs before high tide		
A3	3	18	3	5860	2.724	3 hrs before high tide		
A4	4	22	3	7246	2.266	4 hrs before high tide		
A5	4	26	3	8632	1.838	2 hrs after low tide		
A6	2	10	3	3251	1.684	1 hr after low tide		
A7	3	18	3	6023	1.692	low tide		
A8	6	43	5	8506	1.915	1 hr before low tide		
* it is noted that these samples are collected in the surf rather than sea water and therefore an area of high tubulence and mixing resulting in elevated MP counts potentially due to the linear boundary and mixing effect of the beach and the potential collection of MP from beach sand.								
	mean			6762.06	2.48			
	StDev			1749.19	0.93			
	field filters (n)				8			
	µRaman samples (n)				24			

Appendix 14: Field site for the pilot study, illustrated on ESRI basemaps (used in ArcGIS) provided under the ESRI Master agreement and General Grant of Right and Restrictions basemap datasets

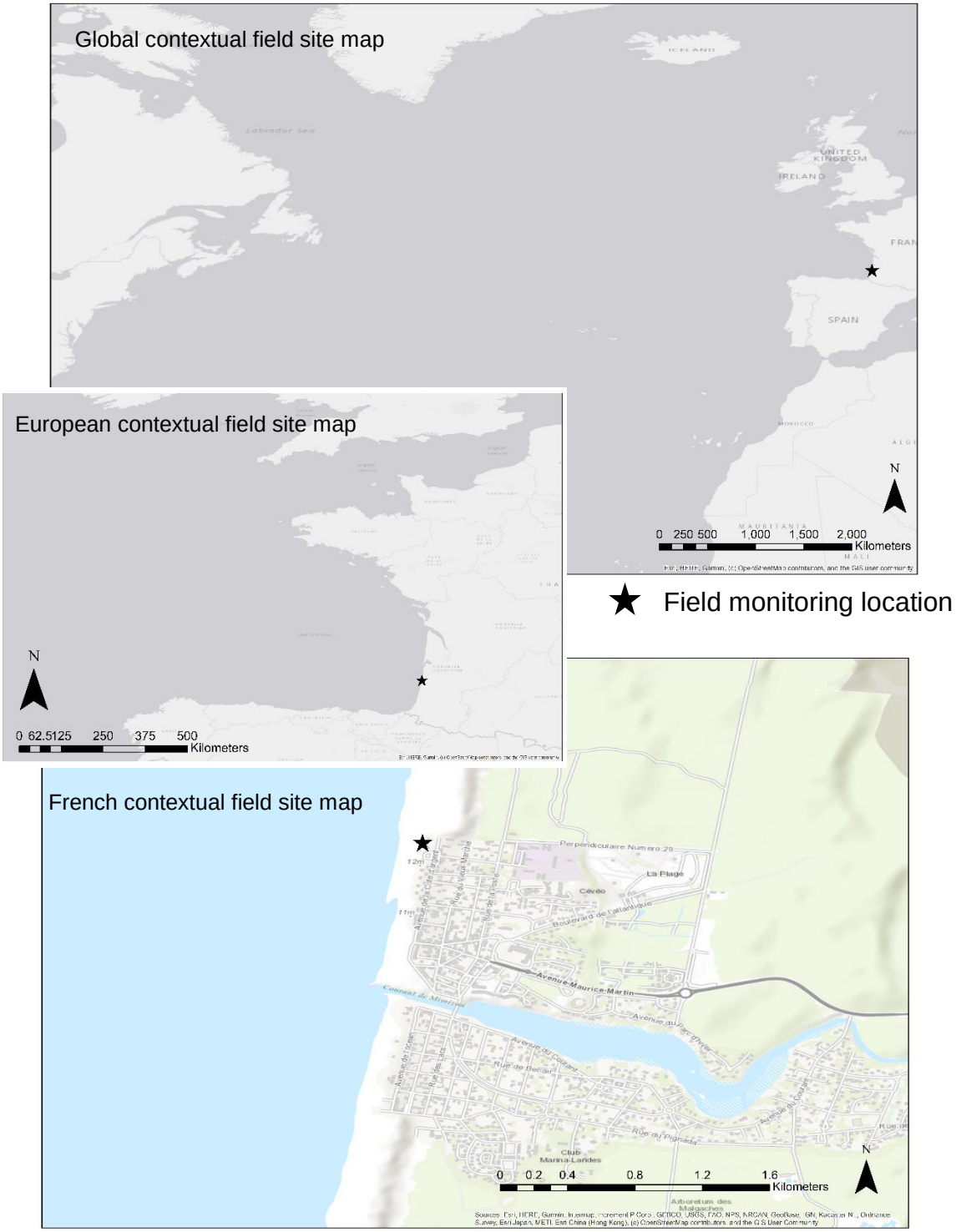

Background maps are provided by ArcGIS (Esri), with permission to reuse as specified in the Esri Master Agreements; Products and Services Terms of Use.

References for basemaps used (also noted in manuscript references):

Esri. “Global contextual field site map” [basemap]. Scale- 1:591M scale to 1:72k scale. “World Light Grey Canvas Base”. April 24, 2019. https://www.arcgis.com/home/item.html?id=87fcdf91a0f14e4a9fda40a763c6f2b8. (January 2, 2020).

Esri. “European contextual field site map” [basemap]. Scale- 1:591M scale to 1:72k scale. “World Light Grey Canvas Base”. April 24, 2019. https://www.arcgis.com/home/item.html?id=87fcdf91a0f14e4a9fda40a763c6f2b8. (January 2, 2020).

Esri. "French contextual field site map” [basemap]. Scale Not Given. "World Topographic Map". June 7, 2013. https://www.arcgis.com/home/item.html?id=6e850093c837475e8c23d905ac43b7d0. January 2, 2020).

Appendix 15: Exploratory extrapolation calculations of MP for 1km and 50% of the global coastline

Volume of microplastic particles (MP)

MP particle diameter = 25µm

MP particle radius = diameter/2 = 12.5µm

MP density = 1 g/cm^3

Equation S1. $MP\ Volume = \frac{4}{3}\pi r^2$

MP mass per MP

MP mass = mass of a single MP particle in kg/MP

Equation S2. $MP\ mass = volume\ x\ density$

MP particles blowing onshore (#MP flux, in MP/sec)

MP in onshore wind = 2.96 MP/m^3 (observations for onshore wind direction samples A1-A4)

= 19.38 MP/m^3 (observations for onshore sea mist sample A8a)

MBL(h) = Marine boundary layer (MBL) height = 200 m

Average onshore wind speed = 5 m/s (Archer and Jacobson 2005, *65*)

Length of coastline being considered = 1000m (for 1km consideration)

= 178000000 m (50% of global coastline, 356000000/2)

Air flow = Volume of air flow onshore, m^3/s

Equation S4. $Air\ flow = MBL(h)\ x\ wind\ speed$

#MP flux = Number of MP particles blowing onshore, MP/s

Equation S5. $\#MP\ flux = air\ flow\ x\ \#MP\ in\ onshore\ wind$

MP mass flux onshore

Mass of MP in onshore wind in kg per second = MP mass flux (kg/s)

Equation S6. $$MP\ mass\ flux = Mass\ (per\ MP)\ x\ \#MP\ flux$$

Mass of MP in onshore wind in tonnes per year = MP mass flux (tons/yr)

Equation S7.

$$MP\ mass\ flux\ \left(\frac{ton}{yr}\right) = \left(MP\ mass\ flux\ \left(\frac{kg}{s}\right) 60\ x\ 60\ x\ 24\ x\ 365\right) x\ 0.01$$